

Hydrodynamics and Morphodynamics in and around Mangrove Forests

Report

September, 2006

WL | delft hydraulics

Hydrodynamics and Morphodynamics in and around Mangrove Forests

Ms.C. Thesis report
Civil Engineering, section Water Engineering and Management
University of Twente

Frank Dekker

Supervisors:
dr. ir. Jan Ribberink
drs. Mindert de Vries

Report

September, 2006

Preface

In Dutch there is a proverb which says: you can't see the forest through the trees, meaning losing the overview by seeing all the details. I often felt like that the last months: so many processes play a role in and around mangrove forests! In this M.Sc. thesis report (to complete my study Civil Engineering at the University of Twente) I tried to present to you the mangrove forest by looking at all the detailed processes. After reading this report I hope you will still see the mangrove forest, once confronted with the details. If this is the case, I have done a good job. Else...

I would like to thank all the people who helped me writing this report and finishing my M.Sc. study Civil Engineering at the University of Twente. Mindert de Vries and Jan Ribberink, thanks for all the discussions, critical reviews, enthusiasm and energy you have put in this project. My fellow graduate at MCM, thanks for all the friendship you offered at WL and all the interest for and input in my thesis. It was great having you guys around me. Hanneke, thanks for your support during the last 9 months. Without you...

Enjoy Reading!

Frank Dekker

Delft, September 2006

Contents

1	Introduction	1—1
2	Physical processes	2—1
2.1	Basic morphodynamic equations	2—1
2.2	Tidal flow and vegetation	2—3
2.2.1	Tidal flows and bed shear stress	2—3
2.2.2	Eddy diffusivity	2—5
2.3	Waves and vegetation	2—7
2.3.1	Introduction into the world of waves	2—7
2.3.2	Waves and sediment transport	2—9
2.3.3	Effects of waves on sediment transport and morphology	2—13
2.3.4	Waves and vegetation	2—15
2.4	Conclusion: modelling morphodynamics	2—16
3	Mangrove forests quantified.....	3—1
3.1	Bathymetry	3—1
3.1.1	Fringe type forests	3—2
3.1.2	Overwash type forests.....	3—2
3.2	Tidal range and currents	3—3
3.3	Wave height and attenuation.....	3—3
3.4	Sediment transport and morphology	3—4
3.4.1	Sediment concentration.....	3—4
3.4.2	Grain size distribution.....	3—4
3.4.3	Sediment accretion	3—5
3.5	Vegetation.....	3—5
3.6	Conclusion.....	3—6

4	Fringe mangroves	4—1
4.1	Non cohesive sediments	4—2
4.1.1	Validation criteria	4—2
4.1.2	Model setup	4—3
4.1.3	Analysis	4—5
4.1.4	Conclusion	4—9
4.2	Cohesive sediments	4—10
4.2.1	Validation Criteria	4—10
4.2.2	Model setup	4—10
4.2.3	Analysis	4—11
4.2.4	Conclusion	4—13
4.3	Discussion	4—14
4.3.1	Difference between model set up and reality	4—14
4.3.2	Shortcomings in the understanding of processes	4—15
4.3.3	Influence of mangroves: trapping of sediments	4—19
4.4	Conclusions	4—20
5	Overwash mangroves	5—1
5.1	Modelling overwash mangroves	5—2
5.1.1	Validation criteria	5—2
5.1.2	Model setup	5—4
5.1.3	Analysis	5—5
5.1.4	Conclusion	5—12
5.2	Sensitivity analysis	5—13
5.2.1	‘Modelling approach’ sensitivity	5—14
5.2.2	‘Physical parameter’ sensitivity	5—16
5.2.3	‘Biological parameter’ sensitivity	5—17

	5.2.4	Conclusion	5—22
5.3		Discussion	5—23
	5.3.1	Model uncertainties	5—23
	5.3.2	Sediment transport inside the forest	5—24
	5.3.3	Modelling vegetation	5—26
5.4		Conclusion	5—27
6		Mangrove management	6—1
6.1		Impact of mangroves on coastlines	6—1
	6.1.1	Time scales of processes	6—1
	6.1.2	Influence of mangroves on waves and tides.....	6—2
	6.1.3	Influence of mangroves on storms.....	6—3
	6.1.4	Conclusion	6—4
6.2		Human impacts on mangrove coastlines	6—4
6.3		Conclusions	6—6
7		Conclusion and Recommendation.....	7—1
7.1		Conclusions	7—1
	7.1.1	Question 1	7—1
	7.1.2	Question 2	7—3
	7.1.3	Question 3a	7—4
	7.1.4	Question 3b	7—4
	7.1.5	Question 4	7—5
	7.1.6	Generally.....	7—5
7.2		Recommendations.....	7—6
A		Mangroves.....	A—1
A.1		Biological aspects	A—1
	A.1.1	Mangrove species	A—1

A.1.2	Root structures	A-3
A.1.3	Growth.....	A-4
A.2	Ecological Aspects.....	A-5
A.2.1	Distribution patterns.....	A-6
A.2.2	Zonation.....	A-7
A.2.3	Environmental settings	A-9
A.2.4	Forest types.....	A-10
B	Delft3D conceptual model.....	B-1
B.1	Grid and bathymetry	B-1
B.2	Delft3D FLOW model.....	B-3
B.2.1	Hydrodynamic equations.....	B-3
B.2.2	Bed shear stress.....	B-6
B.2.3	Turbulence.....	B-7
B.2.4	Sediment transport and morphology	B-8
B.2.5	Mangroves in Delft3D FLOW	B-11
B.3	Delft3D WAVE model	B-13
B.3.1	Background spectral wave analysis.....	B-13
B.3.2	Governing equations	B-16
B.3.3	Vegetation and Delft3D WAVE.....	B-17
C	Delft3D Flow and Wave results.....	C-1
C.1	Delft3D FLOW.....	C-1
C.1.1	Cross-shore tidal flow without vegetation.....	C-1
C.1.2	Velocity profiles	C-3
C.1.3	Eddy viscosity.....	C-4
C.1.4	Conclusion.....	C-7
C.2	Delft3D WAVE model	C-7

	C.2.1	Basics of the linear wave theory.....	C-8
	C.2.2	Checking calculations.....	C-11
	C.2.3	Conclusion.....	C-13
C.3		Wave influences.....	C-14
	C.3.1	Hydrodynamic influences of waves.....	C-15
	C.3.2	Sediment transport and morphology.....	C-17
	C.3.3	Conclusion.....	C-18
	C.3.3	Conclusion.....	C-19
D		Calibration of the vegetation friction factor	D-1
E		Variants on the fringe model	E-1
E.1		Long shore currents.....	E-1
	E.1.1	Model set up.....	E-1
	E.1.2	Analysis.....	E-2
	E.1.3	Conclusion.....	E-5
E.2		A hollow profile.....	E-5
	E.2.1	Model setup.....	E-5
	E.2.2	Analysis.....	E-6
	E.2.3	Conclusion.....	E-6
F		Background sensitivity analysis	F-1
F.1		Model sensitivity.....	F-1
	F.1.1	With waves ~ magnitude.....	F-1
	F.1.2	With waves ~ differences.....	F-3
	F.1.3	Observations.....	F-5
	F.1.4	3D ~ magnitude.....	F-6
	F.1.5	3D ~ Differences.....	F-9
	F.1.6	Observations.....	F-10

F.2	Parameter sensitivity.....	F-11
G	Management issues.....	G-1
G.1	General management issues	G-1
G.2	General hydrodynamic principles.....	G-2
G.2.1	Water levels	G-3
G.2.2	Velocities	G-6
G.2.3	Conclusion.....	G-11

Summary

Mangrove forests cover large parts of the tropical and subtropical shorelines in the world, and are of great economical and biological importance. The recent devastating tsunami attack (26 December 2004) increased the interest in mangrove shorelines by showing their ability to protect coastal regions. By modelling a mangrove forest in the Delft3D modelling package it is tried to get more insight in the hydrodynamics and morphodynamics in and around mangrove forests. This research is confined to the morphodynamics in fringe and overwash mangroves.

It is chosen to model the morphodynamics as a result of tidal flows and waves. The influence of mangroves on tidal flows is taken into account in the momentum equation as an extra force based on vegetation characteristics. Vegetation is often seen as a group of parallel, staggered or randomly arranged rigid vertical cylinders with homogeneous properties. The force F_p per unit area can be expressed as:

$$F_p = \frac{1}{2} \int_0^k C_D(z) m(z) D(z) |u(z)| u(z) dz$$

Where k is the height of the vegetation, C_D the drag coefficient, m the density, D the diameter and u the flow velocity. The continuity equation is corrected for the cross-sectional plant area. In the k - ϵ turbulence model an extra source term is implemented, based on the friction force, the flow velocity and the time-scale of energy dissipation.

The influence of vegetation on waves can be taken into account in the equation for energy dissipation, formulated by Collins (1972). The energy dissipation, based on vegetation characteristics can be expressed as:

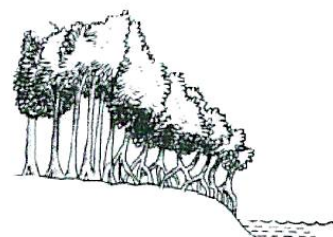
$$S = f_w D m k \rho U_{orb}^3$$

Where f_w is a friction factor, ρ the density of water and U_{orb} the orbital velocity at the bottom.

From literature some general observations can be made considering the following processes and parameters:

- Tidal currents inside mangrove forest are in the order of cm/s
- Wave heights on mangrove coastlines are low (< 20 cm), wave attenuation due to mangroves is between 20% and 50%
- High suspended sediment concentrations are observed in and around mangrove forests (max 400 mg/l)
- Grain sizes inside mangrove forests are low (between 20 and 200 μm)
- The order of magnitude for sediment accretion is mm/yr

Using the above standing influence of mangroves on waves and tidal flows and the results findings from literature, it is tried to model fringe mangroves. Both cohesive and non-cohesive sediments are used in the model calculations, but the model did not generate satisfactory results. It became clear that the cross-shore sediment transport due to waves cannot yet be modelled in a reliable way for the fringe mangrove



Coastal fringe forest

coastline. This observation corresponds with the literature where the cross-shore sediment dynamics are tried to be quantified. The hydrodynamical influence of mangroves was modelled well considering flow velocity, influence on turbulence and wave attenuation. Although the morphological results were not very reliable it seems that inside fringe mangrove forests (for both non-cohesive and cohesive sediments) sediment is trapped and sedimentation takes place.



Overwash forest

For overwash mangroves waves are left out in the first calculations because of the problems with sediment transport due to waves observed in the fringe forest. This can be done because waves play a minor role (tidal currents become more important) in the overwash case. The calculations are carried out in a 2DH setting in order to save calculation time. It turned out that the model generated satisfactory results considering water levels, flow velocity, sediment accretion, levee building (in the case of non-cohesive

sediments) and long term morphological patterns. In the sensitivity analysis it is tried to get more insight in the effect of a different modelling approach, different physical parameters and different biological parameters on the modelling results. Considering the sensitivity of the modelling results to a different modelling approach a '3D approach' and a 'wave approach' are analysed. It is found that the sedimentation/erosion pattern is not sensitive for a different approach. The magnitude of erosion or sedimentation however is highly sensitive for different wave heights. The modelling results did not show a high sensitivity to other physical parameters (wave angle, sediment concentration and settling velocity). Biological parameters like tree density, forest shape and forest length, influenced the sedimentation/erosion pattern only on the long term. With decreasing tree density more sediment transport inside the forest takes place. The most important and general conclusion for the overwash case is that for both sediment types (cohesive and non-cohesive) mangroves trap sediments due to increased sedimentation and reduced erosion inside the forest.

From the modelling experiment can be seen that fringe and overwash mangroves trap sediments, by increased sedimentation due to a reduction in flow velocity and a decrease in erosion due to a reduction in wave height and flow velocity. The consequence of this conclusion for coastal management is that mangroves are able to stabilize coastlines. By their ability to reduce waves and currents, mangroves can also play an important role in safety issues.

It should be kept in mind that the modelling results are not yet validated with a case study. It is therefore recommended to carry out such a study, in order to increase the reliability of the model.

I Introduction

Research framework

Mangrove forests are tidal ecosystems in sheltered saline to brackish wetlands [Quartel, 2000]. Mangrove forests cover large parts of the tropical and subtropical shores in the world [Robertson and Alongi, 1992]. The forests are important for three reasons:

- They are one of the most biologically diverse forests [Burger, 2005]. Several organisms from the sea find a breeding place in these forests. Birds as well find a nesting place.
- They are economically important [Mazda et al., 2002 and Quartel, 2000]. Timber and fuel wood can be found in these forests. Because of the function of mangrove forests as a breeding place they are also important to maintain fisheries production.
- They protect the coastline (and the people behind it) and prevent erosion [Burger 2005, Schiereck and Booij, 1995, Mazda et al., 1997, Mazda et al., 2002].

This importance of mangrove forests asks for good management of these forests. To manage these forests knowledge is necessary about the processes that play a role in the mangrove system and how these processes interact. Three different processes can be distinguished:

- Growth and reproduction processes
- Hydrodynamic processes
- Morphodynamic processes

These processes interact with each other. Mazda et al (2005) summarise this interaction when they state that: *the mangrove ecosystem was constructed over a long span of time through feedback processes including the biotic activity, landform evolution and water flows*. In figure 1.1 this interaction is displayed.

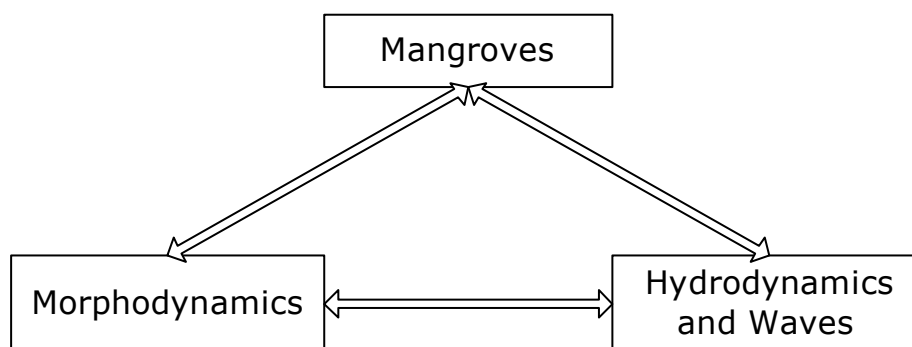


Figure 1-1: interactions in mangrove systems

Good understanding of the processes and good understanding of the interactions between these processes forms the basis of good management of mangrove forests. Several aspects of the triangle presented in figure 1.1 have been studied in mangrove areas around the world (see for example Ellison (1998), who has carried out a literature study on sedimentation in mangrove forests). A comprehensive study of linking the individual processes in mangrove forests to each other has not been carried out.

In order to increase knowledge about the interactions between the individual processes in a mangrove ecosystem and the (morphological) development of such a system a model study shall be carried out. The Delft3D modelling package will be used, which combines a flow model, a wave model and a vegetation model to determine the sediment transport and morphodynamics.

Research objective

The focus of this research is the morphodynamic changes in a mangrove ecosystem. The objective is formulated as:

To get insight in the morphodynamics in and around mangrove forests as the result of the combined processes of waves and (tidal) currents, by modelling the system in Delft3D

Confining the research

It is too complex and difficult at this time to model the full interactive system presented in figure 1.1, especially when ecological aspects like mangrove growth and reproduction have to be taken into account. The objective of this research stated above has already confined the scope of this research into morphodynamic changes by tidal currents and waves. In terms of the triangle of interactions (see figure 1.1) this means that the research will take into account the influence of mangrove trees on the hydrodynamics and waves, the influence of hydrodynamics and waves on the morphodynamics and the influence of the morphodynamics on the hydrodynamics and waves. The system with the interactions presented in figure 1.2 will be the focus of this research.

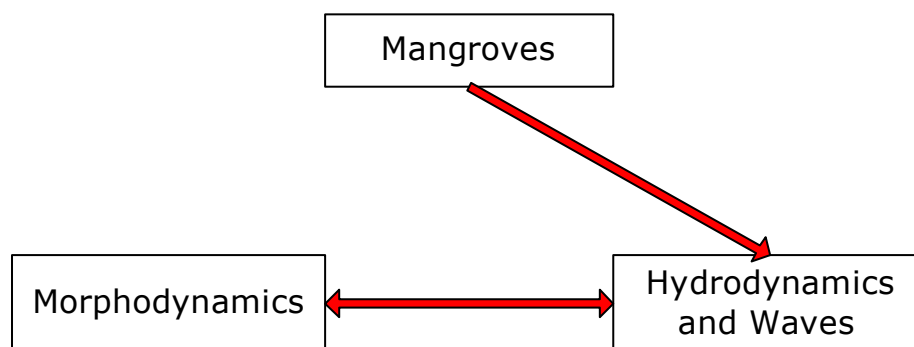


Figure 1-2: modelling sediment transport in mangrove forests

Mangrove forests are not homogeneous. They occur in different environmental settings and differ in types of forest. Lugo and Snedaker (1974) defined six functional types to classify mangrove forests. The types are presented in figure 1.3. More explanation about the types and general (ecological) information on mangrove forests can be found in Appendix A. The hydrodynamic influences in these types of forests are not the same. The biggest difference in hydrodynamic influences can be found in Riverine and Overwash type forests. For Riverine forests the flow is unidirectional (river dominated), for overwash forests the flow is bidirectional (tide dominated). This means also another morphological and ecological development of the forest. Woodroffe (1992) made a triangle, combining the hydrodynamic influences to the six functional forest types of Lugo and Snedaker (2004) (see figure 1.3).

Because this research tries to investigate morphological changes due to tidal currents and waves, tide dominated mangrove forests should be subject of study. These are the overwash and fringe forest types. They are subjected to bidirectional tidal currents and waves from the seaside. Therefore these forest types are the focus of this study. In figure 1.3 the forest types are circled red.

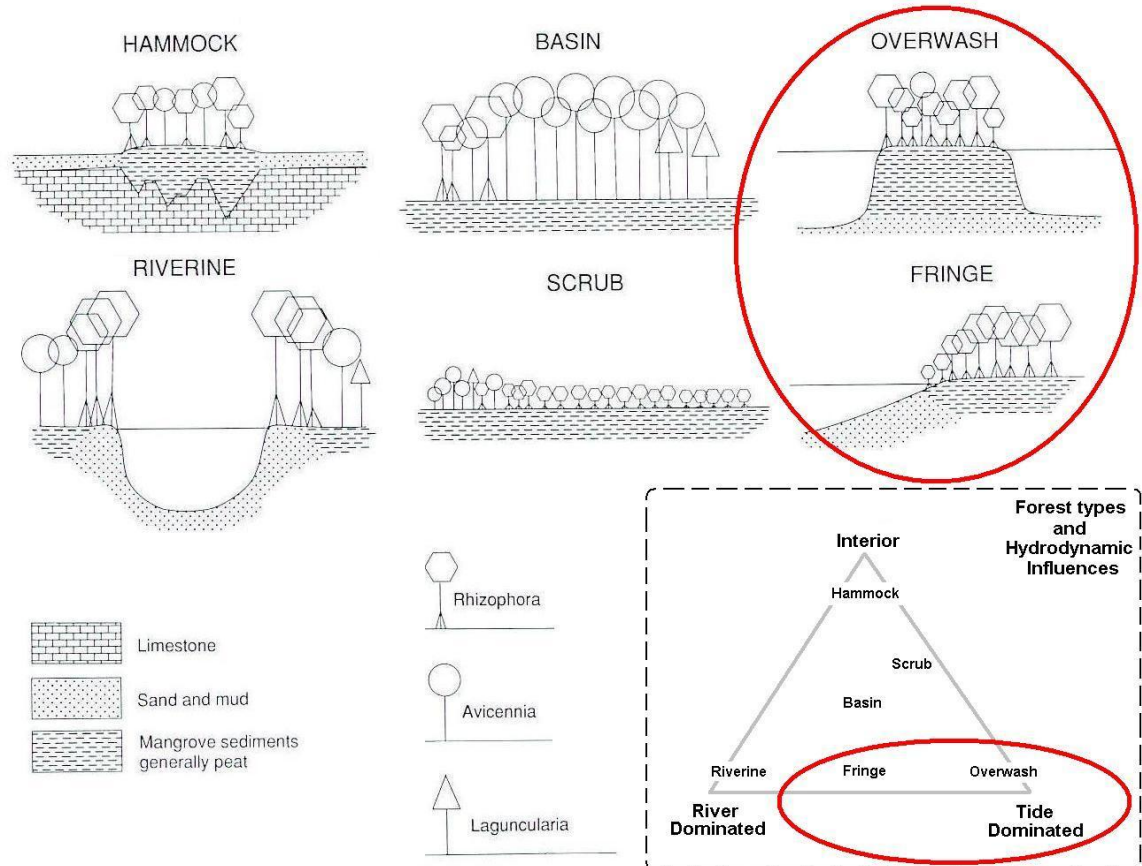


Figure 1-3: Six functional mangrove forest types (after Lugo and Snedaker (1974)) and a classification of the forest types considering their hydrodynamic influences (after Woodroffe (1992)). The red circles represent the focus of this study

Research questions and report structure

Four research questions can be formulated to reach the objective stated above. These questions form the basis for the structure of this report. Each question is elaborated a little and the chapters discussing the question are given as well.

1) Which processes and parameters control morphological changes on (mangrove) coastlines and what is the effect of mangroves on these processes and parameters?

This question tries to get insight in the basic processes of sediment transport, hydrodynamics and waves. The knowledge of physical processes and parameters and the influence of mangroves on these processes and parameters will help in the analysis of the modelling results (chapter 2).

2) What is known about coastal morphology, tidal water levels, tidal currents, waves, and sediments in and around mangrove forest, and vegetation characteristics to parameterize mangrove trees?

Quantification of the processes and the effects of mangroves on these processes will make it possible to check the validity of modelling results. Knowing this, it will also be possible to schematise the mangrove forest and setup the boundary conditions and specific parameters needed by the model. This question is the start to the modelling experiment (chapter 3).

3) How can the fringe and overwash mangrove forest be modelled and what conclusions about the morphodynamic influences and changes can be drawn from the modelling experiment?

The modelling experiment is the heart of this analysis and this question refers to it. Using the information gained with the previous questions it is tried to model fringe mangroves (chapter 4) and overwash mangroves (chapter 5). It is tried to construct a basic model, with which a sensitivity analysis can be carried out.

4) Which possible implications for mangrove management can be drawn from this modelling experiment?

In the research framework three reasons are given for the importance of mangrove forests. Forests have to be managed well in order to keep them useful for human and nature. Answering this question widens the applicability of this research by providing relevant information to end-users.

Research material

As a preparation to this research the effects of mangrove systems on flow, waves, sediment transport and morphodynamics are studied in a literature study (Dekker, 2005). This study starts with an introduction (see appendix A) in the world of mangroves describing biological aspects (like species and root structures) and ecological aspects (like forest types and environmental settings). The introduction is followed by a description of the interaction between vegetation and (1) waves, (2) tides and (3) sediment transport and morphology, which is summarised in chapter 3. The study is used extensively and can be read as an introduction to this research.

Besides the literature study the Delft3D modelling package is an important tool in this research. A general description of this model and an overview of the governing equations are described in the Delft3D FLOW manual and Delft3D WAVE manual. In this research only the used parts of the model are described in chapter 2 and appendix B.

2 Physical processes

Mangroves influence water movements and waves. Waves and currents are responsible for morphological changes. Morphology influences water movements and waves. These interactions are the focus of this study and presented in figure 1.2. Knowledge of physical processes and parameters and the influence of mangroves on these processes and parameters are necessary in analysing the morphodynamics in and around mangrove forest. This chapter tries to describe the interactions in processes and parameters and how (or if) it can be taken into account in Delft3D. The research question is:

Which processes and parameters control morphological changes on mangrove coastlines and what is the effect of mangroves on these processes and parameters?

The question tries to get insight in the basic processes of sediment transport, hydrodynamics and waves. Keeping the triangle of interactions (figure 1.2) in mind, this question can be divided into five sub-questions

- Which basic processes and parameters control morphological changes? (§ 2.1)
- How do tidal flows play a role in morphological changes? (§ 2.2)
- What is the influence of mangroves on currents? (§ 2.2)
- How do waves influence morphological changes? (§ 2.3)
- What is the effect of mangroves on waves? (§ 2.3)

Because this study is a model study the question behind each process is: can it be modelled with Delft3D? To answer this question the processes are tried to be quantified in equations, which are taken into account in Delft3D. The hypothesis is that the individual processes are well understood and can be modelled with Delft3D. In the conclusion of this chapter (§ 2.4) the hypothesis will be reviewed.

2.1 Basic morphodynamic equations

Morphodynamics describes the feedback system of hydrodynamics, sediment transport and bottom changes. The most important processes in sediment dynamics are shown in figure 2.2:

- Suspended sediment transport
- Sediment settling
- Sediment erosion
- Diffusion
- Bed load sediment transport

These processes are driven by hydrodynamic processes and sediment characteristics. In turn the sediment dynamics determine the changes in the bottom. The three dimensional suspended

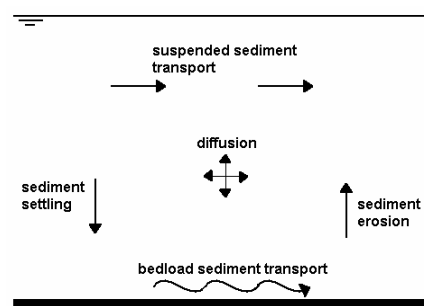


Figure 2-1: most important processes in sediment dynamics

sediment dynamics is determined in Delft3D by solving the three dimensional advection-diffusion equation for sediments:

$$\begin{aligned} \frac{\partial c^\ell}{\partial t} + \frac{\partial uc^\ell}{\partial x} + \frac{\partial vc^\ell}{\partial y} + \frac{\partial (w - w_s^\ell)c^\ell}{\partial z} + \\ - \frac{\partial}{\partial x} \left(\varepsilon_{s,x}^\ell \frac{\partial c^\ell}{\partial x} \right) - \frac{\partial}{\partial y} \left(\varepsilon_{s,y}^\ell \frac{\partial c^\ell}{\partial y} \right) - \frac{\partial}{\partial z} \left(\varepsilon_{s,z}^\ell \frac{\partial c^\ell}{\partial z} \right) = 0 \end{aligned} \quad (2.1)$$

Where:

- $c^{(l)}$ = mass concentration of sediment fraction (l)
- u,v and w = flow velocity components
- ε = eddy diffusivities of sediment fraction (l)
- $w_s^{(l)}$ = (hindered) sediment settling velocity of sediment fraction (l)

In equation (2.1) the most important processes (see figure 2.1) are taken into account, except the bed load sediment transport. It can be seen that the flow velocity (in all directions) and the eddy diffusivity are important hydrodynamic parameters for sediment transport.

The bed load transport in Delft3D is determined using the following equation:

$$S_b = 0.006\eta\rho_s w_s d_{50} M^{0.5} M_e^{0.7} \quad (2.2)$$

Where:

- S_b = bed load transport
- η = relative availability of the sediment in the mixing layer
- ρ_s = density of sediment
- ρ_w = density of water
- w_s = settling velocity of the sediment
- d_{50} = mean grain size diameter
- M = sediment mobility number due to waves and currents
- M_e = excess sediment mobility number

The sediment mobility number depends on the flow velocity and the orbital velocity. For sediment bed load transport there is a minimum flow velocity required, which is expressed in terms of the bed shear stress. The excess sediment mobility number depends on the critical bed shear stress. The critical bed shear stress can be expressed as:

$$\tau_{cr} = (\rho_s - \rho_w) g D_{50} \theta_{cr} \quad (2.3)$$

Where:

- τ_{cr} = critical bed shear stress for initiation of motion
- g = gravity acceleration
- θ_{cr} = the critical Shields parameter

Equation (2.1) to (2.3) show very clear the influence of hydrodynamics on the sediment transport processes and morphodynamics. Flow velocity, orbital velocity, bed shear stress and eddy diffusivity are the most important hydrodynamic parameters. The next two paragraphs will focus on these parameters.

In the Delft3D model equation (2.1) to (2.3) are elaborated much more and more information about these equations can be found in the Delft3D FLOW manual.

2.2 Tidal flow and vegetation

The previous paragraph concluded that the flow velocity, the bed shear stress and the eddy diffusivity are important for sediment transport (considering water movements). In this paragraph the influence of tidal flow on these parameters and the influence of vegetation on tidal flow are explored. The Delft3D model is tested to see if the processes are modelled well. The results of this experiment are given in appendix C: flow and wave model results.

2.2.1 Tidal flows and bed shear stress

Tidal water levels

In a mangrove system important flows are tidal flows, resulting from tidal water level variations. Attractive forces of the earth, moon, sun and other planets and the rotation of the earth are responsible for the water level variations. The variations can be expressed as a number of periodic elements related to the different periodic forcing mechanisms. The basic equation is:

$$h(t) = \sum_{n=1}^N A_n \cos\left(2\pi \frac{t}{T_n} - \theta_n\right) \quad (2.4)$$

Where:

- $h(t)$ = water level at time t
- N = the number of elements
- A_n = the amplitude of component n
- t = time
- T_n = period of component n
- θ_n = phase of component n

Cross-shore and long shore currents

Due to water level variations water will flow in two directions: to or from the coast and along the coastline, cross-shore currents and long shore currents respectively. Cross-shore currents are usually very small, in the order of cm/s. The (time dependent) depth average cross-shore flow velocity $u(t)$ can be derived from equation (2.4) by taking the time derivative and dividing it by the slope of the beach i_b :

$$u(t) = \sum_{n=1}^N -\frac{2\pi A_n}{T_n i_b} \sin\left(2\pi \frac{t}{T_n} - \theta_n\right) \quad (2.5)$$

Equation (2.5) is only valid if the water level differences are resulting only from cross-shore water movements and not from long shore movements. In most cases the tide is propagating along the coast and the tidal water level variations come from long shore currents.

Long shore tidal currents result from phase differences in tidal water levels along the coast and the geometry of the coastline. They are much larger comparing to the cross-shore currents and in the order of 1 dm/s (see for example Winterwerp et al., 2005, Wu et al., 2001). For sediment transport and morphodynamics these currents are much more important than the cross-shore currents.

Influence of vegetation on tidal flows and water levels

The relationship between water levels, flow velocity and friction is usually expressed with the continuity and momentum equations (see appendix B for the equations used in Delft3D). For stationary, uniform flow these equations can be simplified, resulting in the following relation between bed shear stress τ_b and water depth h :

$$\tau_b = \rho g h i \quad (2.6)$$

where ρ is the density of water, g the gravity acceleration and i the water level gradient. By definition the bed shear stress is related to the flow velocity:

$$\tau_b = f \rho u^2 \quad (2.7)$$

where f is a friction factor. By choosing a friction factor and combining equation (2.6) and (2.7), the water level can be related to the flow velocity. Vegetation will lead to an extra force acting on the flow and resisting the flow. Baptist (2005) state that it is common to model vegetation as a group of parallel, staggered or randomly arranged rigid vertical cylinders with homogeneous properties. The resistance force (per area) is defined as:

$$F_p = \frac{1}{2} \rho \int_0^k C_D(z) m(z) D(z) |u(z)| u(z) dz \quad (2.8)$$

Where F_p is the vegetation friction force, C_D the drag coefficient (most of the time set to 1), m the stem density, D the stem diameter and k the height of the stem. A new balance between the bottom friction force, the vegetation force, the water level and the flow velocity has to be established. Expressed in the terms of equation (2.6), (2.7) and (2.8) this balance is:

$$\rho g h i = \tau_b + F_p \quad (2.9)$$

This is the concept to take vegetation into account. In the model calculations the effect of vegetation is taken into account in the complex momentum equations, leading to a new balance between water levels, flow velocity and friction. Model calculations can generate more insight in this balance.

Flow velocity profiles

The velocity profile in the vegetation field will also change. Without vegetation the velocity profile is assumed to have a logarithmic shape, which can be expressed as:

$$u(z) = \frac{u_*}{\kappa} \ln \frac{z}{z_0} \quad (2.10)$$

Where $u(z)$ is velocity at height z , u_* the shear velocity, κ the von Karmann constant ($\kappa = 0.4$), z the height above reference level and z_0 the height above the bottom where the flow velocity is 0 m/s. In figure 2.2 this velocity profile is shown.

Inside the vegetation field the flow velocity profile is supposed to be uniform. Baptist (2005) derived an equation for this flow velocity u_v , depending on vegetation characteristics, considering vegetation as a number of cylinders on the bottom with a certain height k , density m and diameter D :

$$u_v = \sqrt{\frac{2gi}{C_D m D}} \tag{2.11}$$

Using this equation, two different cases can be distinguished: emergent vegetation and submerged vegetation. In the first case the flow velocity is uniform and constant over the water column. For submerged vegetation the flow velocity is only uniform inside the vegetation. Above the vegetation field a transition zone will occur, which will rebuild the original logarithmic profile. Both velocity profiles are also shown in figure 2.2.

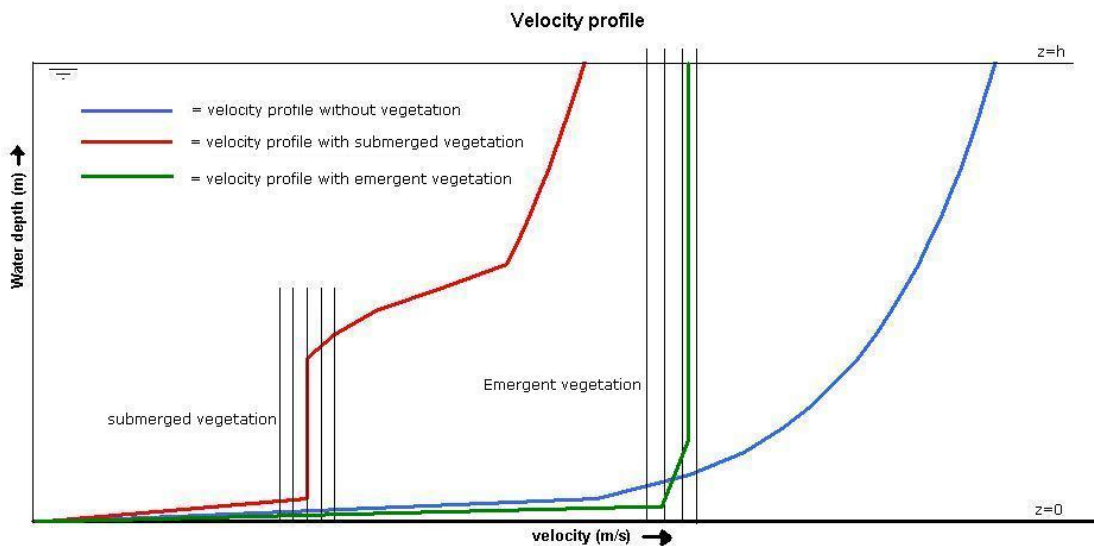


Figure 2-2: flow velocity profiles for submerged (red), emergent (green) and no vegetation (blue)

Influence on sediment transport

In general can be said (using the ‘morphodynamic’ equations (2.1) and (2.2) that vegetation will reduce the flow velocity and bed shear stress, which initially will reduce suspended and bed load sediment transport. However, in what way influences the vegetation the eddy diffusivity and waves, and how is that related to the sediment transport?

2.2.2 Eddy diffusivity

General

The eddy diffusivity expresses the turbulence induced by the flow. More turbulence will lead to a higher erosion flux, more sediment in the water column and more suspended sediment transport (if other parameters are assumed not to vary). It will also lead to more diffusion of the sediment. Generally, the eddy diffusivity can be expressed as:

$$\epsilon_s = c_\mu \frac{k^2}{\epsilon} \tag{2.12}$$

Where ε_s is the eddy diffusivity, c_μ is the empirical constant (= 0.09), k is the kinetic turbulent energy and ε the energy dissipation.

Vegetation and the k- ε turbulence model

The kinetic turbulent energy and the energy dissipation are related to each other and can be calculated with the k- ε turbulence model. The effect of vegetation on kinetic energy and energy dissipation can be taken into account in this turbulence model:

$$\frac{\partial k}{\partial t} = \frac{1}{1-A_p} \frac{\partial}{\partial z} \left\{ (1-A_p) \left(\frac{\nu + \nu_t}{\sigma_k} \right) \frac{\partial k}{\partial z} \right\} + T + P_k - B_k - \varepsilon \quad (2.13)$$

and:

$$\frac{\partial \varepsilon}{\partial t} = \frac{1}{1-A_p} \frac{\partial}{\partial z} \left\{ (1-A_p) \left(\frac{\nu + \nu_t}{\sigma_\varepsilon} \right) \frac{\partial \varepsilon}{\partial z} \right\} + T\tau^{-1} + P_\varepsilon - B_\varepsilon - \varepsilon_\varepsilon \quad (2.14)$$

Where k is the kinetic turbulent energy, A_p the horizontal cross-section plant area, ν the viscosity, T the work on the plants of the flow, τ the time scale, P the production of energy, B the buoyancy and ε the energy dissipation. The equations are more elaborated in appendix B.

Normally the kinetic turbulent energy has a linear profile with a value of 0 at the water surface and a higher value at the bottom. The value at the bottom depends on the roughness of the bed and the flow velocity. The energy dissipation is often assumed to have a logarithmic profile with a low value at the water surface and a high value at the bottom, also dependent on the bed roughness and the flow velocity. The profiles of kinetic turbulent energy and energy dissipation (without vegetation) are shown in figure 2.3. Combining the profiles according to equation (2.12) leads to high eddy diffusivities in the middle of the water column and low eddy diffusivities at the surface and the bottom (a triangle shaped profile).

Vegetation will influence the turbulent kinetic energy and the energy dissipation. Above the vegetation field (for submerged vegetation) both the turbulent kinetic energy and the energy dissipation will be the highest. Inside the vegetation field there will also be a lot of turbulence generated and energy dissipated. However the flow velocity is much smaller comparing to the situation without vegetation. The resulting turbulent energy and energy dissipation will therefore be smaller as well. Possible profiles of the turbulent kinetic energy and energy dissipation for the situation with submerged vegetation, are also shown in figure 2.3.

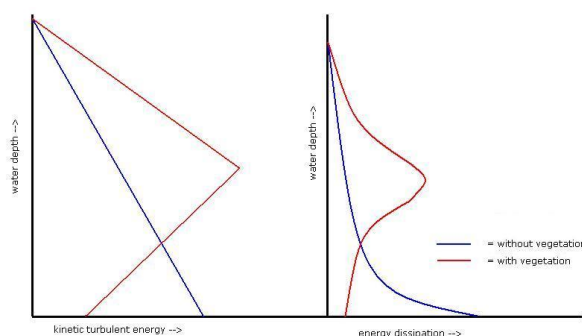


Figure 2-3: possible kinetic turbulent energy (left) and energy dissipation profiles (right) with (red) and without (blue) vegetation. The vegetation is about half the water depth

Influence on sediment concentration

By assuming no change of concentration in time, constant horizontal flow velocities (u and v) and a very low (negligible) horizontal turbulence the sediment balance (see equation (2.1)) reduces to:

$$w_s c = \varepsilon_s \frac{\partial c}{\partial z} \quad (2.15)$$

or:

$$\frac{w_s}{\varepsilon_s} = \frac{1}{c} \frac{\partial c}{\partial z} \quad (2.16)$$

where:

w_s = settling velocity

c = sediment concentration

ε_s = eddy diffusivity

From this equation can be seen that high eddy diffusivity results in a low gradient of the concentration and a flatter concentration profile (if the other parameters remain constant). A high diffusivity corresponds to a high kinetic turbulent energy (see equation (2.12)). More turbulence will result in a better mixing of the sediment in the water column and the change of concentration of sediment in the water depth will be low, so the gradient will be small.

However, the resulting eddy diffusivity inside a vegetation field depends on a number of parameters. Model calculations can generate more insight in the effect of vegetation on the eddy diffusivity and therefore on the sediment concentration profile. This profile is important for the sediment transport.

2.3 Waves and vegetation

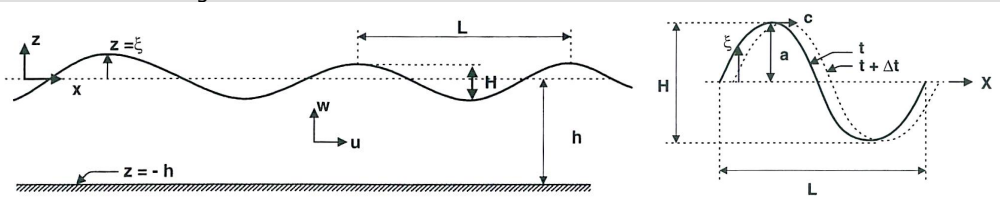
In this paragraph the effects of waves and vegetation on the morphodynamics will be described. It starts with an introduction about waves, where linear wave theory and spectral wave analysis are summarized. Secondly the effects of waves on sediment transport will be described. Thirdly the effects of vegetation on waves are shown. In this way the sub questions 1.d and 1.e are answered.

2.3.1 Introduction into the world of waves

The basics of wave calculations are described by the linear wave theory. In box 2.1 the basic wave parameters and equations are given. This is more elaborated in appendix C. More sophisticated wave calculations can be done with wave spectral analysis, which is used in Delft3D.

Box 2.1: the basics of linear wave theory

The linear wave theory is the basis of most of the wave calculation. The most important parameters are shown in the figure below.



Explanation of parameters in a wave environment and in a wave

Where:

- z = water level
- h = water depth
- H = wave height
- L = wave length
- w = orbital velocity in vertical direction
- u = orbital velocity in horizontal direction
- a = wave amplitude
- c = propagation velocity of the wave

Wave height	Wave orbital velocity	Wave energy
$\eta(x,t) = a \sin(\omega t - kx)$	$u(x,z,t) = \frac{\partial \phi}{\partial x} = \frac{\omega a}{\sinh kh} \cosh k(z+h) \sin(\omega t - kx)$	$E = \frac{1}{8} \rho g H^2$
$a = \frac{1}{2} H, \omega = \frac{2\pi}{T}, k = \frac{2\pi}{L}, c = \frac{L}{T}$	$w(x,z,t) = \frac{\partial \phi}{\partial z} = \frac{\omega a}{\sinh kh} \sinh k(z+h) \cos(\omega t - kx)$	

The basic idea behind this is that the surface elevation $\eta(t)$ can be written as a sum of a large number of harmonic wave components:

$$\eta(t) = \sum_{i=1}^N a_i \cos(2\pi f_i t + \alpha_i) \tag{2.17}$$

Where:

- a_i = wave amplitude of wave i
- f_i = frequency of wave i: $f_i = \frac{1}{T} = \frac{\omega}{2\pi}$
- α_i = phase of wave i

In figure 2.4 the interpretation of the surface elevation into the different wave components is shown.

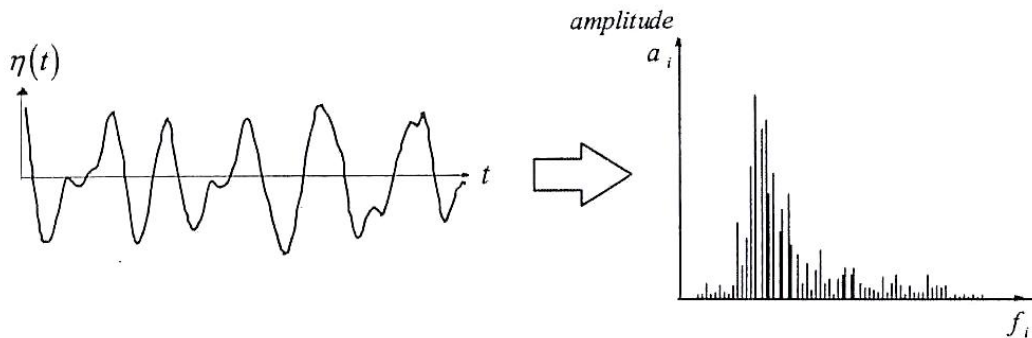


Figure 2-4: from surface elevation to different wave components i with an amplitude a_i and frequency f_i

Taking the expected value of the variance of the amplitude the variance density spectrum can be constructed (see figure 2.5 for the JONSWAP density spectrum). Delft3D uses this density spectrum to calculate a wave field. Providing a peak period, a significant wave

height and a wave direction the spectrum is shaped and ready for the calculation. For more information about wave spectra see appendix B.

A more detailed explanation introduction into the world of waves and a comparison to the Delft3D model calculations can be found in appendix C.

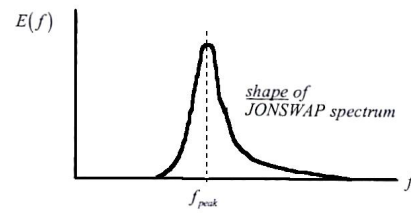


Figure 2-5: the JONSWAP density spectrum

2.3.2 Waves and sediment transport

In coastal regions, waves induce flows, which are able to transport sediments. The occurring flows can be both cross-shore and long shore. Because of the minor tidal cross-shore flow component, waves dominate the cross-shore sediment transport dynamics and morphodynamics.

The interaction between waves, flows and sediment transport is very complex and subject of study and discussion today. The Delft3D model has incorporated five different interactions between waves and flows. These are:

- Stokes drift and mass flux
- Wave set up and wave induced currents
- Streaming
- Wave induced turbulence
- Combined wave – current bed shear stress

More processes are described by Masselink et al (2006) which also give an overview of the resulting sediment transport dynamics. First the ‘Delft3D’ processes are described, followed by other processes described by Masselink et al (2006).

Stokes drift and mass flux

Under waves water particles move along elliptic orbits. In the linear wave theory, see appendix C, the orbit is supposed to be closed (the time averaged velocity is zero!). In reality the orbits are not closed. This can be attributed to the higher velocity on the crest of the wave than at the trough of the wave. Water will be transported in the direction of the wave propagation. This is called the Stokes drift. Figure 2.6 shows the idea of Stokes drift.

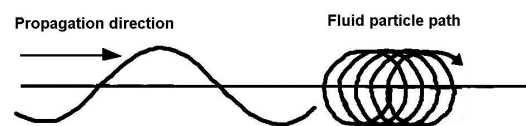


Figure 2-6: principle of the Stokes Drift. The non closed orbital movements lead to a net mass transport in the wave propagation direction

Although the average velocity under waves calculated with the linear wave theory is 0, the velocity can be approximated by calculating the mass flux under a wave. The mass flux M is:

$$M = \frac{E}{c} = \frac{1}{8} \rho g H^2 \frac{k}{\omega} \tag{2.18}$$

Where:

E = wave energy

c = wave propagation velocity

H = wave height

k = wave number = $\frac{2\pi}{L}$

ω = wave frequency = $\frac{2\pi}{T}$

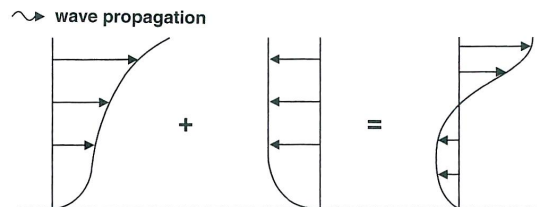


Figure 2-7: resulting velocity profile due to Stokes drift and mass flux

Wave length L and wave period T are related to each other by the dispersion relation (see appendix C). So, the mass flux M only depends on the wave period T , the wave height H and the water depth h . Going to the shore, the mass flux will increase, because the wave height will increase due to shoaling (see appendix C). Because the shoreline is closed the sum of all mass fluxes should be zero (conservation of mass). The onshore directed flux is compensated by a return flow. The velocity profile under waves is shown schematically in figure 2.7. The return flow is called undertow. Due to the return flow sediment can be transported out of the coastal zone.

Wave set up and wave induced currents

Waves exert a net time averaged force on the fluid mass in which they propagate. This force should be taken into account in the equation of motion. An extra force can lead to a water level gradient (water level drops or increases) and/or wave driven currents.

When waves propagate perpendicular to the shore, the water level drops before the breaker zone, and in the breaker zone the water level increases. These processes are called set down and set up respectively. The drop in water level ξ can be approximated by:

$$\xi(h) = -\frac{1}{8} \frac{kh^2}{\sinh(2kh)} \tag{2.19}$$

The increase in water level from the breaking point of waves ($h = h_{br}$) to the coast line ($h = 0$) can be described with:

$$\Delta\xi = \frac{3}{8} \gamma h_{br} \tag{2.20}$$

where γ is the breaking index of a wave.

Because the wave force is directed onshore, the generated currents should also be onshore directed. However, due to the closed boundary of the shore, this onshore current has to be compensated with an offshore current. So, the upper part of the water column has an onshore current and the lower part of the water column has an offshore current. Where the

Stokes drift lead to an offshore current in the lower part of the water column outside the breaker zone, wave set up leads to an offshore current in the lower part of the water column inside the breaker zone. Both processes have the same character, so the velocity field under waves for wave set up is the same as in figure 2.7. In figure 2.8 the effect on the mean water level of both wave set up and wave set down is shown.

When waves propagate under an angle to the shore this will result in long shore currents in the breaker zone. The currents are driven by the wave force, acting in long shore direction, and balanced by the bed shear stress. Combining the wave force and the bed shear stress the long shore current can be approximated by:

$$V = -\frac{5}{8} \pi \frac{g}{f} \xi \gamma h \frac{\partial h}{\partial x} \frac{\sin \theta_0}{c_0} \tag{2.21}$$

Where:

- f = friction factor
- ξ = water level disturbance (wave set up, see equation (2.20))
- γ = wave breaking index (0.5 – 0.8)
- h = water depth
- dh/dx = gradient of the coast
- θ_0 = the wave angle at deep water
- c_0 = the propagation velocity at deep water

This current can lead to long shore sediment transport.

Streaming

With streaming is meant a wave induced current in the wave boundary layer directed in the wave propagation direction. In that layer bottom friction dominates the flow and linear wave theory is no longer applicable. It causes an additional shear stress, which lead to an onshore directed flow. Streaming can be calculated using the dissipation of energy due to bottom friction under waves. The dissipation rate D_f depends on the orbital velocity and can be expressed as:

$$D_f = \frac{1}{2\sqrt{\pi}} \rho f_w u_{orb}^3 \tag{2.22}$$

where f_w is a friction factor. Combining streaming, wave set up and stokes Drift, a general velocity profile under waves can be constructed, shown in figure 2.9. Streaming can be important for (bed load) sediment transport.

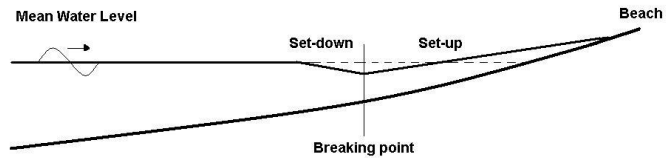


Figure 2-8: mean water level due to wave set-up and wave set-down inside and outside the breaker zone

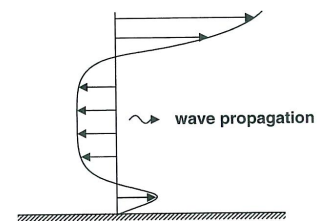


Figure 2-9: mean velocity profile under waves, due to wave set up, stokes drift and streaming

Wave induced turbulence

Waves influence the vertical mixing processes (through wave breaking and orbital velocity) and therefore the sediment concentration profile in the water column. This effect can be taken into account in the eddy diffusivity (see equation (2.12)) by adding terms to the k-ε turbulence model. By these terms there is only kinetic turbulent energy added to the upper part of the water column equal to half the wave height and to the lower part of the water column, equal to the wave boundary layer (see figure 2.10 for a schematisation of the changes in kinetic turbulent energy production). The energy dissipation due to wave breaking depends on the fraction of breaking waves ($D_w \sim -Q_b$), the wave height ($D_w \sim -H^2$) and the wave period ($D_w \sim -1/T$).

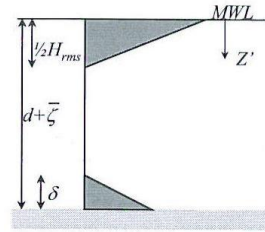


Figure 2-10: changes in kinetic energy production due to waves

The energy dissipation is coupled to the production of energy. The eddy diffusivity results from the kinetic energy production k and the energy dissipation ε (see equation (2.12)). It is difficult to say what the result will be for the sediment transport and morphological processes.

Combined flow-wave bed shear stress

Bed shear stress and flow velocity (near the bottom) are related to each other. The Chezy equation is a good example of a relationship between bed shear stress and flow velocity near the bottom. Waves generate also a velocity near the bottom, influencing the bed shear stress. This velocity is called the orbital velocity. At the bottom this velocity is equal to:

$$u_{orb} = \frac{\omega a}{\sinh kh} \tag{2.23}$$

In box 2.1 the used parameters are explained.

The orbital velocity results in a bed shear stress, depending on the friction factor f_w :

$$\tau_w = \frac{1}{2} \rho f_w u_{orb}^2 \sin^2(\omega t) \tag{2.24}$$

with a maximum bed shear stress of

$$\tau_{w,max} = \frac{1}{2} \rho f_w u_{orb}^2 \tag{2.25}$$

The combined bed shear stress of waves and currents is not just a simple sum of equation (2.7) and (2.24). Soulsby et al (1993) carried out a research to the bed shear stress due to combined waves and currents. The idea on the combination of waves and currents to find a bed shear stress is shown in figure 2.11.

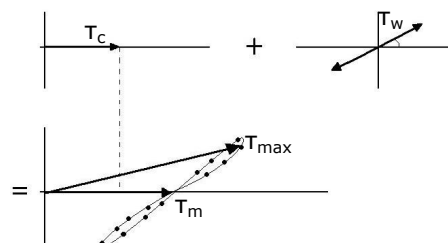


Figure 2-11: Schematic view of non-linear interaction of wave and current related bed shear stresses (after Soulsby et al (1993))

The bed shear stress for combined waves and currents τ_m and the maximum bed shear stress for combined waves and currents τ_{\max} can be calculated with a number of methods. More information can be found in the Delft3D FLOW manual. For now it is sufficient to know that the shear stress due to combined waves and currents is not just a simple sum of the individual bed shear stresses.

Masselink et al (2006)

In their analysis of hydrodynamics and sediment transport processes, Masselink et al (2006) distinguish four groups of processes: shoaling, wave breaking, bores and swash. Shoaling waves can be found seaward of the surf zone and are characterized by larger on-shore than off-shore wave orbital velocity. This results in a net cross-shore sediment transport directed onshore, with increasing sediment transport rate towards the breaking point. The net transport of breaking waves is difficult to determine. Masselink et al (2006) state that cross-shore sediment transport under the breakers is determined by the relative contributions of onshore-directed transport due to wave skewness (larger onshore than offshore orbital velocity), and offshore-directed transport by the bed return flow. Generally this will lead to onshore sediment transport under calm wave conditions and offshore sediment transport under storm conditions. Streaming, Stokes drift and flow acceleration are important when breakers develop into bores. The net sediment transport direction is difficult to determine. See also the description of the individual processes above. Swash motion of waves is very complex and difficult to describe. Generally it promotes net onshore sediment transport (Masselink et al, 2006).

2.3.3 Effects of waves on sediment transport and morphology

The interactions between flow and waves are described in the paragraph above. In the Delft3D Wave module the most important wave parameters which need to be specified are wave height and wave period. Using the processes described above it is possible to describe what the effect will be on sediment transport when wave height is increasing and/or wave period is increasing. It is however difficult what the net effect will be on sediment transport and also in which direction the sediment transport will take place, because of the opposing processes. To increase insight in the morphodynamic processes due to waves, some model calculations are executed and analysed (see appendix C). The general conclusions are that high waves with short wave periods bring sediments to the coast and short waves with long periods transport sediments towards the sea.

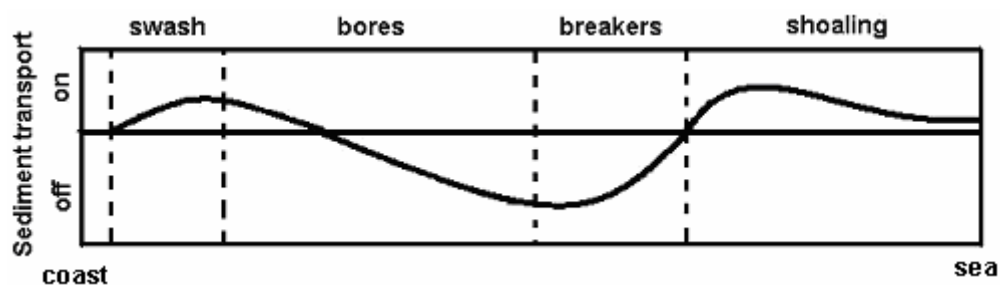


Figure 2-12: cross-shore sediment transport dynamics due to waves (after Masselink et al (2006))

Masselink et al (2006) give a description of the amount and direction of sediment transport due to shoaling, breaking, bores and swash motion of waves. Figure 2.12 summarises their view on sediment transport dynamics (both suspended and bed load transport) under normal wave conditions. Under storm conditions it is expected that the sediment transport is offshore directed throughout the surf zone. It should be kept in mind that this is a snapshot of the sediment transport dynamics. This pattern is travelling up and down the coastal profile with the tidal water level variation. What the resulting tide averaged transport dynamics will be is difficult to say. The conceptual model of Masselink et al (2006) can be used as a validation criterion for the direction of sediment transport under a certain forcing mechanism (e.g. shoaling, breaking etc.)

There is a difference in sediment transport dynamics between cohesive and non-cohesive sediment. The main differences are:

- no bed load transport for cohesive sediments
- lower settling velocities for cohesive sediments.
- Consolidation of the cohesive sediments

Because of the low settling velocities settling lag effects become important (see Van Straaten en Kuenen, (1958) for more information about ‘settling lag’ and ‘scour lag’ effects of cohesive sediments). Figure 2.12 is valid for sandy (non-cohesive) coastlines. For mud (cohesive) coastlines Shi and Chen (1996) propose a conceptual model for cross-shore sediment dynamics, under weak waves and storm conditions (see figure 2.13). The picture represents tide averaged sediment dynamics.

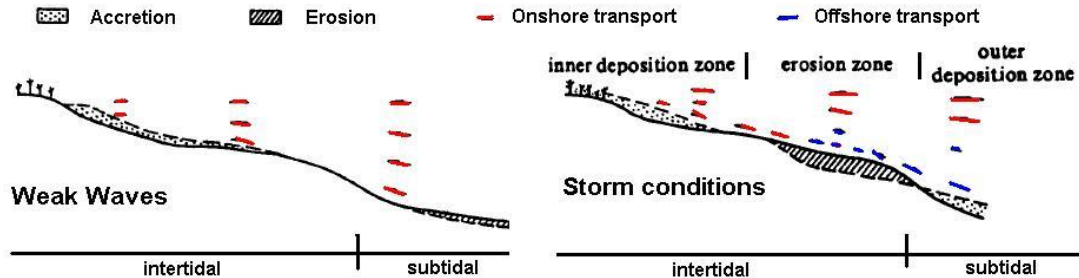


Figure 2-13: cross-shore sediment transport dynamics for cohesive sediments

2.3.4 Waves and vegetation

Until now the influence of vegetation on waves is not discussed. The situation for submerged vegetation is shown in figure 2.14.

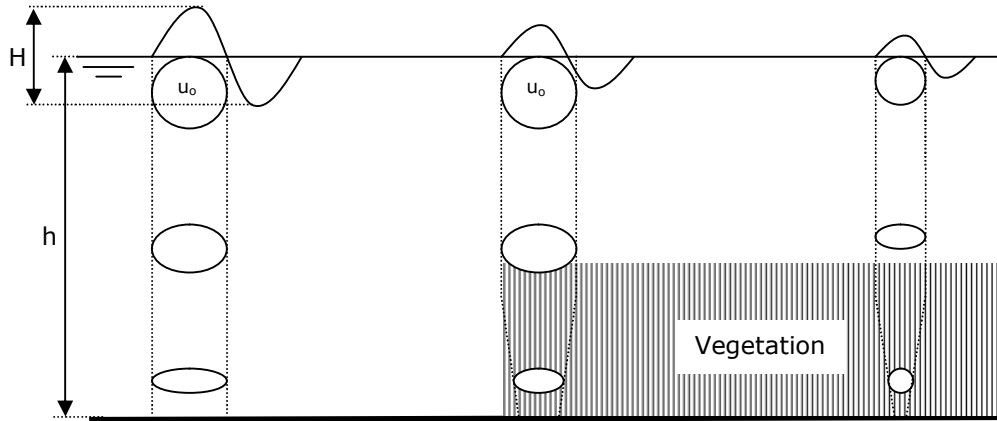


Figure 2-14: waves propagating over vegetation

In shallow water the maximum orbital velocity is constant over the depth. The orbital movement however changes and becomes more flat. When a wave propagates over vegetation, the orbital movement inside the vegetation field is hindered and will be reduced. As a result of this friction effect, energy is dissipated and wave height decreases. This process is called wave attenuation over vegetation

There can be done some calculations to assess the change in wave height over vegetation (see De Vries and Roelvink (2004)). Vegetation can be seen as an extra (bottom)friction component which causes energy dissipation. Due to this dissipation wave height will decrease. Collins (1972) formulated the following expression for wave energy dissipation S :

$$S(\omega, \theta) = -C_{bottom} \frac{\omega^2}{g^2 \sinh^2(kh)} E(\omega, \theta) \quad (2.26)$$

with:

- S = wave dissipation
- ω = wave frequency ($2\pi/T$)
- θ = propagation direction of the wave
- C_{bottom} = bottom friction coefficient
- k = wave number
- h = water depth
- E = total wave energy

Collins related the bottom friction coefficient C_{bottom} to the orbital velocity of waves U_{orb} and a Collins friction factor c_f :

$$C_{bottom} = c_f g U_{orb} \quad (2.27)$$

After filling in the expressions for the wave energy and the wave orbital velocity the following relation for wave energy dissipation S can be obtained:

$$S = -\frac{1}{2}c_f\rho U_{orb}^3 \quad (2.28)$$

De Vries and Roelvink (2004) have shown that it is possible to replace the Collins friction factor c_f with a vegetation factor c_v . The vegetation factor is expressed in terms of vegetation characteristics:

$$c_v = f_w D n dz \quad (2.29)$$

Where f_w is a friction factor, D the diameter of the stems, n the number of stems per square meter and dz the vegetation height

From the equations described above vegetation has only influence on the wave height. When vegetation is added, wave height will decrease, meaning: less orbital velocity, less sediment in the water column and less sediment transport, considering waves. Waves are interacting with the flow and flow changes as well when it enters a vegetation field. What the sum of effects will be on sediment transport is difficult to say. Analysis should explore this relationship.

It remains the question if the decrease in wave height will be the same as the decrease in orbital velocity at the bottom, which is important for the sediment transport. Normally the orbital velocity at the bottom is linear related to the wave height. By submerged vegetation however, the orbital velocity at the bottom is more hindered by the vegetation than the wave height. The decrease in orbital velocity at the bottom could therefore be more than the decrease in wave height. There is however not any research carried out on the relationship between orbital velocity and vegetation. The vegetation should be modelled with the above standing relationships.

2.4 Conclusion: modelling morphodynamics

This chapter presented the basic processes for modelling sediment transport in and around mangrove forests. The resulting morphodynamics is often a balance between opposing processes and it is difficult to say on forehand what it will look like for a mangrove coastline under certain conditions. Modelling is a useful tool to investigate the balance between processes.

Sediment transport under tidal flows (long shore transport) is relatively well understood and described in Delft3D. Interaction between flow and vegetation, when vegetation is modelled as randomly arranged rigid vertical cylinders with homogeneous properties, can also be modelled well with the Delft3D model, according to appendix B. The influence of vegetation on sediment transport under tidal flow conditions will probably lead to good and reliable results.

Waves also play a role in sediment transport processes on coastlines and in most cases waves cannot be neglected. Sediment transport processes under waves are not very well understood. The Delft3D model incorporates five different processes into the hydrodynamic equations, which can lead to sediment transport and morphological changes. Sediment transport due to wave breaking, bores and swash motion (see Masselink et al (2006)), cannot be modelled well with Delft3D, but might be important for sediment transport processes. From Van de Graaf (2003) can be added that the influence of waves on the sediment concentration during a wave period is still not known. Waves are responsible for cross-shore sediment dynamics. Van Rijn (1998) state that profile development of the surf zone cannot be modelled well because of the complexity of processes as wave asymmetry, streaming and wave breaking. Especially at low water depths, where these processes occur, difficulties arise. So, even the processes that are taken into account can be modelled unreliable.

The hypothesis, stated at the beginning of this chapter, was that the interactions between mangroves and water movements can be modelled well with Delft3D. For currents this might be correct, but for waves the hypothesis should be rejected. Rejecting the hypothesis for waves does not mean that it is impossible to model morphodynamic changes due to waves. However, when taking waves into account in the modelling experiment the results should be thoroughly checked and validated with reality.

3 Mangrove forests quantified

In chapter 2 the basic processes and parameters of morphological changes, sediment transport, flow velocity, turbulence and wave development in and around mangrove forests are described. Knowing these processes is the first step in starting a modelling experiment: it helps in analysing the model results. The second step is quantifying processes and parameters as boundary conditions and validation criteria for the modelling experiment. This chapter tries to summarise what other literature has reported about the basic processes and parameters. Research question 2 is shaping the summary:

What is known about coastal morphology, tidal water levels, tidal currents, waves, and sediments in and around mangrove forest, and vegetation characteristics to parameterize mangrove trees?

This question can be divided into the following sub questions:

- a. What is a characteristic bathymetry in and around fringe and overwash mangroves, needed as a boundary condition for the model? (§ 3.1)
- b. What tidal ranges are reported from mangrove coastlines? (§ 3.2)
- c. How large are the tidal currents observed in mangrove forests? (§ 3.2)
- d. Which wave heights are reported on mangrove coastlines? (§ 3.3)
- e. What is the wave attenuation inside mangrove forests? (§ 3.3)
- f. Which sediment properties can be found (and are reported) in and around mangrove forests? (§ 3.4.1 and § 3.4.2)
- g. What is the sedimentation or erosion rate in a mangrove forest? (§ 3.4.3)
- h. What are vegetation characteristics of mangrove trees (height, density and diameter of individual stems), needed to model the trees with Delft3D? (§ 3.5)

The conclusion will review the main research question, by summarizing the results of the sub questions.

NB: The summary of the literature presented in this chapter is derived from Dekker (2005). For more information about each site you are directed to this literature study.

3.1 Bathymetry

In the introduction the research is confined to two types of mangrove forests: overwash and fringe. These types have their own characteristic bathymetry, which should be implemented in the Delft3D model. First the bathymetry of fringe type forests will be described and second the overwash type forest.

3.1.1 Fringe type forests

In figure 3.1 a picture of a fringe type forest, together with a cross-section of a typical fringe type forest is shown. Characteristic for this type of mangrove forest is that it consists of a forest part and a mudflat part in front of the forest. The mudflat and the forest have a different bed level gradient. In table 3.1 an overview is presented for the gradients of the mudflat and the mangrove parts.

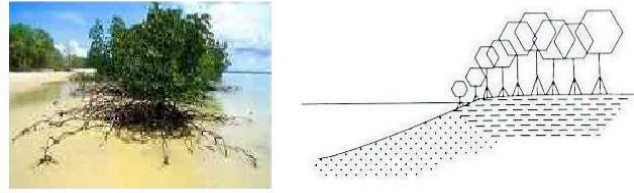


Figure 3-1: picture and cross-section of a fringe type forest

Table 3-1: gradient of fringe mangrove shorelines of the mudflat and the mangrove part

Author	part	gradient
Mazda et al (1997)	mangrove	1/1000
Quartel (2000)	mudflat	1/200
Massel et al (1999)	mangrove	1/150 and 1/50
Bird (1986)	mangrove	1/50
Bird (1986)	mudflat	1/200 and 1/1000
Falconer and Struve (2001)	mangrove	3/1000
Furukawa et al (1997)	mangrove	1/2000
De Vos (2004)	mangrove	1/300 to 1/500
De Vos (2004)	mudflat	1/1000

It can be concluded that the average gradient in mangrove forest is about 1/500 and the average gradient of a mudflat in front of the mangrove forest is 1/200. However, drawing general conclusions on the data presented in table 3.1 should be done with care. The places where these gradients are observed differ much from each other in various aspects. Therefore the data should only be used to get some feeling with the gradients occurring in and around mangrove forest. The conclusion stated above is not meant as ‘the truth’ but has more practical consideration that the model just needs a bathymetry for its calculations.

3.1.2 Overwash type forests

Figure 3.2 shows a picture and a cross section of an overwash type forest. Overwash forest have a uniform bathymetry, slightly above mean sea level (Lugo and Snedaker, 1974). This is enough information to construct a bathymetry of overwash type mangroves.

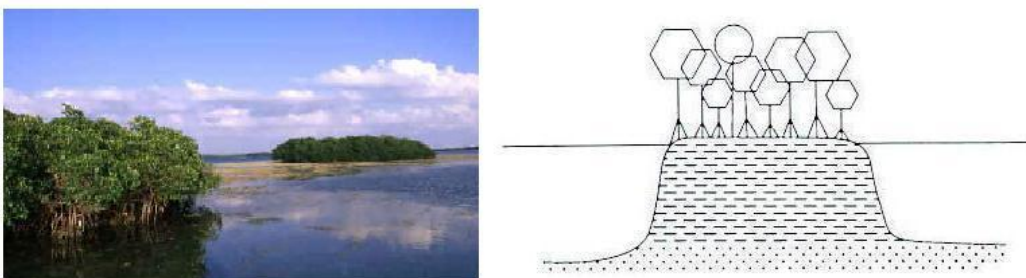


Figure 3-2: picture and cross-section of an overwash type mangrove forest

3.2 Tidal range and currents

Besides the bathymetry, the tidal range is also a boundary condition for modelling. A number of mangrove studies report about tidal ranges in the research area. In table 3.2 just a view tidal ranges in mangrove areas are mentioned. A tidal range of 2 m seems justifiable, considering the information presented in table 3.2

Table 3-2: overview of tidal ranges for different mangrove shores

Author	Location	Tidal Range
Anthony (2004)	Sherbro Bay, West Africa	1.3 – 2 m
Walsh and Nittrouer (2004)	Gulf of Papua, Indonesia	2.4 – 2.8 m
Bird (1986)	Westernport Bay, Australia	2 m
Bryce et al (2003)	Cocoa Creek Australia	2 – 3 m
Mazda et al (1997)	Tong King delta, Vietnam	± 2 m
Winterwerp et al (2005)	Bang Khun Thien, Thailand	1.5 – 2.5 m

To check modelling results tidal currents in mangrove forests can be useful. Table 3.3 presents some tidal currents found in three different researches. The currents are in the order of cm/s.

Table 3-3: summary of tidal currents in mangrove forests

Author	Location	Tidal current (cm/s)
Wolanski et al (1992)	Iriomote Island, Japan	1.2
Furukawa et al (1997)	Middle Creek, Cairns, Australia	7 – 10
Wu et al (2001)	Modelling experiment	± 5

3.3 Wave height and attenuation

Most mangrove shorelines do not receive high waves. The researches found in the survey, reported wave heights smaller than 0.20 m. Table 3.4 gives a short overview. These wave heights are important boundary conditions for modelling mangrove coasts. Considering the values of table 3.4, 15 cm significant wave height forms a good starting point.

Table 3-4: significant wave heights around mangrove forests

Author	Location	Wave height (m)
Mazda et al (1997)	Tong King delta, Vietnam	0.20
Quartel (2000)	Do Son, Red River Delta, Vietnam	0.10 - 0.20
Anthony (2004)	Sherbro Bay, West Africa	< 0.20

Wave attenuation in mangrove forest is an important but complex process of the interaction between mangroves and waves. It is important because of safety reasons, as proved by the tsunami attack of 26th of December 2004 (see Dahdouh-Guebas (2005)). A common way to express the reduction of wave height in mangrove forests is the reduction factor r , defined as:

$$r = \frac{H_s - H_t}{H_s} \quad (3.1)$$

Where r is the wave attenuation per 100 m forest, H_s the wave height of incoming waves and H_1 the wave height after 100 m forest

In table 3.5 several wave reduction factors for different locations are given. The wave reduction factor can be used in calibrating the Delft3D Wave model.

Table 3-5: summary of the wave reduction r

Author	Location	r (per 100 m)
Mazda et al (1997)	Thy Hai, Vietnam	0.05 – 0.20
Quartel (2000)	Do Son, Vietnam	0.5 – 1.1
Massel et al. (1999)	Cocoa Creek, Australia and Iriomote Island, Japan	0.375
Schiereck and Booij (1995)	modelling experiment	0.3 – 0.5

From these findings can be concluded that a mangrove system reduces a wave at least 5% and at most around 100% per 100 m forest. This depends on the mangrove tree itself (type and age) and on the hydraulic conditions (water level and wave height). The results from Quartel (2000) however, seem to be an overestimation of the situation, compared to the other results. A maximum of about 50% per 100 m forest seems more justifiable.

3.4 Sediment transport and morphology

For modelling sediment transport and morphology, there are two important parameters: sediment concentration and sediment grain sizes. An important process is sedimentation. This paragraph will treat these three subjects subsequently.

3.4.1 Sediment concentration

Three researches are found who reported on sediment concentrations near or inside mangrove forests. They are summarised in table 3.6. The values differ a lot from each other and it is not useful to determine the average sediment concentration and use it in modelling. They should be used as a direction for the modelling input.

Table 3-6: suspended sediment concentration (SSC) around mangrove forests for three different locations

Author	Location	SSC (mg/l)
Furukawa et al (1997)	Middle Creek, Cairns, Australia	150
Victor et al (2005)	Pohnpei Island, Micronesia	80
Bryce et al (2003)	Cocoa Creek, Townsville, Australia	400

3.4.2 Grain size distribution

The only good grain size distribution in and around mangrove forest that could be found, is reported by Giana et al (1996). They carried out a research in the Balandra Lagoon, Gulf of California, Mexico. In their research they connect grain size distribution to different tree species (see appendix A for more information). In figure 3.3 their result is presented. It can be seen that on places with no vegetation the grain size distribution shows a peak around 63-20 μm . In mangroves grain sizes are more evenly distributed in the size range of

20 – 200 μm . Another aspect that can be noticed is that under mangroves bigger sediment particles can be found than on a bed with no vegetation.

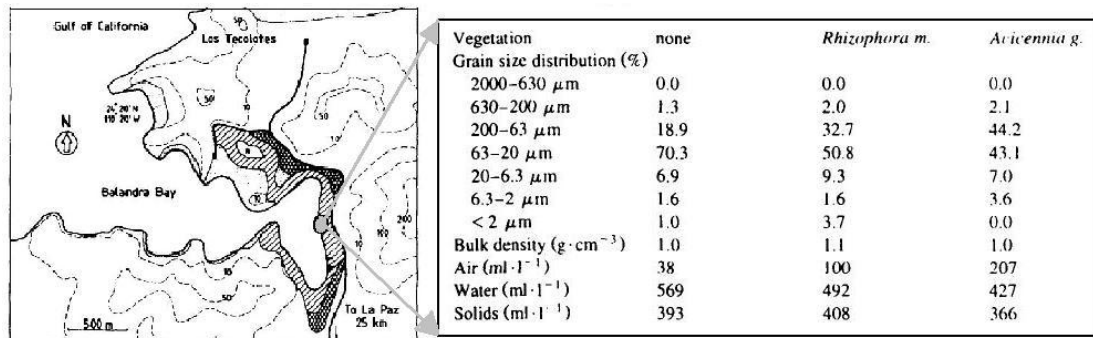


Figure 3-3: Grain size distribution in a mangrove forest in Balandra Bay

3.4.3 Sediment accretion

There are much more reports on sediment accretion in mangrove forests. In table 3.7 an overview is presented. The order of magnitude of sediment accretion in mangrove forests is mm/yr, which is very small. It would be hard to model this kind of accretion. However, on the long run, this small amount of sedimentation can have big effects.

Table 3-7: sediment accretion in mangrove forests (after Ellison (1998))

Author	Location	Rate (mm/yr)
Spencely, 1977, 1982	Magnetic Island	-11 to 9
Furukawa et al., 1997	Cairns, Australia	1.0
Bird and Barson, 1977	Cairns, Australia	3.0 to 10
Bird and Barson, 1977	Melbourne	8.0
Chapman and Ronaldson, 1958	Auckland, NZ	1.7
Lynch et al., 1989	Florida	1.4 to 1.7
Cahoon and Lynch, 1997	Florida	0.6 to 3.7
Lynch et al., 1989	Mexico (Fluvial)	3.2 to 4.4
Lynch et al., 1989	Mexico (Tidal)	1.0 to 2.0
Kraus et al (2003)	Enipoas River Basin, Micronesia	7.2 – 11
Bird (1986)	Westernport Bay, Australia	1.0 – 8.0
Anthony (2004)	Sherbro Bay, West Africa	2.0 – 6.5
Walsh and Nittrouer (2004)	Gulf of Papua, Indonesia	10 – 30

3.5 Vegetation

From Baptist (2005) is known that it is common to model vegetation as a group of parallel, staggered or randomly arranged rigid vertical cylinders with homogeneous properties. De Vries and Roelvink (2004) also use the idea of cylinders with a certain height, density and diameter to calculate a friction factor for wave attenuation (see chapter 2). A schematisation of Burger (2005), who uses this type of schematising a mangrove tree, is given figure 3.4.

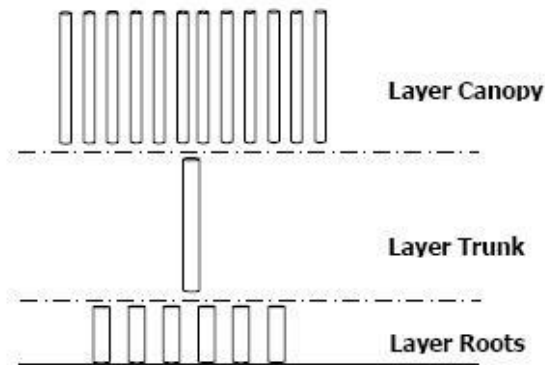
**Reality****Model**

Figure 3-4: schematisation of a mangrove tree

Kraus et al (2003) carried out a research on the relationship between sediment accretion and root system (stilt roots, pneumatophores and knee roots). In three different rivers basins in Micronesia they measured the number of roots per m² and the root diameter. Based on their findings a mean number of roots per m² and a mean root diameter per root type can be calculated. The result is shown in table 3.8. With this information the ‘layer roots’ (see figure 3.4) can be quantified. For the other layers estimations should be used, based on common sense. For wave calculations the friction factor is based on the layer roots.

Table 3-8: number of roots and root diameter for different root systems

Root type	Number of roots (m-2)	Root diameter (cm)
Stilt root	46	2.7
Pneumatophores	48	2.9
Root knee	74	2.5

3.6 Conclusion

This chapter has quantified as much as possible parameters and processes in and around mangrove forests. Based on the presented information the following general conclusions can be drawn:

- Tidal currents inside mangrove forest are in the order of cm/s
- Wave heights on mangrove coastlines are low (< 20 cm)
- There are high sediment concentration in and around mangrove forests (max 400 mg/l)
- Grain sizes inside mangrove forests are low (between 20 and 200 μm)
- The order of magnitude for sediment accretion is mm/yr

Table 3.9 shows the range of parameters and processes described in this chapter. It can be seen that the ranges are wide, indicating that it will be difficult to schematize and model a mangrove forest situation that represents all other mangrove forest situations. Chapter 4 and 5 will try to construct a general fringe and overwash mangrove model, using the information and conclusions presented in this chapter.

Table 3-9: ranges of important parameters and processes

process or parameter	unit	range
Gradient mangroves	-	1/50 – 1/2000
Gradient mudflat	-	1/200 – 3/1000
Tidal range	m	1.3 – 3
Tidal current	cm/s	1.2 – 10
Wave height	m	0.10 – 0.20
Wave attenuation	r	0.05 – 1.1
Sediment concentration	mg/l	80 – 400
Sediment grain sizes	µm	20 – 200
Sediment accretion	mm/yr	-11 – 30

4 Fringe mangroves

Now the basic processes are described, qualitatively (chapter 2) and quantitatively (chapter 3), it is time to carry out the modelling experiment. This research is confined to two mangrove forest types: fringe mangroves and overwash mangroves. Both forest types will be modelled in a modelling experiment in order to increase insight in the morphodynamics in and around mangrove forests. This chapter will discuss the fringe mangroves. The main research question for this chapter sounds:

How can the fringe mangrove forest be modelled and what conclusions can be drawn considering the influence of mangroves on morphodynamics?

This question should be approached with two steps: 1) constructing a basic model and 2) carrying out a sensitivity analysis in order to increase insight.

For step 1 four sub questions should be answered:

- a. What are the validation criteria?
- b. Which model set-up will be used?
- c. What are the modelling results and how can they be explained?
- d. Are the results reliable?

The last question refers back to the first question. If the answer is yes, than sensitivity analysis (step 2) can be carried out. If no, the model setup should be changed, results should be analysed again and compared with the validation criteria (which will be kept the same throughout the modelling experiment), till the results are reliable enough. If no reliable result can be obtained it should be concluded that the situation cannot be modelled well.

The mangrove shoreline can be very constant over a long distance, meaning no change in long shore currents, therefore constant sediment transport and no change in morphology. Cross-shore currents will be responsible for morphological changes. In chapter 2 became clear that waves are very important in cross-shore beach developments, but also very difficult to model. This chapter will show two different cases:

- Non cohesive sediments (§ 4.1)
- Cohesive sediments (§ 4.2)

It will become clear that fringe mangroves cannot be modelled in a satisfactory way, so a sensitivity analysis is not carried out. The two efforts are closed by a general discussion on the results (§ 4.3), followed by conclusions about the modelling experiment (§ 4.4).

No hydrodynamic validation criteria are presented in this chapter because the hydrodynamic validation is carried out in appendix C. The model results are validated on:

- water levels
- cross-shore flow velocity
- flow velocity profile
- kinetic turbulent energy
- energy dissipation
- wave height development (with shoaling and refraction)
- influence of waves on bed shear stress, kinetic turbulent energy, energy dissipation and eddy diffusivity
- Stokes drift

It is found that the modelling results considering the hydrodynamic forcing, are realistic and reliable.

4.1 Non cohesive sediments

4.1.1 Validation criteria

For the fringe mangrove forest the research of Walsh and Nittrouer (2004), carried out in the Gulf of Papua will be used as a validation. With the results of their research they can make a conceptual model which is given in figure 4.1. The sediment accretion on mudflats is around 4 cm/y and inside mangrove forest around 1 cm/y. The pattern of sediment accretion is the only validation possible for this situation. Tidal currents, wave heights and wave attenuation are not reported in the research. It is also not known what the exact situation is. How does the coastline continues? How long (in cross-shore direction) is the fringe forest? Is the forest located along a channel, or along the open sea? About the sediment characteristics there are also uncertainties like, type of sediment (cohesive or non-cohesive) and other sediment properties (grain size, concentration etc.) Walsh and Nittrouer (2004) only constructed this conceptual model on the basis of measurements. They did not connect the conceptual model to hydrodynamic forcing or sediment characteristics. The question arises whether this conceptual model is useful as a validation criterion. There is however no better validation criterion found for the fringe mangrove situation, therefore this conceptual model is used. These uncertainties should be kept in mind when comparing the modelling results with the validation criteria (see § 4.1.4)

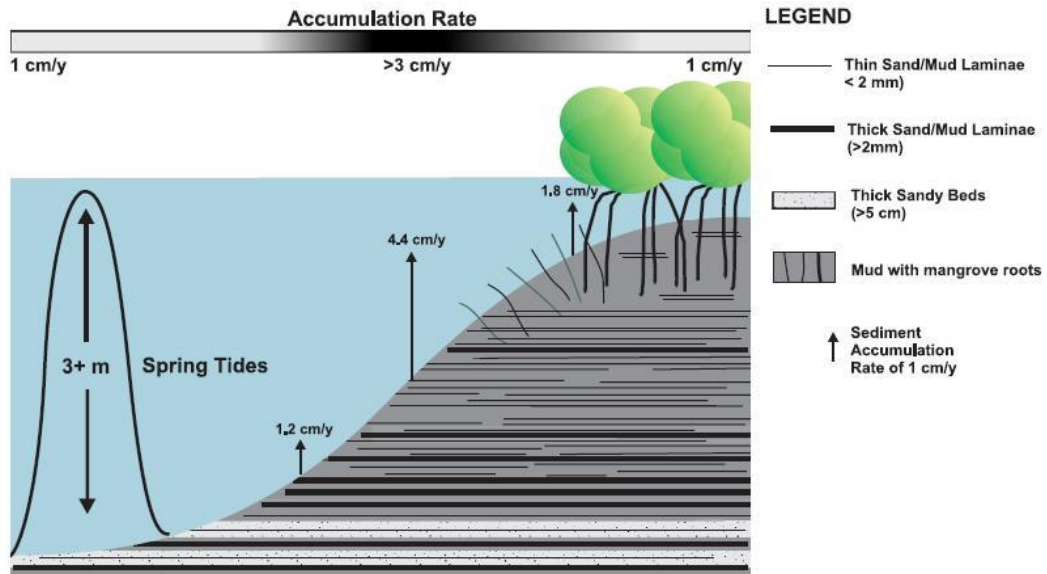


Figure 4-1: conceptual model of sedimentation/erosion, based on measurements in and around mangrove forests in the Gulf of Papua [Walsh and Nittrouer, 2004]

The results can also be validated with the conceptual cross-shore sediment transport model on (non-cohesive) beaches of Masselink (2006). This conceptual model is described in § 2.3.3 and shown here again in figure 4.2. The transport pattern can be validated with that.

The general sediment accretion in mangrove forests, listed in § 3.4.3, can also be seen as a validation criterion. At least there should be some sedimentation inside the mangrove forest.

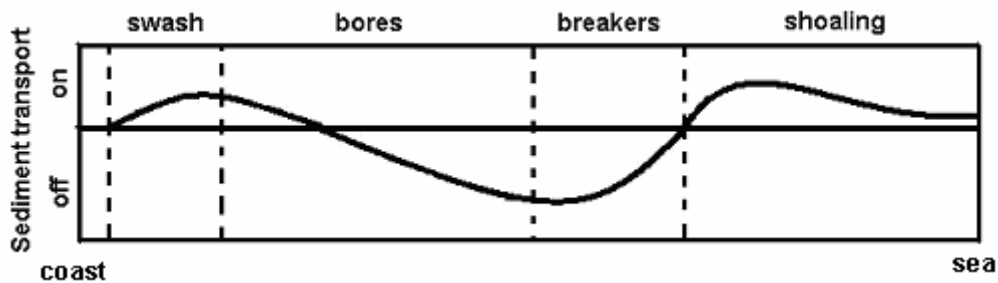


Figure 4-2: cross-shore sediment transport dynamics due to waves (after Masselink et al (2006))

4.1.2 Model setup

Because the validation criteria are based on the conceptual model of Walsh and Nittrouer (2004) the model setup should also be based on the area researched by Walsh and Nittrouer (2004). There is however no useful information about bathymetry, tidal currents, wave height, wave attenuation, sediment type and grain sizes. Therefore the data presented in chapter 3 is used to construct the model. The most uncertainties exist in the bathymetry, the sediment type and the long-shore currents.

Figure 4.3 presents the cross-section modelled and table 4.1 explains figure 4.3. The forest stands above MSL and will increase in density as it goes towards the levee. It is chosen to model the morphological changes during a 12 hr harmonical tide with a tidal range of 2 m. A simple modelling experiment showed a constant behaviour of the sedimentation/erosion pattern after 1 tide.

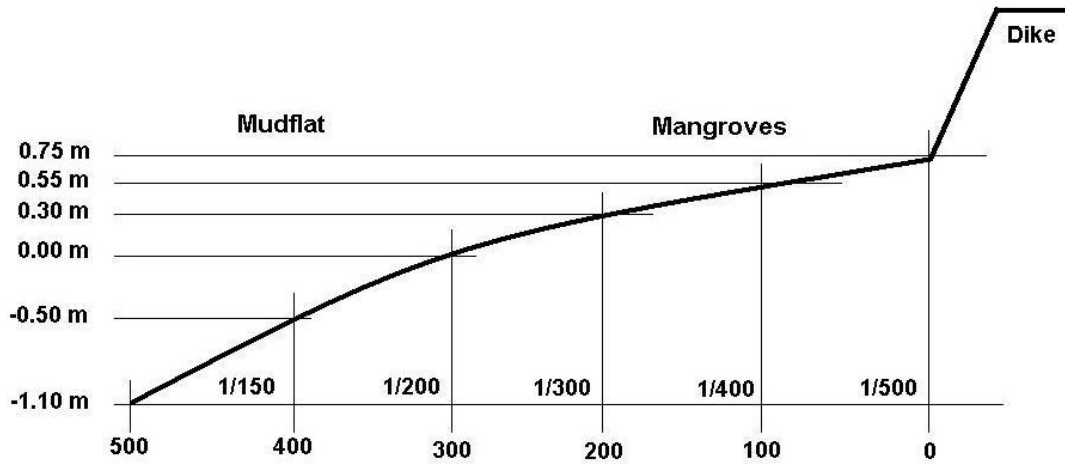


Figure 4-3: a cross-section of the modelled mangrove/mudflat system

Table 4-1: description of the parameters, corresponding to figure 4.2

Location	gradient	height (+MSL)	mangrove forest density
0 – 100 m	1/500	0.75 – 0.55 m	full
100 – 200 m	1/400	0.55 – 0.30 m	decreasing
200 – 300 m	1/300	0.30 – 0 m	decreasing – 0
300 – 400 m	1/200	0 – -0.50 m	none
400 – 500 m	1/150	-0.50 – -1.10 m	none

To get a good view of the water movements in the water column, 16 layers are modelled. The layers are configured in a way that they can take into account the turbulence on the bed and the turbulence generated by the waves in the top of the water column (see figure 4.4). For turbulence the horizontal and vertical eddy viscosity and diffusivity (see chapter 2), will be calculated with the k-epsilon turbulence model. The first calculations are carried out in a 2DV model setting instead of a full 3D. This has two reasons: it saves computation time and it is difficult to specify a 3D coastline, based on chapter 3 and the validation criteria.

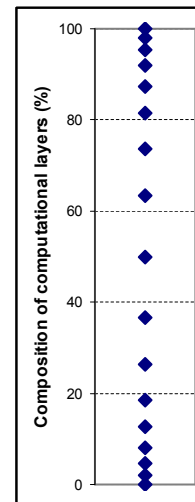


Figure 4-4: distribution of computational layers

It is chosen to take only one sediment type into account. To start, a non-cohesive sediment type is chosen (for cohesive sediments see § 4.2). Chapter 3 shows that grain sizes vary mostly between 20 and 63 µm. The model however is constraint to a minimum grain size diameter of 100 µm (considering non-cohesive sediments). This grain size is used in modelling. The model calculates an equilibrium concentration on the boundary, so there is no need to use a sediment concentration at the boundary.

The roughness will be modelled with a uniform Chezy value of $40 \text{ m}^{1/2}/\text{s}$.

Based on the information presented in chapter 3 waves of 15 cm with a period of 4 seconds are modelled. For waves the vegetation factor c_v should be calibrated. This can be found in appendix D. It is found that the friction factor f_w of 0.69 corresponds well with the data from chapter 3. From this factor a vegetation factor c_v of 0.43 can be calculated, using the root layer of a mangrove tree. The following processes of wave action are taken into account:

- Wave set-up
- Depth induced breaking
- Bottom friction (with a Collins friction factor)
- Refraction
- White-capping

The Delft3D FLOW module will communicate with the WAVE module every 5 minutes, based on careful tuning.

To model mangroves a Rhizophora tree is chosen to represent the typical mangrove tree. It can be schematised with Kraus et al (2003) and Burger (2005) (see also chapter 3). The resulting mangrove tree is presented in figure 4.5. In the schematisation of a forest 200 m is used for the forest to increase from 0 to full density (see also table 4.1).

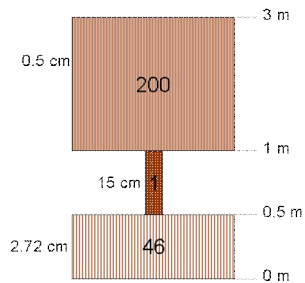


Figure 4-5: vertical composition of a Rhizophora mangrove tree in terms of heights, densities and diameters.

4.1.3 Analysis

From velocities, sediment concentration and sediment transport to bed level changes this fringe type mangrove situation is analysed. In the analysis the parameters for falling and rising tide are often shown. Rising tide represents the situation at 22:00 and falling tide at 14:00. For the modelled water levels see figure 4.6. The water levels at 14:00 and 22:00 are equal (0.5 m +MSL)

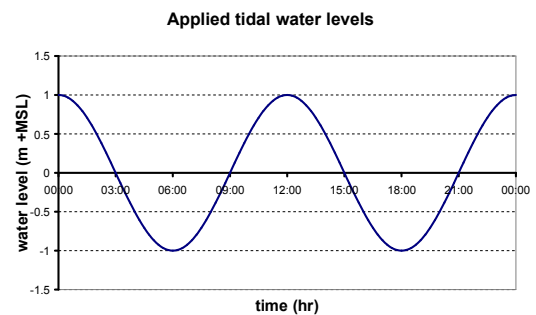


Figure 4-6: waterlevels at the boundary of the model

Velocities

Figure 4.7 shows the velocity during rising and falling tide and the orbital velocity at high tide.

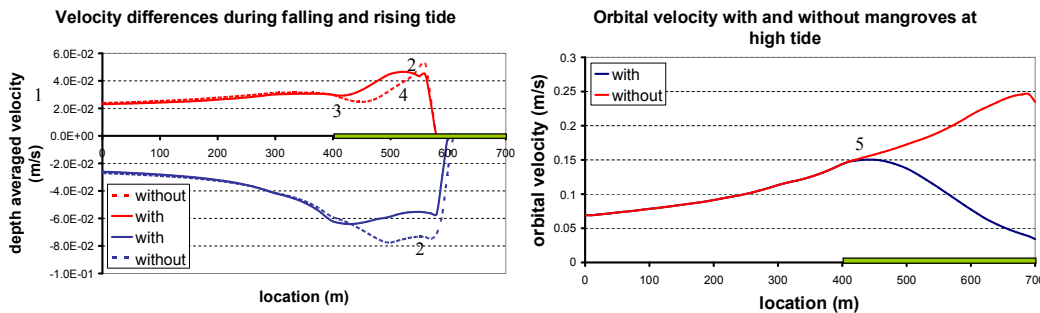


Figure 4-7: velocity differences during falling and rising tide (left) and the orbital velocity during high tide (right). The green bar represents the location of the mangrove forest. A negative velocity is directed off-shore.

The following observations can be made:

1. Cross-shore velocities are very small, in the order of cm/s. Therefore transport of sediment is induced by wave action. The orbital velocities at the bottom are a factor 10 higher.
2. Although the water levels are equal for the falling and the rising tide (see figure 4.6) the velocities are not equal. It can be seen that the off-shore velocities are a little bit higher than the on-shore velocities. A cause for this can be the undertow due to the wave processes Stokes Drift and wave set-up (see chapter 2 for a description). In figure 4.8 the velocity in the water column is presented, during rising tide. Because of the rising tide the velocity should be directed onshore. This is not the case and even the depth averaged velocity is directed offshore. The influence of the wave processes on the velocity in the water column gets very clear in this way. It is however questionable that the wave action is as strong as presented in figure 4.7.
3. The differences in velocity for the situation with and without mangroves start at the beginning of the mangrove forest. For the rising situation the mangrove forest leads to an increase in the depth averaged flow velocity, because the cross-sectional area decreases due to the mangroves. It increase to a certain maximum, depending on the bed level gradient and water level gradient (see Baptist, 2005). It can also be that the undertow reduces, because wave height reduces. This can lead to less off-shore flow and higher depth averaged flow velocity. For the falling tide the velocity with mangrove forest is lower than the velocity without mangroves. The velocity inside the forest increases a little when it goes towards the end of the forest. The lower value of the velocity can be attributed to the fact that the water cannot flow freely through the forest. It is 'blocked' by the trees and therefore it flows slower out of the

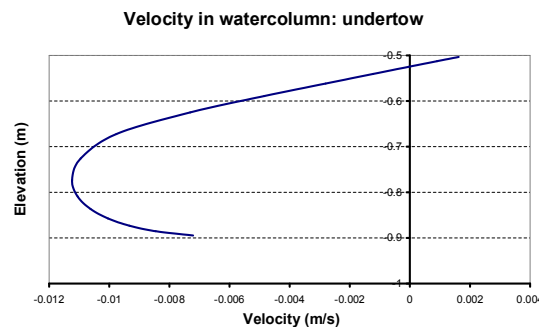


Figure 4-8: velocity in the water column at rising tide (outside the mangrove forest). A negative velocity is directed off shore

- forest. There is also the reduced effect of undertow inside the mangrove forest, leading to lower off-shore flow velocities during the falling tide.
4. The shape in the velocity development without mangrove forests corresponds with the wave set up and wave set down processes. Wave set down occurs just before the breaker zone and leads to more undertow (directed offshore). Wave set up (in the breaker zone) is responsible for the increase in depth averaged velocity.
 5. The development of the orbital velocity at high tide reflects in a very good way the wave attenuation by mangroves. The difference between with and without mangroves is very clear.

Sediment concentration

The sediment concentration in the bottom layer for rising and falling tide is shown in figure 4.9. The differences start, just as the differences in cross shore velocities, at the beginning of the forest. For situations without mangrove forest the concentration is much higher. This can probably be attributed to the wave attenuation of the mangrove forest. Waves are responsible for turbulence, resulting in high sediment concentrations.

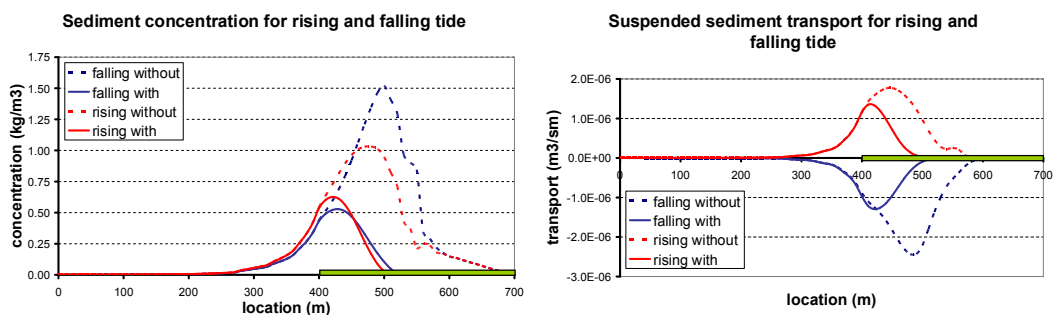


Figure 4-9: sediment concentration in the bottom layer (left) and depth averaged suspended sediment transport (right) for rising and falling tide, with and without mangroves. The green bar represents the location of mangroves.

Where the sediment concentration for the situation without mangrove forests is higher for the falling tide, the sediment concentration for the rising tide is higher for the situation with mangroves. The differences between falling and rising tide concentrations for mangrove forests are however small. The values of the concentration of sediment are very high comparing to the values found in literature (see chapter 3). Although the waves are small they have a very big influence on the sediment concentration in the water column. It is questionable if such small waves can have such big influences on the sediment concentration.

Sediment transport

The depth averaged suspended sediment transport during falling and rising tide is presented in figure 4.9. It can be seen as a combination between sediment concentration and velocity (figure 4.6). From the tide averaged sediment dynamics the morphological changes during 1 tide can be described. Figure 4.10 shows the tide averaged sediment dynamics for depth averaged suspended and bed load transport. The mangrove forest is again responsible for the differences in tide averaged transport. An important aspect is that tide averaged bed load transport is 2 orders of magnitude higher than depth averaged suspended transport. Bed load transport determines therefore the morphological changes. Although the effects of undertow can be seen quite well in mean depth averaged suspended sediment transport pattern (which indicates that this process is modelled well, see also chapter 2), it is completely ruled out by

the bed load transport. Streaming is the only process in this case which causes bed load sediment transport, so streaming is the driving process behind morphological changes.

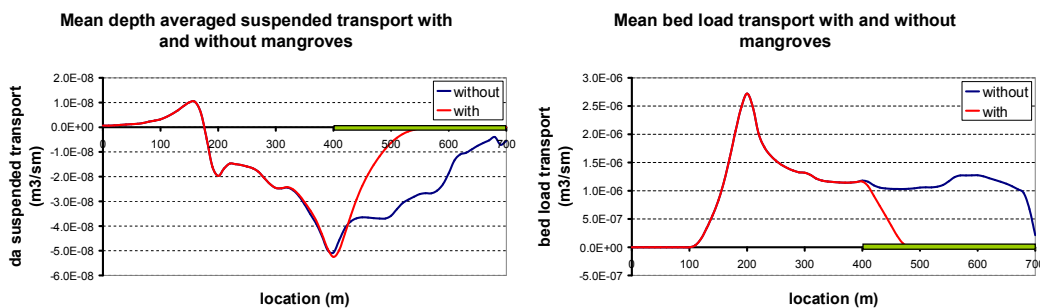


Figure 4-10: mean depth averaged suspended transport and mean bed load transport with and without mangroves

Morphological changes

From the bed load transport the morphological changes can be described. it can be seen in figure 4.10 that there is:

- erosion between 100 and 200 m,
- sedimentation between 200 and 300 m,
- constant bed between 300 and 400 m or 300 and 650 m (depending on the mangrove forest)
- sedimentation between 400 and 500 m (with mangroves) or 650 and 700 m (without mangroves).

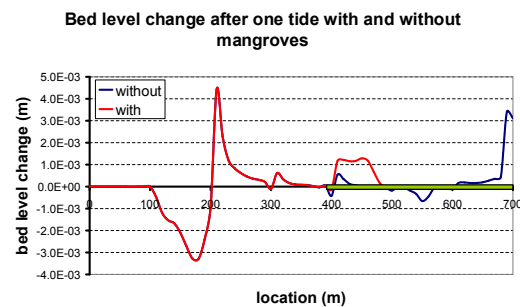


Figure 4-11 sedimentation/erosion pattern after 1 tide, with and without mangroves. The green bar represents the location of mangroves

This pattern is confirmed by figure 4.11, which shows the sedimentation/erosion pattern with and without mangroves. Although the pattern can be explained from the mean bed load transport pattern, the erosion and sedimentation peak around the low water level (200 m) is strange. This is the result from a relatively long wave action because of the turning of the tide. However, such beach development is never observed and the validation criteria also show another development. The pattern is also not a consequence of initial beach development. Some long-term model calculations are carried out (not shown here), in which could be seen that the sedimentation/erosion pattern did not change much.

The influence of mangroves can be seen very well. Sedimentation will take place at the beginning of the mangrove forest, while there would not be any sedimentation if there were no mangroves. Sediment would be transported to the levee. It is however not right to say (on basis of this modelling experiment) that mangroves are trapping the sediment, because sediment transport is mainly directed onshore. In this system sedimentation will always be transported towards the shore, because streaming is the driving process behind morphological changes.

4.1.4 Conclusion

The validation criteria are set in § 4.1.1. For the morphodynamic pattern the conceptual model of Walsh and Nittrouer (2004) is used. The sediment transport pattern can be validated with the conceptual model for sediment transport dynamics of Masselink et al (2006). The last validation criterion is the generally observed sediment accretion inside mangrove forests. For the hydrodynamic validation see appendix C.

Walsh and Nittrouer (2004)

Although the modelling results can be largely explained it should be concluded that the resulting morphological changes do not reflect the morphological changes (looking only to the pattern) of the conceptual model of Walsh and Nittrouer (2004). The modelling results show huge differences comparing to the conceptual model, with the high sedimentation/erosion peak around low water level as the most striking difference.

That the modelling results do not reflect the observed morphological changes of Walsh and Nittrouer (2004) does not mean that the modelling results are unreliable. There are so many things unclear in the situation of the conceptual model that it is not strange that the resulting morphological patterns are not comparable. See § 4.1.1 for the uncertainties concerning the conceptual model.

The resulting erosion/sedimentation peak around low water level is not very realistic. Long term modelling (not shown here) resulted in the same sedimentation/erosion peak, so it is not a case of unstable modelling results. Adding a long shore current or changing the bathymetry (see appendix E) generated the same morphological result. Because of the persisting sedimentation/erosion peak around low water level the modelling results are less reliable. It seems that some processes are not well taken into account in the model.

Masselink et al (2006)

The resulting sediment transport in the model is only driven by bed load transport due to waves (streaming). Streaming is always onshore directed, so the sediment transport pattern calculated by the model is realistic. However, the streaming effect dominates other transport processes under waves like transport due to shoaling or breakers, which also should occur on a sandy beach, according to Masselink et al (2006). This dominated of transport does not seem very realistic, making the modelling results less reliable. The sediment transport due to waves is probably not very well taken into account in the Delft3D model.

Sediment accretion inside the forest

The influence of mangroves however, can be seen very clearly in all the processes: it reduces the flow and the orbital velocity, it reduces the sediment transport and it leads to sedimentation at the beginning of the forest. This reflects the generally observed sediment accretion presented in § 3.4.3.

Conclusion

The hydrodynamic validation (appendix C) was successful and generated realistic and reliable results. The morphodynamic validation presented and analysed in this chapter was not successful because the modelling results did not reflect the validation criteria. The problem seems the overestimation of bed load transport due to waves.

4.2 Cohesive sediments

From the previous paragraph could be concluded that the sedimentation/erosion pattern of the fringe mangrove forest is not modelled well in with this model set up. Long shore currents or another profile did not generate better results. The resulting sedimentation/erosion pattern of cohesive sediments is totally different and will be analysed in this paragraph. This paragraph will follow the four steps identified in the introduction to analyse the cohesive sediment situation.

4.2.1 Validation Criteria

The conceptual model of Walsh and Nittrouer (2004) is also used as validation criteria in this modelling case (see § 4.1.1, watch the remarks made about the model). For the sediment transport pattern the Shi and Chin (1996) conceptual model for weak waves is used, which is presented in figure 4.12. The situation for weak waves should be valid in this case. Sediment concentration can be validated with the data presented in § 3.4.1.

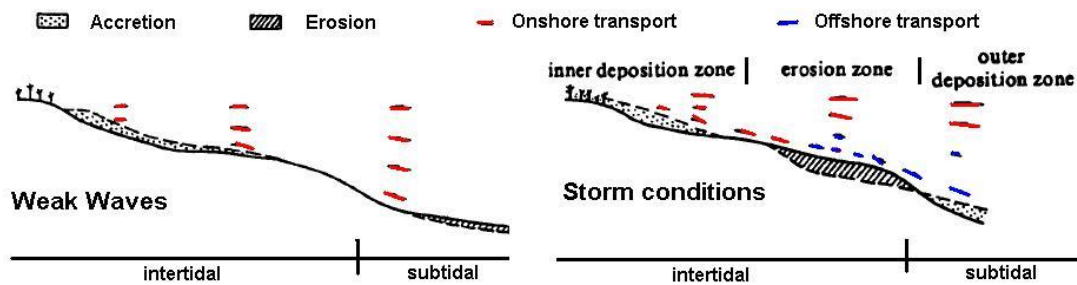


Figure 4-12: cross-shore sediment transport dynamics for cohesive sediments

The general sediment accretion in mangrove forests, listed in § 3.4.3, can also be seen as a validation criterion. At least there should be some sedimentation inside the mangrove forest. With this validation criteria the modelling results can be reviewed.

4.2.2 Model setup

In table 4.2 important sediment parameters and the differences with the previous case are shown. The bathymetry, the bed roughness and the wave parameters are kept the same. With cohesive sediments no equilibrium concentration at the boundary of the model is calculated. This is set to 200 mg/l, based on the data presented in § 3.4.1.

Table 4-2: differences between cohesive and non-cohesive sediments in this modelling experiment

Subject	cohesive	non-cohesive ($d_{50} = 100 \mu\text{m}$)
settling velocity	0.25 mm/s	3.1 mm/s
critical shear stress for erosion (for motion in case of non-cohesive sediments)	0.5 N/m ²	0.2 N/m ²
critical flow velocity	0.29 m/s	0.18 m/s
bed load transport	no	yes

4.2.3 Analysis

Velocities

There is no difference with the basic model considering the hydrodynamic forcing. Flow velocity and orbital velocity during the tide are the same. They can be found in figure 4.7.

Sediment concentration

Figure 4.13 shows the sediment concentration for the rising and the falling tide in the upper and bottom layer of the water column. The influence of mangroves both in the upper and lower layer can be seen very clearly for the falling tide. This can be explained by the less sediment that is picked up by the waves. Waves are attenuated by the forest, as can be seen in figure 4.7. For the rising tide this is different, because the sediment is picked up in front of the mangrove forest and transported towards the forest. Therefore the concentration is high at the beginning of the forest. Differences in concentration will occur from the start of the forest, due to a reduction of the flow velocity and the wave action. Sediment is transported less far, so the concentration decreases more early in the case of mangroves.

The concentration that is set as a boundary condition (0.2 kg/m^3), is lower in the upper layer and higher in the bottom layer. The concentration profile (not shown here) however has an average value of 0.2 kg/m^3 at the sea boundary of the model, so this is modelled well.

Although the critical shear stress and velocity for erosion is higher for the non-cohesive sediments (see table 4.2) the concentration in this case is much higher. The higher concentration can then be attributed to the lower settling velocity. This means that the sediment particles (if they are ‘eroded’) stay longer in the water column, leading to higher concentrations, in comparison with non-cohesive sediments.

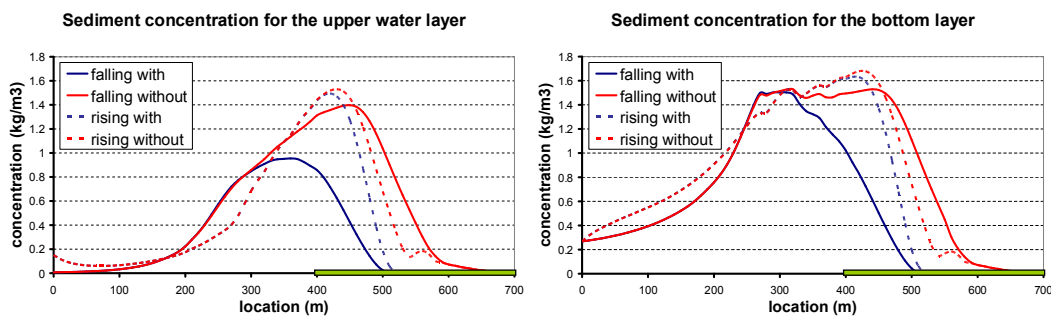


Figure 4-13: sediment concentration for the upper and bottom layer during the rising and the falling tide, with and without mangroves. The green bar represents the location of the forest.

The concentration that is set as a boundary condition (0.2 kg/m^3), is lower in the upper layer and higher in the bottom layer. The concentration profile (not shown here) however has an average value of 0.2 kg/m^3 at the sea boundary of the model, so this is modelled well.

Although the critical shear stress and velocity for erosion is higher for the non-cohesive sediments (see table 4.2) the concentration in this case is much higher. The higher concentration can then be attributed to the lower settling velocity. This means that the sediment particles (if they are ‘eroded’) stay longer in the water column, leading to higher concentrations, in comparison with non-cohesive sediments.

For the bottom layer during the falling tide it looks that the concentration has reached a maximum value, around 1.5 kg/m^3 (see figure 4.10, right picture). For the rising tide the concentration reaches higher values. A possible explanation for this is that all the available sediment is eroded. Therefore the concentration cannot increase any more. The concentration of the rising tide can be a little bit higher, because of the boundary concentration which is set at 0.2 kg/m^3 . This can be observed in figure 4.13, but an analysis of the available sediment (not shown here) showed that there is enough sediment available during the falling tide, to be eroded. In the Delft3D model there is also no maximum sediment concentration used for the calculations. No possible explanation is found for this unusual pattern.

It should also be remarked that the sediment concentration is very high. The highest observed sediment concentration from literature around mangrove forests (see § 3.4.1) is 0.4 kg/m^3 , while the concentrations in this case are exceeding 1.6 kg/m^3 . Waves are responsible for stirring up the sediment. It looks that the wave forces are too high (unless the waves are only 15 cm!) leading to high sediment concentrations. This is an indication of the shortcomings in the understanding of the sediment concentration under waves (see also § 2.4).

Sediment transport

Table 4.2 shows that the settling velocity of cohesive sediment is an order of magnitude smaller than the settling velocity of non-cohesive sediments. The critical shear stress is doubles and no bed load transport takes place. These parameters and the differences between the parameters are all important in explaining the sediment transport for cohesive sediments. Figure 4.14 shows the suspended sediment transport during the tide and the tide averaged version for both with and without mangroves.

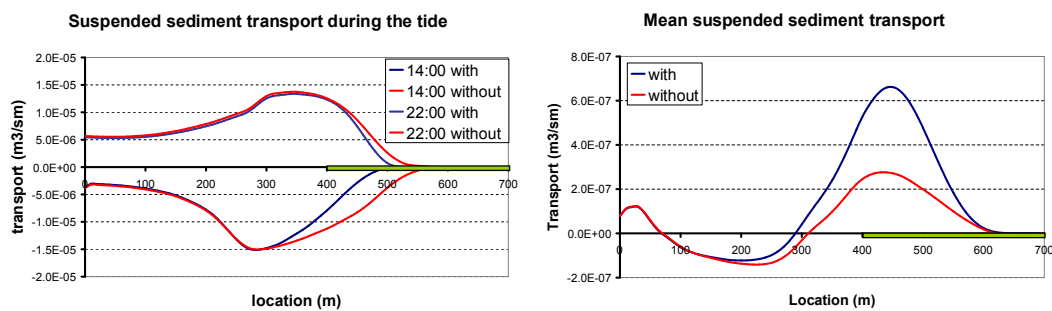


Figure 4-14: suspended sediment transport during the tide and tide averaged suspended transport, with (blue) and without (red) mangroves. Positive means onshore transport (rising tide, 22:00), negative offshore (falling tide, 14:00).

The differences for the rising tide in suspended sediment transport are small. They start to occur at the beginning of the mangrove forest (just as the differences in sediment concentration for the rising tide, figure 4.13). The differences in suspended sediment transport for the falling tide are much larger and not confined to the mangrove area. The sediment concentration is responsible for this difference. Combining the concentration from figure 4.13 and the flow velocity from figure 4.7 the sediment transport is obtained.

Because of the lower off-shore transport in the case of mangroves, the differences between onshore and offshore transport increase. This is shown in the right hand side picture of figure 4.13. The tide averaged suspended sediment transport resembles well the conceptual model on sediment transport of Masselink (2006) (see § 2.3.3, figure 2.14). The pattern of Masselink (2006) however is based on measurements on sandy, non-cohesive, beaches, so the resemblance should be accidental. In the conceptual model of Shi and Chen (1996) (see § 2.3.3, figure 2.15) there is only onshore transport, which increases from the sub tidal area to the intertidal area, remains constant till MSL and decreases again. The pattern of Shi and Chen (1996) can also be found in the conceptual model of Walsh and Nittrouer (2004). This pattern is not observed in figure 4.14.

Doubts are rising about the reliability of the sediment transport, calculated in the model. The sediment transport is a combination between sediment concentration and flow velocity. Assuming that the flow velocity is calculated well the problem can be found in the sediment concentration. In the discussion (see § 4.3) this will be more elaborated.

Morphological changes

Figure 4.15 shows the resulting morphological changes after 1 tide. Knowing that gradients in transport lead to sedimentation or erosion, the sedimentation/erosion pattern is a consequence of the tide averaged sediment transport pattern of figure 4.14. Maximum erosion occurs at MSL (400 m in figure 4.15). Then the erosion decreases fast in the case of mangroves and changes into sedimentation after a 100 m. There the sediment is deposited. Without mangroves it looks that this sediment is not deposited. Erosion till the end of the shore takes place.

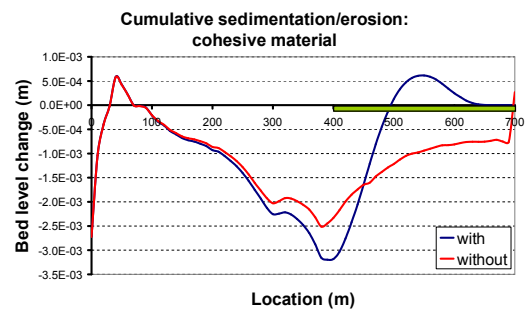


Figure 4-15: sedimentation/erosion patterns after 1 tide for cohesive sediments. The green bar represents the location of the fringe mangroves. The red line is without mangroves and the blue line with mangroves

4.2.4 Conclusion

For the cohesive case 4 validation criteria are used:

- The conceptual model for morphological changes of Walsh and Nittrouer (2004)
- The conceptual model for sediment dynamics of Shi and Chenn (1996)
- The sediment concentrations of § 3.4.1
- The sediment accretion of § 3.4.3

Walsh and Nittrouer (2004)

The sedimentation/erosion pattern (see figure 4.15) does not reflect the pattern of Walsh and Nittrouer (2004). Two conclusions can be drawn: the modelling results are not reliable or the modelled situation does not resemble the conceptual model situation of Walsh and Nittrouer (2004). It is difficult to say which conclusion is true. Both conclusions are defensible.

Shi and Chenn (1996)

The sediment transport pattern of Shi and Chen (1996) is not reproduced as well by the Delft3D model. On average there is however more onshore than offshore transport inside the intertidal zone (see figure 4.14). The tide averaged onshore transport decreases from the mean sea level location at the shore. This also seems the case in the Shi and Chen (1996) conceptual model. So, it can be concluded that some features are reproduced with the Delft3D model calculations, giving a little trust in the modelling results.

Sediment concentration

Looking to the sediment concentration does not lead to more trust in the modelling results. Modelled sediment concentrations are much higher than the observed ones. It is however still possible to lower the modelled concentrations by increasing the critical shear stress for erosion or the settling velocity. Increasing the settling velocity will probably have the most positive effect on the sediment concentration.

Sediment accretion

Sediment accretion in the mangrove forest is observed in the modelling experiment (see figure 4.15). This can be an indication that the processes inside the forest are modelled well.

Conclusion

There is a little more trust in the modelling results for cohesive sediments because of the sediment transport pattern and the sediment accretion inside the forest. However the high sediment concentration and the resulting morphological patterns seem not very reliable, in comparison with the validation criteria.

4.3 Discussion

Although insight in modelling mangrove forests is increased the modelling results were not very positive.

For the difference between the results of the modelling experiment and the conceptual model of Walsh and Nittrouer (2004), two explanations are possible:

- The model set up is too different from the situation where the conceptual model of Walsh and Nittrouer (2004) is based on.
- The processes of sedimentation/erosion are not modelled well

These two explanations will be elaborated below. This paragraph will close with a discussion about the trapping mechanism of mangrove forests.

4.3.1 Difference between model set up and reality

The reality is always much more complex than a model. It is not strange that there are differences between model and reality. A model however tries to summarise the reality in a way that it can be expressed in equations and relations, so that it can predict what will happen. There are good equations and relationships available to predict morphological behaviour of beaches, based on measurements. These equations are available in Delft3D and used in this modelling experiment (see also chapter 2).

However, there is not much known about the situation where the conceptual model of Walsh and Nittrouer (2004) is based on. The tidal range (3 m) is the only thing that is known. In the model a tidal range of 2 m is used. This difference in tidal range does not lead to totally different processes. Only waves will ‘attack’ the beach on different places and different times (see Masselink et al., 2006). The high sedimentation and erosion peak around low water level will stay, while that is the problem in the modelling experiment for non-cohesive sediments.

To get better modelling results for non-cohesive sediments a lot of calculations have been made with varying parameters, like Chezy coefficient or sediment grain sizes. This is not shown here, because the obtained results did show the same morphological development. It is also tried to model with another bathymetry, or adding long shore currents to the fringe situation (see appendix E). Both model setups did not generate different morphological patterns.

The resulting morphological pattern for cohesive sediments showed a huge difference with the pattern for non-cohesive sediments. Also a little sensitivity analysis is carried out. Generally can be said that:

- A larger critical shear stress, settling velocity or sediment concentration on the boundary do not change the sedimentation/erosion pattern for cohesive sediments
- Adding a long shore current does not change the sediment concentration profile, leading to the same errors in sediment transport

These conclusions imply that the model setup does not have to be the same as the reality. There is of course some sensitivity to parameters, but in general can be said that the only big difference is whether the material is cohesive or non-cohesive. Both cases are tested but did not generate satisfactory results.

4.3.2 Shortcomings in the understanding of processes

Modelling sediment transport under waves

Van Rijn (1998) describes that profile developments of beaches inside the surf zone cannot be modelled well with the knowledge of today. The problems arise when sediment transport processes due to the processes wave asymmetry, streaming, wave propagation and wave breaking are tried to model. These processes are still not well understood and much more research is necessary to increase knowledge (see for example Van Rijn, 1998, Masselink and Russel, 2006, Masselink et al, 2006, Zheng and Dean, 1997). Below this is shortly worked out for both non-cohesive and cohesive sediments.

Non-cohesive sediments

For non-cohesive sediments bed load sediment transport is determining the morphological pattern. In Delft3D the bed load transport due to waves and currents (S_b) is calculated with:

$$S_b = 0.006\eta\rho_s w_s d_{50} M^{0.5} M_e^{0.7} \tag{4.1}$$

where η is the relative availability of the sediment fraction in the mixing layer, ρ_s the density of the sediment, d_{50} the sediment grain size and M the sediment mobility number due to waves and currents. The relationship between bed load transport and waves is expressed with the parameter M . M is related to an effective velocity (v_{eff}) and calculated with:

$$M = \frac{v_{eff}^2}{(s-1)gd_{50}} \tag{4.2}$$

and:

$$v_{eff} = \sqrt{v_R^2 + U_{on}^2} \tag{4.3}$$

Where v_R is the depth averaged velocity and U_{on} the onshore directed near bed orbital velocity. Figure 4.16 shows the relationship between orbital velocity and bed load transport. From an orbital velocity of about 0.18 m/s there is bed load sediment transport. This corresponds to the critical shear stress for initiation of motion presented in table 4.2. The relationship between bed load transport and orbital velocity is calculated in a correct way.

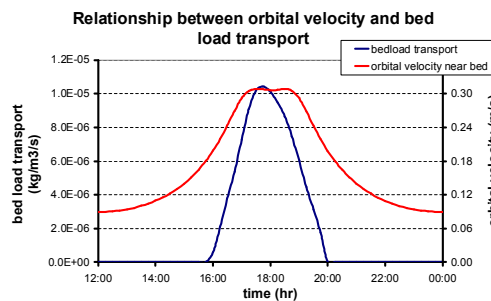


Figure 4-16: Relationship between the wave orbital velocity near the bed and bedload sediment transport at the low water level line (200 m), during the tide.

The problem is not that the bed load transport is not modelled well, but that the bed load transport due to waves is not balanced with the other (suspended) sediment transport components. The parameterisation of the different sediment transport processes in Delft3D (van Rijn 1998 is used) for this kind of problem is not the right one. It can be that another parameterisation generates better results.

There is a preliminary version of Delft3D available which uses another parameterisation (Van Rijn 2004) and is able to take into account very small grain size diameters of non-cohesive sediments (in the previous model the minimum grain size was 100 μ m). Five simulations are carried out with this ‘new’ model (100, 80, 60, 40 and 20 μ m). Figure 4.17 shows the sedimentation/erosion pattern for the five different grain sizes, including the original pattern of 100 μ m used in the analysis (see §4.1).

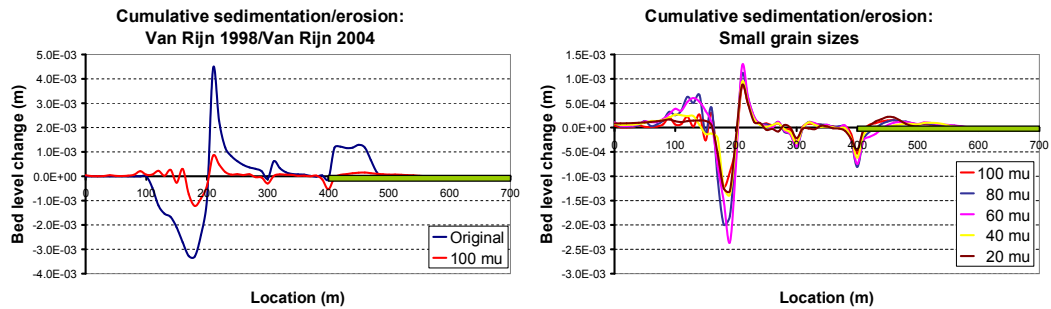


Figure 4-17: sedimentation/erosion pattern for different transport formulas and different (smaller) grain sizes

The differences between the results for the different transport formula are large. The sedimentation/erosion peak around the low water level line appears for both transport formulas, but the peaks for Van Rijn 2004 are much smaller. The sedimentation is smaller inside the forest, but reaches more into the forest, for Van Rijn 2004. There is also a little erosion just in front of the forest. This seems justifiable due to the sudden increase in velocity, when coming out of the forest. A major difference is that the tide averaged bed load sediment transport is much lower when using the Van Rijn 2004 transport formula (not shown here). The system is not only driven by bed load transport any more and suspended sediment transport becomes more important. Sediment transport processes are balanced more. However, the same strange sedimentation/erosion peak around low water level is still observed in figure 4.17.

The sedimentation/erosion pattern for different grain sizes does not vary much from each other. There is a kind of optimum grain size diameter for generating the highest sedimentation/erosion peak around low water level. In this case it is 60 μm . It needs more analysis to find out how this is possible. There are also small differences in patterns, not justifiable by a decreasing sediment size. So it remains unclear whether Van Rijn (2004) is able to model this problem in a reliable way.

For now it is sufficient to see that although the new transport formula (Van Rijn 2004) gives other and a little bit better results, still the same problems (sedimentation/erosion peak) occur in sediment transport. More research can be carried out to the parameterisation of the different cross shore sediment transport processes due to waves and currents.

Cohesive sediments

For cohesive sediments bed load transport due to waves is not the problem, because there is no bed load transport. In this case doubts are rising about the very high sediment concentration. The sediment concentration is a result of sediment dispersion, the sediment erosion flux and the sediment deposition flux. The influence of waves on the sediment dispersion is taken into account by the effects of waves on the k- ϵ turbulence closure model (see § 2.2.2 and 2.3.2). From appendix C can be seen that waves generate high kinetic turbulent energy and energy dissipation, but that the resulting eddy diffusivity is not influenced very much.

The erosion flux depends on the combined bed shear stress for waves and currents (see § 2.3.2), which can be calculated from the flow velocity and the orbital velocity. Figure 4.18 shows the sediment concentration in a cross-section. The orbital velocity is also shown in this graph to illustrate the relationship between sediment concentration and waves. From figure 4.18 can be seen that the orbital velocity shows the same pattern as the sediment concentration: it increases slowly till 400 m, followed by a rapid decrease, as a consequence of breaking waves. Because of the low cross-shore flow velocities (and the low orbital velocities as well) the sediment concentration is probably a consequence of dispersive sediment transport. In this way the sediment concentration is not increasing because of an increasing orbital velocity, but it is decreasing due to dispersive transport of sediments.

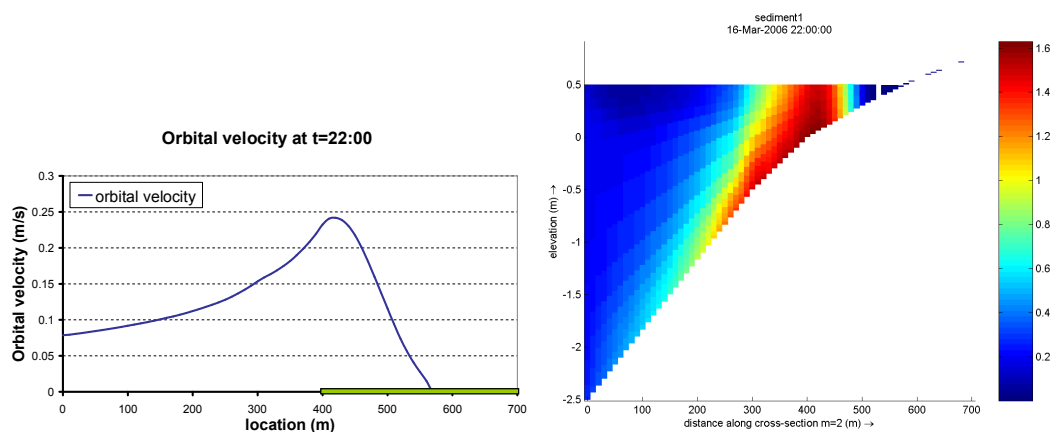


Figure 4-18: Orbital velocity (left) and sediment concentration (right) at time $t = 22:00$ (tide is rising)

The high sediment concentration is probably a result of the low cross-shore flow velocities. Due to the wave action sediment will be picked up from the bottom, but it is not transported away from the point where it is eroded. Therefore the concentration will increase till a certain balance is reached between the deposition flux and the erosion flux. This balance can be seen well in figure 4.13. But because such high sediment concentrations are never reported it remains the question if the high value of the concentration is reliable.

Another interesting aspect is the very steep gradients in sediment concentration at the side of the coastline. Through dispersion it should be expected that the concentration slowly decreases. The steep sediment concentration gradients are probably a consequence of the low water level, with a very low water levels. There is also hardly any wave energy left, taking care for circulation of sediments in the water column.

Keeping this in mind the results for cohesive sediments are becoming more and more reliable.

Simplifications in modelling

Besides the simplifications in the model setup, there are also simplifications in the model. For example:

- Flocculation is not taken into account
- The effect of turbulence due to waves on cohesive sediments cannot be taken into account
- Trees can only be taken into account in the Wave module through an increased bed friction
- Waves and flow cannot be computed at the same time, a communication time is needed
- Because it is a numerical model, some thresholds for calculations are needed to improve the results (like a threshold for sediment computations and a threshold for depth)

4.3.3 Influence of mangroves: trapping of sediments

Although the problem cannot be modelled in a reliable way, the influence of mangroves can be clearly seen in modelling. Inside the mangrove forest the expected processes take place, like reduction of flow, wave height, sediment concentration and sediment transport. Mangroves also promotes sedimentation, which is expected from the sediment accretion data presented in § 3.4.3. About sediment accretion Woodroffe (1992) states that mangrove roots and pneumatophores are efficient sediment trappers. Is the sedimentation in this modelling experiment a consequence of sediment trapping by mangroves? Just a short look to the possible trapping of non-cohesive and cohesive sediments.

Non-cohesive sediments

Sediment trapping is the process that sediment is transported into the forest, but cannot be transported out of the forest. To analyse this for non-cohesive sediments figure 4.9 is the key. The mean suspended sediment transport pattern shows a negative value, which means that the tide averaged transport is directed off-shore. So there is more transport out of the forest than into the forest and no trapping of sediments. For bed load transport there is only a onshore transport and sediment is trapped inside the mangrove forest. The sedimentation the beginning of the forest is a sign of trapping of sediments. This trapping effect leads to levee formation. Augustinus (1978) shows the same levee formation for mangrove forests along the Surinam coastline. He states that levees are only formed in the case of non-cohesive sediments. This corresponds with the modelling results (see also § 5.1.4)

Cohesive sediments

Cohesive sediments are behaving much different comparing to non-cohesive sediments. The settling velocity is responsible for this. Cohesive sediments have much lower settling velocities, causing the sediment to be transported further into the forest. The sediment cannot be picked up from the bottom at that point and is trapped in that way. This is called the concept of ‘settling lag’ and ‘scour lag’ (Van Straaten en Kuenen, 1958). This process can be seen in figure 4.14.

4.4 Conclusions

The objective of this modelling experiment was to increase insight in the hydrodynamics and morphodynamics in and around fringe mangrove forests. The main research question was:

How can the fringe mangrove forest be modelled and what conclusions can be drawn considering the influence of mangroves on morphodynamics?

To answer this question it was tried to model a fringe mangrove forest, resembling the conceptual model of Walsh and Nittrouer (2004), see figure 4.1. Considering the hydrodynamics (in terms of water level, flow and wave characteristics) the model is reproducing satisfactory results (see appendix C).

For the morphodynamics (for both the non-cohesive and cohesive sediment case) in and around fringe mangroves it should be concluded that they are not modelled in a satisfactory way. This can be attributed to the lack of understanding of the balance between cross-shore sediment transport processes due to waves. For non-cohesive sediments the bed load transport due waves (streaming) is probably overestimated comparing to the other processes. For cohesive sediments it seems that the sediment concentration due to waves is overestimated. The pattern of sediment concentration however seems reasonable. This modelling experiment confirms the research that is needed to understand sediment transport processes due to waves.

What should be kept in mind is that there is not much background knowledge about the used conceptual models to validate the results. It is possible that differences between modelling results and validation criteria occur because of this reason. It is advised to search for more specific validation criteria.

One important conclusion that can be made is that mangroves lead to sedimentation inside the forest: in both cases sediment is trapped. For non-cohesive sediments this trapping can lead to levee formation.

5 Overwash mangroves

The objective of this research is to increase insight in morphodynamics in and around mangrove forests, by modelling the mangroves in Delft3D and carrying out a sensitivity analysis. The research is confined to fringe and overwash mangroves. Fringe mangroves are modelled and analysed in chapter 4. Overwash mangroves will be the focus of this chapter. The main research question is:

How can the overwash mangrove forest be modelled and what conclusions can be drawn considering the influence of mangroves on morphodynamics?

Just as the fringe mangroves this question can be divided into two parts: constructing a model and doing a sensitivity analysis. The model constructing will follow the same path as the fringe mangrove model constructing:

- a. What are the validation criteria?
- b. Which model set-up will be used?
- c. What are the modelling results and how can they be explained?
- d. Are the results reliable?

The model constructing is carried out in § 5.1, where also a distinction is made between cohesive and non-cohesive sediments. It will be seen that the results are reliable, so a sensitivity analysis can be carried out. There are two reasons to carry out a sensitivity analysis. The first reason is to increase insight in how the model works and to justify the simplifications made in the modelling approach. The question ‘What is the influence of another modelling approach and/or other physical parameter values on the modelling results?’ is the main question in this part of the sensitivity analysis.

The second reason for the sensitivity analysis is to see what the influence of the mangroves on morphodynamics in and around mangrove forests is. The main question is: What is the influence of forest parameters on the modelling results? This is the most important part of the sensitivity analysis, because it answers directly the second part of the main research question. In this case only forest parameters will be varied. These are tree density, forest length and forest shape.

The analysis is carried out in § 5.2. It is followed by a discussion on the results (§ 5.3) and a conclusion on modelling the overwash mangrove case (§ 5.4).

5.1 Modelling overwash mangroves

5.1.1 Validation criteria

It is difficult to find validation criteria for the overwash mangrove case. No reports are found focussing on the overwash mangroves. The situation of tidal creeks along mangrove forests is comparable to the overwash case because of the possible high currents in the creeks. These high currents can also be found in the overwash case around the forest.

Wolanski et al (1992) did some research on the tidal hydrodynamics in and around tidal creeks in mangrove forests. Inside the Coral Creek in northern Australia they observed currents between 1 and 2 m/s for a tidal water level differences of 2 m. Results of water level differences and currents inside a mangrove forest on Iriomote Island, Japan (for more details see Wolanski et al (1992)) are shown in figure 5.1. Velocity inside the forest is around 1.2 cm/s. In the water level differences between station 3 and 4 a certain lag can be observed. It looks that the water level rises faster trough the forest than it falls. This concept of water level differences can be used as a validation criterion. The flow velocity inside the forest from figure 5.1 (and also from table 3.3) can be used as validation criterion as well. The flow velocity should not exceed 10 cm/s. Another check in velocity is to use the equation for uniform flow velocity in a vegetation field (Baptist, 2005):

$$u_v = \sqrt{\frac{2gi}{C_D n D}} \quad (5.1)$$

Where i is the water level gradient, C_D the drag coefficient, n the density of vegetation and D the diameter of vegetation.

For sediment concentration and sediment accretion the data presented in chapter 3 can be used to validate the modelling results. It should be kept in mind that the pattern of processes is more important than the magnitude of the processes. During calibration the magnitude can be tuned to the observed values. Patterns however are rather consistent and much more difficult to tune. Considering the morphological development (both short and long term) it is tried to find aerial photographs of overwash mangrove island. Figure 5.2 presents the

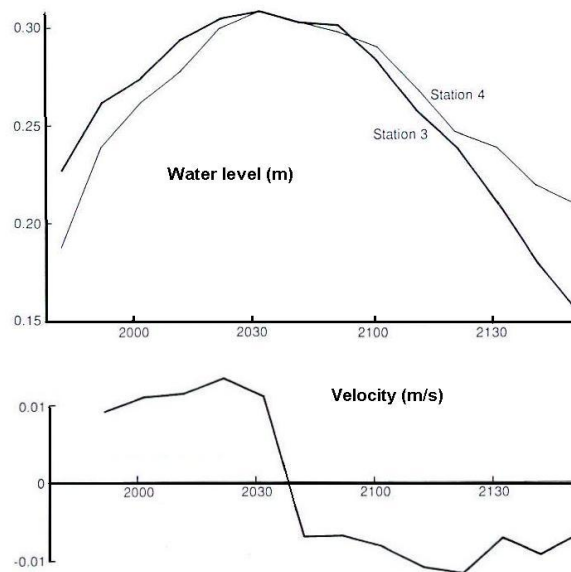


Figure 5-1: water levels and velocity inside a mangrove forest. Station 4 is located further inside the forest than station 3 (after Wolanski et al (1992)). The vertical axis is the height above MSL (m) and the horizontal axis is the time (hr)

morphological pattern of overwash mangroves in Tampa Bay Florida. The bay is ebb dominated, resulting in a residual current, with a certain direction (see the white arrows in figure 5.2). The overwash mangrove islands are expanding in the direction of the current. At the other side hardly any expansion can be observed. It should be noticed that the exact hydrodynamic forcing is not known. The question is also what the influence is of the harbour, located a few hundred meters from the mangroves, on the morphological development.



Figure 5-2: morphological development of overwash mangroves in Tampa Bay, Florida (pictures after Google Earth)

Figure 5.3 shows an overwash mangrove island in Tanzania inside a river branch in the Rufiji Delta, where the flow is unidirectional. It can be seen that the island tends to expand in the direction of the current. For this case also many questions can be raised about the hydrodynamical forcing, sediment characteristics etc... Both cases should be used with care for the validation of the model

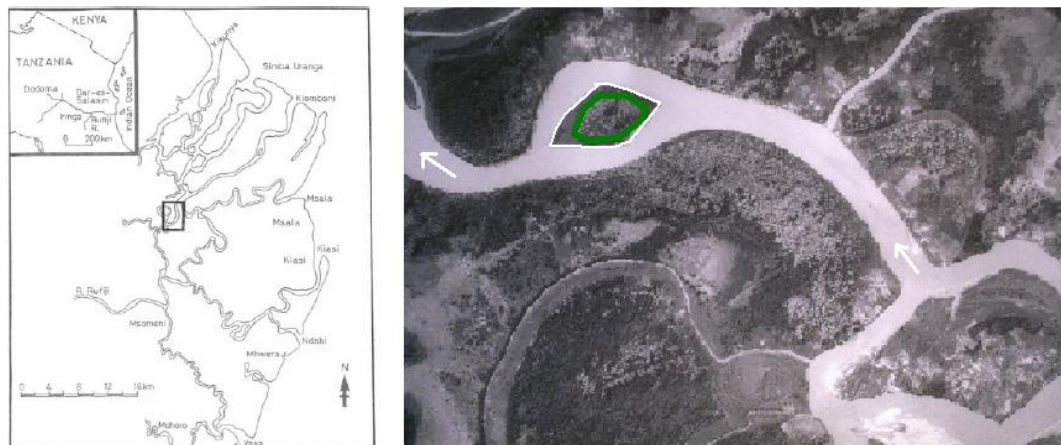


Figure 5-3: Overwash mangrove island in a river branch of the Rufiji Delta, Tanzania (after Erfemeijer and Hamerlynk, 2004)

5.1.2 Model setup

Chapter 3 describes the bathymetry of an overwash forest as uniform and slightly above mean sea level. Considering the modelling experiences from the fringe mangrove case a problem arises when the modelling area is exposed to very low water levels or falls dry during modelling. To avoid this problem it is chosen to model the forest below mean sea level in a way that it never becomes dry. In this case the sediment transport will be overestimated, because there is always sediment transport. The morphological pattern that develops will however be the same. Other important parameters are:

- Bathymetry
 - Horizontal bed level at -2m NAP
 - Bed roughness (Chezy) is uniform, $40 \text{ m}^{1/2}/\text{s}$
 - Modelled area of $1000 \times 1000 \text{ m}$ with grid cells of $10 \times 10 \text{ m}$
- Hydrodynamics
 - Tidal currents around 1 m/s (after Wolanski et al. (1992))
 - Tidal range 2 m (see chapter 3)
 - Harmonical tide
- Mangroves
 - Forest $200 \times 200 \text{ m}$, with a border of 100 m where the density of the forest slowly increases
 - Forest on the bottom and not on an Island, in the middle of the modelled area
 - Forest exist of Rhizophora trees (see figure 4.6 for stem height, densities and diameters)
- Sediment
 - non cohesive, $100 \mu\text{m}$ equilibrium concentration on the boundaries
 - cohesive, critical shear stress of 0.5 N/m^2 , boundary concentration is 200 mg/l , settling velocity is 0.25 mm/s

Figure 5.4 summarises the schematisation

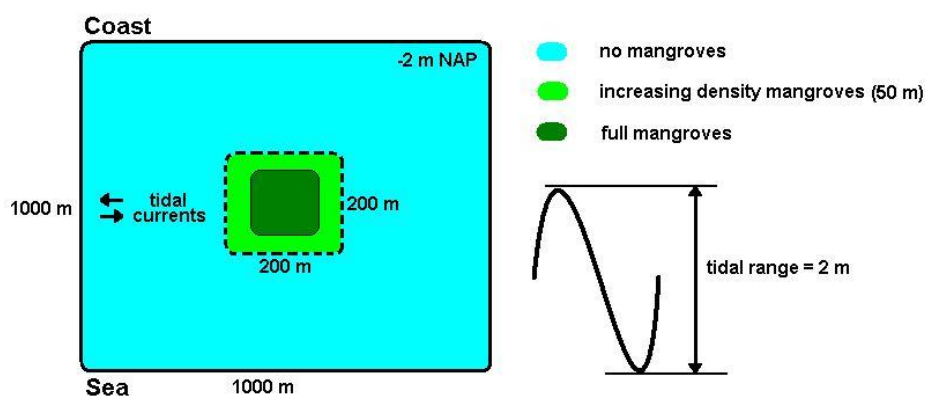


Figure 5-4: schematisation of the overwash mangrove case

It is chosen to model first a 2D case in order to decrease the computation time. The effect of a 3D simulation will be analysed in § 5.2. For the forest schematisation this means that there can only be one layer taken into account in modelling. It is chosen to use the root layer, because this layer is the most important layer in morphological computations. The effect of applying this layer on the full water depth is an overestimation of the friction of mangroves, leading to a more reduced flow inside the forest, and less sediment transport into the forest.

In the basic schematisation waves are also not included. This is done because waves have most influence on the cross-shore cross shore currents. Tidal water level differences are responsible for long shore currents and much larger than the cross-shore currents generated by waves. The effect of long shore currents is therefore also much larger and the cross-shore currents can probably be neglected (see also § 5.2). A consequence of this simplification is less sediment transport into the forest and lower sediment concentrations which also lead to less sediment transport in general.

To get a tidal current a phase difference is applied on both sides of the model (see figure 5.5). A phase difference of 7 degrees results in tidal currents of max 0.9 m/s in this schematisation.

Applying these settings in Delft3D leads to strange a-symmetric sedimentation / erosion patterns. The cause of this are that velocities at the right hand side of the model (directed to the left) are higher, comparing to the velocities at the left hand side, directed to the right (see for example figure 5.6). The attempts to get the model symmetric did not succeed. This should be kept in mind when analysing the modelling results.

5.1.3 Analysis

Showing velocities, sediment concentrations, suspended transport, bed load transport and ending with morphological changes the overwash case will be analysed. From sediment concentrations the analysis will be splitted in non-cohesive and cohesive sediments.

Hydrodynamics

Figure 5.5 presents the depth averaged velocity patterns for both the left directed and right directed long shore tidal currents, 14:00 hr (falling tide) and 22:00 hr (rising tide) respectively (see figure 5.3). The following observations can be made:

1. The velocity is reduced in front of the mangrove forest.
2. The forest functions like a blocking mechanism and the current is directed around the mangrove forest (see also Wu et al (2001) for blocking effects of mangroves)
3. At the corners of the forest and at the sides the velocity increases. At the corners the velocity is at its highest value
4. The velocity decreases and goes back to its original pattern at the end of the forest. Behind the forest the velocity increases again
5. The patterns is rather consistent

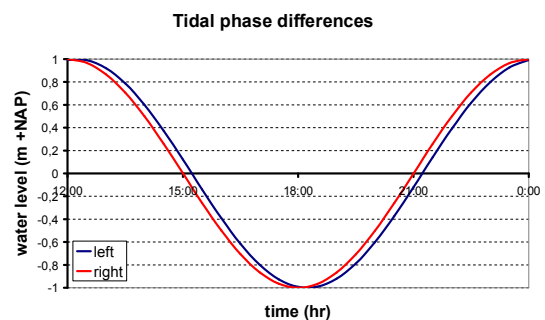


Figure 5-5: applied phase differences in tidal water levels

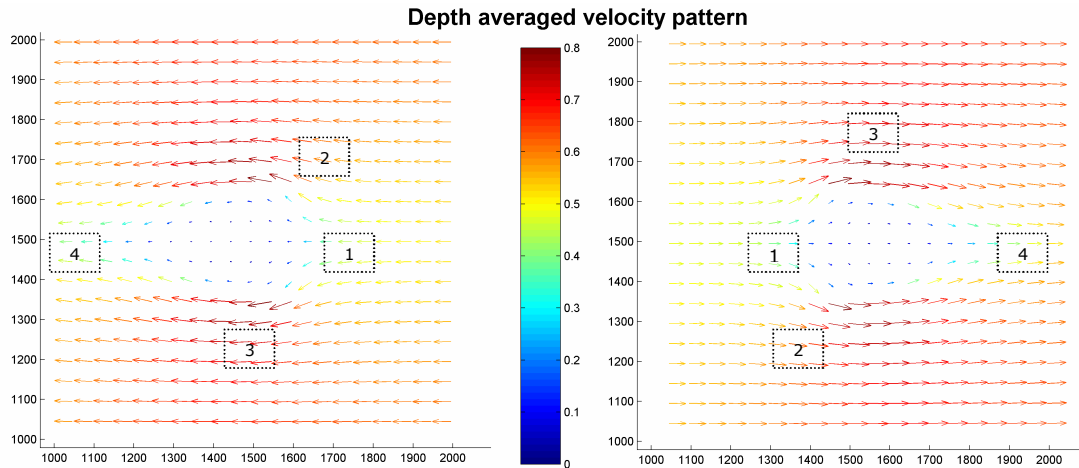


Figure 5-6: depth averaged velocity patterns (unit m/s). The numbers in the figure corresponds to the numbers of the observations. The right picture presents the velocity pattern at 14:00, the left at 22:00. At this time the water levels should be the same

During the tide the velocity in the forest reaches a maximum of about 7 cm/s. This corresponds with the literature presented in § 3.2. An approximation on the flow velocity inside the forest can be made with (Baptist 2005):

$$u_v = \sqrt{\frac{2gi}{C_D n D}} \tag{5.2}$$

Where:

- i = water level gradient
- C_D = drag coefficient
- n = density of vegetation
- D = diameter of vegetation

With the water levels in front and behind the forest the water level gradient can be calculated. This gradient is different from the water level gradient existing between the borders of the model and driving the flow. From figure 5.7 the water level gradient in the forest is $(0.11 - 0.03) / 200 = 0.0004$. With a gravity force of 9.8 m/s^2 , a drag coefficient of 1, a density of 46 and a diameter of 0.0246 m, the velocity in the forest becomes 6 cm/s. At the same time (15:00) the model calculated a velocity of 7 cm/s. The approximation made with equation (5.2) generates a good result.

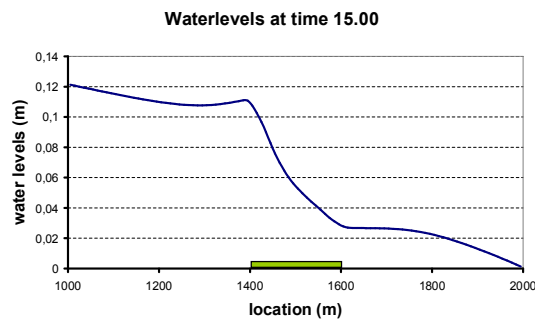


Figure 5-7: cross-section of the water level at 15.00 hr

Because of the friction caused by the vegetation field there is a much steeper water level gradient above the vegetation field. In figure 5.7 the water levels through the vegetation at 15.00 hr is shown to illustrate the difference between both water level gradients. The lag in water levels inside the forest, reported by Wolanski et al (1992) can also be observed in figure 5.8. In this figure the water levels between 10:00 and 14:00 are plotted for two points in the forest. The differences between water levels when they are increasing are smaller than when they decrease. See figure 5.1 for the same lag in water levels.

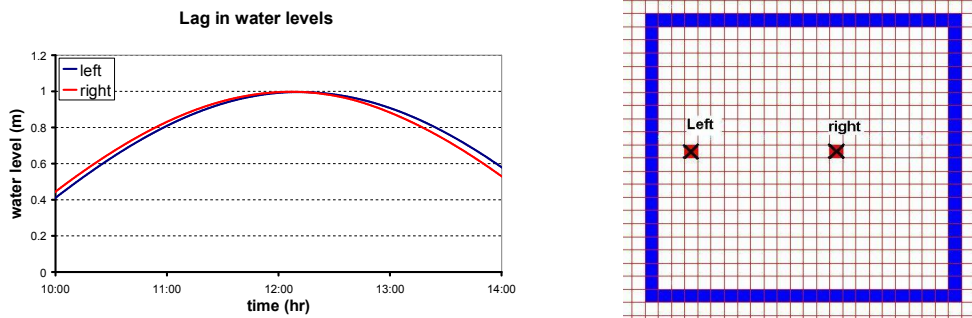


Figure 5-8: lag in water levels (left picture) for two locations inside the forest (right picture). The blue square in the right picture indicates the forest boundary.

Non cohesive sediments

Sediment concentration

The sediment concentration in the water column depends on a number of factors like the flow velocity, bed roughness, grain size diameter, water depth and the turbulence. It is difficult to say on forehand or based on the velocities (see figure 5.6) where the sediment concentration will be the highest. The sediment concentrations are shown in figure 5.9A for two different moments during the tide (14:00 and 22:00), where the water level is the same, but the tidal current is directed the other way. The first thing that is very obvious is that the two different moments are a-symmetric. With the turning tide some lag effects are observed in the currents resulting in stronger left directed currents. It could also be that the mangrove forest is not exactly in the middle of the schematisation, leading to a-symmetric effects. However the a-symmetry is also observed in the situation without mangroves, therefore this is not the reason for a-symmetry. It should be noticed that the a-symmetry is only in the magnitude of the transport and not in the transport pattern.

Other observations that can be made are the half circle in front of the forest, the ‘rain-drop’ like shape of the high concentrations at the sides of the forest and a ‘tail’ with low sediment concentrations behind the forest. It can be concluded that where the velocities are high, the concentrations are also high, and when the velocities are low, the concentrations are also low.

Sediment transport

Suspended sediment transport is a combination of the current and the sediment concentration. Figure 5.9B presents the suspended sediment transport and the pattern is a copy of the sediment concentration figure. The observations for the depth averaged velocity and the sediment concentrations can also be applied here and does not have to be repeated again. It would be expected that there also a little transport would occur inside the forest. If transport takes place in front of the forest and the flow velocity does not reach the critical shear stress any more, the sediment would settle. The settling velocity of the non-cohesive sediment is 3.1 mm/s. For a 2 m water depth and a velocity of 0.2 m/s (the critical flow velocity for the sediment), a sediment particle in top of the water column would be transported 130 m, before it settles. This can't be observed in figure 5.9B. However, before the forest the concentration is low and the sediment is not very high in the water column. Therefore the sediment is not transported far into the forest. It stays at the boundaries (see also § 5.4.2).

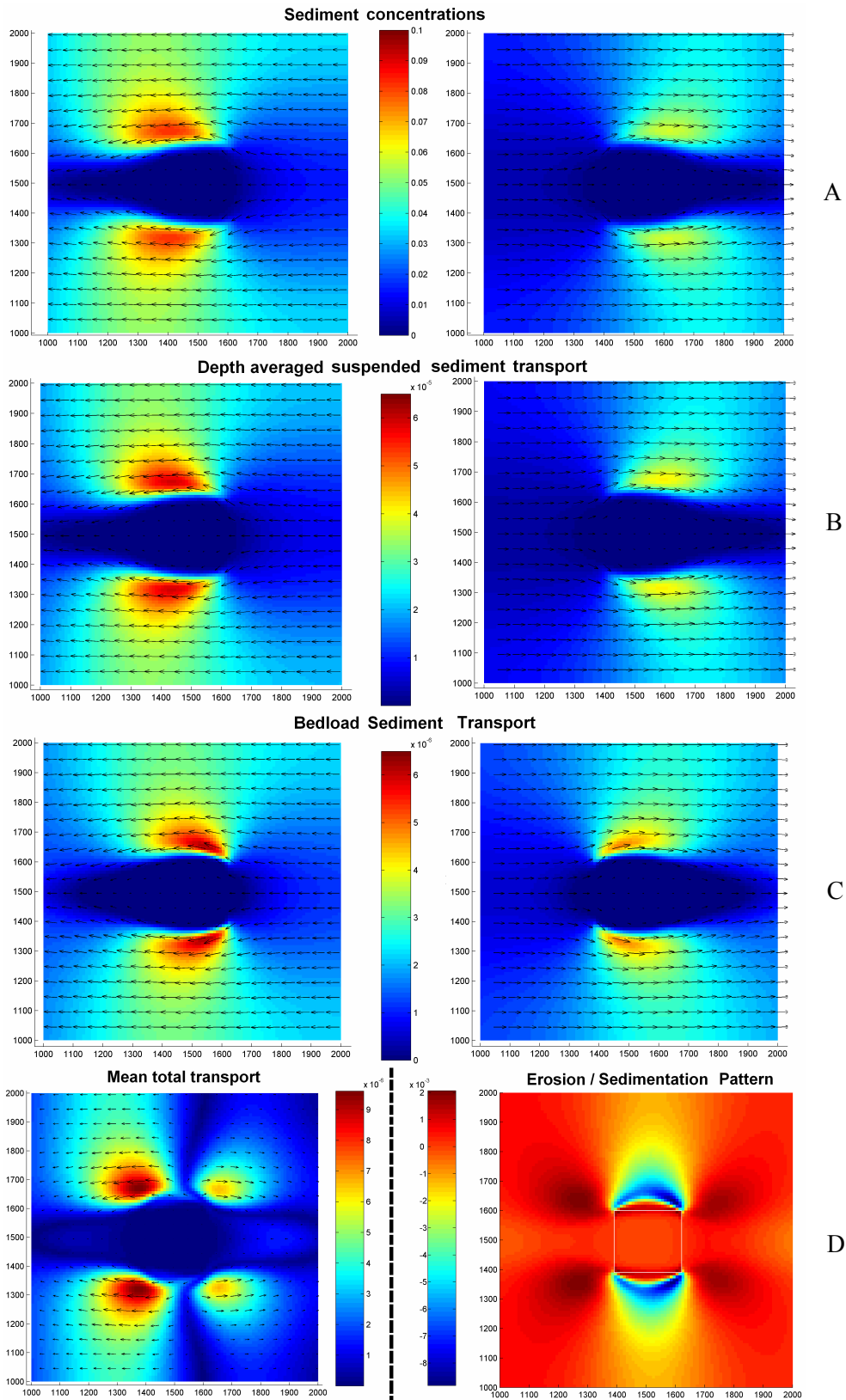


Figure 5-9: sediment concentrations (kg/m^3) (A), sediment transport (m^3/sm) (B and C) and sedimentation/erosion pattern (m) (D) for non-cohesive sediments. The concentration and transport graphs show the magnitude and direction at 14:00 (right) and 22:00 (left). The white square in the sedimentation/erosion pattern represents the location of the mangrove forest.

Considering the bed load sediment transport, presented in figure 5.9C, the pattern of the flow velocity is followed. The high values at the corners of the forest results in high values of bed load transport. There is an increase in bed load transport at the corners and the sides of the mangrove forest. A ‘tail’ of no bed load sediment transport occurs behind the forest. The differences between suspended transport and bed load transport is an order of magnitude (10^{-5} versus 10^{-6}), so the influence of bed load transport is small.

From the suspended load and bed load transport graphs it can be noticed that there is only at the borders of the forest a little sediment transport and no sediment transport inside the forest. This can be attributed to the low velocity in the forest, resulting in low bed shear stress. The critical bed shear stress for the sediment to move can be calculated with Van Rijn (1998) and is 0.21 N/m^2 . With a Chezy value of $40 \text{ m}^{1/2}/\text{s}$ the critical flow velocity is 0.18 m/s . The velocity inside the forest does not reach 0.1 m/s (see figure 5.6) so the sediment in the forest is not moved and no transport takes place.

Morphological changes

In figure 5.9 no sediment transport could be observed in the mangrove forest, resulting in no changes in morphology. At the corners and the sides of the forest a lot of sediment transport takes place. Gradients in sediment transport result in sedimentation or erosion. Figure 5.9D presents the tide averaged total transport. Although there is a little asymmetry around the vertical axis in values, the patterns are the same. Looking to morphological changes after 1 tide the residual currents are important. These are at the corners of the forest, directed outside.

Looking to the gradients in mean total transport the morphological changes can be predicted. At the corners of the forest there will be sedimentation and at the sides of the forest there will be erosion. A little sedimentation occurs at the boundaries of the forest, just inside the forest. The pattern is also presented in figure 5.9D.

Cohesive sediments

Figure 5.10 presents the sediment concentrations, sediment transport and sedimentation/erosion pattern for cohesive sediments.

Sediment concentration

The sediment concentration, presented in figure 5.8A, slowly increases in the direction of the current. At the boundary the concentration is 0.2 kg/m^3 , which is set as a boundary condition. It slowly increases till a maximum value of 0.4 kg/m^3 , because sediment is picked up from the bottom and staying in the water column. Inside the forest the sediment concentration slowly decreases. This can be attributed to the decrease in velocity, which is not exceeding the critical velocity of 0.29 m/s , needed for erosion. Because of the low settling velocity the sediment concentration decreases slowly inside the forest. The downstream effect of the forest can also be seen quite well in figure 5.8A.

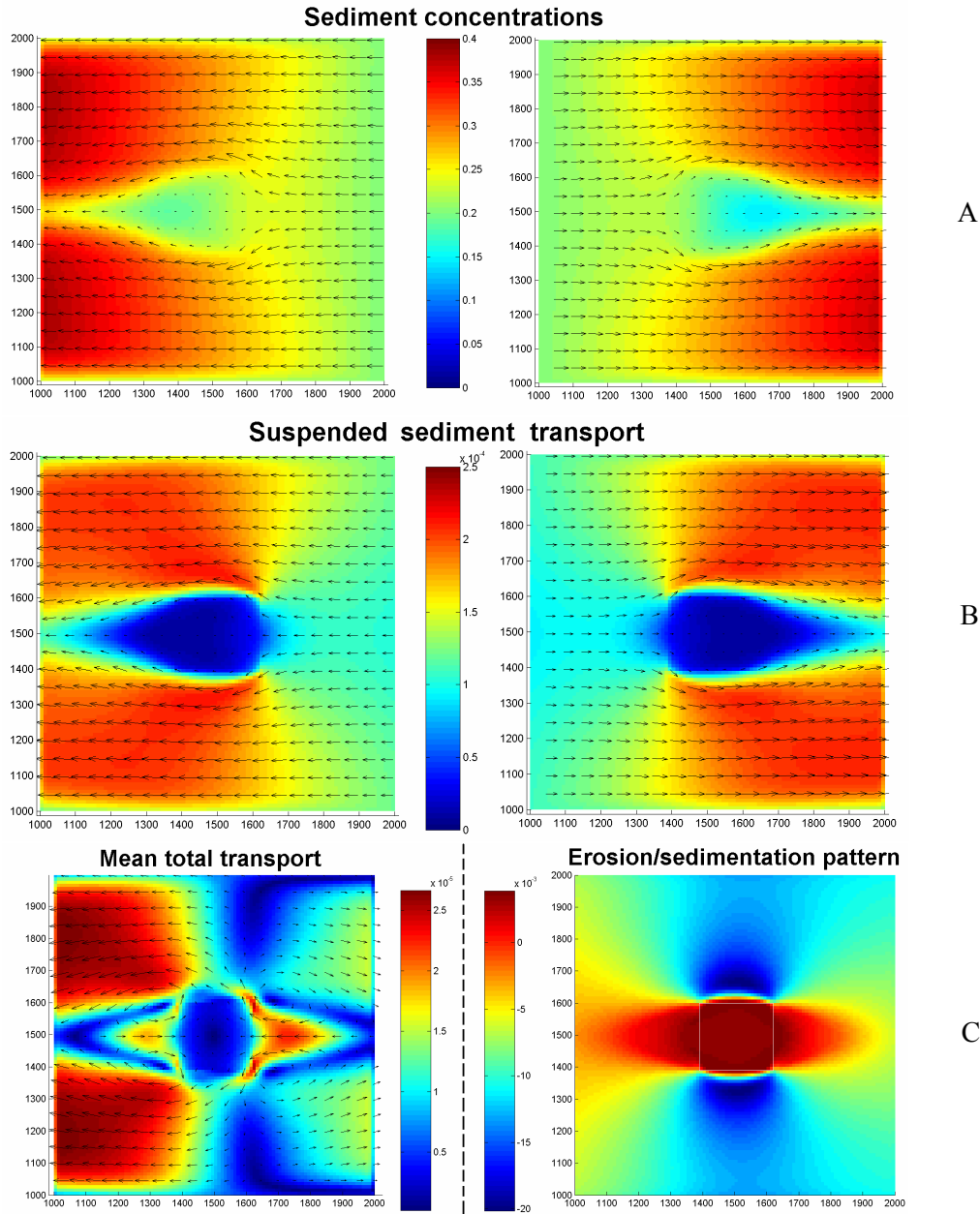


Figure 5-10: sediment concentrations (kg/m^3) (A), suspended sediment transport (m^3/sm) (B) and sedimentation/erosion pattern (m) (C) for cohesive sediments. The concentration and transport graph show the magnitude and direction at 14:00 (right) and 22:00 (left). The white square in the sedimentation/erosion pattern represents the location of the mangrove forest.

Sediment transport and sedimentation/erosion pattern

Figure 5.10B presents the depth averaged suspended sediment transport for cohesive sediments. It is a combination of the currents from figure 5.6 and the sediment concentration of figure 5.10A. Some sediment transport occurs inside the forest, which is logical considering the low settling velocity of the sediment. Looking to the tide averaged transport pattern it can be seen that sediment is brought into the forest and that the forest is expanded at both sides perpendicular to the current direction. The tails of less sediment transport observed in figure 5.10B are filled up.

The sedimentation/erosion pattern (see figure 5.10C) confirms the tide averaged sediment transport pattern. It can be observed that there is high sedimentation inside the forest. It should be noticed that for cohesive sediments also a little levee is established after one tide in the mangrove forest. There is more sedimentation at the borders of the forest than inside the forest. The differences however are small. Around the forest erosion takes place with the highest values at the sides of the forest which are in line with the current direction. No strange elements can be observed in figure 5.10.

Long term analysis

The resulting long term sedimentation pattern for non-cohesive sediments is shown in figure 5.11. It can be seen that levees are built around the mangrove forest. Hardly any sedimentation is observed inside the forest. This is consistent with the short term sedimentation/erosion pattern. Around the mangrove forest a canal develops. The areas of sedimentation at the corners of the forest after 1 tide (see figure 5.9D) are disappeared. Because of the low flow velocity behind the forest a rhombus shaped island will develop. This is consistent with the morphological validation criteria presented in figure 5.2 and 5.3. Outside the canals there is also high sedimentation. It is unclear what the origin is from the sediment. The model calculates an equilibrium sediment concentration at the boundaries of the model, which results (probably) in sedimentation outside the canals. In the last computation steps during modelling only small morphological were observed (compared to the morphological changes in the beginning), which justifies the conclusion that this morphological pattern presents an equilibrium pattern after constant tidal flow forcing.

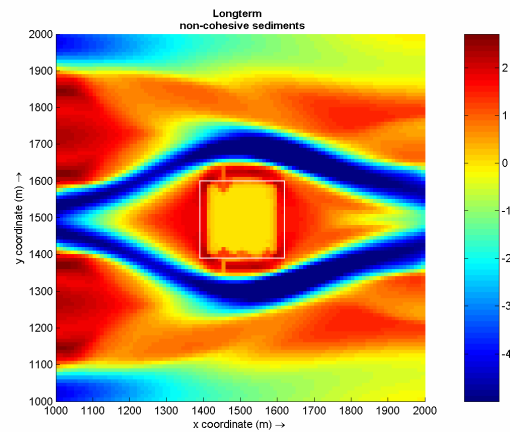


Figure 5-11: Longterm morphological pattern (unit: m) for non-cohesive sediments

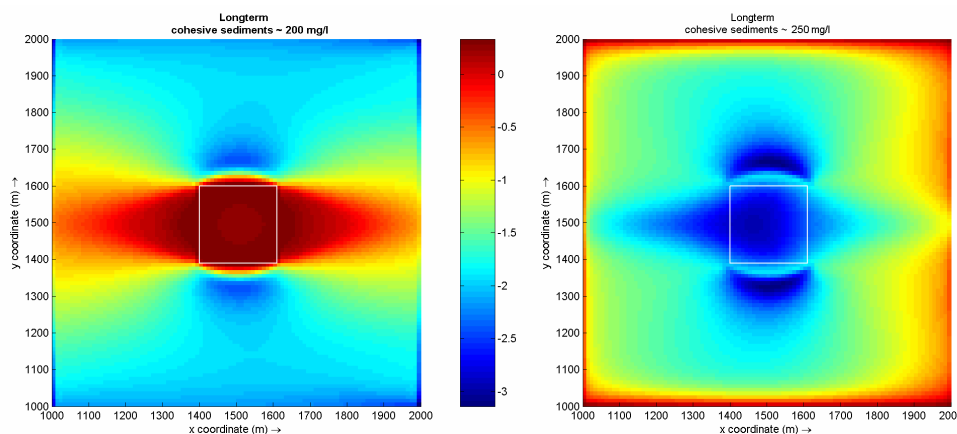


Figure 5-12: Long term morphological development (unit: m) for cohesive sediments with two different sediment concentrations at the boundary: 200 mg/l (the left picture) and 250 mg/l (the right picture)

For cohesive sediments no equilibrium pattern was reached. If there is too little sediment available from the model boundaries (200 mg/l), there is a constant erosion of the bed around the mangrove forest. Only inside the forest and at lee sides of the forest there is sedimentation (or reduced erosion). When there is too much sediment available at the boundaries (250 mg/l) only sedimentation is observed and the basin is slowly filled up. In this case it takes more time to fill up the mangrove forest, because of the reduced flow and the reduced sediment transport inside the forest. The resulting long term morphological pattern for cohesive sediments for two different boundary conditions is shown in figure 5.12. In nature the availability of sediment is probably variable, resulting in a dynamic equilibrium of the system.

For the erosive case (figure 5.12, left picture) a rhombus shaped development of the overwash mangrove island can be observed. This corresponds with the shapes of the islands shown in figure 5.2 and 5.3. However, the system is very sensitive for the availability of sediment. This is illustrated by the two morphological developments shown in figure 5.12. A difference in sediment concentration of only 50 mg/l results in a totally different morphological development.

5.1.4 Conclusion

In § 5.1.1 hydrodynamic and morphodynamic validation criteria are presented. In this paragraph the modelling results are summarised and checked on their validity with the validation criteria.

Hydrodynamic validation

The modelling results from the previous paragraph should be compared with the validation criteria presented in § 5.1.1. Looking to the hydrodynamics it can be observed that the results correspond well with the validation criteria. A tidal current of 7 cm/s lies inside the range presented in table 3.3. The 'water level lag' inside the mangrove forest (observed by Wolanski et al 1992) is also observed in the modelling results.

Morphodynamic validation

Looking to the non-cohesive sedimentation/erosion pattern levees are formed around the forest. It is difficult to say if this is a reliable pattern. No validation criterion (presented in § 5.1.1) reports this levee building capacity of mangroves. Augustinus (1978) made some comments about levee formation around mangrove forests. He states that (for the mangroves along the Surinam coast) only in the case of non-cohesive sediments (sands) levees are formed. Figure 5.13 shows this levee development of a part of the Surinam coast. Because of the currents and the waves sediment is transported along the coastline and levees are formed. The old levees are growing too high, leading to the death of the mangroves behind the old levees (the cause is hyper salinisation). Between the old and new levees new mangrove areas are formed. Augustinus (1978) did not investigate the influence of mangroves on levee formation. Considering the information presented by Augustinus (1978) levee formation is only observed in the case of non-cohesive sediments (see also Augustinus (1995 and Woodroffe (1992)). This corresponds with the modelling results.

The aerial photographs showed in figure 5.2 and 5.3 presents a certain morphological development. Both islands show rhombus like shapes and they grow in the direction of the current. This is observed in the long-term calculations for both cohesive and non-cohesive sediments, indicating that the modelled patterns are not unrealistic.

Other validation criteria are the general information about sediment concentration and sediment accretion inside the mangrove forest. The modelled sediment concentration values for cohesive sediments and non-cohesive sediments lies in the range of 400 mg/l (see figure 5.9 A, figure 5.10A and table 3.6). Sediment accretion is observed for both sediment types which also corresponds to the general sediment accretion information (see § 3.4.3).

Conclusion

Considering the positive results of the hydrodynamical and morphological validation it can be concluded that the model produces realistic and reliable results. A sensitivity analysis will be carried out in the next paragraph.

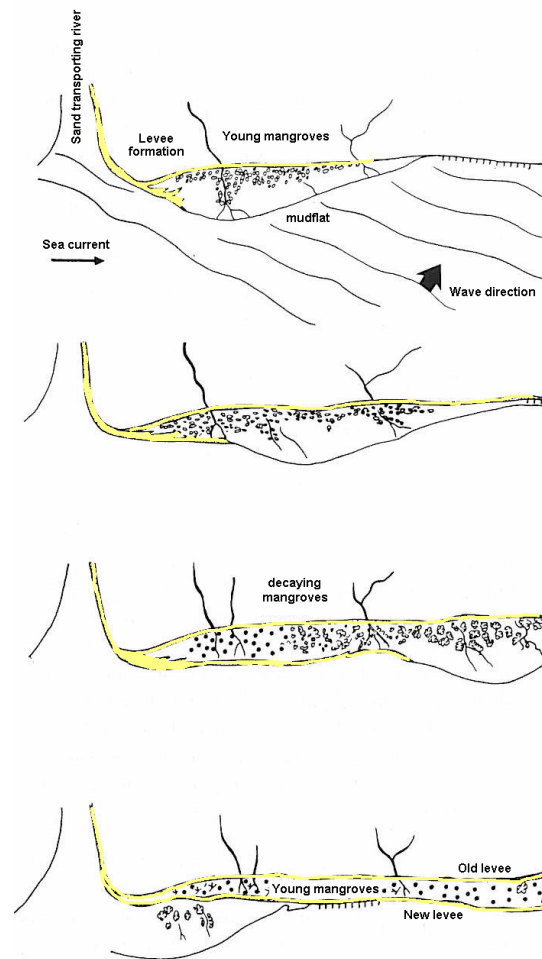


Figure 5-13: conceptual levee formation along the surinam mangrove coastline (after Augustinus, 1978)

5.2 Sensitivity analysis

In the previous paragraph the basic model is analysed for both cohesive and non-cohesive sediments. The modelling results were found realistic and reliable, so it is useful to carry out a sensitivity analysis. In this way more insight is generated in the modelling results. The modelling results are sensitive to:

- the modelling approach
- changes in physical parameters
- changes in biological parameters

These three aspects will be elaborated in the following three sub-paragraphs. The focus in this paragraph is on the morphological sensitivity to modelling approach and parameter values, because morphology is a result of both hydrodynamics and sediment dynamics. By showing the resulting morphodynamical patterns both processes are taken into account. It is chosen to analyse the sensitivity to modelling approach, physical parameters and biological parameters, of only the basic non-cohesive model. There is no time left for the analysis of the sensitivity of the basic cohesive model.

5.2.1 'Modelling approach' sensitivity

First a way to analyse the sensitivity is explained, followed by an analysis of the sensitivity to the 'waves' and '3D' modelling approaches.

Analysing the sensitivity

To analyse where the differences occur and how big they are, the following equation is used:

$$\text{difference} = \frac{A - B}{A} \quad (5.3)$$

Where

A = the researched factor (like 3d, waves, cohesive)

B = the 'standard' factor (the '2d-without waves-non cohesive material' run)

By dividing it through the researched factor the differences are made relative and it is easy to compare them with each other.

Values of equation (5.3) can have different meanings depending on the magnitude and the sign of the value. Sedimentation has a positive sign and a magnitude, erosion has a negative sign with a certain magnitude. Knowing this the following values of equation (5.3) can be distinguished:

Value > 2 → B is larger than A and the process (sedimentation or erosion) is different

Value = 2 → B has the same magnitude as A, but another process

1 < Value < 2 → B is smaller than A and the process differs

Value = 1 → B has no influence on A and is negligible comparing to A

0 < Value < 1 → B is smaller than A and has the same process

Value = 0 → B has the same magnitude and process as A

Value < 0 → B is larger than A and the process is the same

Equation (5.3) can be used to analyse the differences in magnitude and the differences in direction between two cases. To know whether case A shows more/less sedimentation or erosion, or shows sedimentation instead of erosion, the sedimentation and erosion locations in the original situation have to be known. This is presented in figure 5.14. This pattern is plotted in the 'difference-plot'.

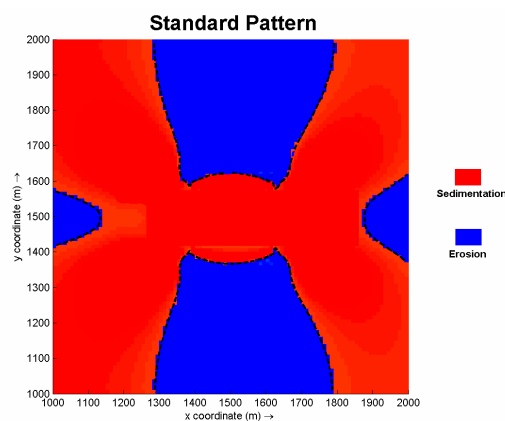


Figure 5-14 the erosion/sedimentation pattern in the basic model

Wave sensitivity

Waves of 0.5 m, directed perpendicular to the tidal flows, are added to the model. The vegetation friction factor calculated in chapter 4 is used to take the influence of vegetation into account. The resulting hydrodynamics and sediment transport dynamics can be found in appendix F, including the differences with the basic model. Figure 5.15 shows the sedimentation/erosion pattern for the situation with waves and the differences between this

situation and the basic model. The observations made from figure 5.15 can also be found in appendix F.

From figure 5.15 it can be concluded that waves do not have a big influence on the sedimentation/erosion pattern (most values are < 1). There is however a big influence on the amount of sedimentation or erosion. Sedimentation or erosion is most of the time 50% to 80% larger for the situation with waves.

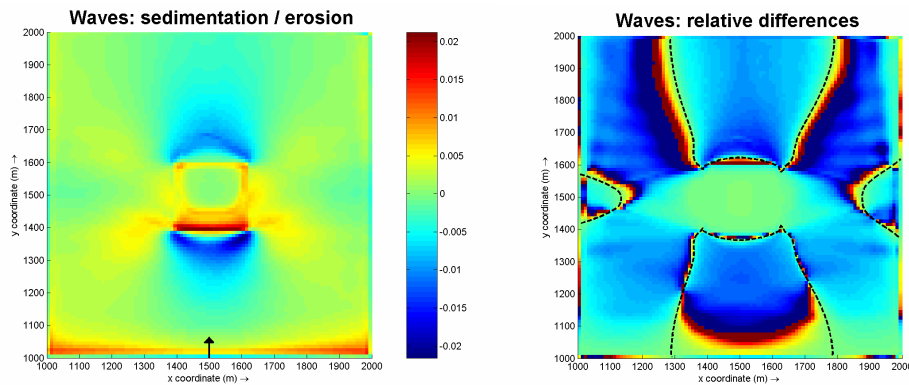


Figure 5-15: sedimentation/erosion pattern for the situation with waves and the differences between the basic model and the wave model. The erosion is in meters, the array shows the direction of the waves

3D

The basic situation is modelled in 2 dimensions. The main reason for this is that it saves a lot of computation time, comparing to 3D modelling. However, trees are 3 dimensional objects with important variations in height. To take this into account a three dimensional model simulation is done. The 3D-model has the same model setup of the fringe mangrove model (see § 4.1.2): 16 layers are implemented with on top and on the bottom more computation layers than in the middle (see figure 4.4). The influence on hydrodynamics and sediment transport dynamics is shown in appendix F, together with the observations. The sedimentation/erosion pattern and the difference with the original 2D model simulation are shown in figure 5.15.

It can be concluded from figure 5.15 that 3D modelling does not show very different results. Inside the forest the difference is large: there is much more sedimentation comparing to the basic non-cohesive model. The magnitude of the sedimentation however is still very small.

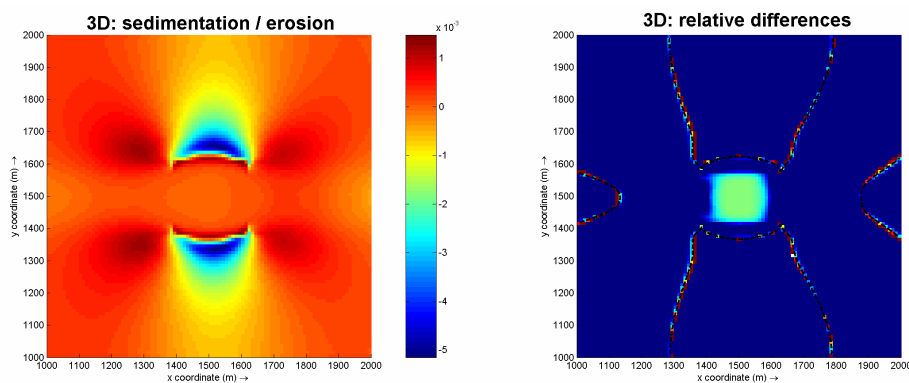


Figure 5-16: sedimentation/erosion pattern (in meters) of a 3D simulation and the difference with a 2D simulation

Conclusions

When waves are added to the basic model, they influence the magnitude of erosion and sedimentation, but they do not change sedimentation into erosion, or other wise. A 3D simulation instead of a 2D simulation does not lead to different results.

5.2.2 ‘Physical parameter’ sensitivity

First the variations in physical parameters are described, followed by an analysis of the sensitivity of the modelling results to these variations.

Description of variations in physical parameters

It is chosen to analyse the sensitivity of the modelling results to the wave height and wave angle (using the ‘wave’ modelling approach) and to the settling velocity and sediment concentration (using the ‘cohesive’ modelling approach). The wave parameters are chosen because wave situations occur frequent in mangrove forest areas. Therefore it is useful to generate more insight in the effect of waves on the modelling results. The cohesive sediment parameters are chosen because cohesive sediments are abundant in and around mangrove forests. Therefore it is also useful to generate more insight in the effect of these physical parameters.

The sensitivity of the modelling results to these parameters is analysed with the Individual Parameter Variation study (IPV) (see Janssen et al., 1990). Only one parameter is varied, while the others are kept constant. The influence of the individual parameter to the modelling results can be seen very clearly in this way. There are other methods as well to do a sensitivity analysis. Janssen et al (1990) gives a good overview by describing 5 different methods to carry out a sensitivity analysis¹. The IPV however is the easiest one and shows the influence of the parameter on the modelling results in the most direct way. A disadvantage of this study is that the interactions between parameters and the influence on the modelling results cannot be taken into account in this study.

It is chosen to vary the parameters with a constant factor of 20%. In table 5.1 an overview of the parameter values is given. For the wave angle perpendicular waves (180 degrees) are 100% and parallel waves (90 degrees) are 0%. The modelled wave height in § 5.1.1 is the 60%-value of the waves. The other modelled values are taken to be 100%. They will decrease in this sensitivity study.

Table 5-1: variations in parameters

Physical parameter	wave height (m)	wave angle (degrees)	settling velocity (mm/s)	concentration (mg/l)
100%	0.833	180	0.25	200
80%	0.667	162	0.20	160
60%	0.5	144	0.15	120
40%	0.333	126	0.10	80
20%	0.167	108	0.05	40

¹ *The Individual Parameter Variation, Differential sensitivity analysis, Response Surface method, Monte Carlo and the Hornberger-Spear-Young method*

Modelling results

For morphodynamics in and around mangrove forest the sediment transport dynamics are very important. Gradients in sediment transport determine the sedimentation and erosion. To get a good view of the morphodynamics in and around mangrove forest the net sediment transport into (or out of) the forest is assessed. The result is shown in figure 5.17. In appendix F an extensive analysis of the sediment transport into and out of the forest can be found.

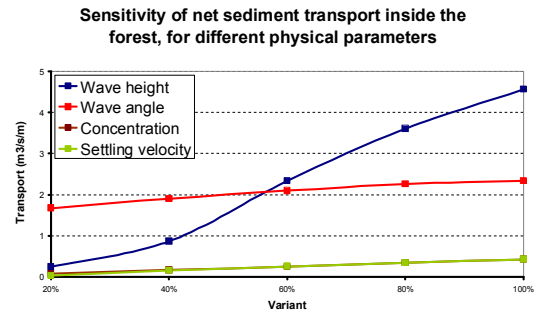


Figure 5-17 net sediment transport into the mangrove forest for different physical parameters and parameter values

Conclusions

From figure 5.17 can be concluded that:

- for all parameters there is a net sediment transport into the forest, and therefore sedimentation inside the forest.
- the sedimentation inside the forest is much higher in the case of non-cohesive sediments with waves, compared to cohesive sediments
- sediment inside the forest is very sensitive for wave height, but not very sensitive for the other three parameters (what should be kept in mind is the scale of figure 5.17)
- for increasing sediment concentration and settling velocity the sedimentation inside the mangrove forest increases

5.2.3 ‘Biological parameter’ sensitivity

There is a wide variation between mangrove forests around the world, illustrated with the data presented in chapter 3. This paragraph tries to analyse the sensitivity of the modelling results for different mangrove forests. In the sensitivity analysis there will be varied in:

- Tree density
- Forest length
- Forest shapes

Again the IPV method for the sensitivity analysis is used.

Tree density

It is chosen to vary the tree density in the same way as the other parameters from § 5.3.1 (see table 5.2). The resulting sedimentation/erosion patterns for the 100%, 60% and 20% tree densities are presented in figure 5.18. It can be seen that both the sedimentation and erosion around the forest decreases with decreasing density. There is also more sedimentation inside the forest (which is hard to see from figure 5.18). This effect is logical because for a decreasing tree density, the flow is less obstructed and it flows faster through the forest.

Table 5-2: variations in parameters

Biological Parameter	tree density (no roots /m2)
100%	46
80%	36.8
60%	27.6
40%	18.4
20%	9.2

Therefore the flow can take more sediment into the forest. This also explains the decreasing morphological effects around the mangrove forest. From figure 5.19 the effect of the tree density on morphological changes looks non-linear: as the density decreases the effect increases more. The non-linear effect is illustrated in figure 5.19 where the sediment transport into the forest and out of the forest is shown.

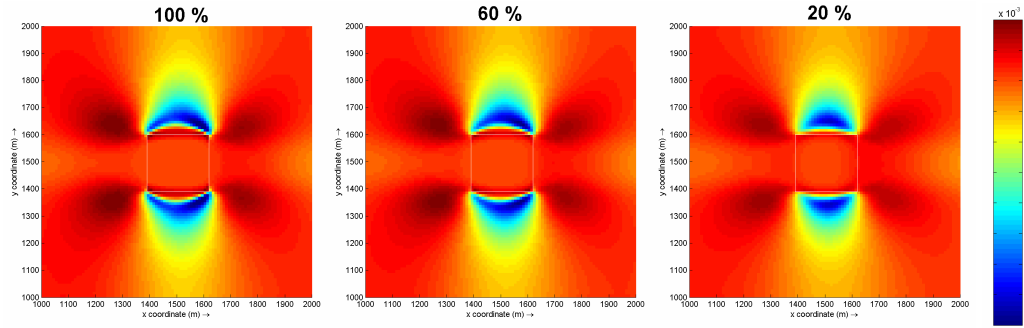


Figure 5-18: sedimentation/erosion patterns for different tree density. The white square presents the location of the mangrove forest

In figure 5.19 can be seen that as the density decreases there is more sediment transport into the forest and also more sediment transport out of the forest. This increase is non-linear. The difference between these two parameters results in sedimentation (or erosion if there is more transport out than in). This is also plotted in figure 5.19. It can be seen that the difference between transport in and transport out of the forest is increasing slowly in a non-linear way, which is a proof of the non-linearity in morphological changes.

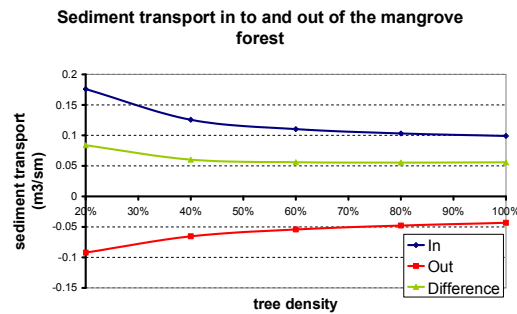


Figure 5-19: sediment transport into and out of the forest, including the differences between the two transport values. The transport out of the forest is negative

Forest length

To investigate the influence of the length of the forest on sedimentation/erosion patterns in and around overwash mangroves the square forest shape (see §5.1.2) will be increased from 200 m to 1200 m, with steps of 200 m. It is expected that with increasing forest length the velocity will stabilize along the forest resulting in no erosion alongside the forest. The erosion at the corners of the forest remains, but the erosion areas are cut into halves. It is hard to predict at which forest length this will happen. The six resulting sedimentation/erosion patterns are shown in figure 5.20.

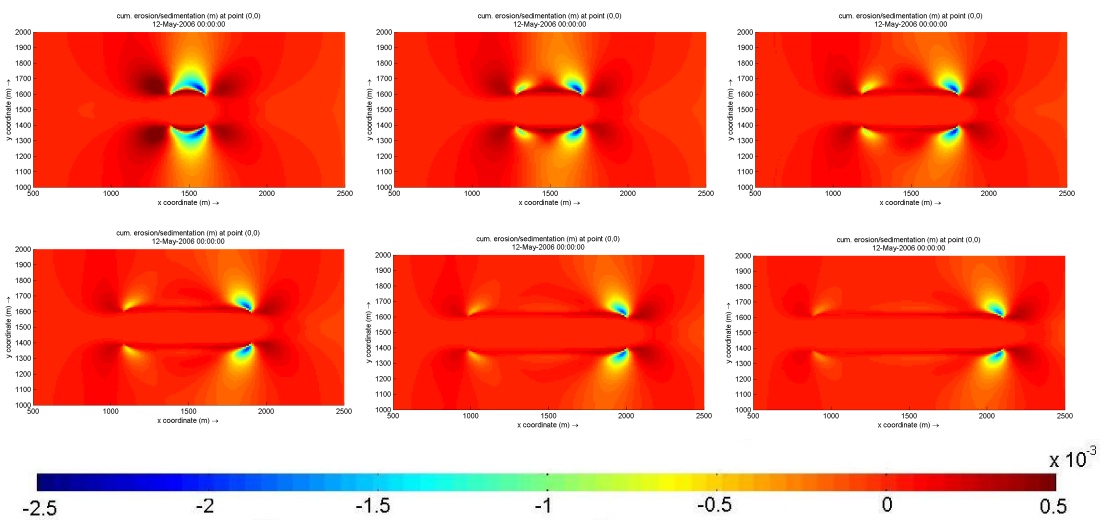


Figure 5-20: sedimentation/erosion patterns (in m) after one tide, for different forest lengths. The forest length increases from 200 m (upper left) to 1200 m (lower right)

From the sedimentation/erosion pattern the following can be observed:

- For a forest length of 400 m, the erosion spots at the corners of the forest are not connected to each other anymore.
- There is sedimentation over the full length of the forest till 800 m forest, building a levee around the forest. From 800 m this levee is not build over the full length anymore. It should be kept in mind that this is the pattern after 1 tide, and does not have to represent the long term sedimentation/erosion pattern. It is possible that after one year of morphological modelling the erosion spots at the corners are connected to each other and that the levees are build around the mangrove forest.
- The pattern remains very consistent. From the small forests in figure 5.20 it looks that the sediment that is eroded at the corners of the forest at the front (from the ‘current perspective’), is dropped at the corners at the back of the forest. This is because there is more erosion on the right side of the forest and more sedimentation on the left side (the system is a little bit a-symmetric). However, the sedimentation at the right side of the forest remains constant, while the erosion at the left side of the forest decreases. Suspended sediment transport is the driving factor of the sedimentation/erosion pattern. Figure 5.21 presents the suspended sediment transport pattern for two times during the tide, and for three different forest lengths (200, 400 and 600m). The three patterns of the upper part of figure 5.21 should be symmetric with the patterns of the lower part. This is not the case, resulting in a constant sedimentation/erosion at the right side of the forest, and a decreasing sedimentation/erosion at the left side of the forest. The cause can probably be found in the model setup. An asymmetric tide, with velocities close to the critical velocity for sediment transport, can result in these different patterns. It is already tried to move the asymmetric tide, but the attempt was not successful. The difference can also be a consequence of the morphological changes during the tide. These morphological changes can (theoretically) influence the flow velocity pattern, resulting in a different sediment transport pattern. However, bed level changes are so small that the influence on the flow velocity can result in such big differences in sediment transport patterns.

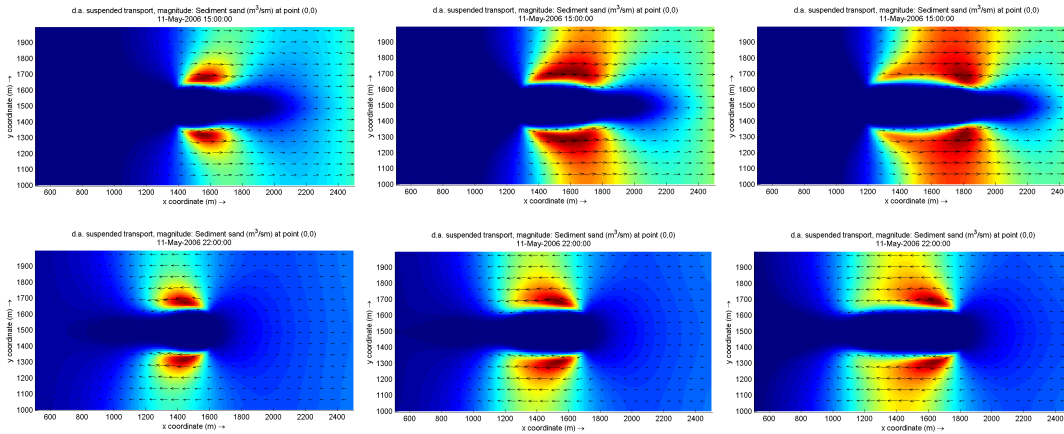


Figure 5-21: suspended sediment transport pattern for two times during the tide (22:00 first line and 14:00 second line) and three different forest lengths (from left to right: 200, 400 and 600 m mangrove forest). The pattern is important and not the magnitude, therefore the unit is not presented here.

It is difficult to say in what way the morphological development of the bottom is related to the length of the forest. I would expect more symmetric patterns at both corners of the forest, but this cannot be observed in figure 5.21. It is not clear if this represents a modelling problem, or the true morphological development. The only valid conclusion seems that after a certain forest length, the erosion along the forest is not closed anymore, resulting in slower canal shaping along the forest, on the long term.

The long term morphological development is shown in figure 5.22. The pattern is different, comparing to the 200 m forest model results (see figure 5.11). little Islands are growing at both sides of the forest. The sediment is eroded at the corners of the forest. Because the long forest length the velocity reduces a little, leading to sedimentation and a little increase in bed level. The levee along the forest is fully established. This corresponds with the study of Augustinus (1978).

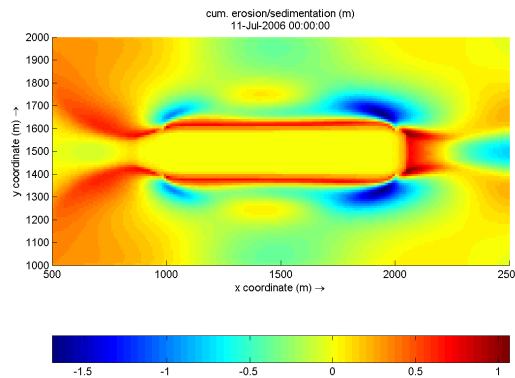


Figure 5-22: long term morphological development of the overwash mangrove case with a forest length of 1000 m (unit m).

Forest shapes

For overwash mangroves it is chosen to model the forest as a square. On the long term this resulted in a rhombus shaped forest. What the influence is of the shape of the forest on the initial morphological pattern is hard to say on forehand. To analyse the influence of the shape two other forest shapes are modelled (see also figure 5.23):

- A rhombus shaped forest of 200 m width and 400 m long
- A circle shaped forest with a diameter of 200 m

The other parameters (tree characteristics, grain sizes, bed roughness and tidal water level variant) are kept the same as the basic overwash case. The resulting sedimentation/erosion pattern of these forests, including the basic square overwash mangrove case, is shown in figure 5.24.

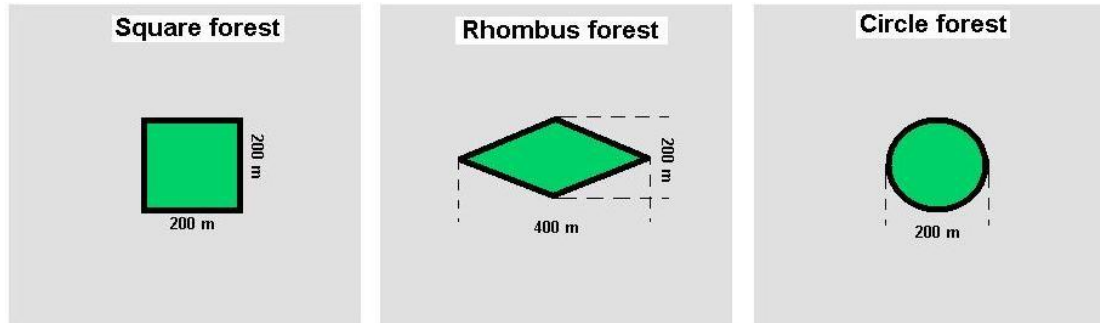


Figure 5-23: three different forest shapes which will be modelled under the same conditions as the basic model.

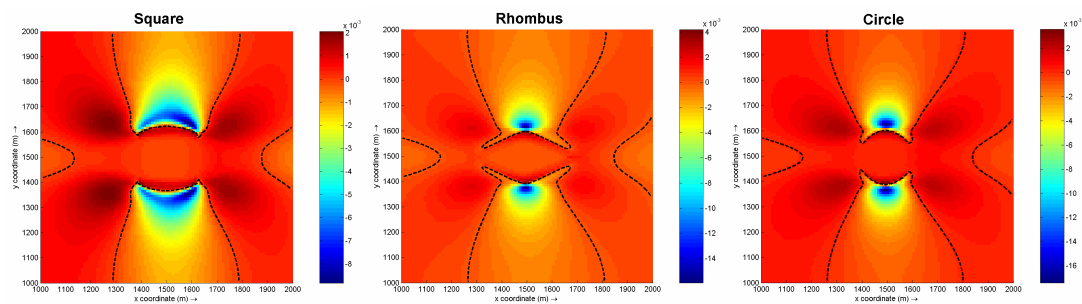


Figure 5-24: sedimentation/erosion pattern (in m) after one tide for three different forest shapes. Watch the different scales of the individual patterns

It can be seen that the square, rhombus and circle variant show the same sedimentation/erosion pattern, indicating that the pattern is not very sensitive for different forest shapes. Differences can be found in the amount of sedimentation or erosion between these three situations. The erosion is much higher and concentrated in a smaller spot for the rhombus and the circle shape forest, in comparison with the square shape forest. The sedimentation peaks at the corners of the forest can be less observed for the rhombus variant comparing to the circle and square variant. For the rhombus and the circle pattern it would be expected that the flow is less obstructed comparing to the square forest. This should lead to less or more spread sedimentation at the sides of the forest comparing to the square variant. The erosion peak should also be confined to a smaller spot, because the change in velocity is less abrupt. The rhombus variant show the expected behaviour for sedimentation: it is more spread and less levees are formed around the borders of the forest. Less levees are also formed at the borders of the circle variant, but the sedimentation peaks at the corners can still be observed. This difference can be attributed to the fact that the flow pattern cannot follow the circle, leading to more abrupt changes (and therefore more concentrated sedimentation) in comparison with the rhombus shape. For erosion the expected values are also observed in the rhombus and circle variant: a smaller area of erosion. The magnitude of erosion however is larger, comparing to the square variant.

The conclusion from modelling these variants is that the shape has influence on the sedimentation/erosion pattern. The more the shape is reflecting the velocity direction, the less sedimentation there will be at the corners of the forest.

Conclusion

The focus of this sub-paragraph was the influence of different forest parameters on morphological changes in and around mangrove forests. Tree density, forest length and forest shape are varied. Three conclusions can be drawn, corresponding to the three different variants:

- For decreasing tree density the morphological effects around the forest are decreasing and inside the forest the sedimentation is increasing. The effects are non-linear
- The longer the forest the less sedimentation or erosion occurs along the forest. On the long term little islands will develop alongside the forest, depending on the length of the forest.
- The shape of the forest has some influences on the sedimentation/erosion pattern. The more the shape is reflecting the velocity direction, the less sedimentation there will be at the corners of the forest.

5.2.4 Conclusion

This paragraph showed the results and the analysis of the sensitivity analysis. Considering the sensitivity of the modelling results to different model approaches it can be concluded that the pattern of the basic model is not sensitive for a 3D or a Wave modelling approach. Looking to the sensitivity of the modelling results to different physical parameters (wave height, wave angle, settling velocity and sediment concentration) the modelling results were highly sensitive for different wave heights and a little sensitive for different wave angles, settling velocities and sediment concentrations.

The sensitivity of the modelling results to different tree densities is that the erosion outside the forest decreased and sedimentation inside the forest increases for decreasing tree densities. The length of the forest influences the sedimentation/erosion pattern alongside the forest and the shape of the forest showed only a little influence on the general sedimentation/erosion pattern.

What should be kept in mind is that these conclusions are only valid for the non-cohesive sediment case. In most cases only the initial response of the model is assessed. On the long term the modelling results can be less sensitive or more sensitive to the same parameter. It is recommended to investigate also the sensitivity of the modelling results with cohesive sediments.

5.3 Discussion

The discussion will review modelling uncertainties, sediment transport inside the forest and another way of modelling vegetation (with a decreased Chezy value).

5.3.1 Model uncertainties

Uncertainties in modelled processes and model schematisation influence the reliability of the modelling results. There are a lot a uncertainties in the modelling set-up already. The shape of the forest, the tidal currents, the sediment properties, the tree shapes and sizes, the tidal water levels, the bathymetry etc... The uncertainties in the equations can be added to the uncertainties in the modelling set-up. How reliable will the result of the modelling experiment be?

Looking to the schematisation of the overwash mangrove case it is not really realistic to model a mangrove area on a flat bed at -2 m MSL. Mangroves always stand above mean sea level (De Vos, 2004) and a flat bed does also not occur in reality, especially where mangroves exist. The reason for the schematisation of the overwash mangrove case is given in the first paragraph of this chapter. For tidal currents the model set-up should not be a problem. The model is built in a way that the generated currents are around 1 m/s. These currents are also observed in Wolanski et al (1992) and are not overestimations.

There can be a problem in this schematisation with sediment transport. With increasing water depth there can be more sediment in the water column, which can be transported further comparing to lower water depths. This depends on the settling velocity of the sediment. The sedimentation inside the forest is probably overestimated for both non-cohesive and cohesive sediments. It is difficult to say how big the error is.

When waves are taken into account problems with the schematisation will also arise. Wave processes like wave set up, wave induced currents, wave breaking etc. (see chapter 2 for an overview of these processes) are induced by the water depth. So, increasing the water depth changes the processes, leading to another morphological development. Chapter 4 concluded that it was not possible to model morphological development of beaches due to the complex sediment transport processes generated by waves. The problems occurred in chapter 4 are not present in this chapter, for the situation with waves. However, important processes are not taken into account, which do play a role in the morphological development of overwash mangroves.

It is impossible to quantify all the uncertainties and quantify with that the reliability of the modelling results. There are so much variations possible! The sensitivity analysis however showed constant and predictable results, which increases the reliability of the results. It would be even better if measurements would be done in a mangrove forest for real validation and calibration of the model.

5.3.2 Sediment transport inside the forest

Differences in sediment transport inside the forest occur between (non-cohesive) 2D and 3D calculations (see § 5.2.1) and 2D non-cohesive and cohesive calculations (see § 5.1.3). Both differences will be elaborated below.

Differences between 2D and 3D calculations

The differences in sediment transport inside the mangrove forest (and therefore sedimentation/erosion inside the forest) between 2D and 3D calculations are large in a relative way (see figure 5.12). The differences can be attributed to the different ways in which suspended sediment transport is calculated. For 3D calculations the three dimensional advection/diffusion equation is used (see §2.1). In 2D calculations a depth averaged version of the 3D advection/diffusion equation is used:

$$\frac{\partial c_s}{\partial t} + \alpha_u \left(u \frac{\partial c_s}{\partial x} + v \frac{\partial c_s}{\partial y} \right) + \frac{\partial}{\partial x} \left(\varepsilon_x \frac{\partial c_s}{\partial x} \right) + \frac{\partial}{\partial y} \left(\varepsilon_y \frac{\partial c_s}{\partial y} \right) = \frac{c_{se} - c_s}{T_s} \quad (5.4)$$

where:

c_s = the sediment concentration

α_u = coefficient for the vertical sediment concentration gradient

ε = horizontal eddy diffusivity

c_{se} = equilibrium concentration of suspended sediment

T_s = adaptation time for vertical sediment concentration profile

The vertical elements in the 2D equation are replaced by the parameters α_u and T_s . This is the first difference between a 2D and 3D approach. The second difference is the calculation of the eddy diffusivities. In the 3D model the $k-\varepsilon$ turbulence model is used to calculate the eddy diffusivity in horizontal (x and y) and vertical (z) direction. For 2D calculations the horizontal eddy diffusivity need to be specified by the user. In the calculations it is chosen to set the eddy diffusivity to 1. By enlarging the eddy diffusivity there is more diffusive sediment transport and there will also be sediment transport (and sedimentation or erosion inside the forest). This is shown in figure 5.25 where the sedimentation/erosion pattern can be seen, calculated with an eddy diffusivity of 10. The white square represents the mangrove forest.

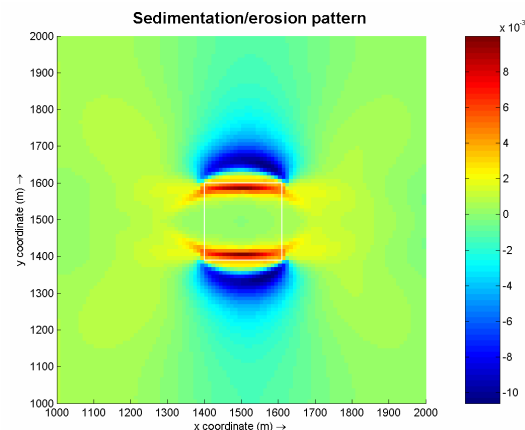


Figure 5-25: Sedimentation/erosion pattern (unit: m) for a 2D-non cohesive setting with an eddy diffusivity set to 10. The white square represents the mangrove forest

Differences with the basic non-cohesive model are large. It can be seen that the sediment is deposited more inside the forest and also about 3 times higher (comparing to the basic model, see figure 5.9). Also the sedimentation/erosion pattern is different. The results show the importance of this parameter and the impact of it on the modelling results. In the initial

Delft3D setting for 2D calculations this parameter is set to 10. Comparing the 2D modelling results where this parameter is set to 1, to 3D calculations (§ 5.2.1), there are not much differences observed outside the forest, indicating that the value 1 is more representative comparing to a value of 10. In this case advective transport governs the suspended sediment transport. Inside the forest differences between sediment transport and sedimentation are (relatively) large. This can be attributed to the decrease in flow velocity and advective transport. Diffusive transport becomes more important. Based on these observations it is recommended for 2D calculations to specify the eddy diffusivity for each grid-cell, with high diffusivities inside the forest and low diffusivities outside the forest. The importance of this parameter for 2D sediment transport calculations should not be underestimated.

Cohesive and non-cohesive differences

Considering the sediment transport inside the forest the most important factor responsible for the differences between cohesive and non-cohesive sediments is the settling velocity (assuming the same hydrodynamic forcing). Figure 5.26 shows the differences between tide averaged suspended transport for high settling velocity (3.1 mm/s, the same as sand, see § 4.2.1) and low settling velocity (0.25 mm/s, the initial Delft3D value). The differences between sediment transport inside the forest can be seen very clearly, showing the influence of the settling velocity on sediment transport (see also § 5.2.2). Hardly any sediment transport inside the forest occurs in the case of a high settling velocity.

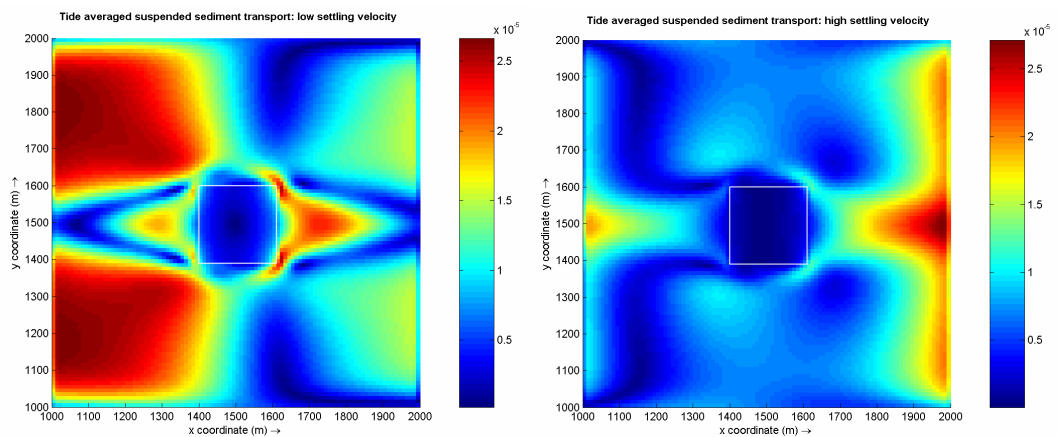


Figure 5-26: tide averaged suspended sediment transport pattern (unit: $m^3/s/m$) for low and high settling velocities (in case of non cohesive sediments). The white square represents the mangrove forest

5.3.3 Modelling vegetation

In this modelling experiment vegetation is modelled as a group of parallel, staggered or randomly arranged rigid vertical cylinders with homogeneous properties. The resistance force is defined as:

$$F_p = \frac{1}{2} \rho \int_0^k C_D(z) m(z) D(z) |u(z)| u(z) dz \quad (5.5)$$

Where F_p is the vegetation friction force, C_D the drag coefficient, m the cylinder density, D the cylinder diameter and k the height of the cylinder.

Baptist et al. (2005), describe two ways of modelling vegetation. One of them is the above standing method, the other one is modelling vegetation as an increased bed roughness. The question raises: what is the difference in result between both modelling approaches? And which one is better? Baptist et al (2005) concluded that both approaches are able to model the remote effects of vegetation (redirection of the flow with erosion or sedimentation as a consequence), but that the local effects (very close or inside the vegetation field) cannot be modelled well with the increased bed roughness approach. They state that the sediment transport is overestimated with this approach, because bed roughness is increased, resulting in increased bed shear stress, leading to more sediment transport. By replacing the mangrove forest with a decreased Chezy value of $8 \text{ m}^{1/2}/\text{s}$, this hypothesis is tested. The results are shown in figure 5.27.

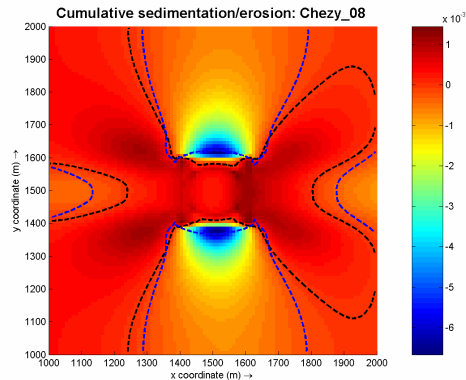


Figure 5-27: sedimentation/erosion pattern (in meters) after one tide, when vegetation is modelled as an increased bed roughness. The black dotted line indicates the difference between erosion and sedimentation in the Chezy sedimentation/erosion pattern. The blue dotted line indicates the sedimentation/erosion pattern when vegetation is modelled as cylinders.

From figure 5.27 it can be concluded that the remote effects of the vegetation are modelled in a comparable way (looking to the pattern, and not to the magnitude of the process). The results show that the Chezy coefficient could probably be something lower in order to get better results. This is however not the focus of this research and therefore it will not be done. Figure 5.27 indicates that the conclusion of Baptist et al (2005) on modelling the remote effects of vegetation can be modelled with both approaches.

Looking to the local effects two differences can be noticed:

- No levees at the sides of the mangrove forest are formed when mangroves are modelled as increased bed roughness
- The shape of the erosion pattern near the forest goes into the forest when mangroves are modelled as increased bed roughness and stays out of the forest when mangroves are modelled as cylinders.

The local differences also indicate that the hypothesis of Baptist et al (2005) can also be applied for mangrove forests.

5.4 Conclusion

This chapter tried to model the overwash mangrove case, to increase insight in the morphodynamics in and around mangrove forests. The main question was:

How can the overwash mangrove forest be modelled and what conclusions can be drawn considering the influence of mangroves on morphodynamics?

First a basic model is constructed for the overwash mangroves. It can be concluded that the overwash mangrove forest can be modelled in a satisfactory way, because:

- The hydrodynamic modelling results (water levels and flow velocities inside the forest) are comparable and in the range of the validation criteria.
- The morphological development based on aerial photographs is comparable with the modelling results. The levee building in the case of non-cohesive sediments can also be found back in the literature (Augustinus, 1978). Sediment accretion inside the forest occurs and sediment concentration for both non-cohesive and cohesive sediments are in the range of reported values.

Secondly a sensitivity analysis is carried out to justify the made simplifications in modelling approach and analyse the influence of both physical and biological parameters. The sensitivity analysis is carried out using the basic non-cohesive model. It can be concluded that the modelled morphodynamic pattern is not sensitive for another modelling approach. Considering the physical parameters there is a high sensitivity of net sediment transport into and out of the forest for wave height. The results are less sensitive for different wave angles, settling velocities and sediment concentrations. The sensitivity of the modelling results to different tree densities is that the erosion outside the forest decreased and sedimentation inside the forest increases for decreasing tree densities. The length of the forest influences the sedimentation/erosion pattern alongside the forest and the shape of the forest showed only a little influence on the general sedimentation/erosion pattern.

What should be kept in mind when drawing these conclusions is that the used bathymetry is not very realistic, leading to an overestimation of the sediment transport. Besides this, the user specified eddy diffusivity for 2D calculations has a large influence on the modelling results, especially inside the forest.

The most important influence of mangroves on morphology is that mangroves trap sediments by a reduction of erosion and an increase in sedimentation due to reduced currents.

6 Mangrove management

The objective of this research is to increase insight in morphodynamics in and around mangrove forests (see chapter 1). To widen the scope of this research it is tried to find implications for coastal zone management using this modelling experiment. The following research question can be asked:

Which possible implications for coastal zone management considering the influence of mangroves on hydrodynamic and morphodynamic processes can be drawn from this modelling experiment?

One of the definitions of coastal zone management is (Hoozemans, 2004): *To analyse the autonomous coastal processes and their interaction with the human activities with a view to develop the best strategy for management of existing and development of future activities.* Mangroves play a role in the first part of this definition: the autonomous coastal processes. The first sub-question refers to this influence:

- a) What are the impacts of mangroves on hydrodynamical and morphological processes along coastlines? (§6.1)

The second sub question refers to the interaction of human activities on the autonomous coastal processes along mangrove coastlines:

- b) What is the impact of human activities on mangrove coastlines? (§6.2)

In the conclusion (§6.3) the answers on the sub questions are summarised and it is tried to find an answer to the main question of this chapter.

6.1 Impact of mangroves on coastlines

6.1.1 Time scales of processes

Characteristic about hydrodynamical and morphological processes along coastlines is that they occur on different timescales. In general five different geomorphological processes corresponding to five different timescales can be distinguished (after Woodroffe, 1992). They are presented in figure 6.1. The ecological processes in mangrove forests also occur on different timescales, interacting with the geomorphological processes occurring on the same time scale. Twilley et al., (1998) defines six processes, which are also shown in figure 6.1.

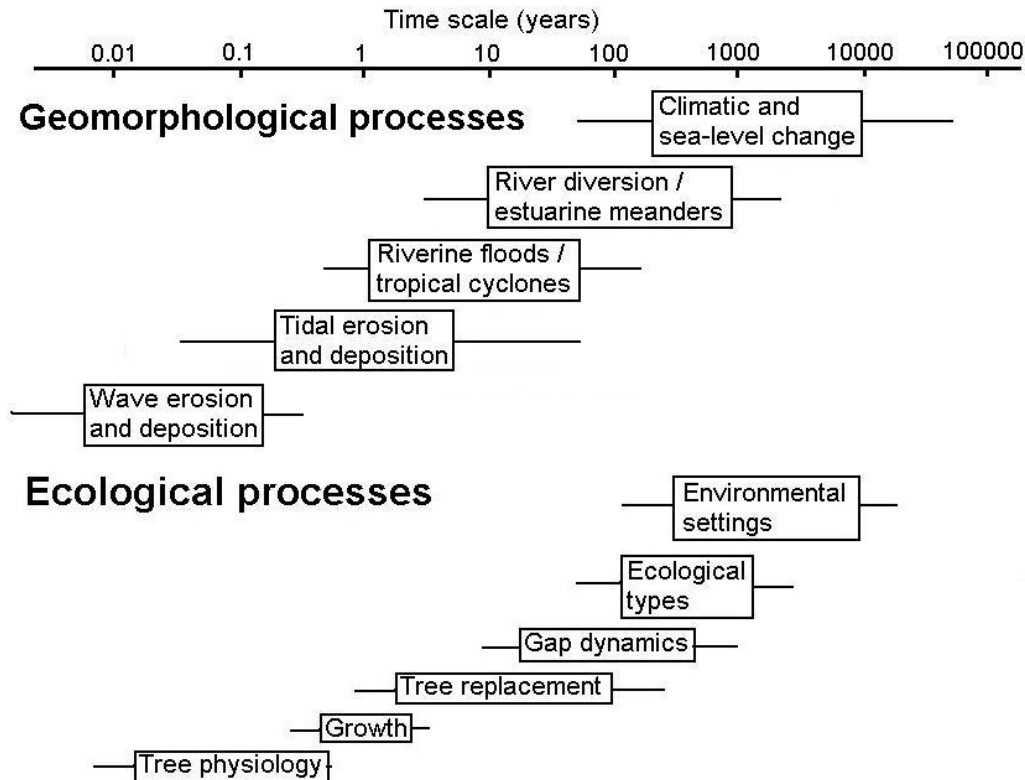


Figure 6-1: timescales of different geomorphological and ecological processes (after Woodroffe, 1992 and Twilley et al., 1998)

6.1.2 Influence of mangroves on waves and tides

During modelling the interaction between mangroves and hydrodynamics or mangroves morphodynamics is not taken into account. The mangrove forest can be seen as static structure in the model influencing both processes. Looking to figure 6.1 it can be seen that the relevance of this model is on timescales smaller than about 10 years, because a uniform forest is used (no gap dynamics, ecosystem changes of environmental setting changes). Therefore it is only useful to assess the possible influences of mangroves on floods/cyclones, tidal erosion/deposition and wave erosion/deposition with the used model.

In this modelling experiment the influence of mangroves on sediment erosion and deposition due to waves and tides is analysed. From literature it is known that mangroves attenuate waves. Table 3.5 shows a wide range of wave attenuation with an average value r (wave attenuation per 100 m forest) about 50%. Wave attenuation is taken into account during modelling. The impact of the reduction in wave height can be seen in chapter 4 for the fringe mangrove forest and § 5.2.1 for the overwash mangrove forest. Due to the reduction in wave height, sediment is deposited.

Looking to the fringe mangroves, the tidal water level variations are responsible for the location of erosion or deposition due to waves. Cross-shore tidal currents are so small that they do not affect the erosion process. Considering the sediment deposition cohesive sediment (eroded by waves) is transported much further inside the forest, because of the low settling velocities. This leads to a general sediment accretion inside the mangrove forest. For

non-cohesive sediments the tidal currents are not able to transport the sediment far, so it is deposited at the sea-side of the forest, leading to levees. The levees are a combination of the low cross-shore velocities and the reduction of the wave action inside the forest. Levees around fringe mangroves are also reported by Augustinus (1978) for the Surinam coastline.

The effect of long shore currents can be seen well in the overwash mangrove case. At the lee sides of the forest sedimentation takes place for both cohesive and non-cohesive sediments. This corresponds with the aerial photographs showed in § 5.1. The mangroves stabilize the island and are even responsible for expansion of the island. Considering cohesive sediments there is high and uniform sedimentation inside the forest, For non-cohesive sediments levees are formed in line with the long shore currents (see also Augustinus, 1978).

One important implication for coastal zone management can be derived from this modelling experiment (underlined by observations from literature). Mangroves stabilize coastlines by reducing wave height and flow velocity, leading to sedimentation around and inside the forest and a reduction of the erosion.

6.1.3 Influence of mangroves on storms

Mangroves are very stable trees and can withstand huge floods and cyclones, with the advantage of coastal protection. The recent tsunami attack of 26th December 2004 proves this statement (Dahdouh-Guebas et al., 2005, Vermaat and Thampanya, 2006). Mazda et al., (1997) underline the coastal protection function of mangroves by assessing the wave attenuation by mangroves and showing. They conclude that the wave reduction of full grown mangroves over 100 m was as large as 20%.

It is tried to model the impact of a mangrove coastline on the resulting water levels due to the tsunami, in order to gain some insight in the effect of mangroves. Therefore a profile model (1DV) is constructed, with a 200 m mangrove fringe, starting at MSL. The trees are modelled as a single stem with a diameter of 10 cm and 1 tree per m². The water levels occurring during the tsunami of 26 December 2004 are a boundary condition for the water levels in the model. The effects of mangroves on the water levels are shown in figure 6.2. It can be seen that mangroves are blocking the water (see also Wu et al., 2001 for blocking effects). Some water is slowly getting through the forest and the other water is bounced back to the sea. This leads to lower water levels and less penetration of the water levels on the shore. The impact of this forest on the resulting water levels (not shown in figure 6.2) was more than 1000 m (compared to the without mangrove situation). Because of the simplifications in modelling, like that trees can resist the tsunami force and the tree schematisation, this conclusion is questionable. However, the generally accepted view that mangroves protect coastlines is underlined by this modelling result.

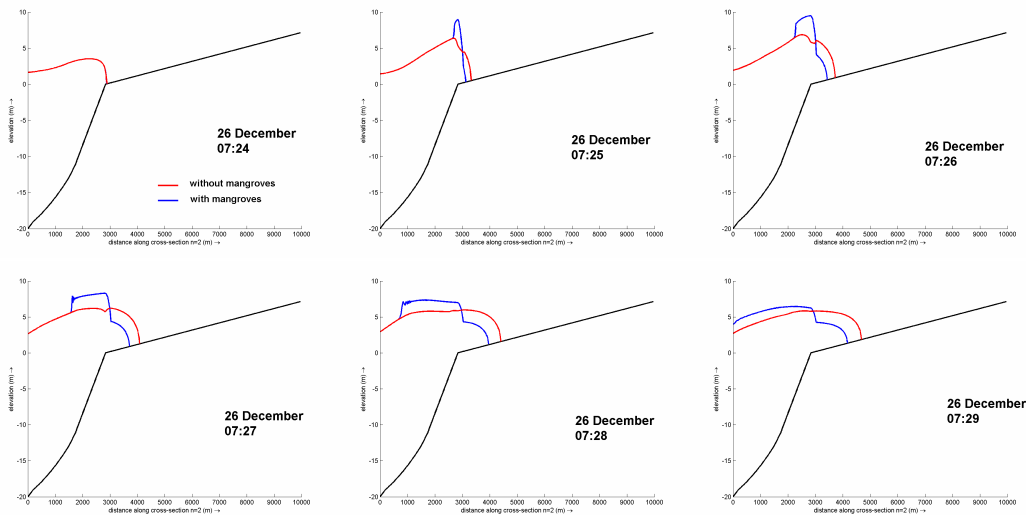


Figure 6-2: influence of mangroves on water levels during the 26th December 2004 tsunami. The pictures are 1 minute behind each other. The red line represents the water levels without mangroves and the blue line with mangroves, the black line shows the bed level

Dahdouh-Guebas et al (2005) make another remark about the protection function of mangrove forests. They state that by clearance and re-growth of mangroves infusion of non-mangrove species can take place. These non-mangrove species can resist less friction and shear stress comparing to mangrove species, resulting in less coastal protection.

The resistance effect of mangroves to occurring shear stress, is not modelled in this study, but by translating mangrove resistance into a critical shear stress it should be possible to take this effect into account. Mangroves can withstand higher shear stresses than non-mangrove species.

6.1.4 Conclusion

This paragraph analysed the impact of mangroves on coastlines. The main conclusion that can be drawn, using the modelling experiment is that mangroves stabilize coastlines due to a reduction of the erosive force by waves and a reduction of the tidal currents. Because of the reduction in tidal currents more sedimentation will take place inside the forest. Mangroves also offers protection to floods and cyclones. By the stabilizing and the reduction effect of mangroves, they play an important role in safety issues of coastal management.

6.2 Human impacts on mangrove coastlines

Humans have had a big devastating impact on natural ecosystems throughout the world. Ecosystems are degraded and destroyed for human well being (Dahdouh-Guebas 2005). Already expressed in § 6.1, mangroves ecosystems are not an exception to this fact. Shortly the effects of human are:

- Wood cutting (Armitage, 1994, EJJ, 2006))
- Constructing fishponds/shrimp farms (Winterwerp et al, 2005, WRM, 2002, EJJ, 2006))
- Land reclamation (EJJ, 2006)

- Diversion of fresh water (EJF, 2006)
- Dam construction, which reduces sediment availability and can lead to erosion (Winterwerp et al. 2005)
- Oil and gas exploitation, which can lead to subsidence and spilling can lead to a direct pollution of mangrove forest (WRM, 2002)
- Dredging can lead to too high sediment concentrations in the water column and too high sedimentation rates in the mangrove forest (WRM, 2002)
- Building tourist resorts in mangrove areas (EJF, 2006)

Figure 6.3 gives an overview of the amount of loss of mangrove forests due to the different impacts. By these losses the stabilizing and protective effect of mangroves, concluded in the previous paragraph, is also reduced. An example of human impacts on mangrove coastline is given by Winterwerp et al. (2005). He describes a pilot study on the erosion and rehabilitation of a mangrove mud coast, where he couples the erosion to the shrimp farm construction.

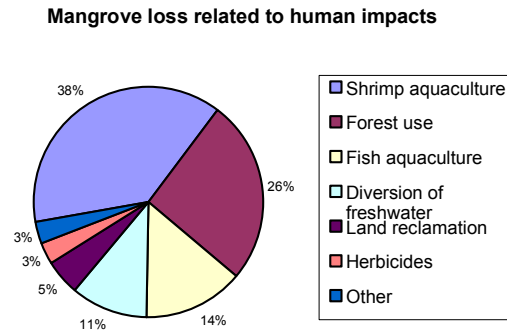


Figure 6-3: area of mangrove habitat destroyed worldwide by different human activities (EJF, 2006)

Winterwerp et al., (2005) identifies the construction of fish and shrimp ponds (protected with a levee at the sea side) as the main cause of erosion. The levees of the shrimp ponds reduce the onshore sediment transport by tidal filling, due to the significant decreased cross-shore flow velocity component, while the long shore component stayed constant. The coastline is not filled up with sediment any more and the sediment that stays in the water column is only transported long shore. This leads to erosion of the coastline. Figure 6.4 shows this present situation. The former situation, without shrimp or fish ponds, has a much higher cross-shore velocity component, leading to the filling of the coastline. A solution is found in the increase in cross-shore flow velocity by replacing the dikes of the shrimp farm and the decrease of long-shore flow velocity by construction groynes. This is also sketched in figure 6.4.

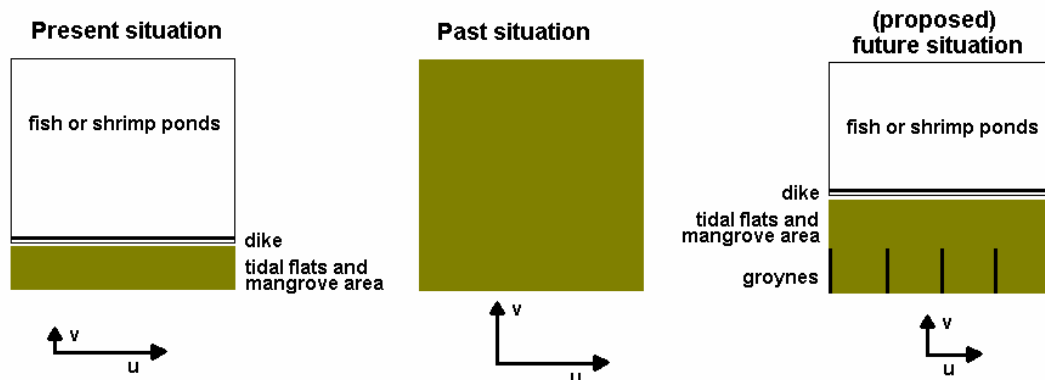


Figure 6-4: sketch of past, present and (proposed) future situation in the study area (Ban Kun Thien). u and v represent the long-shore and cross-shore currents and sediment transport components, respectively.

This is just an example of what the effects of human impacts on coastlines can be. By removing mangroves, the coastline is destabilised and erosion will take place. Modelling can be a useful tool for the ‘coastal zone manager’ in getting insight in the effects of removing mangroves from a coastal zone. The Delft3D model showed his ability (in chapter 4 and 5) to take into account the mangrove vegetation (in a 3 dimensional way) in morphological modelling.

In appendix G some general management issues are described and a detailed analysis is carried out on the effects of overwash and fringe mangroves on hydrodynamics in order to gain general insights, useful for the ‘coastal zone manager’. From this analysis can be concluded that:

- The effect of mangroves on water levels is not significant
- The effect on flow velocity is significant, resulting in an increase outside both the fringe and overwash forest, and a decrease inside the overwash mangrove forest. The increase in cross-shore flow velocity for fringe mangroves depend on the incoming velocity. The decrease in flow velocity for overwash mangroves is not

related to incoming velocity or tree density. it can be approximated with $\frac{1}{\sqrt{(0.05x)}}$

6.3 Conclusions

In this chapter it is tried to answer the following research question:

Which possible implications for coastal zone management considering the influence of mangroves on hydrodynamic and morphodynamic processes can be drawn from this modelling experiment?

The following implications can be derived:

- Mangroves stabilize the coastline by reducing erosion due to a reduction in wave height and tidal currents. They also increase sedimentation due to a reduction in flow velocity
- Mangroves can serve as a protection to tsunamis, because of their ability to reduce wave heights and currents
- Humans have a large devastating impact on mangrove coastlines, reducing the positive effects of mangroves on coastlines
- The Delft3D model can be a useful tool in analyzing the effects of human construction along mangrove coastlines.

7 Conclusion and Recommendation

This chapter summarises the conclusions from other chapters, by answering the research questions. The conclusions are followed by some recommendations, based on the discussion described in chapter 4 and 5.

7.1 Conclusions

Mangrove forests cover large parts of the tropical and subtropical shorelines in the world, and are of great economical and biological importance. The recent devastating tsunami attack (26 December 2004) increased the interest in mangrove shorelines by showing their ability to protect coastal regions. The mangrove ecosystem is constructed over a long span of time, through feedback processes including biotic activity, landform evolution and water flows (Mazda et al, 2005). This interactive system was the focus of this study. The research objective is:

To get insight in the morphodynamics in and around mangrove forests, as the result of the combined processes of waves and currents, by modelling the system in Delft3D.

Because it is too complex to model the whole interactive system ‘only’ the influence of mangroves on hydrodynamics and waves and the feedback processes between hydrodynamics, waves and morphodynamics are taken into account. This is shown in figure 7.1. The research is further confined to fringe and overwash mangroves. Four research questions lead to more insight in the morphodynamics in and around mangrove forests. They will be discussed below.

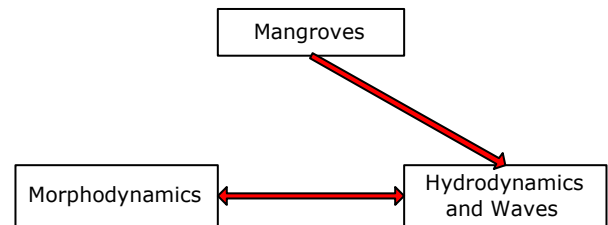


Figure 7-1: modelled interactions between mangroves, hydrodynamics and morphodynamics

7.1.1 Question I

Which processes and parameters control morphological changes on (mangrove) coastlines and what is the effect of mangroves on these processes and parameters (qualitatively)?

Chapter 2 describes many parameters and processes. Morphodynamics describes the feedback system of hydrodynamics, sediment transport and bottom changes. For suspended sediment transport the most important parameters are 1) sediment concentration, 2) flow velocity, 3) eddy diffusivity and 4) the settling velocity. Bed load transport depends on the flow velocity, keeping in mind that a minimum critical velocity should exist to move the sediment. The first three parameters depend on a number of processes. When waves are taken into account the number of processes increases, resulting in a complex situation.

The influence of vegetation can be taken into account in the momentum equation by expressing the vertical distribution of the friction force per area caused by the stems of the vegetation:

$$F(z) = \frac{1}{2} \rho C_D D(z) m(z) |u(z)| u(z) \quad (7.1)$$

Where F_p is the vegetation friction force, C_D the drag coefficient (most of the time set to 1), m the stem density, D the stem diameter and u the flow velocity. The continuity equation is corrected for the cross-sectional area of the vegetation. Water levels and flow velocities are influenced and new balances will be established. Interesting is the conclusion of Baptist (2005) who states the flow velocity u_v inside a vegetation field will be uniform over the depth and can be determined with:

$$u_v = \sqrt{\frac{2gi}{C_D m D}} \quad (7.2)$$

Where i is the water level gradient. Vegetation also influences turbulence (the eddy diffusivity) which can be taken into account in the k - ϵ turbulence model. It is difficult to say if vegetation leads to extra turbulence, because turbulence is a combination between kinetic turbulent energy and energy dissipation. Both will increase in a vegetation field, so the net effect depends on the situation. In general it can be said that high turbulence leads to flatter sediment concentration gradients and more spreading of sediment in the water column.

The effect of vegetation on waves can be taken into account with the vegetation friction factor (a modified Collins friction factor (De Vries and Roelvink, 2004)):

$$c_v = f_w D n dz \quad (7.3)$$

Where c_v is the vegetation friction factor, f_w a friction factor and dz is the height of the vegetation. With this factor the energy dissipation S over a vegetation field can be calculated, resulting in wave attenuation:

$$S = c_v \rho U_{orb}^3 \quad (7.4)$$

where U_{orb} is the orbital velocity at the bottom and ρ the density of water. It should be kept in mind that the influence of vegetation on orbital velocity is connected to the influence of wave height. The reduction in wave heights lead to reduced orbital velocity, but the vegetation field can reduce the orbital velocity near the bottom more than would be expected of the effect on the wave height.

A remark which should be made is that there are difficulties in modelling sediment transport under waves at shorelines. Two conceptual models give more insight in the cross-shore sediment dynamics due to waves and can be used as validation criteria:

- Masselink et al (2006) for non cohesive sediments
- Shi and Chenn (1996) for cohesive sediments

7.1.2 Question 2

What is known about coastal morphology, tidal water levels, tidal currents, waves, and sediments in and around mangrove forest, and vegetation characteristics to parameterize mangrove trees?

To get a feeling with the processes and parameters that play an important role and are analysed with the previous question, processes and parameters are quantified. This information can serve as validation criteria or can be used in the model setup. Table 7.1 gives a possible range of several processes and parameters. The ranges represent values from literature for different situations. Table 7.1 illustrates how different mangrove shorelines can be.

Table 7-1: ranges of important parameters and processes

Process or parameter	unit	range
Tidal ranges on mangrove coastlines	m	1.3 – 3
Tidal currents in mangrove forests	cm/s	1.2 – 10
Wave heights on mangrove coastlines	m	0.10 – 0.20
Wave attenuation inside mangrove forest	r	0.05 – 1.1
Sediment concentration in front of mangroves or in tidal creeks	mg/l	80 – 400
Sediment grain sizes inside mangroves	µm	20 – 200
Sediment accretion inside mangrove forest	mm/yr	-11 – 30
Number of roots	m ⁻²	46 – 74
Root diameter	cm	2.5 – 2.9
Gradient mudflat	-	1/200 – 1/1000
Gradient mangroves	-	1/50 – 1/1000

The ranges are very wide, showing that every mangrove forest situation is unique. This makes it difficult to check the modelling results on their validity. However, some general remarks can be made:

- Tidal currents inside mangrove forest are in the order of cm/s
- Wave heights on mangrove coastlines are low (< 20 cm), wave attenuation due to mangroves is between 20% and 50%
- High suspended sediment concentrations are observed in and around mangrove forests (max 400 mg/l)
- Grain sizes inside mangrove forests are low (between 20 and 200 µm)
- The order of magnitude for sediment accretion is mm/yr

It was the objective that with this quantification a ‘general mangrove forest’ could be constructed, but because of the wide range in values and the little literature for some parameters, a ‘general mangrove forest’ could not be constructed.

7.1.3 Question 3a

How can the fringe mangrove forest be modelled and what conclusions can be drawn considering the influence of mangroves on morphodynamics?

This question can be divided in a ‘model building’ part and a ‘sensitivity analysis’ part. It is only useful to do the ‘sensitivity analysis’ part if the other part is successfully completed. For fringe mangroves this was not the case, which will be explained.

The ‘model building’ part can be separated into four steps: validation criteria, model building, analysis and conclusion. The conclusions for both non-cohesive and cohesive sediments are:

- Non-cohesive: going back to the validation criteria it can be seen that neither the conceptual model of Walsh and Nittrouer (2004) nor the conceptual model of Masselink et al (2006) resembles the modelling results. The conclusion should be that the fringe mangrove case with non-cohesive sediments is not modelled in a satisfactory way. The difficulty is the high bed load sediment transport due to waves.
- Cohesive: looking to the validation criteria (conceptual model of Walsh and Nittrouer (2004) and Shi and Chenn (1996)) it should also be concluded that the criteria are not met, making the modelling results less reliable. The cause is probably the high sediment concentrations under waves, which are transported by tidal currents.

It looks like the balance between sediment transport processes due to waves is not well understood for both cohesive and non-cohesive sediments, leading to erroneous results. However, the hydrodynamics of the fringe mangrove forest can be modelled well (see appendix C). Also the reducing capacity of mangroves on currents and waves can be seen in modelling, leading to sedimentation inside the mangrove forest. This shows the trapping of sediments effect inside the forest. Because of the unsatisfactory modelling results it remains the question if the sedimentation process inside the mangrove forest is not influenced by the other errors in sediment transport.

7.1.4 Question 3b

How can the overwash mangrove forest be modelled and what conclusions can be drawn considering the influence of mangroves on morphodynamics?

Here also the question can be divided into a ‘model building’ part and a ‘sensitivity analysis’ part. Considering the ‘model building’ part the conclusion is that the hydrodynamic modelling results show the same features as the hydrodynamic validation criteria. These features are a lag in water levels (Wolanski et al., 1992) and decrease in flow velocity inside the forest according to Baptist (2005). It can be concluded that the hydrodynamics are modelled satisfactory. Considering the morphodynamics, there is sedimentation inside the forest for cohesive sediments and just at the border of the forest (till 40 m inside) for non-cohesive sediments. In this way the general validation criterion of sediment accretion in mangrove forests is met for both sediment types. The long term development represents also

the expected behaviour of overwash mangroves (based on aerial photographs): a cone shaped extension of the overwash island in the direction of the current. In the case of non-cohesive sediments, levees are formed around the forest, corresponding to the observations made by Augustinus (1978).

In the sensitivity analysis the sensitivity of the modelling results to a different modelling approach, different physical parameters and different biological parameters is analysed. Considering another modelling approach the sedimentation/erosion pattern was not sensitive for a '3D approach' or a 'wave approach. The magnitude of the sedimentation and erosion however showed a high sensitivity for different wave heights. Other analysed physical parameters are wave angle, sediment concentration and settling velocity. A little sensitivity of the modelling results was observed for different values of these parameters.

In the case of different biological parameters, the sensitivity of the modelling results to different tree densities is that the erosion outside the forest decreased and sedimentation inside the forest increases for decreasing tree densities. The length of the forest influences the sedimentation/erosion pattern alongside the forest and the shape of the forest showed only a little influence on the general sedimentation/erosion pattern.

The most important conclusion for overwash mangroves is that they are very efficient in trapping sediment by their capacity to reduce erosion and increase sedimentation, as a consequence of the reduction in tidal currents.

7.1.5 Question 4

Which possible implications for coastal zone management considering the influence of mangroves on hydrodynamic and morphodynamic processes can be drawn from this modelling experiment?

In general can be said that mangroves have a stabilizing effect on the coastline by their reducing capacity on waves and currents, leading to a reduction in erosion and more sedimentation. They can also play an important role as a protection to tsunamis or cyclones, by their ability to reduce wave heights and currents. Humans have a large devastating impact on mangrove coastline. Shrimp farm construction is the largest contributor to the worldwide reduction in mangrove forests, responsible for 35% of the total reduction.

7.1.6 Generally

The objective of this research was to gain insight in the morphodynamics in and around fringe and overwash mangrove forests. It is shown that the effects of mangroves on the hydrodynamics and morphodynamics can be modelled in a satisfactory way with Delft3D. The most important and general insight from this model study is that mangroves trap sediments, by reducing erosion and increasing sediment due to a reduction in wave action and tidal currents. The consequence for coastal management is that mangroves stabilize coastlines and offer some protection against floods, storms and tsunamis.

7.2 Recommendations

Based on the discussion of the modelling results described in the chapters 4 and 5 the following recommendations can be given:

1. *Model validation* → during modelling it became clear that there is a shortage of measurements of specific locations to really validate the model. The sensitivity analysis showed that the sedimentation/erosion pattern is only sensitive for the type of sediments. This implies that with relatively little measurements (bathymetry, water level variation, tree characteristics and sediment type) the hydrodynamics, sediment dynamics and sedimentation/erosion pattern can be modelled. Model validation should lead to more confidence in the modelling results. To validate the model it is recommended to go to a specified mangrove forest location and measure flow velocities inside and outside the forest (especially on locations where high velocities are expected), sediment concentrations, bed load transport and sediment accretion inside and outside the forest. At this moment (September 2006) a PhD research is carried out at the Vrije Universiteit van Brussel (the Mangrove Management Group) to propagule (seed of mangroves) transport inside and outside mangrove forest. One of the objectives is to model the propagule transport, so a hydrodynamical model is needed as a boundary condition for this transport. Together with the VUB a hydrodynamical model can be developed using Delft3D. This can be used for both propagule transport and sediment transport. This is a great opportunity to validate the Delft3D model for mangrove shorelines using the vegetation module.
2. *Modelling sediment transport under waves* → for the fringe mangrove forest it was concluded that sediment transport under waves for both cohesive and non-cohesive sediment did not show reliable results. For non-cohesive sediments bed load transport due to waves (streaming) was a problem, for cohesive sediments the high concentrations of sediment seemed erroneous. In the discussion of chapter 4 another transport equation (Van Rijn 2004) is used for the non-cohesive situation in the attempt to get better results. The results with this equation showed a less high bed load transport and generated better results. It is recommended to use more different sediment transport equations in order to get better results for both cohesive and non-cohesive sediments.
3. *2D and 3D modelling* → in chapter 5 it is chosen to model the ‘basic overwash’ case in 2 dimensions. The effect of 3D modelling is analysed in § 5.2.1 and discussed in § 5.4.2. It became clear that the most important difference between 2D and 3D sediment transport modelling can be found in the determination of the diffusive suspended sediment transport. The largest observed differences can be found inside the forest, because there the suspended sediment transport depends on diffusion. In 2D calculations this effect can be taken into account by specifying higher eddy diffusivities inside the forest. Because 2D modelling decreases computation time about 20 times compared to 3D calculations, it is recommended to analyse the differences between 2D and 3D more thoroughly. The result should be a way to calculate an eddy diffusivity, based on tree characteristics, which can be used in the Delft3D model calculations.

4. *Modelling vegetation* → the approach to model vegetation as a group of parallel, staggered or randomly arranged rigid vertical cylinders with homogeneous properties, seems promising. Besides some validation in the flume (scale: 10^1) this approach is not much used in modelling large scale (10^2 - 10^3) situations (Temmerman et al, 2005). Baptist (2005) has showed the possibilities of this approach for rivers and Temmerman et al (2005) applied this method to a tidal marsh system. Both applications of this approach showed promising results. It is recommended to do more research to this approach on large scale situations. This can be done by the application of this approach to mangrove forest situations (larger scale than tidal marshes). In this way this recommendation can be connected to recommendation 1.

5. *Ecosystem modelling* → this study modelled the influence of mangroves on hydrodynamics, and the interaction between hydrodynamics and morphodynamics. However hydrodynamics and morphodynamics influence also the locations of mangroves. It is recommended to do more research to this influence in order to define rules (in terms of inundation time (a combination of bed level and water level) and maximum bed shear stress) where mangrove trees can stand. In this way the full interactive system between mangroves, morphodynamics and hydrodynamics can be modelled (see figure 1.1).

References

- [Anthony, 2004] Edward J. Anthony (2004), Sediment dynamics and morphological stability of estuarine mangrove swamps in Sherbro Bay, West Africa, *Marine Geology*, 208, pp. 207-224
- [Armitage 2002] Derek Armitage, Socio-institutional dynamics and the political ecology of mangrove forest conservation in Central Sulawesi, Indonesia, *Global Environmental Change*, Vol 12, pp 203-217, 2002
- [Augustinus, 1987] P.G.E.F. Augustinus, the changing shoreline of Surinam, Natuurwetenschappelijke studiekkring voor Suriname en de Nederlandse Antillen, Utrecht, No 95, 1978
- [Augustinus, 1995] P.G.E.F. Augustinus, Geomorphology and sedimentology of mangroves, in *Geomorphology and Sedimentology of Estuaries, Developments in Sedimentology*, 53, edited by G.M.E. Perillo
- [Baptist, 2005] M.J. Baptist (2005), Modelling floodplain biogeomorphology, Delft University Press, Delft, ISBN: 90-407-2582-9
- [Baptist et al 2005] M.J. Baptist, L.V. van den Bosch, J.T. Dijkstra and S. Kapinga, Modelling the effects of vegetation on flow and morphology in rivers, *Large Rivers* Vol 15, No. 1-4, pp 339-357, May 2005
- [Bird, 1986] E.C.F. Bird (1996), Mangroves and intertidal morphology in Westernport Bay, Victoria, Australia, *Marine Geology*, 69, pp. 251-271
- [Bryce et al., 2003] S. Bryce, P. Larcombe, P.V. Ridd (2003), Hydrodynamic and geomorphological controls on suspended sediment transport in mangrove creek systems, a case study: Cocoa Creek, Townsville, Australia, *Estuarine, Coastal and Shelf Science*, 56, pp. 415-431
- [Bunt, 1996] J.S. Bunt (1996), Mangrove Zonation: an examination of data from seventeen riverine estuaries in tropical Australia, *Annals of Botany* 78, pp. 333 – 341, 1996
- [Burger, 2005] B. Burger (2005), Wave Attenuation in Mangrove Forests, Numerical modelling of wave attenuation by implementation of a physical description of vegetation in SWAN, TUDelft, Faculty of Civil Engineering and Geosciences, Msc Thesis, September 2005

- [Clough, 1992] B.F. Clough, Primary productivity and growth of mangrove forests, in: *Tropical Mangrove Ecosystems* (A.I. Robertson and D.M. Alongi, Eds.), Coastal and Estuarine Studies 41, American Geophysical Union, Washington, 1992
- [Dahdouh-Geubas Et al, 2005] F. Dahdouh-Guebas, L.P. Jayatissa, D. Di Nitto, J.O. Bosire, D. Lo Seen and N. Koedam, How effective were mangroves as a defence against the recent tsunami?, *Current Biology*, Vol 15, No 12, pp. R443-R447, June 2005
- [Duke, 1992] N.C. Duke (1992) Mangrove floristics and biogeography, in: *Tropical Mangrove Ecosystems* (A.I. Robertson and D.M. Alongi, Eds.), Coastal and Estuarine Studies 41, American Geophysical Union, Washington, 1992
- [EJF, 2006] Mangroves: nature's defence against tsunamis – a report on the impact of mangrove loss and shrimp farm development on coastal defences, Environmental Justice Foundation, London, UK, ISBN: 1-904523-05-7
- [Ellison, 1998] J.C. Ellison (1998), Impacts of sediment burial on mangroves, *Marine Pollution Bulletin*, 37, pp. 420-426
- [Erftemeijer and Hamerlynck, 2004] Paul L.A. Erftemeijer and Olivier Hamerlynck, Die-Back of the mangrove *Heritiera Littoralis* Dryand, in the Rufiji Delta (Tanzania) Following El Nino floods, *Journal of Coastal Research*, 42, pp. 106-113, Fall 2004
- [FLOW User Manual, 2005] User Manual Delft3D-FLOW (2005), WL Delft Hydraulics, January 2005
- [Furukawa et al., 1997] K. Furukawa, E. Wolanski and H. Mueller (1997), Currents and Sediment Transport in Mangrove Forests, *Estuarine, Coastal and Shelf Science*, 44, pp. 301-310
- [Giani et al., 1996] L. Giani, Y. Bashan, G. Holguin, A. Strangmann (1996), Characteristics and methanogenesis of the Balandra lagoon mangrove soils, Baja California Sur, Mexico, *Geoderma*, 72, pp 149-160
- [Van de Graaf, 2003] J. van de Graaf, Coastal Morphology and Coastal Protection, Lecture notes CT5309, University of Delft, Faculty of Civil Engineering and Geosciences, September 2003.
- [Holthuijsen, 2005] Leo H. Holthuijsen (2005), Waves in Oceanic and Coastal Waters, Wind Waves, Delft University of Technology, Faculty of Civil Engineering and Geosciences, subject code CT 5316, September 2005

- [Hoozemans et al., 2004] F.J.M. Hoozemans, R.J.T. Klein, A. Kroon, H.J. Verhagen, M. van der Wegen, The coast in conflict - an interdisciplinary introduction to Coastal Zone Management, UNESCO-IHE, 34 pp., 2004
- [Huiskes et al 1995] A.H.L. Huiskes, B.P. Koudstaal, P.M.J. Herman, W.G. Beeftink, M.M. Markrusse and W. De Munck, Seed dispersal of halophytes in tidal salt marshes, *Journal of Ecology*, Vol 83, pp 559-567, 1995
- [Hulscher et al., 2004] Marine Dynamics II (2004), S.J.H.M. Hulscher, J.S. Ribberink and M.A.F. Knaapen, University of Twente, Faculty of Civil Engineering, subject code 221033, August 2004.
- [Janssen et al 1990] PH.M. Janssen, W. Slob and J. Rotmans, Gevoeligheidsanalyse en Onzekerheidsanalyse: een Inventarisatie van Ideeën, Methodes en Technieken, National Institute of public health and environmental protection, Rapport nr 958805001, July 1990
- [Kraus et al., 2003] K.W. Kraus, J.A. Allen and D.R. Cahoon (2003), Differential rates of vertical accretion and elevation change among aerial root types in Micronesian mangrove forests, *Estuarine, Coastal and Shelf Science*, 56, pp. 251-259
- [Lewis, 2005] Roy R. Lewis III, Ecological engineering for successful management and restoration of mangrove forests, *Ecological Engineering*, Vol 24, pp 403-418, 2005
- [Lewis and Marshall 1997] R.R. Lewis and M.J. Marshall, 1997, Principles of successful restoration of shrimp Aquaculture ponds back to mangrove forests. Programa/resume de Marcuba '97, September 15/20, Palacio de Copnvencciones de La Habana, Cuba, p 126
- [Massel et al., 1999] S.R. Massel, K. Furukawa, R.M. Brinkman (1999), Surface wave propagation in mangrove forests, *Fluid dynamics research* 24, pp. 219-249
- [Masselink et al 2006] G. Masselink, A. Kroon, R.G.D. Davidson-Arnott, Morphodynamics of intertidal bars in wave-dominated coastal settings – A review, *Geomorphology* 73, pp. 33-49, 2006
- [Mazda et al., 1997] Yoshihiro Mazda, Michimasa Magi, Motohiko Kogo, Phan Nguyen Hong (1997), Mangroves as a coastal protection from waves in the Tong King delta, Vietnam, *Mangroves and Salt Marshes* 1, 127-135, 1997
- [Mazda et al. 2005] Yoshihiro Mazda, Daijiro Kobashi and Satoshi Okada (2005), Tidal-scale hydrodynamics within mangrove swamps, *Wetlands Eco. Manage.*, (in press)

- [Quartel, 2000] S. Quartel (2000), Quantification of Wave attenuation in a Mangrove Forest, Physical Geography, Utrecht University, December 2000
- [Ribberink and Hulscher, 2003] J.S. Ribberink and S.J.H.M. Hulscher, Ondiepwaterstromingen, lecture notes pakket W8: Oppervlaktewater, subject code 221011, University of Twente, faculty of Civil Engineering and Management, March 2003
- [Van Rijn, 1998] L.C. van Rijn, Principles of Coastal Morphology, Aqua Publications, Amsterdam, The Netherlands, ISBN 90-800356-3-7
- [Ruitenbeek 1994] H. Jack Ruitenbeek, Modelling economy-ecology linkages in mangroves: Economic evidence for promoting conservation in Bintuni Bay, Indonesia, *Ecological Economics*, Vol 10, pp 233-247, 1994
- [Schierreck and Booij, 1995] Gerrit Jan Schierreck and Nico Booij (1995), Wave transmission in mangrove Forests, paper presented on the international conference on coastal and port engineering in Developing Countries, September 1995 Brazil
- [Shi and Chen 1996] Z. Shi and J.Y. Chen, Morphodynamics and sediment dynamics on intertidal mudflats in China (1961-1994), *Continental Shelf Research*, Vol. 16, No. 15, pp. 1909-1926, 1996
- [Smith III, 1992] T.J. Smith III (1992), Forest structure, in: *Tropical Mangrove Ecosystems* (A.I. Robertson and D.M. Alongi, Eds.), Coastal and Estuarine Studies 41, American Geophysical Union, Washington, 1992
- [Van Straaten and Kuenen 1958] L.M.J.U van Straaten, Ph.H. Kuenen, Tidal action as a cause of clay accumulation, *journal of sedimentary petrology*, Vol 28, No. 4, pp. 406-413, December 1958
- [Temmerman et al, 2005] S. Temmerman, T.J. Bouma, G. Govers, Z.B. Wang, M.B. de Vries and P.M.J. Herman, Impact of vegetation on flow routing and sedimentation patterns: three dimensional modelling for a tidal marsh, *Journal of Geophysical Research*, Vol. 110, F04019
- [TIDE User Manual, 2005] User Manual Delft3D-TIDE (2005), WLDelft Hydraulics, May 2005
- [Twilley et al, 1998] Robert R. Twilley, Victor H. Rivera-Monroy, Ronghua Chen and Leonor Botero, Adapting an ecological mangrove model to simulate trajectories in Restoration ecology, *Marine Pollution Bulletin*, Vol 37, pp. 404-419, 1998

- [Victor et al., 2005] Steven Victor, Leinson Neth, Yimnang Golbuu, Eric Wolanski, Robert H. Richmond (2005), Sedimentation in Mangroves and Coral Reefs in a wet tropical Island, Pohnpei, Micronesia, *Estuarine, Coastal and Shelf Science*, in press.
- [Vermaat and Thampanya, 2006] Jan. E. Vermaat and Udomluck Thampanya, Mangroves mitigate tsunami damage: a further response, *Estuarine, Coastal and Shelf Science*, Vol 69, pp 1-3, August 2006
- [De Vos, 2004] Willem-Jan de Vos (2004) Wave attenuation in mangrove wetlands; Red River Delta Vietnam, TUDelft, Faculty of Civil Engineering and Geosciences, Msc Thesis, June 2004
- [De Vries and Roelvink 2004] M.B. de Vries and D. Roelvink, Vegetation friction factor algorithm, Delft Hydraulics, March 2004
- [Walsh and Nittrouer, 2004] J.P. Walsh, C.A. Nittrouer (2004), Mangrove-bank sedimentation in a mesotidal environment with large sediment supply, Gulf of Papua, *Marine Geology*, 208, pp. 225-248
- [WAVE User Manual, 2003] User Manual Delft3D-WAVE (2003), WLDelft Hydraulics, March 2003
- [Winterwerp et al. 2005] Johan C. Winterwerp, William G. Borst and Mindert B. de Vries, Pilot Study on the erosion and rehabilitation of a mangrove mud coast, *Journal of Coastal Research*, Vol 21, No 2, pp 223-230, March 2005
- [Wolanski et al., 1992] Eric Wolanski, Yoshihiro Mazda and Peter Ridd (1992), Mangrove Hydrodynamics, in: Tropical Mangrove Ecosystems (A.I. Robertson and D.M. Alongi, Eds.), Coastal and Estuarine Studies 41, American Geophysical Union, Washington, 1992
- [Woodroffe, 1992] Colin Woodroffe (1992), Mangrove Sediments and Geomorphology, in: Tropical Mangrove Ecosystems (A.I. Robertson and D.M. Alongi, Eds.), Coastal and Estuarine Studies 41, American Geophysical Union, Washington, 1992
- [WRM, 2002] Mangroves: Local livelihoods vs corporate profits, World Rainforest Movement, Montevideo, Uruguay, ISBN: 9974-7719-1-9, December 2002, retrieved from www.wrm.org.uy
- [Wu et al., 2001] Y. Wu, R.A. Falconer, J. Struve (2001), Mathematical modelling of tidal currents in mangrove forests, *Environmental Modelling & Software*, 16, pp 19-29

A Mangroves

This appendix describes the biology and ecosystem of mangroves. Only the characteristics and processes are described that play a role in modelling the interaction between mangrove trees, waves and tides and determining the influence of mangroves on morphodynamics. The first paragraph considers the biological aspects and the second paragraph ecological aspects.

A.1 Biological aspects

The biological aspects that will be treated in this chapter are different mangrove species, different root structures and the growth process. The objective is to learn more about specific trees that exist inside mangrove forest. With this information an individual tree can be schematised and implemented in a computer model. The growth factors are described for the possibility to extend the computer model with an equation for the growth of mangroves.

A.1.1 Mangrove species

A mangrove is a tree, shrub, palm or ground fern, generally exceeding one half metre in height, and which normally grows above mean sea level in the intertidal zone of marine coastal environments, or estuarine margins [Duke, 1992]. Although it is difficult to identify mangrove species, it is clear that mangroves are not a genetic entity but an ecological one. Recognizable attributes of mangrove species are:

salt excreting glands or a system inside the tree or roots to control the salt water
special breathing structures (prop roots, pneumatophores, small air breathing lenticels)
structures to support the above ground mass of the tree
viviparous propagulus, their way to reproduce

From the literature three main mangrove species can be distinguished (see also figure A.1) [De Vos, 2004]:

- *Avicennia germinans* (black mangrove)
- *Rizophora mangle* (red mangrove)
- *laguncularia racemosa* (white mangrove)

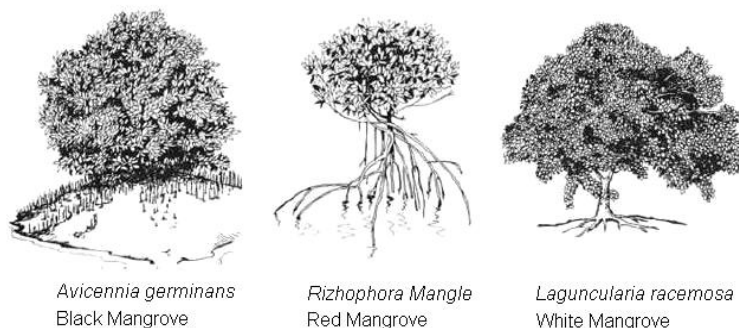


Figure A.1: black, red and white mangrove

Because of their occurrence on both hemispheres and their distinctive root structures the *Avicennia* and *Rizhophora* are the main characters in mangrove literature [De Vos, 2004]. The names and pictures of nine major mangrove species are shown below in figure A.2.



Avicennia



Bruguiera



Ceriops



Kandelia



Laguncularia



Lumnitzera



Nypa



Rizhophora



Sonneratia

Figure A.2: pictures of the nine major mangrove species around the world

A.1.2 Root structures

The surface on which mangroves grow is inundated at least part of the day. A consequence is that the substrate (ground on which mangroves grow) is of anaerobic nature. In order to ventilate the root system they need to expose their roots directly to the air, at least a part of the day. Mangrove trees develop special aerial root structures to ventilate their roots. Although the various types of aerial roots may look quite different from one another, their function is the same and their existence is one of the features that distinguishes mangroves from other trees [De Vos, 2004]. In figure A.3 the main types of aerial roots are shown.

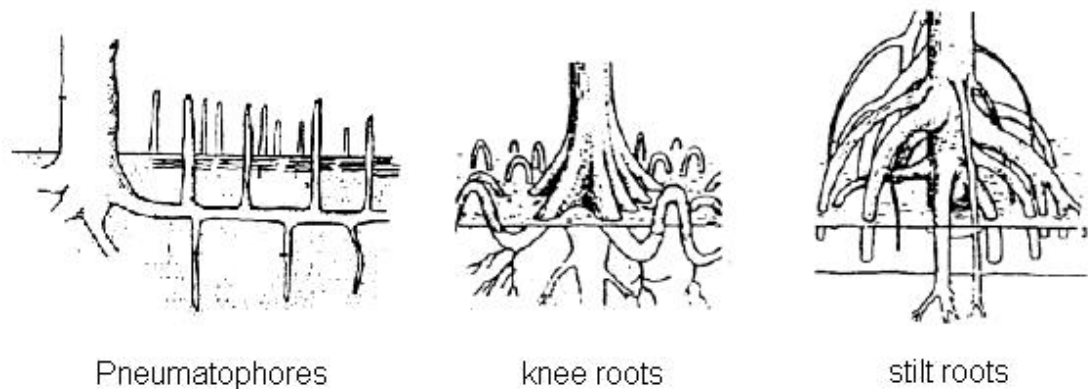


Figure A.3: root structures of mangroves

De Vos (2004) gives an overview of the different roots according to Tomlinson (1986). This is shortly summarized below.

Pneumatophores are erect lateral branches of the horizontal cable roots, which themselves are growing underground. The pencil-like pneumatophores are the visible part of the root system of several mangrove species. The length of pneumatophores depends on the species. *Avicennia* aerial roots reach a maximum of 30 cm, *Sonneratia* aerial roots can reach heights up to 3 m and *Laguncularia* roots have a maximum of 20 cm.

Knee roots differ from tree to tree. In *Bruguiera* and *Cerriops* the horizontal cable component of the root system surfaces periodically while growing away from the tree. The surfacing root forms a loop before continuing its horizontal growth. In *Xylocarpus* knee roots are formed by local secondary growth in the primary cable components, in contrast with *Bruguiera* and *Cerriops* where knee roots are formed by primary growth.

Stilt roots are branched looping aerial prop roots that arise from the trunk and lower branches of the species of the *Rizophora* genus. Stilt roots are rarely found in other species. The name 'stilt' refers to the supportive character these roots have.

A.1.3 Growth

In this chapter a number of important factors influencing the growth of mangroves will be discussed.

Tidal range

Tidal range determines where mangrove trees can grow. Trees with knee roots or pneumatophores grow mostly in the upper tidal zone. This is because these trees have not very large aerial roots and to let them inundate as short as possible they will grow the best in the upper tidal zone. Trees with stilt roots can grow also in the lower tidal zone, like the *Rizophora Mangel*. The tidal range, together with the gradient of the substrate, determines which area is suitable for growth of mangroves.

Protection from wave action

This plays a role in the settlement of propagules and seedlings. They require a low (wave) energy environment to settle [De Vos, 2004].

Air Temperature

Mangroves can cope with a wide range of temperature. The minimum temperature under which mangroves can grow is about 15 °C average during the coldest months of the year. The maximum temperature of the air may be as high as 35 °C average during the warmest months of the year [Clough, 1992]. Although this is a wide range, in general can be said that if the temperature decreases, the growth rate, the forest height, the species richness and the maximum size of the mangrove trees will decrease [Clough, 1992 and De Vos, 2004]

Water temperature

There seems to be a correlation between the areas where the water exceeds 24 °C during the warmest months and the presence of mangrove forests. There is, however, not a clear maximum for water temperature to allow growth of mangrove forests.

Salinity

Mangroves grow in salt water, but the level of tolerance of salt varies by species. In general can be said that soil salinities of 10 – 20‰ are best for mangrove growth [Clough, 1992]. Between 30 and 72‰, tree height was found to be inversely proportional to soil salinity [De Vos, 2004].

Substrate

Mangroves can grow on sand, mud, peat and coral rock. However, the most extensive forests are found on muddy soils, typical in deltas, lagoons, bays and estuaries. These muddy soils depend on the input of sediments by tidal currents or river discharges. The substrate is fertilized by nutrients in freshwater run-off, river discharges or organic litter produced within the forest itself [De Vos, 2004].

Aridity

Aridity can cause two problems: an increasing salinity and less import of sediments and nutrients. So, rainfall is important for mangrove forests. The degree of aridity which a tree can deal with varies with the tree species.

Summary

Considering all these factors, different species stand on different locations in a mangrove habitat. These locations are summarised in figure A.4 and will be explained more in the next paragraph. In table A.1 the 9 major mangrove species (see figure A.2) are listed, including their ability to cope with certain circumstances and their location in a mangrove habitat.

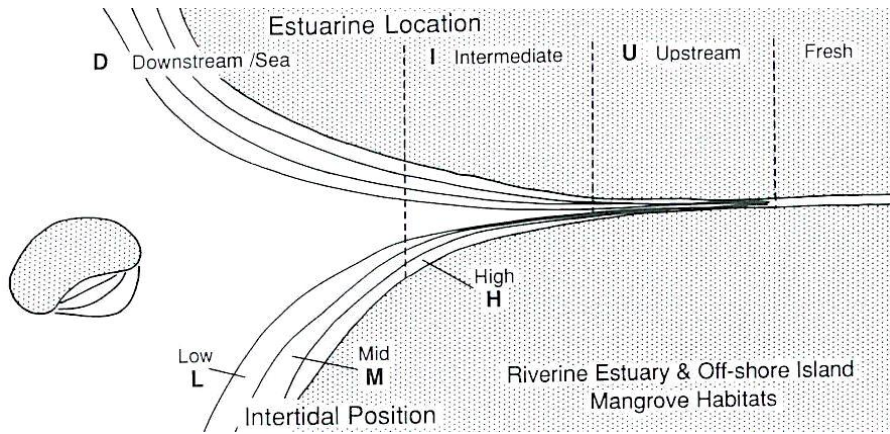


Figure A.4: Mangrove locations in a habitat [Duke, 1992]

Table A.1: Relative tolerances of 9 mangrove species, +++++ = very tolerant, += not tolerant, H = high, M = mid and L = low intertidal position [Clough, 1992]

Species	Salinity	Aridity	Low Temperature	Intertidal Level
Avicennia	+++++	+++++	+++++	H,M,L
Bruguiera	+++	+++	++	H,M
Ceriops	++	++	+	H,M
Kandelia	+++?	+++?	+++	H,M
Laguncularia	?	?	?	?
Lumnitzera	++++	++++	+++	H
Nypa	+	+	+	M,L
Rizhophora	+++	+++	++	M,L
Sonneratia	+++	+++	++	M,L

A.2 Ecological Aspects

In this paragraph the distribution of mangroves over the world, the zonation of mangroves, the settings in which mangrove can occur and the types of mangrove forests which can be recognised, will be described in this chapter. The objective of this paragraph is to view mangroves in their environment and learn more about it. This can help to schematise shorelines with mangroves for modelling.

A.2.1 Distribution patterns

Duke (1992) states that mangroves are distributed over the world according to three important scales:

- Coastal range
- Location within an estuary
- Position along the intertidal profile

These scales will be discussed below.

Coastal range

On a global scale, mangrove plants are found throughout tropical regions of the world. The locations of mangrove forests match with the presence of warm and cold oceanic currents. That is why the latitudinal ranges of mangroves tend to be broader on eastern continental coasts and more constraint on their western sides [Duke, 1992]. Generally mangroves match the winter 20 °C isotherm, but the warm oceanic currents can extend the warmer coastlines. Three exceptions exist to this pattern. The coastlines around Australia, across the North Island of New Zealand and of eastern South America. Continents and oceans can form a barrier in the distribution of mangroves. Two barriers, the Africa and Euro-Asia continent and the Pacific Ocean are very effective and divide mangrove species into two global hemispheres:

- Atlantic East Pacific or New World
- Indo West Pacific or Old World

These hemispheres can each be divided into three regions according to the presence of species. This is all summarised in figure A.5. There is a spectacular difference in floristic distribution between the *New World* and the *Old World*. Mangroves reach their maximum development and diversity in the *Old World* and the ratio between the number of species in the Old World and the New World is five to one.

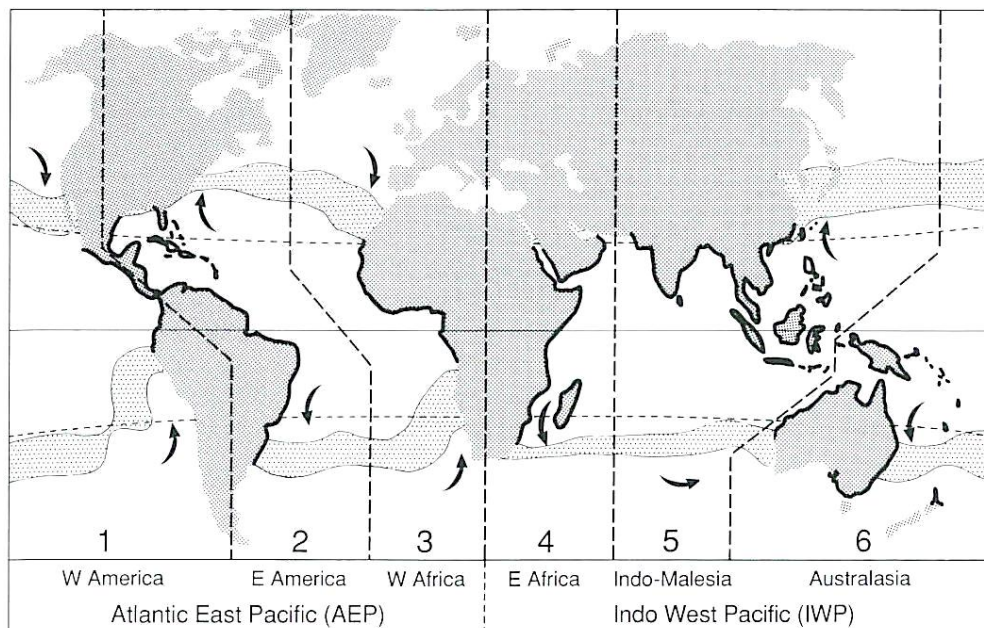


Figure A.5: global mangrove distribution

Location within an estuary and position along intertidal profile

In figure A.4 the division of mangrove locations in an estuary and along the intertidal profile is given. Six categories can be defined in two groups: intertidal position and location in estuary [Duke, 1992]. The tree categories of the intertidal position are:

- Low intertidal position → areas inundated by medium high tides and flooded more than 45 times a month
- Mid intertidal position → areas inundated by normal high tides and flooded 20 to 45 times a month
- High intertidal position → areas inundated less than 20 times a month

The division in estuary locations is less clear. Three regions can be distinguished:

- Downstream location, including off-shore islands
- Intermediate location
- Upstream location

Duke (1992) uses a division of downstream/intermediate/upstream of 1/1/1 from the mouth of the estuary. Hence, for example a species might be known as a high intertidal, intermediate specialist.

A.2.2 Zonation

Smith III (1992) starts his description of the forest structure of mangroves with the statement that the most noted feature of mangrove forest structure is the often conspicuous zonation of tree species into monospecific bands parallel to the shoreline. However, this feature has attracted the interest of a lot of scientists it is difficult to generalize conclusions from local observations. Describing zones in general has to be done with care. For vegetation along open shorelines the following zonation can be recognised, from land to sea (Bunt, 1996):

- Landward fringe
- Landward *Avicennia*
- *Ceriops* thickets
- *Bruguiera* forests
- *Rhizophora* forests
- Seaward fringe (*Avicennia* and/or *Sonneratia*)

This is summarised in figure A.6.

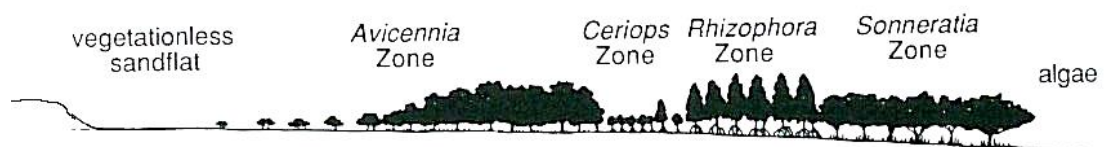


Figure A.6: zonation of mangroves

The abovementioned zonation pattern describes the position of mangroves along the intertidal profile. The species shown in figure A.6 correspond with the characteristics of mangrove species in table A.1. There is not only a zonation along the intertidal profile, but also in the length of the estuary. A combination of both zonation patterns is shown in figure A.7 for a mangrove forest in Madagascar.

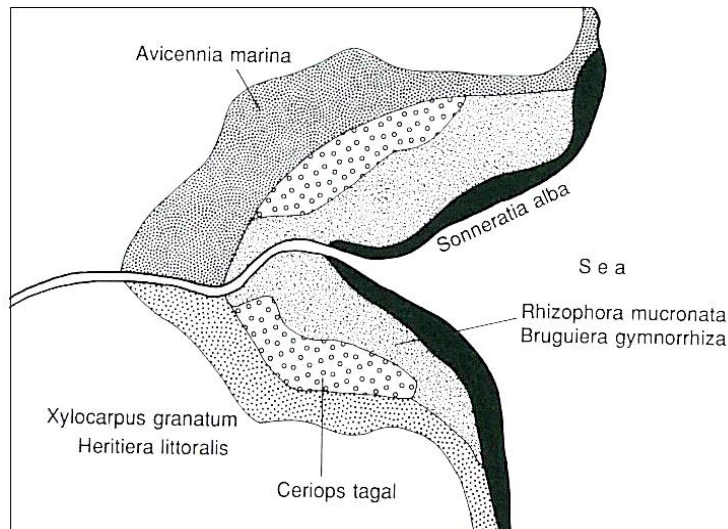


Figure A.7: zonation along intertidal position and estuary location

Two different explanations exist about the cause of zonation:

- Land building and plant succession
- Competition

Smith III (1992) summarises the development in the first explanation. He states that Curtis (1888) makes one of the earliest claims regarding the ability of mangroves to build land, specifically for *Rhizophora mangle* in Florida. Davis (1940) expanded the supposed land building role of *Rhizophora* into a complete successional sequence in which sea grasses colonized bare, sub tidal areas and trapped sediments to the point that *R. mangle* would colonize the area and trap more sediment; *Rhizophora* would then be replaced by *Avicennia germinans*, which in turn would give way to a tropical forest climax association. Chapman (1976) provided a synthesis of the “zonation represents succession” theory and provided examples from around the world.

The other view is competition. It is suggested that zonation of mangroves depends on frequency of tidal inundation, salinity and soil type [De Vos, 2004]. The factors described in paragraph A.1.3 are responsible for the zonation. So, it can be concluded that mangroves are not responsible for geomorphologic changes (land building) but they respond to these changes [Smith III, 1992]. This view is accepted throughout the world. Succession in mangrove forests does occur (as in every forest in the world), but are not responsible for land building and zonation.

A.2.3 Environmental settings

Mangroves occur in a number of environmental settings, comprising particular suites of recurring landforms and differing in the physical processes responsible for sediment transport and deposition [Woodroffe, 1992]. Five different terrestrial settings are described by Thom (1982) and are shown in figure A.8. The geophysical characteristics (climate, tides and sea-level) the geomorphological characteristics (the dynamic history of the land surface and contemporary geomorphological processes) and the biological characteristics (micro topographic, elevation and sediments, drainage and nutrient status) define the setting. The different settings are described below.

River dominated	The river distributes enormous loads of sediments into the delta. This makes the delta extremely dynamic. In river dominated settings there is an active and abandoned deltaic plain. Along the abandoned deltaic plain mangroves will grow.
Tide dominated	This setting is characterised by areas of high tidal range (>4 m) where there is an extensive, low-gradient intertidal zone available for mangrove colonisation [Woodroffe, 1992].
Wave dominated	This setting is characterised by the presence of barrier islands that enclose drowned river valleys or lagoons and act to dissipate wave energy [De Vos, 2004]. The wave dominated setting occurs in two other settings: composite river and wave dominated and drowned river valley.
Composite river and wave dominated	As already said, this setting is a form of wave dominated setting, combined with the river setting. The river brings large volumes of sediments to the wave dominated coast and different landforms occur. Inside the lagoons that are formed, mangroves will occur (see figure A.8).
Drowned bedrock valley	Many large coastal embayments in the tropics and subtropics have been drowned by the post-glacial rise in sea level. These areas provide sheltered environments within which mangrove forest develop on muddy substrates [Woodroffe, 1992].

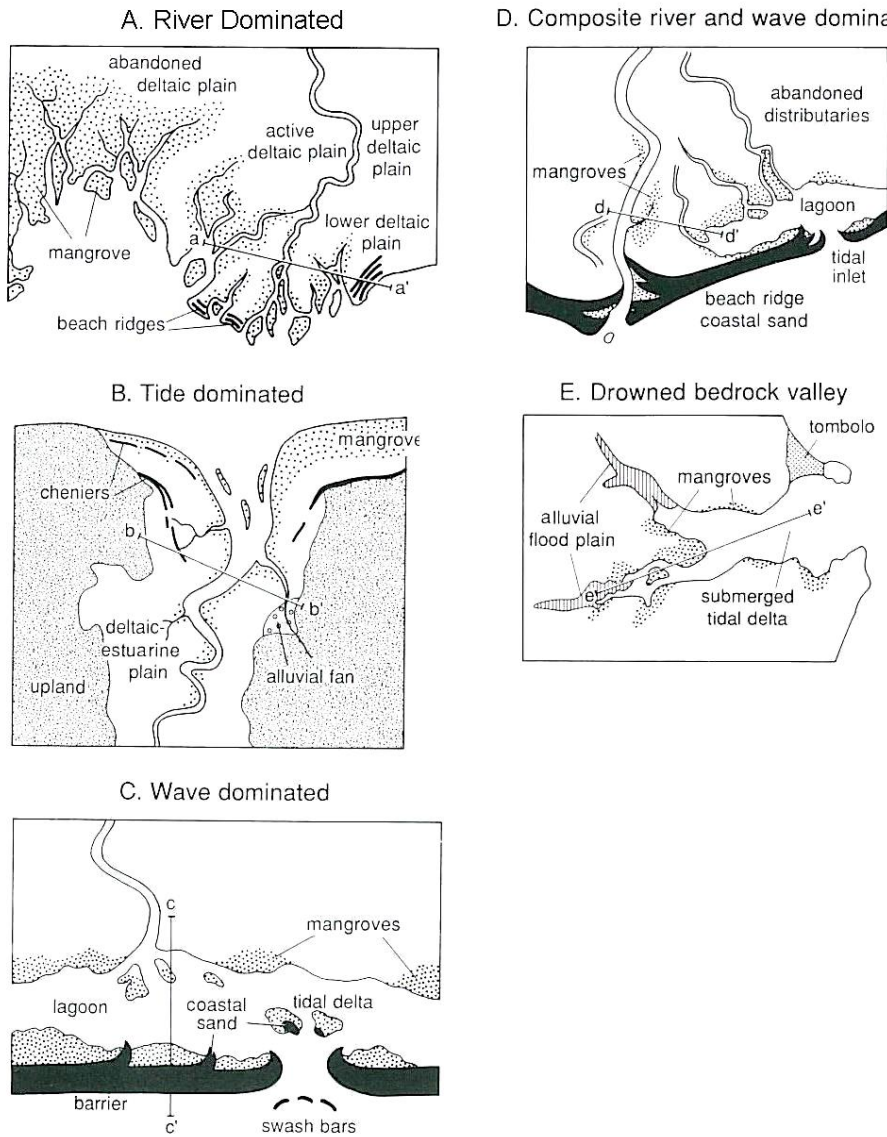


Figure A.8: five environmental settings

A.2.4 Forest types

Lugo and Snedaker (1974) developed a functional classification of mangrove forests, which is widely used and accepted. This classification consists of six categories and is shown in figure A.9. Woodroffe (1992) gives a good description of these categories:

- Overwash mangroves → small Islands, generally composed of Rizhophora, completely overwashed and often underlain by mangrove peat but not characterised by litter accumulation
- Fringe mangroves → a Rizhophora dominated littoral fringe inundated by daily tides, but with litter accumulation.
- Riverine mangroves → tall, productive Rizhophora dominated mangrove stands flanking a river channel receiving nutrient rich freshwater flushing

- Basin mangroves → typically mixed, or *Avicennia* dominated characteristic of interior areas of mangrove forests.
- Scrub mangroves → a dwarfed stand especially of *Rhizophora* <1.5 m tall, often in nutrient poor areas
- Hammock mangroves → a special form of basin mangrove found in the Everglades, forming small islands of mangrove over a mangrove derived peat which infills a depression in the underlying limestone substrate.

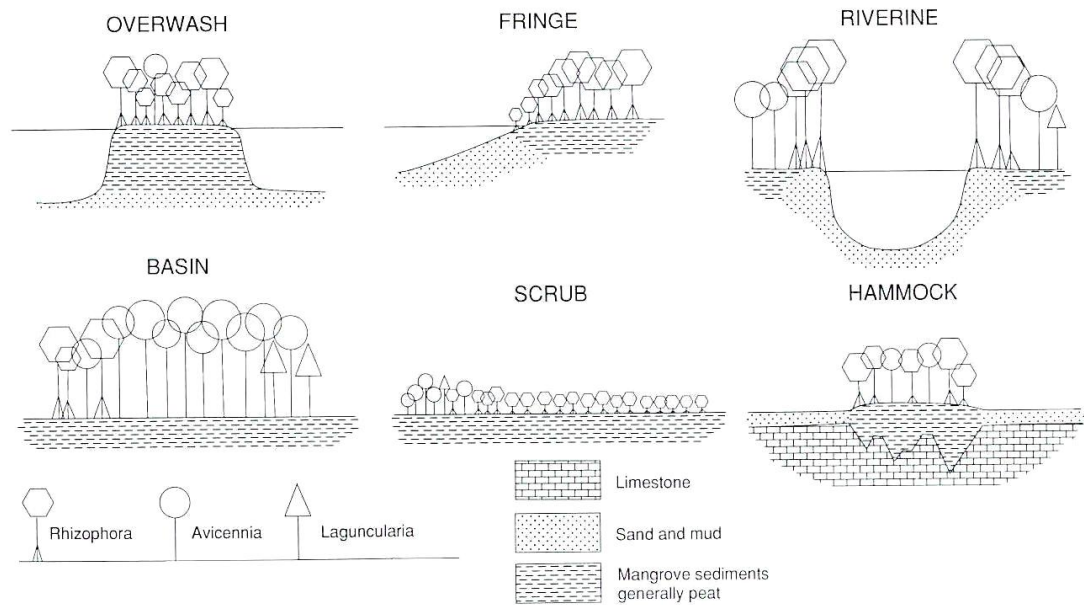


Figure A.9: Functional mangrove forest types

B Delft3D conceptual model

This appendix describes and explains the basics of Delft3D FLOW and WAVE model. Before going into the details of the individual models some basic aspects of grids are explained to. This is followed by a description of Delft3D FLOW and WAVE. Each description ends with the way that vegetation is taken into account in the model.

B.1 Grid and bathymetry

In numerical models (like Delft3D-FLOW) grids are used to solve the partial differential equations that describe the system. Boundaries in river or coastal systems are in general curved and not smoothly represented on a rectangular grid. To model the boundaries well an orthogonal curvilinear coordinate system is used. The equations in Delft3D-FLOW are formulated in orthogonal curvilinear coordinates (ξ, η). An example of a grid is given in figure B.1. Figure B.2 explains the coordinate system (ξ, η). In the vertical direction the same problem occurs, because bottoms do not have a rectangular shape. A σ coordinate system is used. This system is defined as:

$$\sigma = \frac{z - \zeta}{d + \zeta} = \frac{z - \zeta}{H} \quad (\text{B.1})$$

Where:

z = vertical coordinate in physical space

ζ = free surface elevation above the reference plane (at $z = 0$)

d = water depth below the reference plane

H = total water depth

At the bottom $\sigma = -1$ and at the free surface $\sigma = 0$. An example of this grid system is given in figure B.3.

Grids can be made by the module Delft3D-RGFGRID. A bathymetry on this grid can be generated by the module Delft3D-QUICKIN

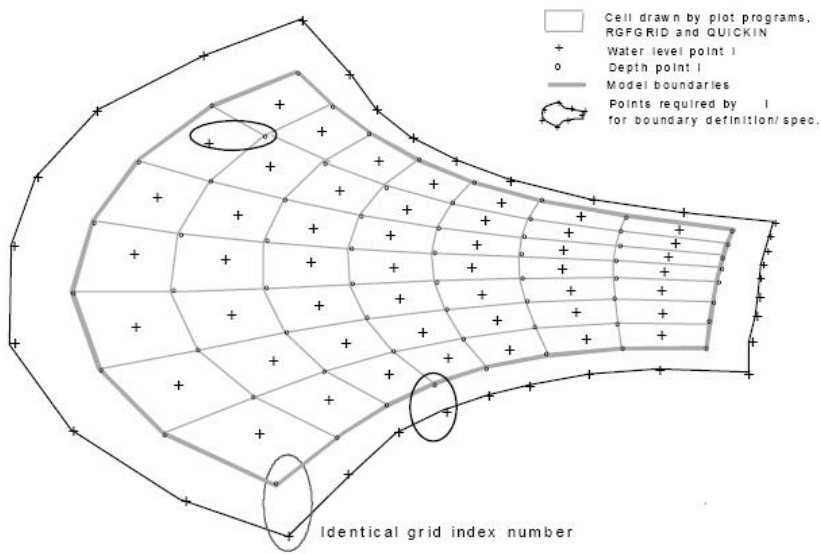


Figure B.1: example of a grid

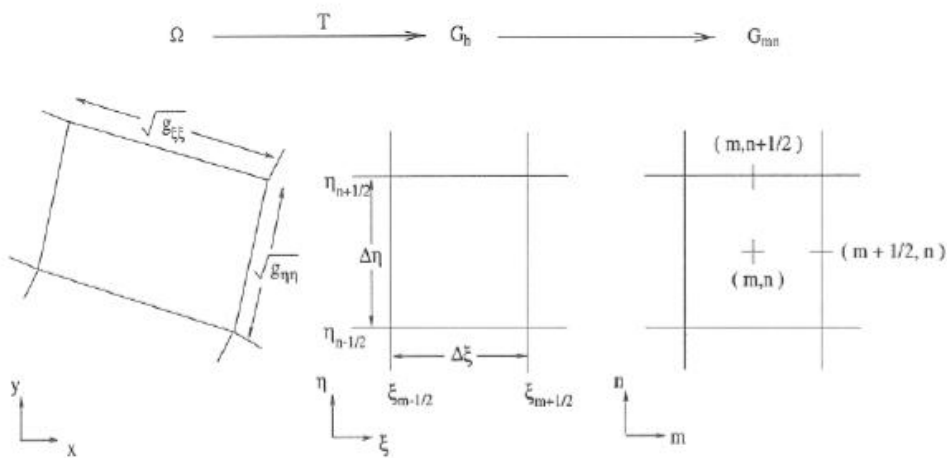


Figure B.2: coordinates in the grid-system.

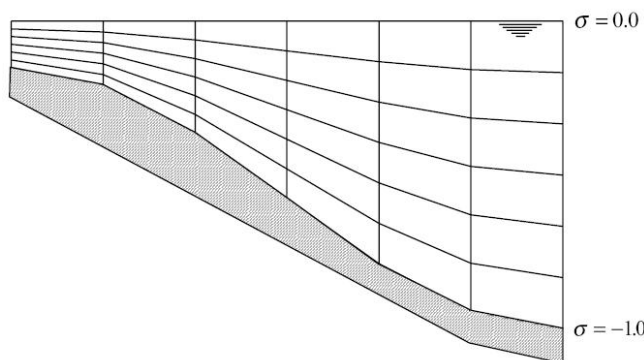


Figure B.3: example of a σ grid

B.2 Delft3D FLOW model

B.2.1 Hydrodynamic equations

The basis of all flow equations are the continuity equation and the momentum equation.

The depth average continuity equation used in Delft3D FLOW is given by:

$$\frac{\partial \zeta}{\partial t} + \frac{1}{\sqrt{G_{\xi\xi}} \sqrt{G_{\eta\eta}}} \frac{\partial \left[(d + \zeta) U \sqrt{G_{\eta\eta}} \right]}{\partial \xi} + \frac{1}{\sqrt{G_{\xi\xi}} \sqrt{G_{\eta\eta}}} \frac{\partial \left[(d + \zeta) V \sqrt{G_{\xi\xi}} \right]}{\partial \eta} = Q \quad (\text{B.2})$$

$$Q = H \int_{-1}^0 (q_{in} - q_{out}) d\sigma + P - E \quad (\text{B.3})$$

With Q representing the contributions per unit area due to the discharge or withdrawal of water, precipitation and evaporation.

In table 1.1 the symbols used in equations (B.2) and (B.3) are listed and explained. The first term on the left hand side of equation (B.2) represents the change of water level in the time. The second and the third term represent the changes of current velocities U and V in ξ and η direction.

The momentum equations used in Delft3D FLOW in the ξ and η direction are given by:

$$\begin{aligned} \frac{\partial u}{\partial t} + \frac{u}{\sqrt{G_{\xi\xi}}} \frac{\partial u}{\partial \xi} + \frac{v}{\sqrt{G_{\eta\eta}}} \frac{\partial u}{\partial \eta} + \frac{\omega}{d + \zeta} \frac{\partial u}{\partial \sigma} + \frac{uv}{\sqrt{G_{\xi\xi}} \sqrt{G_{\eta\eta}}} \frac{\partial \sqrt{G_{\xi\xi}}}{\partial \eta} + \\ - \frac{v^2}{\sqrt{G_{\xi\xi}} \sqrt{G_{\eta\eta}}} \frac{\partial \sqrt{G_{\eta\eta}}}{\partial \xi} - fv - \frac{1}{\rho_0 \sqrt{G_{\xi\xi}}} P_\xi + F_{\xi\eta} + \frac{1}{(d + \zeta)^2} \frac{\partial}{\partial \sigma} \left(v_\nu \frac{\partial u}{\partial \sigma} \right) + M_\xi \end{aligned} \quad (\text{B.4})$$

and:

$$\begin{aligned} \frac{\partial v}{\partial t} + \frac{u}{\sqrt{G_{\xi\xi}}} \frac{\partial v}{\partial \xi} + \frac{v}{\sqrt{G_{\eta\eta}}} \frac{\partial v}{\partial \eta} + \frac{\omega}{d + \zeta} \frac{\partial v}{\partial \sigma} + \frac{uv}{\sqrt{G_{\xi\xi}} \sqrt{G_{\eta\eta}}} \frac{\partial \sqrt{G_{\eta\eta}}}{\partial \xi} + \\ - \frac{u^2}{\sqrt{G_{\xi\xi}} \sqrt{G_{\eta\eta}}} \frac{\partial \sqrt{G_{\xi\xi}}}{\partial \eta} + fu - \frac{1}{\rho_0 \sqrt{G_{\eta\eta}}} P_\eta + F_{\eta\xi} + \frac{1}{(d + \zeta)^2} \frac{\partial}{\partial \sigma} \left(v_\nu \frac{\partial v}{\partial \sigma} \right) + M_\eta \end{aligned} \quad (\text{B.5})$$

A list of the symbols, the unit and what they mean is given in table B.1.

The first term on the left hand side in equation (B.4) and (B.5) is the acceleration. The second, third and fourth term describe the advection. The last term on the left hand side in equation (B.4) and (B.5) is the coriolis force. On the right hand side the first term is the pressure gradient, the second term describes the stress, the third term the viscosity and the last term the contributions due to external sources or sinks of momentum (external forces).

Table B.1: symbols, their units and their meaning

Symbol	Unit	Meaning
ζ	m	water level above some horizontal plane of reference (datum)
t	s	time
$\sqrt{G_{\xi\xi}}$	m	coefficient used to transform curvilinear to rectangular coordinates
$\sqrt{G_{\eta\eta}}$	m	coefficient used to transform curvilinear to rectangular coordinates
d	m	water depth below some horizontal plane of reference (datum)
U	m/s	depth average velocity in ξ - direction
ξ, η		horizontal curvilinear coordinates
Q	m/s	global source or sink per unit area
q_{in}	1/s	local source per unit volume
q_{out}	1/s	local sink per unit volume
H	m	total water depth
σ		scaled vertical coordinate
P	m/s	Precipitation
E	m/s	evaporation
u	m/s	flow velocity in x- or ξ - direction
v	m/s	flow velocity in y- or η - direction
f	1/s	coriolis coefficient
P	$\text{kg/m}^2\text{s}^2$	gradient hydrostatic pressure
F	m/s^2	turbulent momentum flux
ν_v	m^2/s	vertical eddy viscosity
M	m/s^2	source or sink of momentum

The Delft3D FLOW model needs the following parameters for solving the equations (B.2) - (B.5):

- Grid and bathymetry (see paragraph A.1)
- Time frame; the start and stop time of the simulation.
- Time step; this is an important parameter. When the time step is too large, the results of the model calculations cannot be trusted. The model can become unstable. When a time step is too small the computing time will increase and it will take a long time before a model-run is finished. To estimate a good time step the following equation can be used:

$$Cr = \frac{\Delta t \sqrt{gh}}{\{\Delta x, \Delta y\}} \quad (\text{B.6})$$

Where:

Cr = Courant Number (≤ 10)

Δt = time step [s]

g = gravity acceleration

h = total water depth

$\{\Delta x, \Delta y\}$ = minimum value of the grid spacing in either direction

Example: for a model with a maximum water depth of 2 m and a minimum grid spacing of 10 m a time step of 20 seconds is good enough.

- The initial conditions; this can be initial water level conditions and initial sediment concentrations
- Boundary conditions. On the boundary certain conditions can be specified. For this modelling experiment only water level variations are important. The water level variation need to be specified in terms of Astronomic conditions, Harmonic conditions, a QH-relation or a water level time-series. For the modelling experiment I will use the Harmonic conditions. For these conditions a frequency of the tide (in deg/hr), a phase of the tide (in deg) and an amplitude of the tide (in m). For a tide of 12 hr starting on $h = 0$ the frequency is $360 / 12 = 30$ deg/hr and the phase is 90 deg.
- Roughness and viscosity; for roughness can be chosen four different methods: Chezy, Manning, White-Colebrook and Z0. Each method has its own parameters which need to be specified. The roughness and viscosity can also be specified by area. This can be done by making a file with the required information per grid-cell.
- Some numerical parameters

B.2.2 Bed shear stress

In Delft3D FLOW the bed shear stress for three dimensional simulations is calculated with:

$$\tau_b = \frac{g \rho_0 \bar{u}_b |\bar{u}_b|}{C_{3D}^2} \quad (\text{B.7})$$

Where

- τ_b = bed shear stress
- g = gravity acceleration
- ρ_0 = density of water
- u_b = velocity at the bottom
- C_{3D} = three dimensional Chezy coefficient

The velocity at the bottom is determined by assuming a linear velocity profile and can be calculated with:

$$\bar{u}_b = \frac{\bar{u}_*}{\kappa} \ln \left(1 + \frac{\Delta z_b}{2z_0} \right) \quad (\text{B.8})$$

Where:

- u^* = shear velocity
- κ = Von Karman constant (0.4)
- z_b = point above the bottom where velocity u_b is determined
- z_0 = point at the bottom where velocity is 0 m/s

In equation (B.7) a three dimensional Chezy coefficient is used because the depth average velocity is larger than the velocity at the bottom. Using the same Chezy values for two dimensional computations will result in much lower bed shear stresses than in reality. The three dimensional Chezy value can be approached with the following equation:

$$C_{3D} = C_{2D} + \frac{\sqrt{g}}{\kappa} \log \left(\frac{eh}{2H} \right) \quad (\text{B.9})$$

Where:

- C_{2D} = two dimensional Chezy value (which is available as a boundary condition)
- e = natural logarithm
- h = thickness of the lowest computational layer
- H = water depth

B.2.3 Turbulence

In the calculations the k-ε turbulence closure model is used. This closure model calculates the turbulent kinetic energy k and the energy dissipation ε. They are related in the following way:

$$\frac{\partial k}{\partial t} = \frac{1}{1-A_p} \frac{\partial}{\partial z} \left\{ (1-A_p)(\nu + \nu_T / \sigma_k) \frac{\partial k}{\partial z} \right\} + T + P_k - B_k - \varepsilon \quad (\text{B.10})$$

and

$$\frac{\partial \varepsilon}{\partial t} = \frac{1}{1-A_p} \frac{\partial}{\partial z} \left\{ (1-A_p)(\nu + \nu_T / \sigma_\varepsilon) \frac{\partial \varepsilon}{\partial z} \right\} + T\tau^{-1} + P_\varepsilon - B_\varepsilon - \varepsilon \quad (\text{B.11})$$

Where:

- k = kinetic turbulent energy
- A_p = the horizontal cross-section plant area (will be explained later)
- ν = viscosity
- T = the work on the plants of the flow
- τ = time scale
- P = production of energy
- B = buoyancy
- ε = energy dissipation

The meaning of the terms and the way they are calculated can be found in the FLOW USER manual.

In the k-ε turbulence closure model a mixing length L can be defined from ε and k according to:

$$L = C_D \frac{k\sqrt{k}}{\varepsilon} \quad (\text{B.12})$$

Where C_D is a drag coefficient. Two important assumptions are made in the turbulence closure model:

- The production, buoyancy and dissipation terms are the dominating terms
- The horizontal length scales are larger than the vertical ones (shallow water, boundary layer type of flows)

From the turbulence closure model the eddy diffusivity can be calculated. This parameter is very important for sediment transport processes. It is defined as:

$$\varepsilon_s = c_\mu \frac{k^2}{\varepsilon} \quad (\text{B.13})$$

Where

ε_s = eddy diffusivity

c_μ = empirical constant (0.09)

k = kinetic turbulent energy

ε = energy dissipation

B.2.4 Sediment transport and morphology

Suspended sediment transport

The 3 dimensional transport of suspended sediment is calculated by solving the three dimensional advection-diffusion (mass balance) equation for the suspended sediment:

$$\begin{aligned} & \frac{\partial c^{(\ell)}}{\partial t} + \frac{\partial uc^{(\ell)}}{\partial x} + \frac{\partial vc^{(\ell)}}{\partial y} + \frac{\partial (w - w_s^{(\ell)})c^{(\ell)}}{\partial t} + \\ & - \frac{\partial}{\partial x} \left(\varepsilon_{s,x}^{(\ell)} \frac{\partial c^{(\ell)}}{\partial x} \right) - \frac{\partial}{\partial y} \left(\varepsilon_{s,y}^{(\ell)} \frac{\partial c^{(\ell)}}{\partial y} \right) - \frac{\partial}{\partial z} \left(\varepsilon_{s,z}^{(\ell)} \frac{\partial c^{(\ell)}}{\partial z} \right) = 0 \end{aligned} \quad (\text{B.14})$$

Where:

$c^{(\ell)}$ = mass concentration of sediment fraction (l)

u, v and w = flow velocity components

ε = eddy diffusivities of sediment fraction (l)

$w_s^{(\ell)}$ = (hindered) sediment settling velocity of sediment fraction (l)

For morphology calculations the sediment deposition flux and the erosion flux are important. The balance between these two processes determines whether sedimentation or erosion takes place.

Deposition flux

In a simple way can be said that the deposition flux is:

$$D = w_s c \quad (\text{B.15})$$

Where:

D = deposition flux

w_s = settling velocity

c = concentration

The settling velocity is very important in the deposition flux. The larger the settling velocity, the higher the deposition flux of sediment. The settling velocity is calculated with:

$$w_s = \left(1 - \frac{c_s^{tot}}{CSOIL} \right) w_{s,0} \quad (B.16)$$

Where:

c_s^{tot} = the total mass concentration of the sediment

CSOIL = Reference density (this parameter should be specified in the Delft3D FLOW model)

And:

$$w_{s,0} = \frac{(s-1)gd_s^2}{18\nu} \quad (B.17)$$

Where:

s = relative density of sediment fraction = $\frac{\rho_s - \rho}{1000}$

g = gravity acceleration

d_s = representative diameter of the sediment fraction (depends on d_{50} and d_{50} can be specified in the Delft3D FLOW model)

ν = kinematic viscosity

With the above standing equations the deposition flux can be fine-tuned.

Erosion Flux

The erosion flux can be determined with the expression:

$$E = \varepsilon_s \frac{dc}{dz} \quad (B.18)$$

Where:

ε = eddy diffusivities of sediment fraction

dc/dz = the change in the concentration over the vertical

dc/dz can be calculated with a specified profile: the Rouse profile. More information about this profile can be found in the literature study 'interactions between Mangrove Forests, Hydrodynamics and Morphodynamics (Dekker, 2005)

Bed-load transport

The basic equation for bed-load transport, used in Delft3D FLOW, is:

$$|S_b| = 0.006\eta\rho_s w_s d_{50}^{(\ell)} M^{0.5} M_e^{0.7} \quad (\text{B.19})$$

Where:

- S_b = bed-load sediment transport
- η = relative availability of the sediment fraction in the mixing layer
- ρ_s = density of sediment
- w_s = settling velocity of sediment
- $d_{50}^{(l)}$ = mean grain size diameter of the sediment
- M = sediment mobility number due to waves and currents
- M_e = excess sediment mobility number

An important parameter for bed-load sediment transport is the critical bed shear stress (θ_{cr}). There is no transport if the bed shear stress does not exceed this critical value. The critical bed shear stress can be calculated with the following equations:

$$\begin{aligned} \tau_{cr} &= (\rho_s - \rho_w) g d_{50} \theta_{cr} \\ \theta_{cr} &= 0.14 D_*^{-0.64}, \rightarrow 4 < D_* \leq 10 \\ D_* &= d_{50} \left[\frac{(s-1)g}{v^2} \right]^{1/3} \end{aligned} \quad (\text{B.20})$$

The bed shear stress depends on the velocity and the roughness. The higher the velocity, the higher the bed shear stress, the more chance that the critical value of the bed shear stress is exceeded. Another strategy to get more bed-load sediment transport is to decrease the grain size diameter d_{50} . This works in a double positive way, lowering the critical bed shear stress.

Morphological changes

The equation Delft3D uses to calculate the morphological changes, represents the same concept, but looks more complex:

$$\Delta_{SED}^{(n,m)} = \underbrace{\frac{\Delta t f_{MORFAC}}{A^{(n,m)}}}_{\text{factor}} \left\{ \left(\underbrace{S_{b,uu}^{(n,m-1)} \Delta y^{(n,m-1)}}_{in} - \underbrace{S_{b,uu}^{(n,m)} \Delta y^{(n,m)}}_{out} \right) + \left(\underbrace{S_{b,vv}^{(n-1,m)} \Delta x^{(n-1,m)}}_{in} - \underbrace{S_{b,vv}^{(n,m)} \Delta x^{(n,m)}}_{out} \right) \right\} \quad (\text{B.21})$$

Where:

- $\Delta_{sed}(n,m)$ = change in bed level
- Δt = computational time step
- f_{MORFAC} = user specified morphological acceleration factor
- A = area of computational cell
- $S_{b,uu}$ = computed bed load sediment transport vector in u direction, held at the u point of the computational cell
- Δx = cell width in x-direction
- Δy = cell width in y-direction

User specified parameters

In Delft3D FLOW the following things need to be specified when modelling the sediment transport and morphodynamics:

- How much sediment fractions will be used (maximum of 5) and if the sediment is cohesive or non-cohesive.
- The initial concentration of each sediment fraction
- The boundary concentrations of each sediment fraction
- The eddy diffusivity
- The reference density for hindered settling
- Specific density
- Dry bed density
- Mean sediment diameter
- The sediment layer thickness
- The MORFAC

B.2.5 Mangroves in Delft3D FLOW*Resistance force of mangroves*

The effects of mangrove forests on tides can be determined using the momentum equations. Mangrove forests are incorporated in this equation as a force. The force can be expressed as:

$$F_p(z) = \frac{1}{2} \rho \int_0^k C_D(z) m(z) D(z) |u(z)| u(z) dz \quad (\text{B.22})$$

Where:

- ρ = density of water
- k = plant height
- $C_D(z)$ = drag coefficient
- $m(z)$ = cylinder density per unit area
- $D(z)$ = cylinder diameter
- $u(z)$ = time averaged, horizontal flow velocity

This way of presenting the force of mangrove forest is used by Mazda et al (2005) and Wu et al, (2001). Vertical variations of the force generated by mangrove forests are large due to the root-trunk-canopy structure of a tree. These vertical variations are included in Delft3D-FLOW by making the stem diameter, the vegetation and the current velocity a function of height z . A typical schematisation is shown in figure B.5.

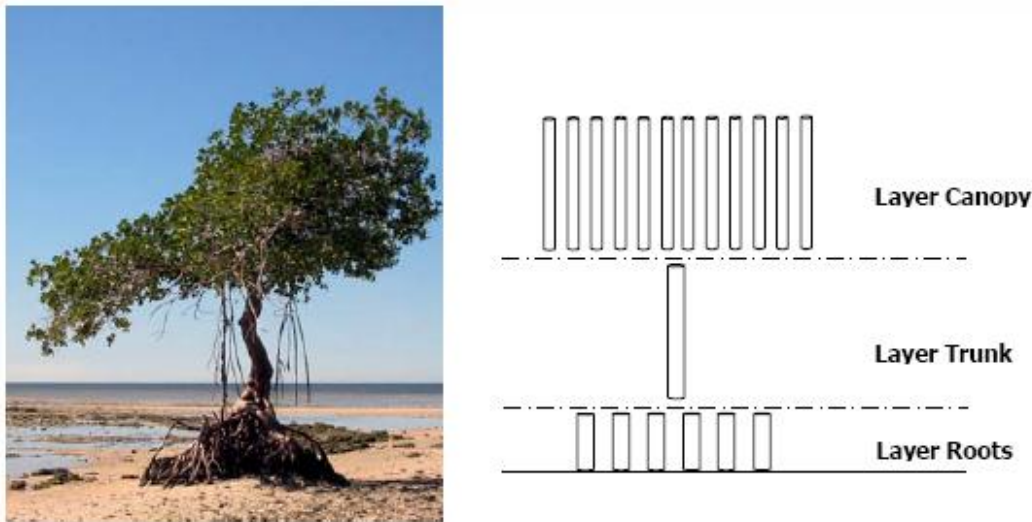


Figure B.5: schematisation of a mangrove tree in Delft3D FLOW [Burger, 2005]

Vertical mixing

Mangroves also have influence on the vertical mixing in the flow. This is reflected in an extra source term in the kinetic turbulent energy equation:

$$\frac{\partial k}{\partial t} = \frac{1}{1 - A_p} \frac{\partial}{\partial z} \left\{ (1 - A_p) (v + v_T / \sigma_k) \frac{\partial k}{\partial z} \right\} + T + P_k - B_k - \varepsilon \quad (\text{B.23})$$

with A_p the horizontal cross sectional plant area:

$$A_p(z) = \frac{\pi}{4} \phi^2(z) n(z) \quad (\text{B.24})$$

with $T(z)$ the work spent by upon the fluid:

$$T(z) = F(z) u(z) \quad (\text{B.25})$$

and an extra source term in the epsilon equation,

$$\frac{\partial \varepsilon}{\partial t} = \frac{1}{1 - A_p} \frac{\partial}{\partial z} \left\{ (1 - A_p) (v + v_T / \sigma_\varepsilon) \frac{\partial \varepsilon}{\partial z} \right\} + T \tau^{-1} + P_\varepsilon - B_\varepsilon - \varepsilon_\varepsilon \quad (\text{B.26})$$

with τ the minimum of:

the dissipation time scale of free turbulence:

$$\tau_{free} = \frac{1}{c_{2\varepsilon}} \left(\frac{k}{\varepsilon} \right) \quad (\text{B.27})$$

the dissipation time scale of eddies in between the plants:

$$\tau_{veg} = \frac{1}{c_{2\varepsilon} \sqrt{c_\mu}} \left(\frac{L^2}{T} \right)^{1/3} \quad (B.28)$$

that have a typical size limited by the smallest distance in between the stems:

$$L(z) = C_l \left\{ \frac{1 - A_p(z)}{n(z)} \right\}^{1/2} \quad (B.29)$$

C_l is a coefficient reducing the geometrical length scale to the typical volume averaged turbulence length scale. Uittenbogaard presents a closure and finds that a C_l value of 0.07 is applicable for grid generated turbulence. For vegetation this coefficient may be tuned, values of 0.8 are found applicable.

Required parameters

The parameters required for including the plants in Delft3D FLOW cannot be specified in the flow module itself, but need to be specified in a special file. In this file the following values should be presented:

- C_{lplant} ; the turbulent length scale coefficient between the stems, usually 0.80
- It_{plant} , number of time steps between updates of plant arrays, usually 50
- The height with for each height the diameter, density and drag coefficient. The drag coefficient is usually 1.
- A file where the location of the plant is specified, including the number of plants per m^2 .

B.3 Delft3D WAVE model

B.3.1 Background spectral wave analysis

Delft3D WAVE uses the model SWAN to calculate wave parameters. SWAN is a spectral wave model and uses a wave spectrum in its calculations. Basically the idea is that waves can be seen as the sum of a large number of harmonic wave components. A possible observed surface elevation is shown in figure B.6. The waves are on first sight quite irregular. However, the surface elevation can be reproduced as the sum of a large number of harmonic wave components:

$$\eta(t) = \sum_{i=1}^N a_i \cos(2\pi f_i t + \alpha_i) \quad (B.30)$$

Where:

- $\eta(t)$ = free surface elevation
- α_i = phase
- a_i = amplitude
- f_i = frequency

From the observed free surface elevation amplitude and phase can be determined for each frequency, and so an amplitude spectrum and a phase spectrum can be composed (see figure B.6). It can be seen from figure B.6 that the phases turn out to have any value between 0 and 360 without any preference for any one value. Only the amplitude spectrum remains to characterise the wave record. [Holthuijsen, 2005].

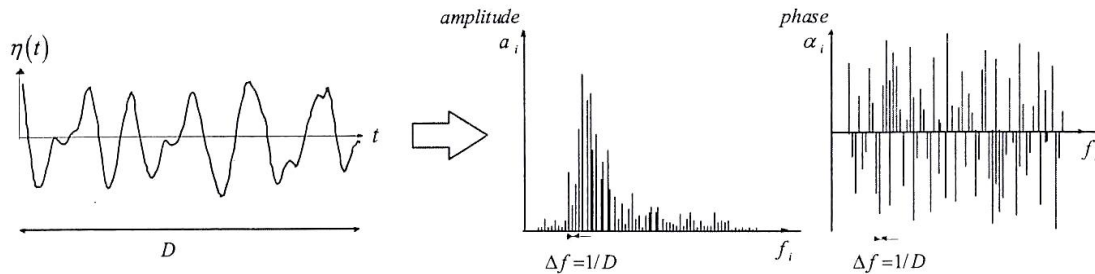


Figure B.6: The observed surface elevation and its amplitude and phase spectrum

When repeating the experiment the observed free surface elevation would be different and so would be the amplitude spectrum. But after a number of measurements and taking the average of all measurements an average amplitude spectrum will be found. The spectrum is not continuous and gives only for discrete frequencies f_i an amplitude a_i . It is believed however that a wave spectrum is continuous, so the discontinuous wave spectrum should be transformed to a continuous one. This is done in three steps (see also figure B.7):

1. Taking the variance of each wave component: $\frac{1}{2} \overline{a_i^2}$
2. Dividing the expected value of the variance ($E \left\{ \frac{1}{2} a_i^2 \right\}$) of the amplitude between each wave component by Δf
3. Let the frequency interval approach zero ($\Delta f \rightarrow 0$).

The formal definition of the variance density spectrum becomes:

$$E(f) = \lim_{\Delta f \rightarrow 0} \frac{1}{\Delta f} E \left\{ \frac{1}{2} a_i^2 \right\} \quad (\text{B.31})$$

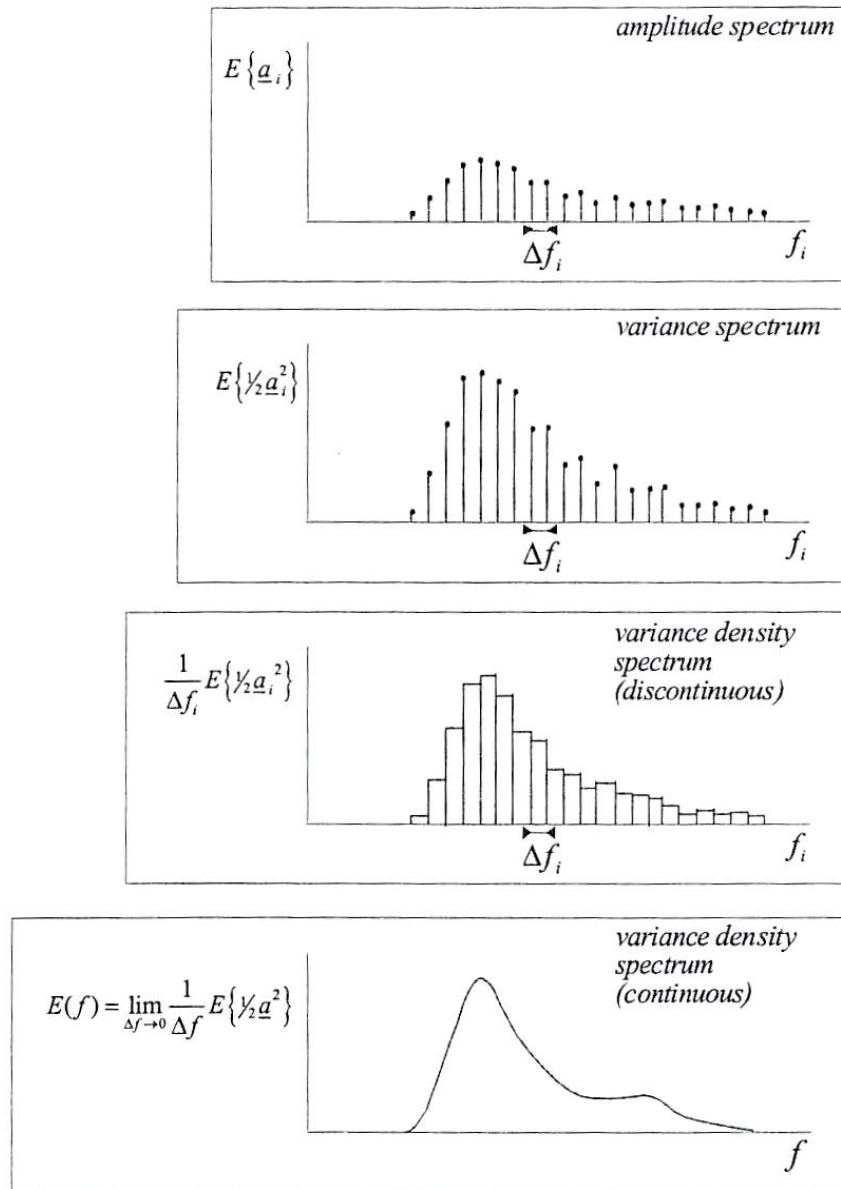


Figure B.7: the transformation of the discrete amplitude spectrum to the continuous variance density spectrum

By multiplying the variance density spectrum with the density of water ρ and the gravity acceleration g the energy density spectrum can be obtained. This spectrum provides the basis for modelling the physical aspects of the waves [Holthuijsen, 2005]. In figure B.8 three different spectra are shown with their irregular character for free surface elevation. The Delft3D WAVE module uses also the energy density spectrum to calculate a wave field. This will be more elaborated in the supplement ‘Modelling in Delft3D’.

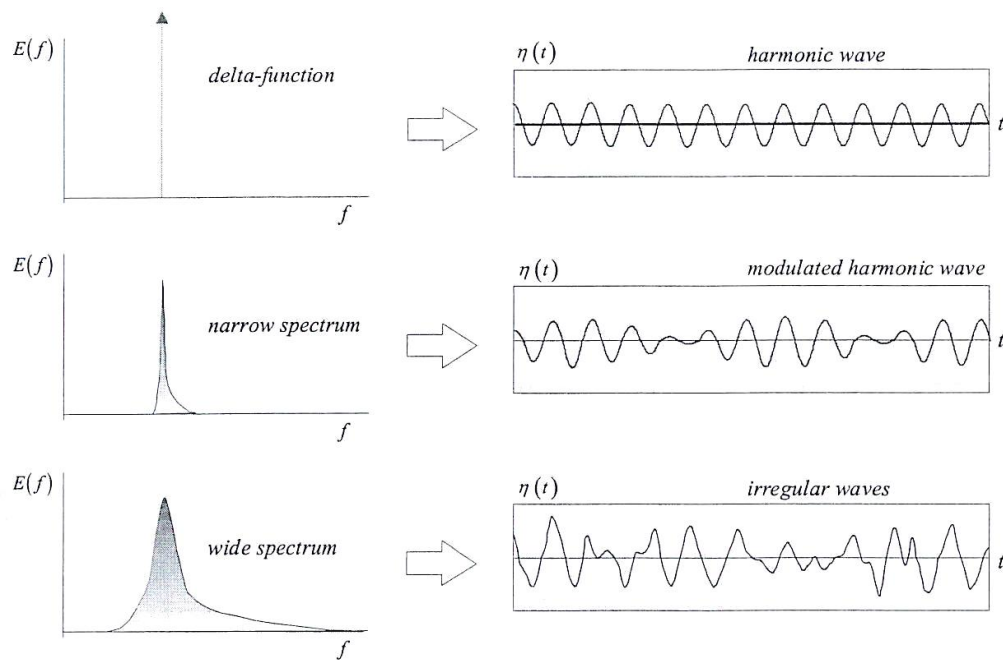


Figure B.8: The (ir)regular character of the waves for three different widths of the spectrum

B.3.2 Governing equations

Delft3D-WAVE uses a action density spectrum to model waves. The action density is:

$$N(\sigma, \theta) = \frac{E(\sigma, \theta)}{\sigma} \tag{B.32}$$

where:

- N = action density
- σ = relative frequency
- θ = wave direction

In WAVE the evolution of the wave spectrum is described by the spectral action balance equation which for Cartesian co-ordinates is:

$$\frac{\partial}{\partial t} N + \frac{\partial}{\partial x} c_x N + \frac{\partial}{\partial y} c_y N + \frac{\partial}{\partial \sigma} c_\sigma N + \frac{\partial}{\partial \theta} c_\theta N = \frac{S}{\sigma} \tag{B.33}$$

in this spectral action balance a lot of processes can be taken into account (if they can be expressed in terms of energy dissipation). The input of energy is only done by wind. The expression is:

$$S_{in}(\sigma, \theta) = A + BE(\sigma, \theta) \tag{B.34}$$

Where:

- A = linear growth term
- BE = exponential growth term

The dissipation of energy can be attributed to:

- White capping
- Bottom friction
- Depth induced breaking

These three processes are taken into account in Delft3D WAVE. They have their own expression which can be found in the Delft3D WAVE User Manual.

B.3.3 Vegetation and Delft3D WAVE

Vegetation cannot be implemented in the same way as in Delft3D FLOW. It should be implemented in a more implicit way. One way to do this is using a collins friction factor. This factor can be used to calculate the energy dissipation of waves over a bottom. The energy dissipation and the collins friction factor are related with the following equations:

$$S_{ds,b}(\sigma, \theta) = -C_{bottom} \frac{\sigma^2}{g^2 \sinh^2(kd)} E(\sigma, \theta) \quad (\text{B.35})$$

With:

$$C_{bottom} = c_v g U_{rms} \quad (\text{B.36})$$

Where:

- S = energy dissipation
- C_{bottom} = bottom friction coefficient
- σ = relative frequency
- E = energy
- c_v = Collins Friction factor
- U_{rms} = orbital velocity

To relate this to vegetation the collins friction factor can be approximated by:

$$c_v = f_w^* \cdot D \cdot n \cdot dz \quad (\text{B.37})$$

Where:

- f_w = friction coefficient (about 0.9)
- D = plant diameter
- n = plant density
- dz = plant height

C Delft3D Flow and Wave results

Although the Delft3D FLOW and WAVE model is widely used, it is always good to check the model performance with some simple cases. This appendix describes the model checking, focussing on the flow velocity (as the driving force behind bed shear stress) and eddy diffusivity. First cross-shore tidal flows, flow velocity profiles and eddy diffusivity are analysed and, because these are the most important parameters for sediment transport processes and morphodynamics. In this way, the Delft3D Flow module is tested. Secondly the Delft3D Wave module is tested on the processes shoaling and refraction, by comparing the results with the linear wave theory. Thirdly the influence of waves on bed shear stress, turbulence sediment concentration, sediment transport and sedimentation/erosion processes is analysed, for varying wave height and period. No check is made because of the complexity of the processes and no measurements. It generates insight in the effect of waves.

C.1 Delft3D FLOW

Three processes are analysed and checked in this paragraph:

- Cross-shore tidal flows
- Flow velocity profiles
- Eddy viscosity

They will be treated subsequently

C.1.1 Cross-shore tidal flow without vegetation

For tidal flow the situation is shown in figure C.1. Imagine a beach with a slope of $\sin \beta$. The water level is increasing so $h_{t+\Delta t}$ is higher than h_t . Because of the rise in water level the water will flow in the direction of the beach. This flow is caused by gravity forces F_g . The bed shear stress τ_b (or the friction force F_s) act in opposite direction to the flow. The acting forces will cause a gradient in the water level with a slope of $\sin \alpha$.

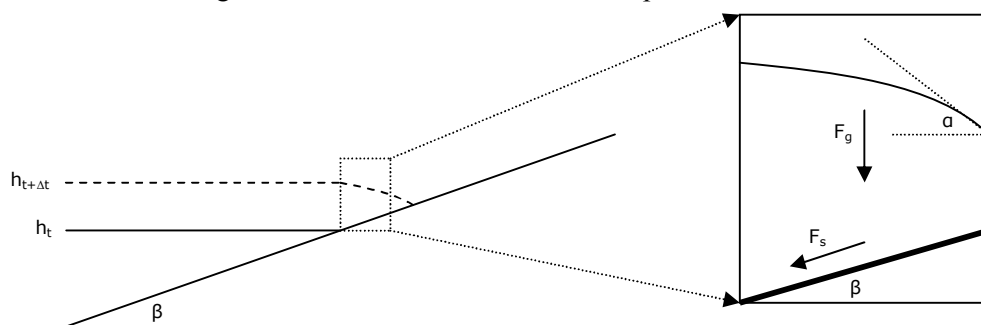


Figure C.1: tidal water level variations on the beach

The tidal water level variation can be described by:

$$h(t) = A \cos(\omega t) \tag{C.1}$$

Where:

$h(t)$ = water level on time t

A = amplitude

ω = the frequency

The vertical velocity u_v of the water level is:

$$\frac{dh}{dt} = -\omega A \sin(\omega t) = u_v \tag{C.2}$$

The velocity in the upward direction can also be translated to a horizontal flow velocity u_h using the slope of the beach i_b :

$$u_h = \frac{u_v}{i_b} = -\frac{\omega A \sin(\omega t)}{i_b} \tag{C.3}$$

Hand calculations

For the calculations a 2 m high 12 hr tide is used. The beach slope i_b is 0.006. This lead to the following equation for the water level and the flow velocity:

$$h(t) = 2 \cos\left(\frac{\pi}{21600} t\right) \tag{C.4}$$

Where t is the time in seconds

The horizontal flow velocity is:

$$u(t) = -\frac{2\pi \sin\left(\frac{\pi}{21600} t\right)}{21600 i_b} \tag{C.5}$$

Model calculations

The results are almost the same. There are some little fluctuations in the flow velocity when the water level is rising. These fluctuations can be attributed to the fact that Delft3D is a discrete model. This results in little jumps in the water level when an area is becoming wet. These little jumps have also influence on the flow velocity and that can be seen in the graph above. When an area is getting dry the effect of these jumps on the flow velocity are smaller.

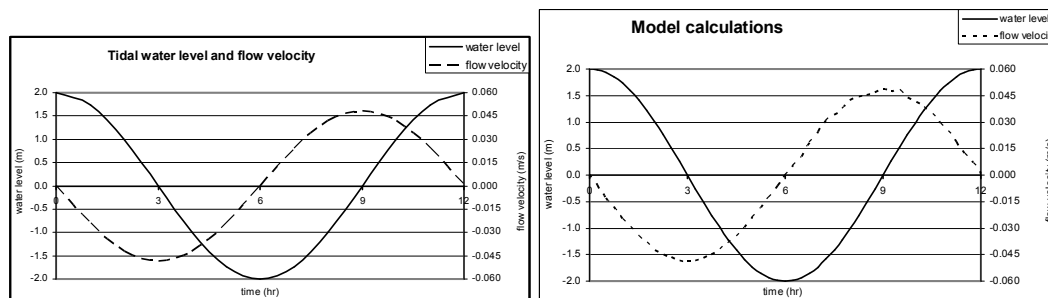


Figure C.2: water level variations and flow velocities during a tide calculated with equation (C.4) and (C.5) (left) and model calculations of water level variation and tidal flow velocities (right)

C.1.2 Velocity profiles

The situation of the combination of tidal flow and vegetation is schematised in figure C.3.

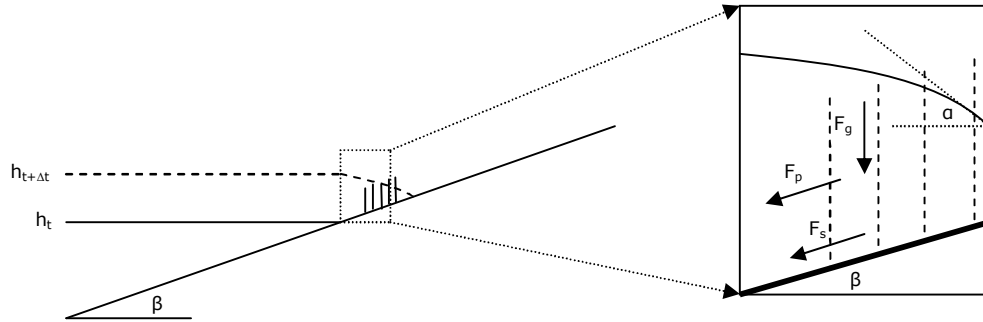


Figure C.3: tidal water level variations in combination with vegetation

The vegetation will lead to an extra force F_p acting in opposite direction of the flow. The bed shear stress will remain constant, so the gravity force should increase to balance F_p . This will result in a steeper water level gradient and in a lower flow velocity.

When the water level is decreasing and water flows out of a vegetation field, the opposite will take place. The water level inside the vegetation field will remain higher than outside the vegetation field, because of the friction force of the vegetation. On the border of the vegetation field the water will suddenly find less friction to flow and will flow faster.

The velocity profile in the vegetation field will also change. It is often assumed that inside the vegetation field the flow is uniform (depending on the flow velocity and the vegetation characteristics). The profile for emergent vegetation, submerged vegetation and no vegetation is shown in figure C.4. The figure shows characteristic profiles. These profiles should also be found in the model calculations.

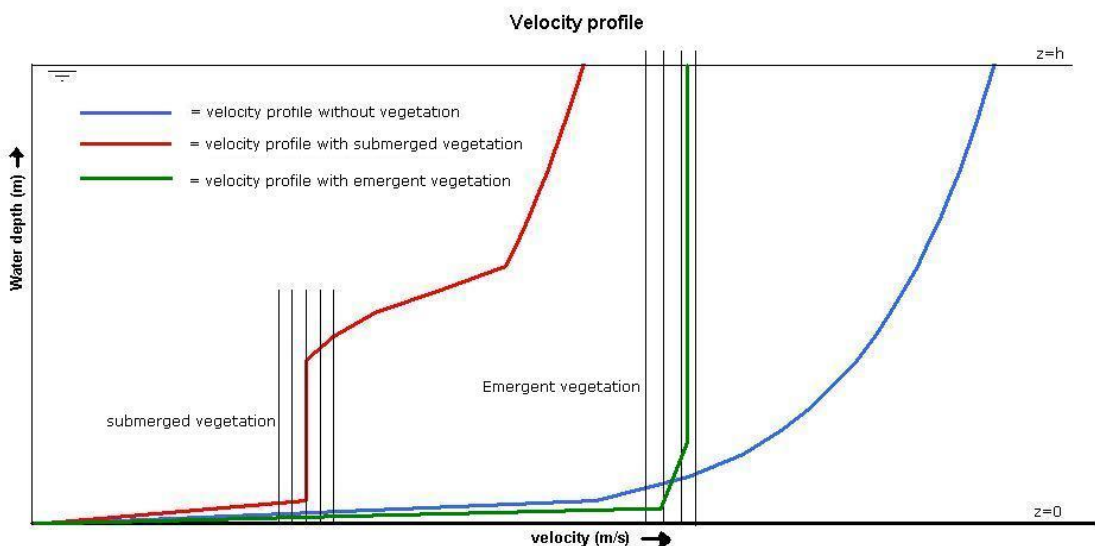


Figure C.4: velocity profiles for submerged, emergent and no vegetation

Model calculations

The result of the model is shown in figure C.5. From this figure the profiles from figure C.4 can be recognised easily. It can be concluded from this figure that the processes considering the velocity profile are modelled well in Delft3D.

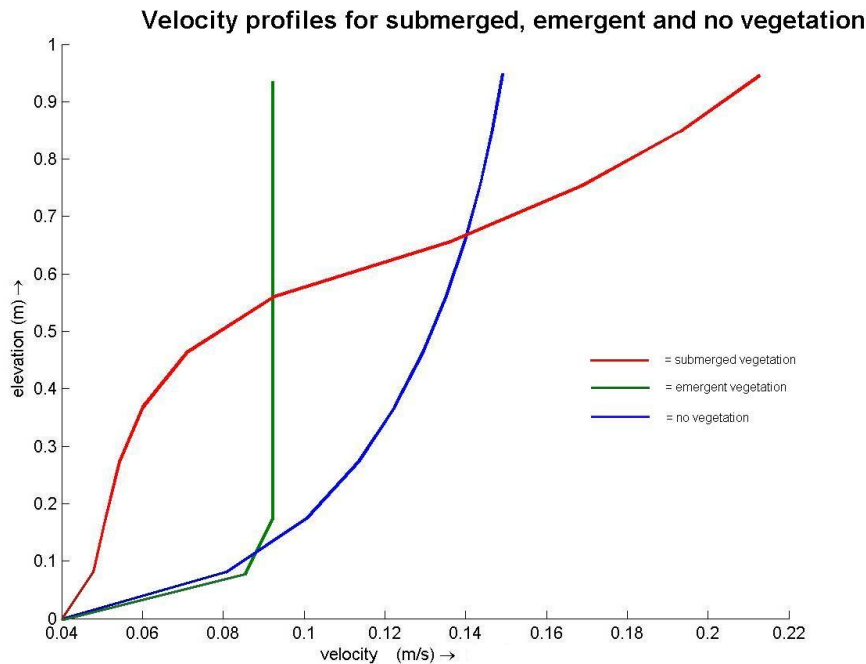


Figure C.5: velocity profiles for the situation with emergent vegetation, submerged vegetation and no vegetation, calculated with the Delft3D FLOW model

C.1.3 Eddy viscosity

For the sedimentation and erosion process not only the bed shear stress is important, but also the kinetic energy (turbulence) and the energy dissipation. These two parameters determine the eddy viscosity, which is important for the calculation of the erosion flux. The relation is:

$$E = \varepsilon_s \frac{dc}{dz} \quad (C.6)$$

Where:

E = erosion flux

ε_s = eddy diffusivity

dc/dz = concentration gradient

The eddy diffusivity can be expressed as:

$$\varepsilon_s = c_\mu \frac{k^2}{\varepsilon} \quad (C.7)$$

Where

ε_s = eddy diffusivity

c_μ = empirical constant (0.09)

k = kinetic turbulent energy

ε = energy dissipation

The kinetic turbulent energy and the energy dissipation are related to each other and influenced by the vegetation. The equations for the kinetic turbulent energy and the energy dissipation are:

$$\frac{\partial k}{\partial t} = \frac{1}{1-A_p} \frac{\partial}{\partial z} \left\{ (1-A_p)(\nu + \nu_T / \sigma_k) \frac{\partial k}{\partial z} \right\} + T + P_k - B_k - \varepsilon \quad (C.8)$$

and

$$\frac{\partial \varepsilon}{\partial t} = \frac{1}{1-A_p} \frac{\partial}{\partial z} \left\{ (1-A_p)(\nu + \nu_T / \sigma_\varepsilon) \frac{\partial \varepsilon}{\partial z} \right\} + T\varepsilon^{-1} + P_\varepsilon - B_\varepsilon - \varepsilon_\varepsilon \quad (C.9)$$

With:

$$A_p(z) = \frac{\pi}{4} \phi^2(z) n(z) \quad (C.10)$$

$$T(z) = F(z)u(z) \quad (C.11)$$

Normally the kinetic turbulent energy has a linear profile with a value of 0 at the water surface and a higher value at the bottom. The value at the bottom depends on the bed shear stress. The energy dissipation is often assumed to have a logarithmic profile with a low value at the water surface and a high value at the bottom. When vegetation is added the vertical profiles of the kinetic turbulence energy and the energy dissipation will change. There will be a lot of turbulent energy just above the vegetation. Inside the vegetation the kinetic turbulent energy will be lower than the original value, because there is almost no velocity and therefore a very low shear stress. The dissipation of energy is also high in the upper part of the vegetation, because of the (relatively) high flow velocity in the vegetation. It decreases at the bottom again, because of the low flow velocity. The possible profiles of kinetic turbulent energy and energy dissipation are shown in figure C.6.

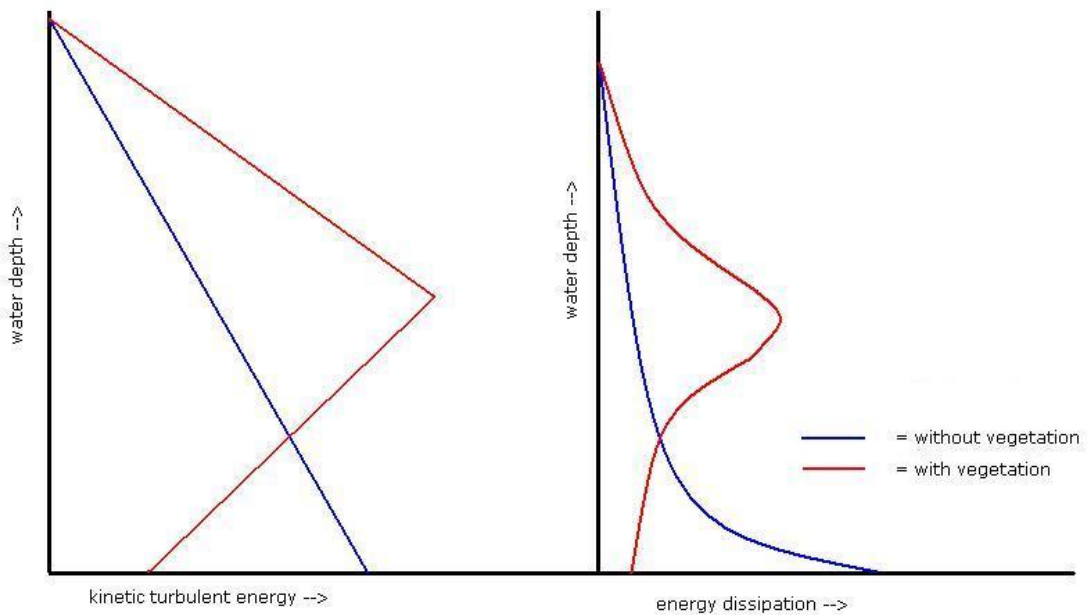


Figure C.6: possible kinetic energy and turbulent energy profiles

It is difficult to say which situation will result in higher eddy diffusivities. The eddy diffusivity is of influence on the concentration profile of the sediment. By assuming no change of concentration in the time, constant horizontal flow velocities (u and v) and a very low (negligible) horizontal turbulence the sediment balance reduces to:

$$w_s c = \varepsilon_s \frac{\partial c}{\partial z} \quad (\text{C.12})$$

or:

$$\frac{w_s}{\varepsilon_s} = \frac{1}{c} \frac{\partial c}{\partial z} \quad (\text{C.13})$$

where:

w_s = settling velocity

c = sediment concentration

ε_s = eddy diffusivity

From this equation can be seen that a high eddy diffusivity results in a low gradient of the concentration and a flatter concentration profile. A high diffusivity corresponds to a high kinetic turbulent energy. More turbulence will result in a better mixing of the sediment in the water column and the change of concentration of sediment in the water depth will be low, so the gradient will be small. A Rouse profile is often used to represent the sediment concentration in the water column. In figure C.7 a sediment concentration profile with and without vegetation is shown.

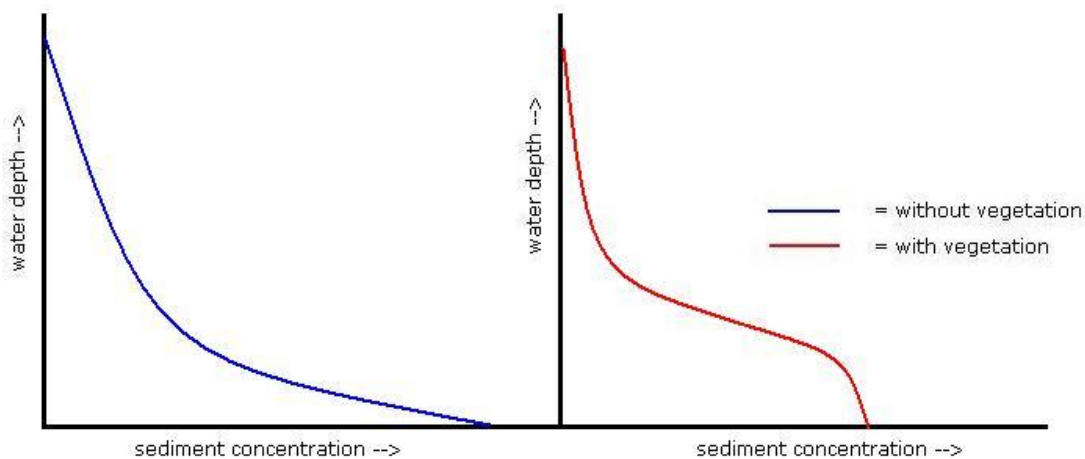


Figure C.7: possible sediment concentration profiles with (right) and without (left) vegetation

Model calculations

During the model calculations three situations are reviewed: no vegetation, submerged vegetation and emergent vegetation. In figure C.8 the results for these three situations are shown. It is very similar as described above according to the theory. So, the conclusion is that the processes responsible for energy dissipation and kinetic energy are modelled well.

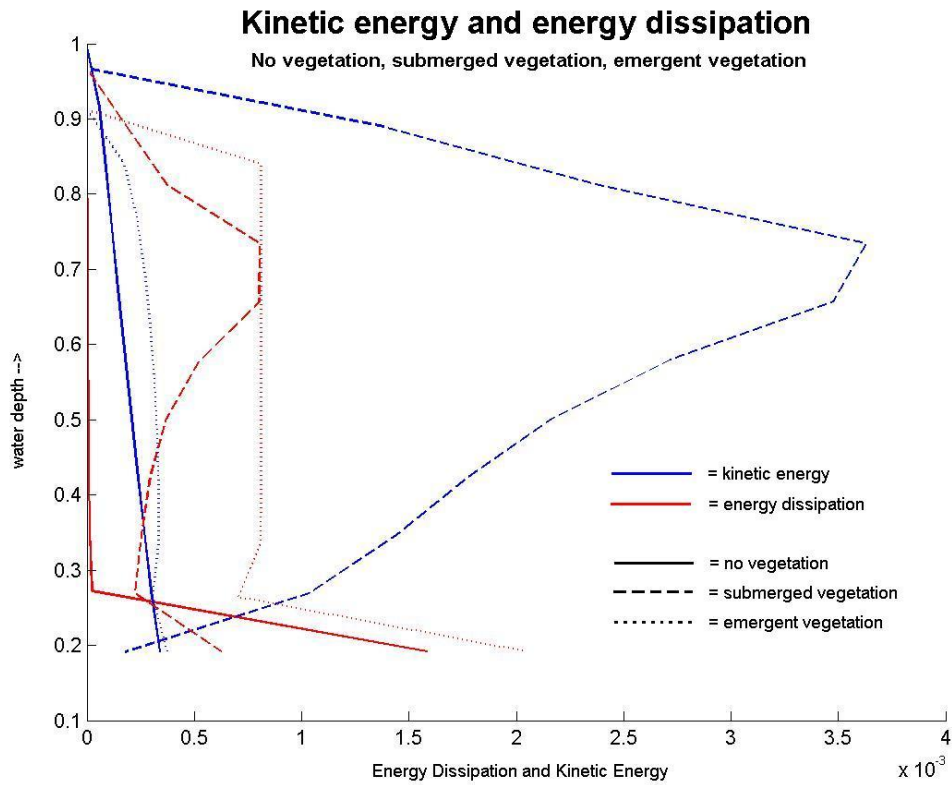


Figure C.8: kinetic energy and energy dissipation for no vegetation, submerged vegetation and emergent vegetation

C.1.4 Conclusion

In this paragraph the Delft3D FLOW model is checked. The model corresponds very well to the hand calculations and conceptual models also presented in this paragraph. The discretisation of the reality into different grid cells has some influence on the results of the model and may lead to some differences between hand and model calculation. However, the differences are not too big and both graphs of model and hand calculations show the same pattern. It can be concluded that the Delft3D FLOW model performs good and will be useful in the analysis of the morphodynamics in and around mangrove forests.

C.2 Delft3D WAVE model

This paragraph will check the Delft3D WAVE model by comparing the linear wave theory calculations to the model calculations. First the linear wave theory will be described and the used equations will be listed. In the second place the hand and model calculations will be executed and compared with each other. This results in conclusions about the Delft3D WAVE model.

C.2.1 Basics of the linear wave theory

The linear wave theory is the basis of most of the wave calculation. The most important parameters are shown in figure C.9 and C.10.

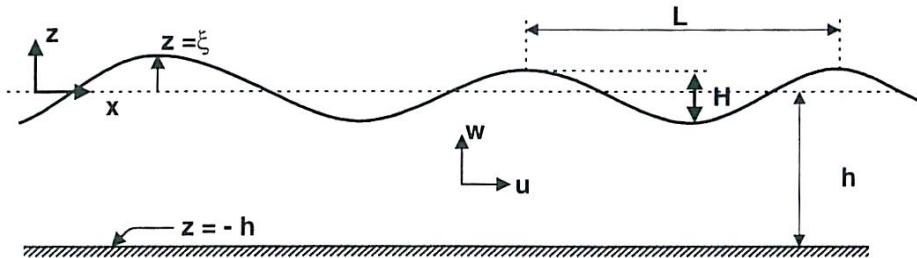


Figure C.9: explanation of parameters in a wave environment

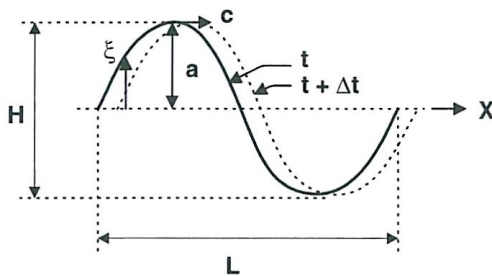


Figure C.10: explanation of parameters in a wave

Where:

- z = water level
- h = water depth
- H = wave height
- L = wave length
- w = orbital velocity in vertical direction
- u = orbital velocity in horizontal direction
- a = wave amplitude
- c = propagation velocity of the wave

The linear wave theory has the following assumptions:

- Constant water depth
- Two dimensional wave motion
- Waves are constant of form thus do not change with time
- Incompressible fluid
- Viscosity, turbulence and surface tension are neglected
- The wave height H is small compared to the wave length L and the water depth h .

The basic equations are:

The continuity (or Laplace) equation:

$$\frac{\partial^2 \phi}{\partial x^2} + \frac{\partial^2 \phi}{\partial z^2} = 0 \quad (\text{C.14})$$

The momentum (Bernouilli) equation:

$$\frac{\partial \phi}{\partial t} + \frac{p}{\rho} + gz = 0 \quad (\text{C.15})$$

To solve these equations boundary conditions should be specified at the flow boundaries [Hulscher et al., 2004]:

$$\text{Bottom:} \quad \rightarrow z = -h \quad \rightarrow \quad \frac{\partial \phi}{\partial z} = 0 \quad (\text{C.16})$$

$$\text{Water surface:} \quad \rightarrow z = 0 \rightarrow \quad \frac{\partial \phi}{\partial t} + g\eta = 0$$

$$\frac{\partial \phi}{\partial z} = \frac{\partial \eta}{\partial t} \quad (\text{C.17})$$

The general solution for the wave height is:

$$\eta(x, t) = a \sin(\omega t - kx)$$

$$a = \frac{1}{2} H, \omega = \frac{2\pi}{T}, k = \frac{2\pi}{L}, c = \frac{L}{T} = \frac{\omega}{k} \quad (\text{C.18})$$

The wave length L can also be calculated with the so-called dispersion relation:

$$L = L_0 \tanh \frac{2\pi h}{L} \quad (\text{C.19})$$

And:

$$L_0 = \frac{gT^2}{2\pi} \quad (\text{C.20})$$

Where:

L = wave length

L₀ = wave length at deep water

T = wave period

When the wave period and the wave height are known the wave height can be calculated at any place and any time.

The orbital velocity can be written as:

$$\phi(x, z, t) = \frac{\omega a}{k} \frac{\cosh k(z+h)}{\sinh kh} \cos(\omega t - kx) \quad (\text{C.21})$$

The horizontal and vertical orbital velocities are (the velocity field):

$$\begin{aligned} u(x, z, t) &= \frac{\partial \phi}{\partial x} = \omega a \frac{\cosh k(z+h)}{\sinh kh} \sin(\omega t - kx) \\ w(x, z, t) &= \frac{\partial \phi}{\partial z} = \omega a \frac{\sinh k(z+h)}{\sinh kh} \cos(\omega t - kx) \end{aligned} \quad (\text{C.22})$$

The energy inside a wave can be calculated with:

$$E = \frac{1}{8} \rho g H^2 \quad (\text{C.23})$$

Where:

E = wave energy

H = wave height

Using the wave energy the processes shoaling and refraction can be calculated. Shoaling is the process that the wave height increases when the water depth decreases. Refraction of waves mean that waves when they propagate to the shore under an angle they turn in a way that their propagation direction is perpendicular to the shore. with a shoaling factor K_{sh} and a refraction factor K_r these processes can be calculated:

$$K_{sh} = \sqrt{\frac{1}{\tanh\left(1 + \frac{2kh}{\sinh 2kh}\right)}} \quad (\text{C.24})$$

$$K_r = \sqrt{\frac{\cos \theta_0}{\cos \theta}} \quad (\text{C.25})$$

Where θ is the angle of the wave ray to the shore and can be calculated with Snell's law:

$$\frac{\sin \theta}{c} = \text{constant}$$

And

$$c = \frac{\omega}{k} \quad (\text{C.26})$$

Using these equations and the relation

$$\frac{H}{H_0} = K_{sh} * K_r \quad (\text{C.27})$$

the wave height can be calculated at any position and water depth in front of the shore. The only parameters that have to be known are the wave height H, the wave period T, the angle under which the wave is propagating and the water depth h. The process of diffraction is not described here, because it is not incorporated in Delft 3D WAVE.

C.2.2 Checking calculations

Hand calculations

The situation is shown in figure C.11.

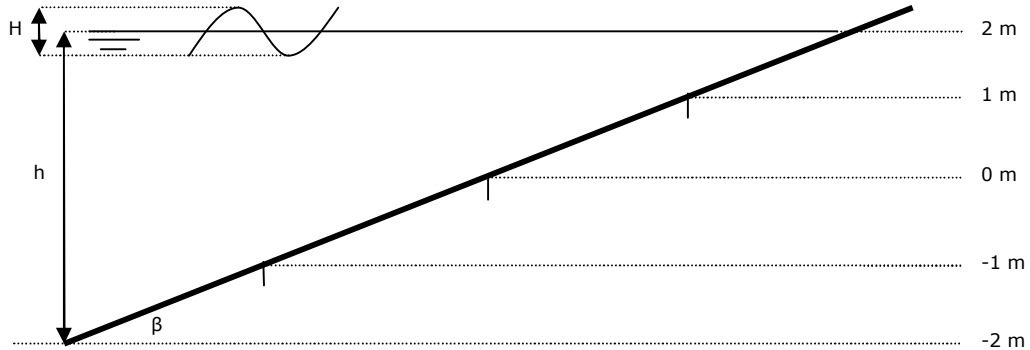


Figure C.11: situation of wave calculations

A wave with wave height $H = 0.215$ m (in order to get a wave height of 0.2 m at a water depth of 4 m) and period $T = 5$ sec (at deep water) is propagating in the direction of the shore. The shore has a slope of $\sin \beta = 0.002$. The wave height is calculated for the points shown in figure B.13. The result is given in table C.1. For a wave propagating under an angle of 45 degrees the wave height is also calculated and the results are shown in table C.2. The parameters shown are h is the water depth, L the wave length, c the wave propagation velocity, n the coefficient, K_{sh} the shoaling factor, H the wave height, θ the wave angle, K_r the refraction factor.

Table C.1: results of wave calculation with shoaling

h (m)	L (m)	c (m/s)	n (-)	K_{sh} (-)	H (m)
4	28	5.6	0.81	0.93	0.20
3	25	5.0	0.85	0.96	0.21
2	21	4.2	0.90	1.02	0.22
1	15	3.0	0.95	1.16	0.25

Table C.2: results of wave calculation with shoaling and refraction

h (m)	θ	K_{sh} (-)	K_r (-)	H (m)
4	30	0.93	0.90	0.18
3	27	0.96	0.89	0.18
2	22	1.02	0.87	0.19
1	16	1.16	0.85	0.21

Model calculations

In the Delft3D WAVE module the situation shown in figure C.11 is implemented. The wave height at the boundaries is set at 0.2 m and a period of 5 sec. For the refraction calculation the wave angle at the boundary of the model is set at 30 degrees. The results for the ‘shoaling’ calculation are shown in table C.3. The ‘refraction and shoaling’ result can be found in table C.3. It is difficult to determine the angle of the wave in the model because of

the influences of the border of the model. To find a wave angle it is tried to follow one wave ray, propagating in the direction of the coast. This is shown in figure C.12, including the coordinates for which the wave angle is determined.

Table C.3: results model calculation shoaling (left) and refraction (right)

h (m)	L (m)	H (m)	L (m)	θ	H (m)
4	19	0.20	19	30	0.18
3	18	0.21	18	27	0.18
2	16	0.22	16	23	0.19
1	13	0.24	13	16	0.21

Comparison of the results

The calculations of the model, considering the wave angle and the wave height coincide with the hand calculations. The wave length L is different however. This can be attributed to the way of calculation in Delft3D WAVE. Delft3D WAVE uses the model SWAN to calculate wave parameters. SWAN is a spectral wave model and uses a wave spectrum in its calculations (see appendix B for explanation).

The wave length L is calculated with the average wave number k. The wave number k and the angular wave frequency ω are related by the dispersion relation:

$$\omega^2 = gk \tanh kh \tag{C.28}$$

where g is the gravity acceleration and h the water level. The frequencies are transformed into a wave number and an average wave number is calculated from it. The average wave number does not coincide with the average frequency, therefore the mean wave length does is not the same as the wave length calculated with the linear wave theory. In table C.4 this is shown that the wave number of corresponding to the average frequency (calculated with equation (C.28)) is always lower than the average wave number. Therefore the wave length calculated with the average frequency is always higher than the wave length calculated with the average wave number.

Table C.4: relation between average wave frequency and average wave number (for a water depth of 2 m)

T (s)	f	w	k	L (m)
10	0.10	0.63	0.14	43.70
9	0.11	0.70	0.16	39.22
8	0.13	0.79	0.18	34.69
7	0.14	0.90	0.21	30.16
6	0.17	1.05	0.25	25.59
5	0.20	1.26	0.30	20.94
4	0.25	1.57	0.39	16.23
3	0.33	2.09	0.56	11.31
2	0.50	3.14	1.04	6.05
1	1.00	6.28	4.03	1.56
AVERAGE				
5.5	0.29	1.84	0.72	22.94

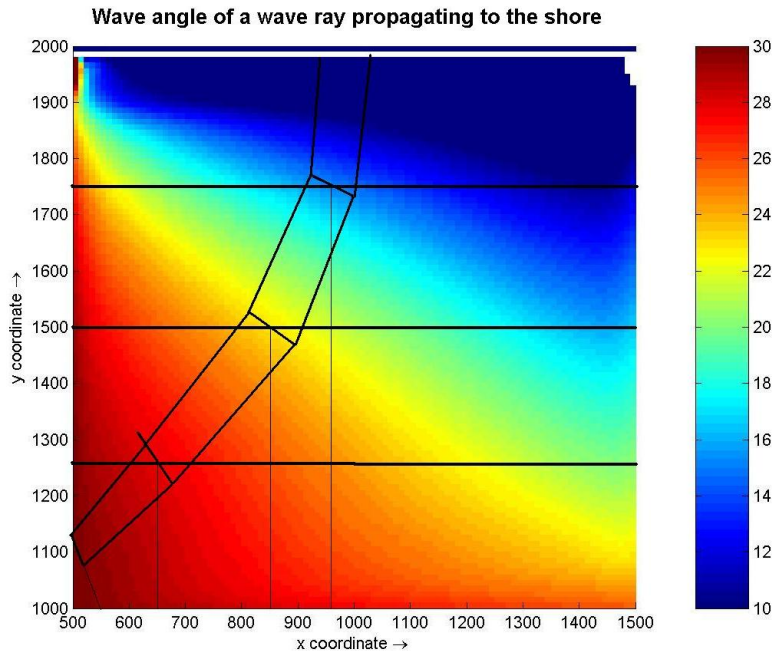


Figure C.12: wave angle of a wave ray propagating to the shore. The side influences of the boundaries of the model can also be seen clearly

In the wave module a peak period of 5 seconds is used. This period is also used in the hand calculations. Because the wave number corresponding to the peak period is lower than the average wave number, the wave length the model calculates is lower. This difference can be up to more than 10 m, but decreases when the water level decreases.

C.2.3 Conclusion

The model results coincide with the linear wave theory. A difference can be found in the wave length L , which can be attributed to the different way of calculation between the model and the hand calculations (harmonic waves versus wave spectra). From this observation can be concluded that wave height development is modelled well in the Delft3D WAVE model. This does not say anything about the capability to model sediment transport under waves. This depends on how the wave acting is communicated to the Delft3D FLOW model. The next paragraph will touch this issue.

C.3 Wave influences

This paragraph deals with the influences of waves on sediment transport processes. Modelled is a coast with a slope 1/500, a tidal water level variation of 4 m (between high tide and low tide), a Chezy value of 40 m^{1/2}/s and a JONSWAP wave spectrum with a JONSWAP bottom friction of 0.067 m²/s³. Wind and wave set-up are not taken into account. Wave breaking is taken into account with a breaking index of 0.73. The waves are not modelled under an angle. First the hydrodynamic components are subject of analysis and secondly the sediment transport components. The analysis is splitted in wave height and wave period influences. A lot of ‘strange’ effects occur when waves interact with flow and result in sediment transport and morphodynamic changes. This analysis only focuses on the influence of wave height and wave period to get some feeling with the model. It does not explain the ‘strange’ things. This will be done during the analysis of the real cases.

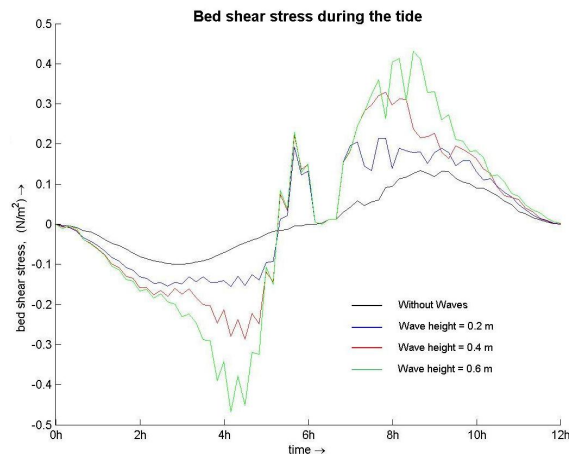


Figure C.13: bed shear stress during the tide

C.3.1 Hydrodynamic influences of waves

Wave height

The bed shear stress during the tide is shown in figure C.13. It can be seen that when the wave height increases the bed shear stress also increases. The jumps in the development of the bed shear stress correspond to the number of times the flow module and the wave module of Delft3D communicate. If they communicate more often the jumps will be less large.

The turbulent kinetic energy and the energy dissipation, shown in figure C.14 and C.15, show the expected behaviour. It can be seen that waves have a great influence on the kinetic turbulent energy and the energy dissipation, and, the larger the waves the more kinetic energy is produced and the more energy is dissipated. The kinetic energy and the energy dissipation results in a eddy diffusivity (see figure C.16). The diffusivities of a situation with waves do not differ much from the situation without waves. In general can be said that in the upper and lower part of the water column the eddy diffusivities are larger with waves than without waves. In between the eddy diffusivity without waves is larger. What the result will be for the sediment transport is difficult to say from this picture. More analysis is necessary.

An example of the Stokes Drift is shown in figure C.17. In the upper part of the water column the velocities are directed onshore. In the lower part the velocities are directed offshore. The velocities however seem to be very small, and this only occurs when the tidal flow velocities are small. The effect on the sediment balance will therefore also be small.

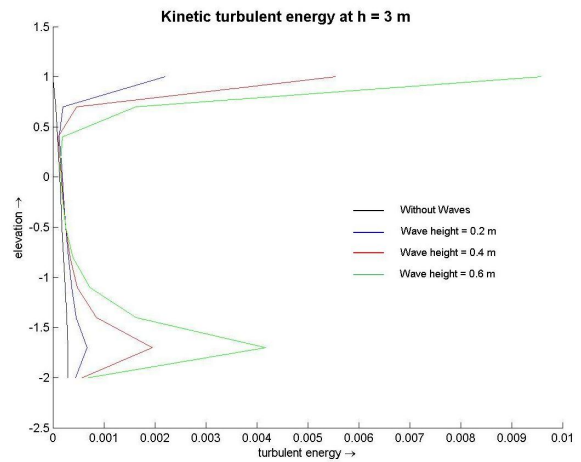


Figure C.14: kinetic turbulent energy

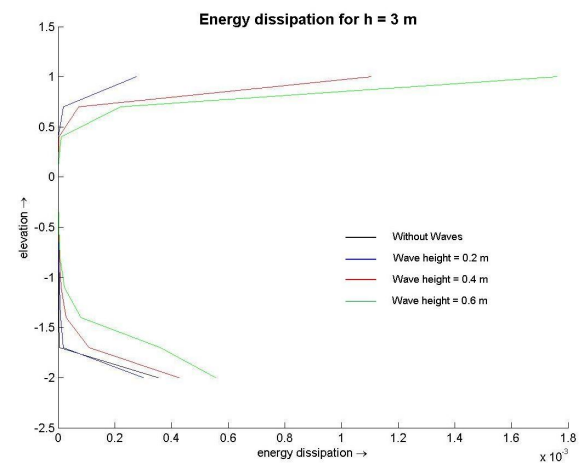


Figure C.15: Energy dissipation

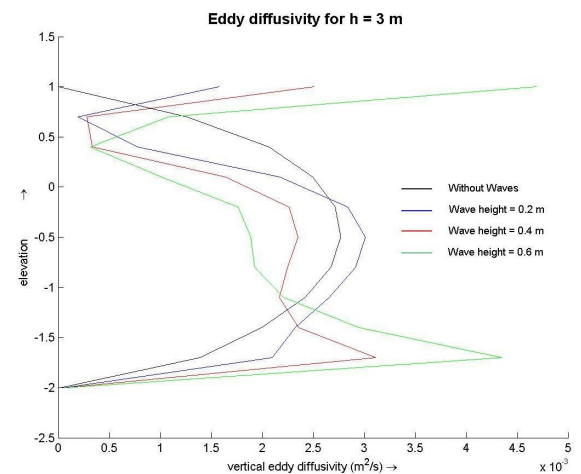


Figure C.16: eddy diffusivity

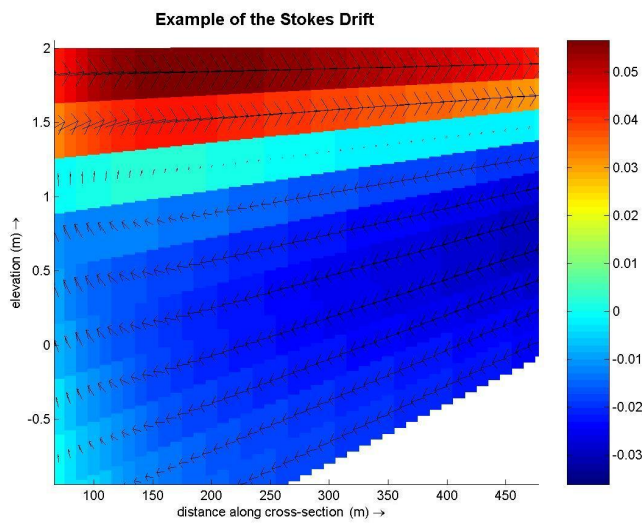


Figure C.17: example of the Stokes Drift

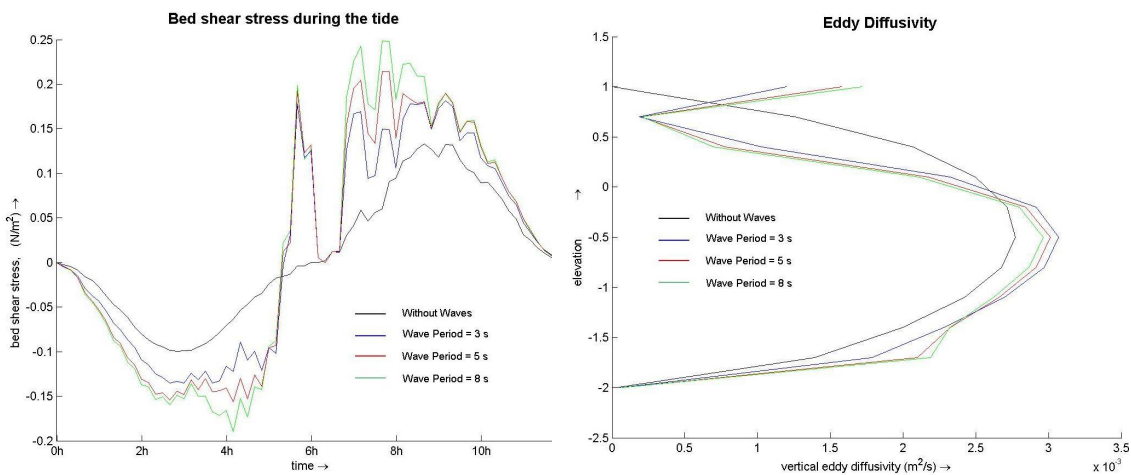


Figure C.18: Influence of wave period on bed shear stress; Figure C.19: influence of the wave period on the eddy diffusivity

For a wave period the same parameters are checked as above: the bed shear stress, the kinetic turbulent energy, the energy dissipation and the eddy diffusivity. The results are shown and analysed below. This is done for a wave height of 0.2 m.

Considering the bed shear stress (see figure C.18), it can be concluded that waves increase the bed shear stress and that a larger wave period results in a higher bed shear stress. The jumps in the line of the bed shear stress can be attributed to the number of communication times between the flow and the wave module of Delft3D. Comparing the influence of the wave period to the wave height, the wave period seem to have less influence on the bed shear stress than the wave height. The differences between the bed shear stress for different wave periods are smaller compared to the differences in bed shear stress for different wave heights.

The kinetic turbulent energy, the energy dissipation and the eddy diffusivity show the same effect for an increasing wave period as for an increasing wave height. Therefore only the eddy diffusivity is shown in figure C.19. The effect of an increasing wave period is, however, much smaller than the effect of an increasing wave height.

C.3.2 Sediment transport and morphology

Looking to the influence of the wave height and the wave period on the bed shear stress and the eddy diffusivity, it should be concluded that there is more sediment transport in the situation with waves than without waves. Moreover, larger waves and longer wave periods generate larger transports. However, in which direction takes the transport place? Onshore or offshore? And where does it depend on? In this paragraph these questions shall be tried to answer.

Wave height

Considering the influence of the wave height on the eddy diffusivity, the wave height should also have influence on the sediment concentration in the water column. This is shown in figure C.20 and it can be concluded that the larger the waves, the more sediment in the water column can be found.

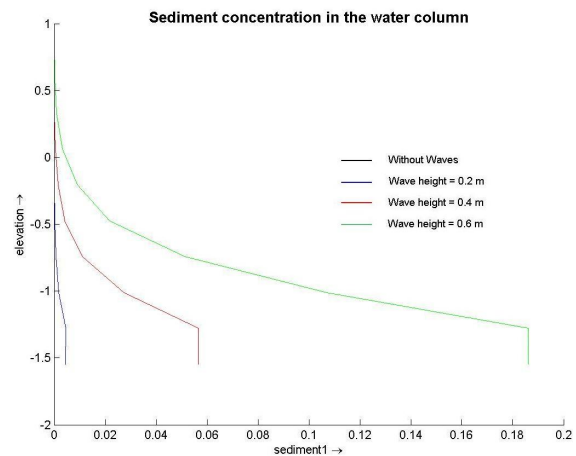


Figure C.20: influence of wave height on the sediment concentration profile

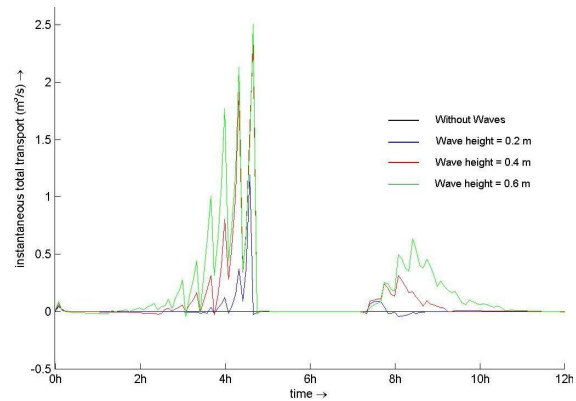


Figure C.21: influence of the wave height on sediment transport

More sediment in the water column and a larger bed shear stress should also generate more transport. This is shown in figure C.21. It can be seen that larger waves influence the bottom earlier than shorter waves. Therefore the period over which larger waves transport material is also larger. The end and the start of the period of transport can be attributed to the fact that the point becomes dry and wet again. When there is no water also no transport occurs. The transport is also very jump-like. This can be attributed to the number of communications between the flow and the wave module of Delft3D. The more the modules communicate, the smoother the line will be.

Than one question remains: in which direction takes the transport place. Will there be on this point erosion or sedimentation? Figure C.22 makes this clear. It shows the accretion of the bottom during the tide. First erosion takes place as the water level falls. When the water level rises again sedimentation takes place. The rate of erosion and of sedimentation depends on the wave height. Small waves give much erosion and less sedimentation. Large

waves give less erosion and much sedimentation. The differences in sedimentation and erosion between the different wave heights should be attributed to the Stokes drift and the sediment in the water column.

Wave period

The influence of the wave period is assessed in the same way as the influence of the wave height. The sediment concentration is shown in figure C.23. It can be seen that the sediment concentration in the water column decreases for an increasing wave period. This coincides with the fact that the kinetic turbulent energy decreases for an increasing wave period. The conclusion can be drawn that when kinetic turbulent energy increases vertical mixing increases and more sediment from the bottom will be picked up.

The sediment concentration is also important for the sedimentation – erosion process. The sedimentation and / or erosion is shown in figure C.24. When the water level is falling waves get more influence on the bottom, erosion takes place. When the water level rises again the waves do not bring in enough sediment to the coast to undo the erosion. The erosion is more as the wave period is small. The differences however are very small. This result corresponds with the previous result where the sediment concentration decreases as the wave period increases.

C.3.3

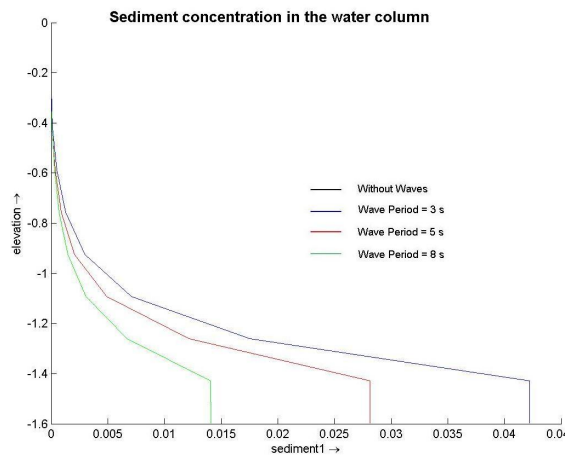


Figure C.23: influence of wave period on sediment concentration in the water column

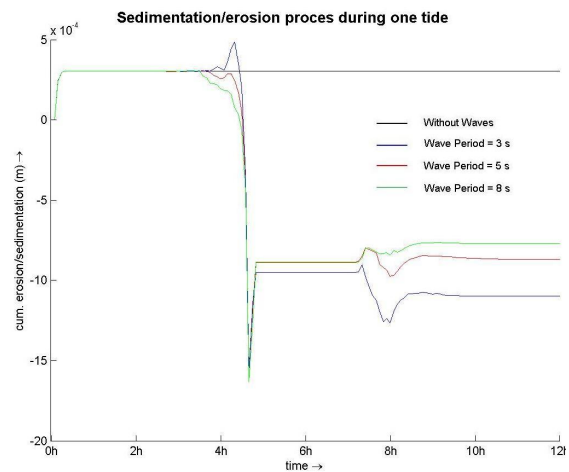


Figure B.26: influence of wave period on the sedimentation/erosion proces

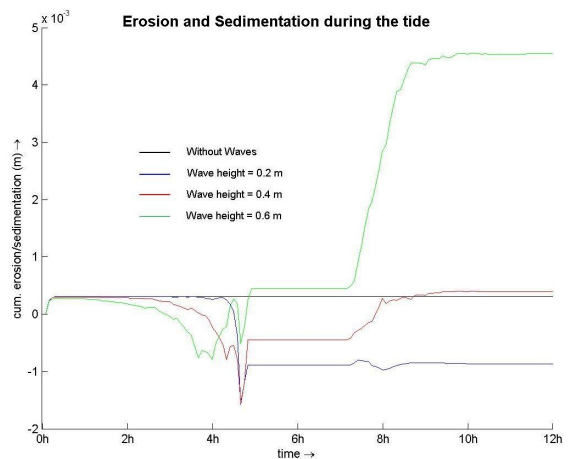


Figure C.22: influence of wave height on erosion and sedimentation during a tide

Conclusion

The analysis above focussed on the influence of wave height and wave period on the hydrodynamics and sediment dynamics. From this analysis can be concluded that high waves with a short wave period bring sediments to the coast. Short waves with long periods transport sediments towards the sea. This analysis is not checked with field observations and therefore no conclusions about the validity of the modelled processes can be drawn. It is even possible that the opposite will happen in reality. The analysis of the different mangrove forests should give more insight in the 'shape' and reality of the sediment transport processes due to waves.

No modelling results are added on waves and vegetation, because only the wave height will change, due to an increased value of the bed shear stress, which represents vegetation. The influence of the wave height on various hydrodynamic and sediment transport processes is assessed and described above.

D Calibration of the vegetation friction factor

The wave model uses a Collins friction factor to take the effect of vegetation into account. This factor should be calibrated, leading to a good reduction of the wave height. The wave height depends on the water level and so does the wave attenuation. Wave attenuation is usually expressed with:

$$r = \frac{H_{in} - H_{100}}{H_{in}} \tag{D.1}$$

Where:

- r = wave reduction factor
- H_{in} = incoming wave height
- H_{100} = wave height after 100 m forest

Values for the wave reduction factor r varies between 0.3 and 0.5 (see Mazda et al (1997), Quartel (2000), Massel et al (1999) and Schiereck and Booij (1995)). Because the wave attenuation depends on the water level, for three different water levels (1, 1.5 and 2 m) and for four different friction factors (0.5, 0.8, 1, 1.5) the wave attenuation will be determined, using the model explained in chapter 4. Table D.1 and figure D.1 present the results.

Table D.1: wave reduction factor for different water depths and friction factors.

friction factor f_w	r at h = 1m	r at h=1.5m	r at h=2m
1	0.58	0.37	0.24
0.8	0.54	0.33	0.21
0.5	0.44	0.24	0.15
1.5	0.65	0.46	0.31

From figure D.1 the following observations can be made:

- The relationship between friction factor and wave attenuation looks linear
- The differences between wave attenuation for the different water depths does not depend on the friction factor. The influence of the factor is constant.

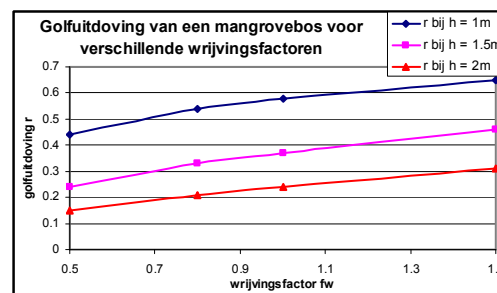


figure D.1: relatie tussen wrijvingsfactor en golfuitdoving

Because of the linear relationship it is possible to choose a friction factor. Assuming a maximum wave reduction factor of 0.5 at 1 m water depth, the friction factor will be 0.69 (see figure D.1). This value is used in the model calculations.

E Variants on the fringe model

The basic variant in chapter four was not able to reproduce the conceptual model of Walsh and Nittrouer (2004). Two other variants that are tried but gave the same erroneous results are described and analysed in this appendix. It starts with the long shore currents variant, followed by the hollow profile variant.

E.1 Long shore currents

E.1.1 Model set up

To take long shore currents into account another model setup is chosen. Modelled is a coast with a gradient of 1/200, a constant water level, and a water level gradient. The water level gradient is responsible for the long shore current, and should result in currents of about 1 m/s. Because of complexity in model set up the water level will be kept constant. The difference with tidal water level variations is that the waves are only acting on one spot on the coast and that the processes are overestimated at that point. The sedimentation/erosion pattern and all the processes leading to this pattern are analysed after one hour of modelling. The wave height is increased to 0.5 m and the sediment diameter also increased to 200 μm . This is done to get better results with modelling, because the chosen parameters are in the middle of the valid range for parameters (see chapter 4).

Figure E.1 shows the model setup, including the locations of mangroves. Two spots of mangroves are chosen, in order to analyse also the influence of the location of mangroves on a coast.

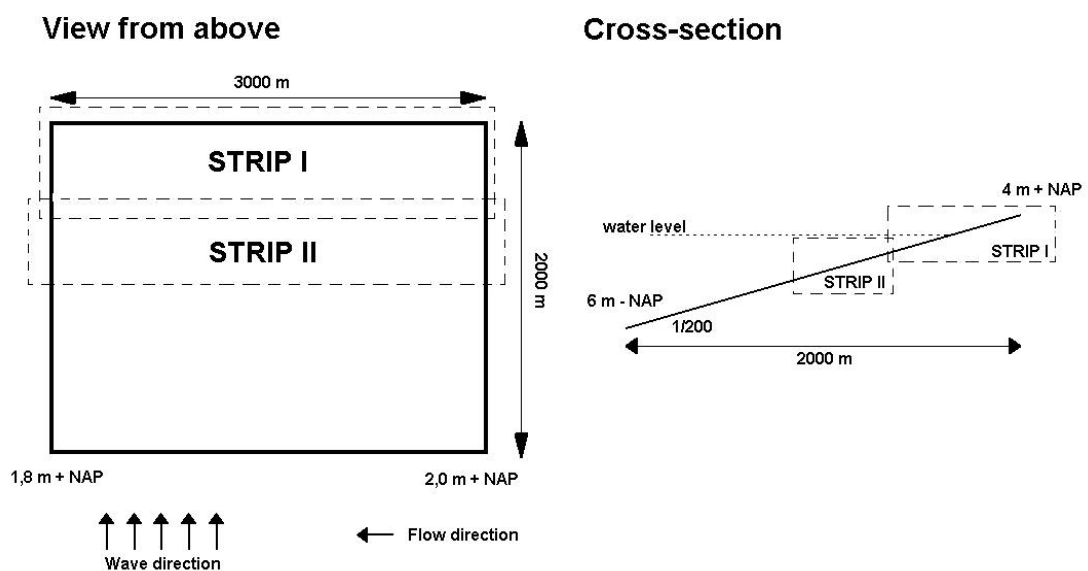


Figure E-1: view from above and aside of the coast where the effects of long shore currents on sediment transport are combined with the effects of waves. The two strips indicate the two different locations of fringe mangroves

E.1.2 Analysis

The analysis of this situation with long shore currents will be carried out in the same way as previous analysis.

Velocities

The long shore and cross-shore velocities are presented in figure E.2. The cross-shore currents are induced by waves and the long currents by a water level gradient.

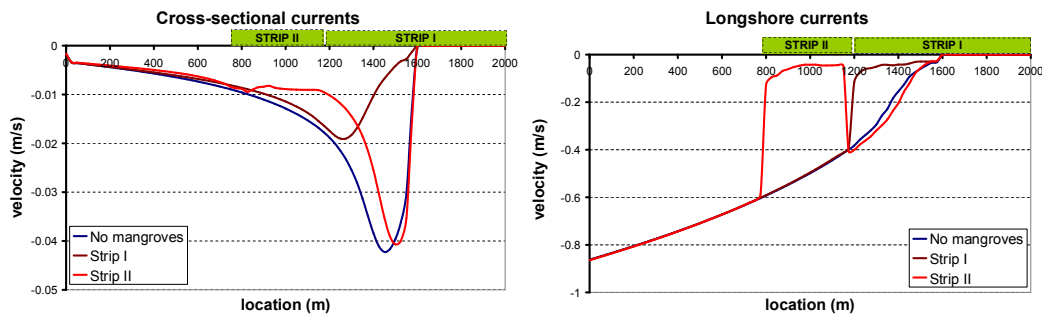


Figure E-2: (depth averaged) cross-shore (left) and long shore currents (right) for three different situations. The locations of the mangroves are presented by the green bar on top. A negative cross-shore current is directed offshore; a negative long shore current is directed to the left.

The following observations can be made:

- Cross-shore currents are much lower than long shore currents (factor 20!).
- The reduction in long shore currents is much higher than the reduction in cross shore currents. The resulting currents in long shore direction inside the mangroves however are with 4 cm/s higher than the cross-shore currents in general. The cross-shore current will be halved due to the mangroves.
- The long shore currents show a nice increase in magnitude from the beach (0 m/s) to open sea (0.9 m/s).
- The cross-shore currents are negative, which means that they are directed offshore. This can be attributed to the undertow of waves (see also chapter 2), which is the dominate process. Figure E.3 shows the cross-shore velocity in the water column. It can be seen that the undertow is so strong that even in the upper part of the water column the direction of the flow is onshore. Generally this is only in the lower part of the water column, where the name of the process also refers to. It is an indication that the processes are still not modelled well (see the previous section).
- The cross-shore currents show a peak value, directed onshore, around the breaking point of waves. This is confirmed in figure E.4, where the wave height development and the wave orbital velocity are shown. The peak value of the orbital velocity corresponds with the peak value in cross-shore currents. The peak value for mangrove strip I shows a low peak. This can be attributed to waves are not

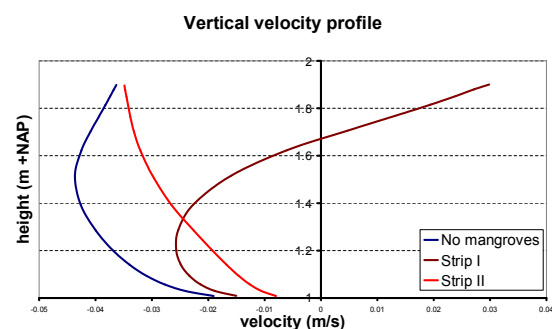


Figure E-3: vertical cross-shore velocity profile due to waves

breaking but attenuated by the forest. The breaking of waves leads to the high peak values in other situations. The peak values seem to depend only on the fact that waves are breaking or not, and not to the peak value in orbital velocity, or to the wave height values. This also indicates that the cross-shore currents due to waves are not modelled well.

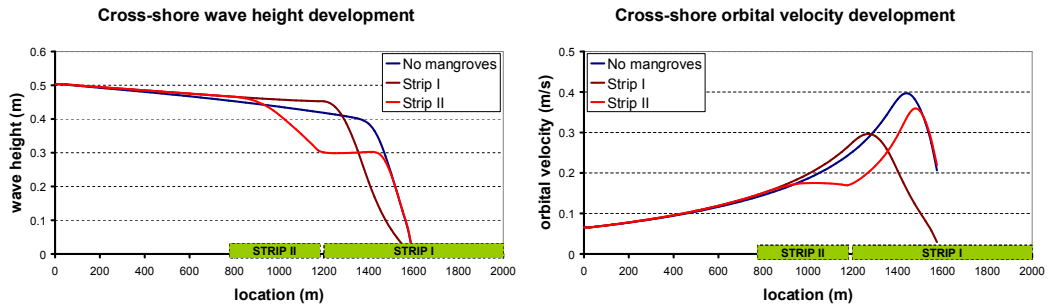


Figure E-4: wave height and orbital velocity development

Sediment concentration and transport

By combining the sediment concentration and the current the suspended sediment transport can be determined. Figure E.5 shows both the sediment concentration and the suspended sediment transport.

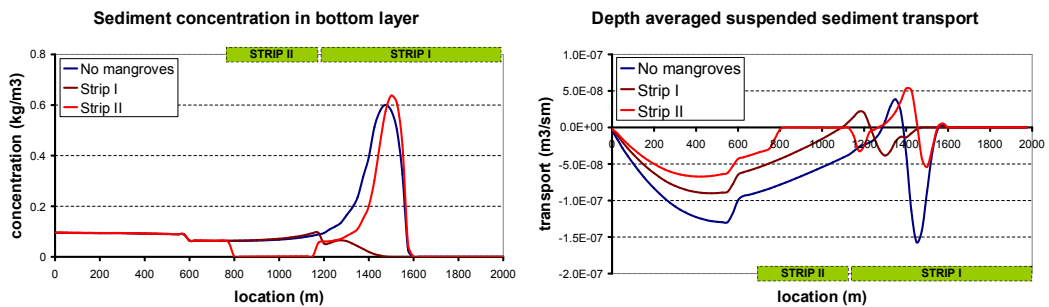


Figure E-5: sediment concentration and depth averaged sediment transport

It can be seen that the sediment concentration for strip II inside the mangrove forest is 0. Although waves can stir up the sediment, they are not able to do that inside the mangrove forest. It is probably too deep. The sediment can be stirred up in strip I. The concentration however is not very high. The highest concentrations occur at the breaking point of waves. The concentration for strip II mangroves is even higher than there are no mangroves. How this is possible is not clear. It cannot be related to the high orbital velocity, or to the high cross-shore velocity. It can only be said that waves are breaking a little bit later for strip II mangroves (see figure E.4). The water depth is lower at that point, resulting in higher sediment concentration. The concentration of sediment is than only related to the water depth and the fact that waves are breaking.

Combining the sediment concentration with the cross-shore currents (figure E.2) the suspended sediment transport can be determined. Looking to the cross-shore currents suspended sediment transport should increase till the breaking point and be directed off shore. This is not what figure E.5 is showing. The first 800 m shows an increasing suspended sediment transport, directed offshore. There are however differences between the three modelled situations, where there no differences occurred in sediment concentration or depth averaged velocity. The differences could be a consequence of the different structure in cross-shore velocity profile (see for example figure E.3), but that would probably also result in different depth averaged velocity. It can also be that the minor differences in cross-shore currents (see figure E.1) result in much larger differences for suspended sediment transport. Transport is related to velocity to the power 3-5. Therefore a small difference in velocity can lead to huge differences in transport. This seems the most logical explanation. The little drop in concentration around 600 m is responsible for the drop in sediment transport. It is not clear where this drop in sediment concentration can be attributed to.

There is no suspended sediment transport in strip II corresponding to no sediment concentration in strip II. Just before the breaking point the suspended sediment transport shows a peak directed on shore. How this is possible is not clear either. It cannot be attributed to the cross-shore currents. At the breaking point the suspended sediment also shows a peak value but directed offshore. This corresponds to the sediment concentration and the cross-shore currents. The peak values however do not correspond with each other. The modelling results considering suspended sediment transport remain a mystery.

The cross-shore bed load transport is shown in figure E.6. It can be seen that streaming is the dominating process, because bed load transport is directed onshore. The peak values of strip I mangroves and the other two situations show more differences than expected, looking to the orbital velocities (figure E.4). The water depth is probably also an important factor. The peak values for bed load transport are again much larger comparing to the peak values for suspended sediment transport. This means that the bed load transport is the leading process in morphological development. It can be seen that the orbital velocity should reach a critical velocity to start the bed load transport. This critical orbital velocity is just above 0.20 m/s.

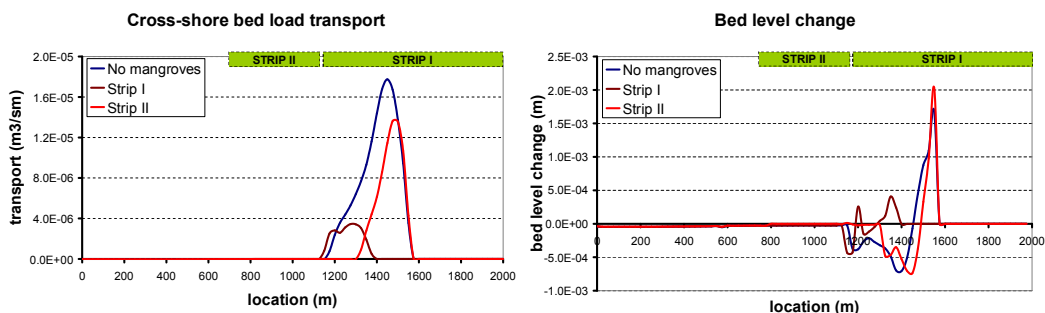


Figure E-6: bed load transport and bed level change

Sedimentation/erosion pattern

From the bed load transport pattern the sedimentation/erosion pattern can be derived. The influence of the suspended transport can be seen in the minor variations on this pattern. The pattern shows high erosion just for the breaking point and high sedimentation just after the breaking point. This is confirmed in figure E.6. The pattern shows the same pattern and therefore also the same problem as the situation without long shore currents.

E.1.3 Conclusion

Long shore currents and higher waves and grain sizes did not bring us closer to the conceptual model of Walsh and Nittrouer (2004). It should be concluded that it remains too difficult to model morphological changes of beaches, taking into account waves and long shore currents.

E.2 A hollow profile

E.2.1 Model setup

A model with another profile is used to test the influence of the shape of the profile. By changing the profile the locations of the important processes are changed as well, which can result in another (more reliable) sedimentation/erosion pattern. Figure E.7 shows the used profile. It is hollow comparing to the initial roundly profile. The other parameters and processes (Chezy value, tidal range, sediment type, grain size diameter and wave processes that are taken into account) are kept the same as the basic model from chapter 4. The mangroves forest starts at MSL (so at 400 m in figure E.7)

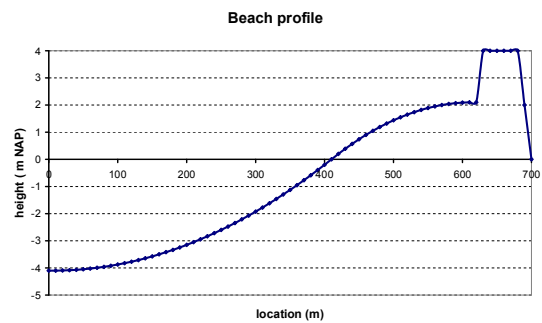


Figure E-7: a hollow beach profile

E.2.2 Analysis

Figure E.8 shows the resulting sedimentation/erosion pattern of this modelling experiment. Some differences can be observed comparing to the basic model of paragraph 4.1. The most important difference is that there is no sedimentation at the beginning of the mangrove forest, but halfway the mangrove forest. This can be attributed to the differences in wave action. Where the shoreline in the basic model has a gradient of 1/300 at the beginning of the mangrove forest, here it is only 1/50.

Waves get more change to act on the same spot on the shore face when the gradient is high. The mangrove forest however is able to stabilise the sediment in this case, so no erosion takes place at the beginning of the forest. When mangroves will be removed there will be erosion.

The sedimentation halfway the mangrove forest can be attributed to the water level variation. The water rises till that point (about 470 m), so the sediment is transported to that point. This is the same as described in chapter four for the basic model, where without mangroves a huge amount of sediments will be transported towards the shoreline.

E.2.3 Conclusion

In spite of these variations in results, this model resembles the same errors as the basic model and it should be concluded that this is not the way to model mangrove forests.

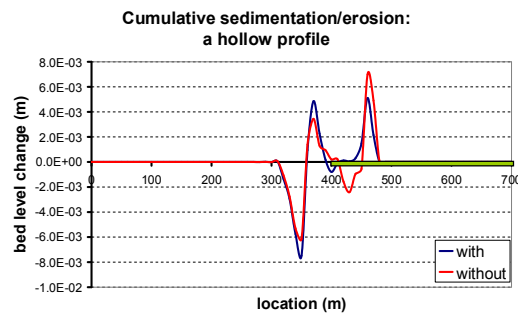


Figure E-8: resulting sedimentation/erosion pattern for a hollow profile. The green bar represents the location of mangroves

F Background sensitivity analysis

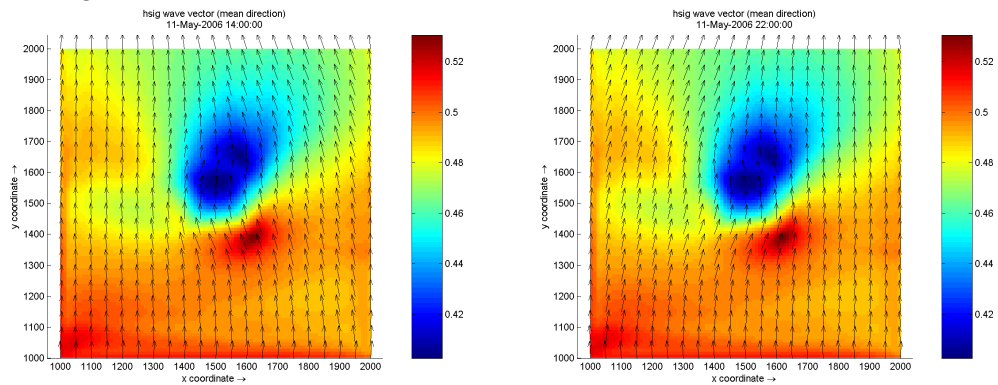
This appendix gives some background information about the sensitivity analysis carried out in chapter 5. It starts with showing the influence of different model set-ups on the hydrodynamics and sediment dynamics, followed by an extensive analysis of the parameter sensitivity graph.

F.1 Model sensitivity

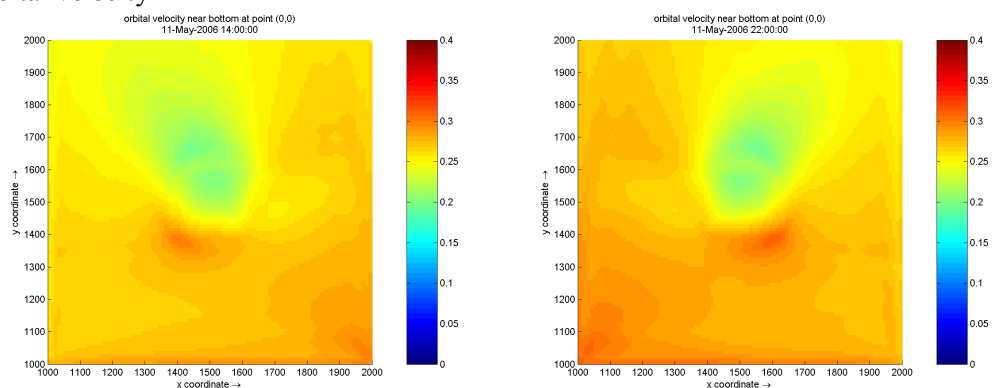
F.1.1 With waves ~ magnitude

The resulting hydrodynamic, sediment dynamic and morphodynamic patterns for the wave model calculations are shown below.

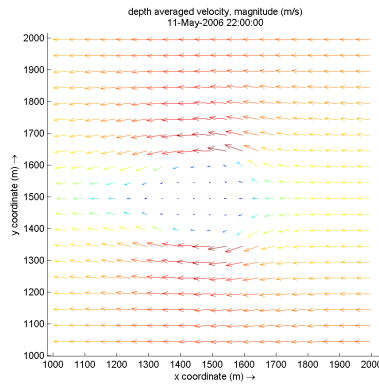
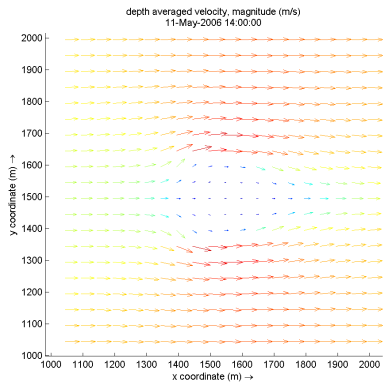
Wave heights



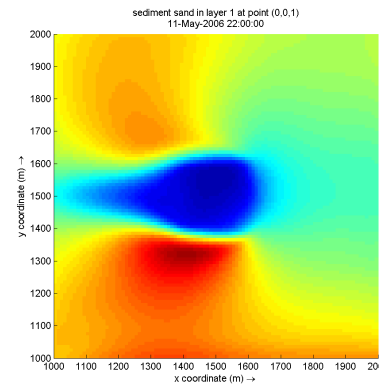
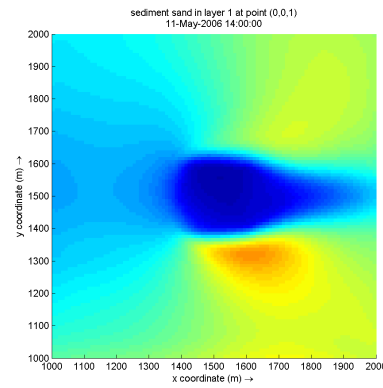
Orbital velocity



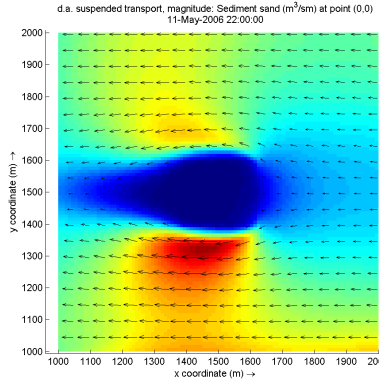
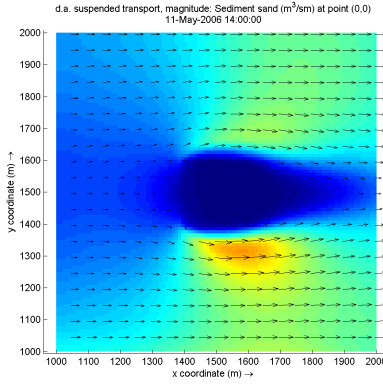
Velocity



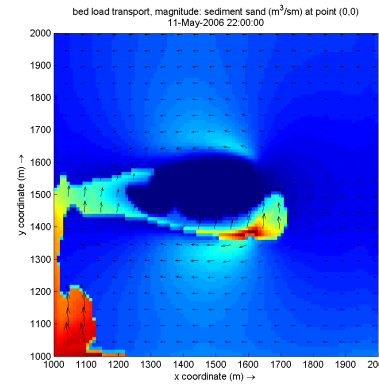
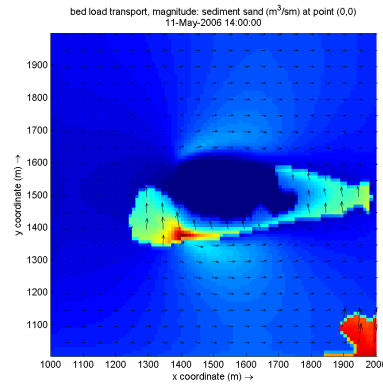
Sediment concentration



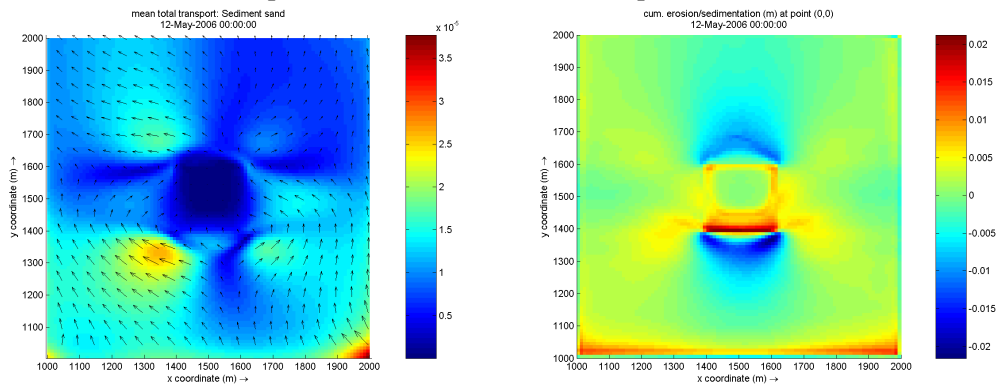
Suspended sediment transport



Bed load transport



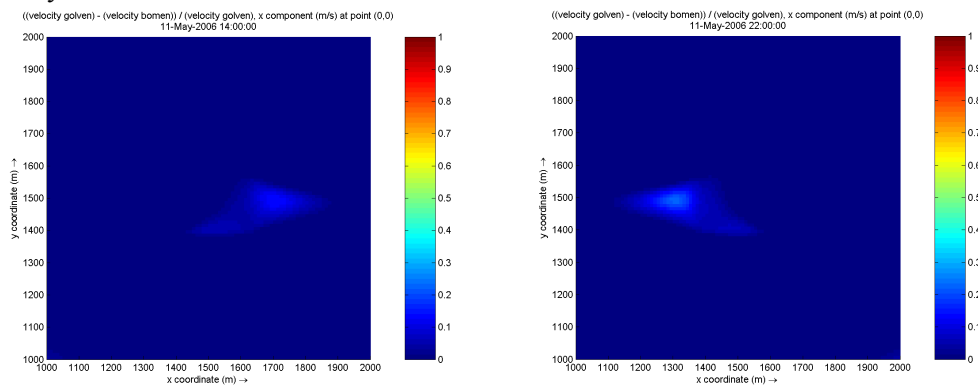
Mean total sediment transport and sedimentation erosion pattern:



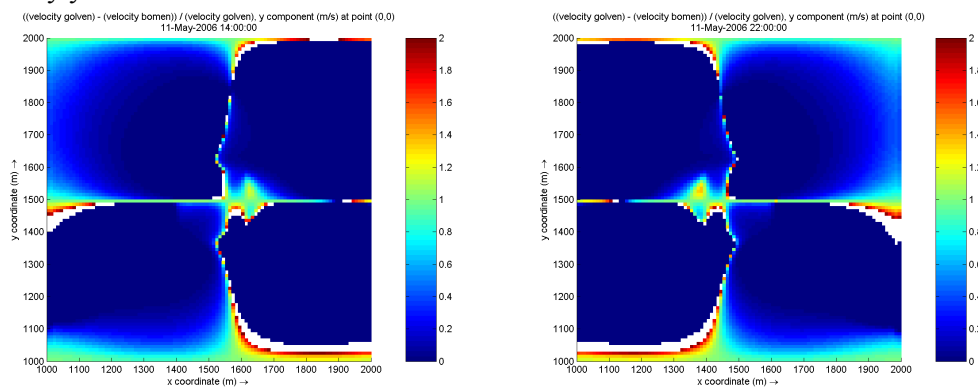
F.1.2 With waves ~ differences

The differences with the standard 2D, non-cohesive sediments modelling results are shown below.

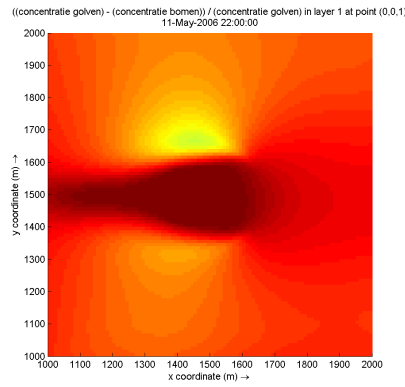
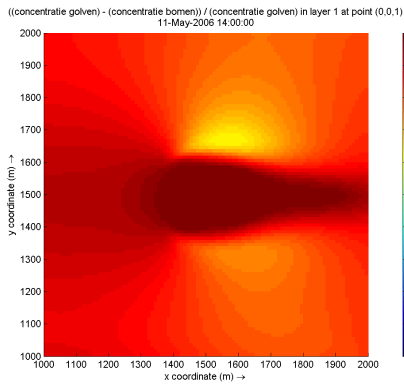
Velocity x-direction



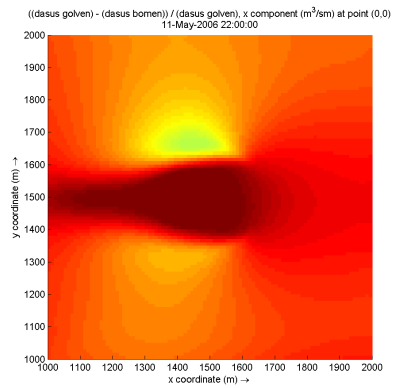
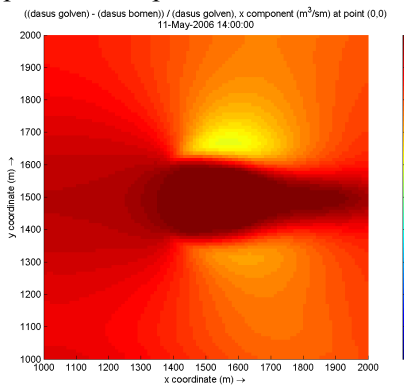
Velocity y-direction



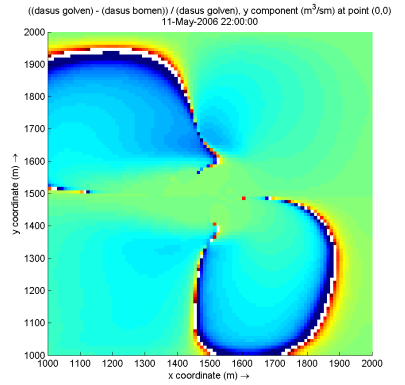
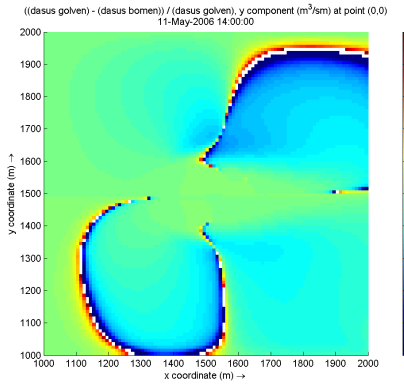
Concentrations



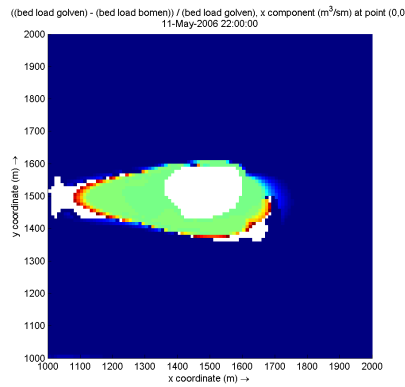
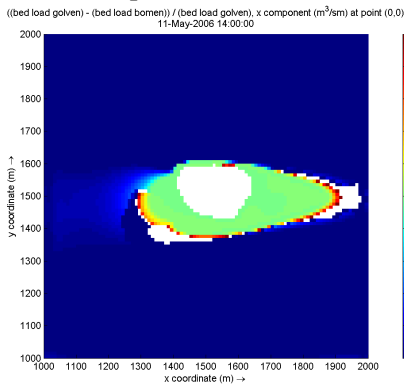
Suspended transport x-direction



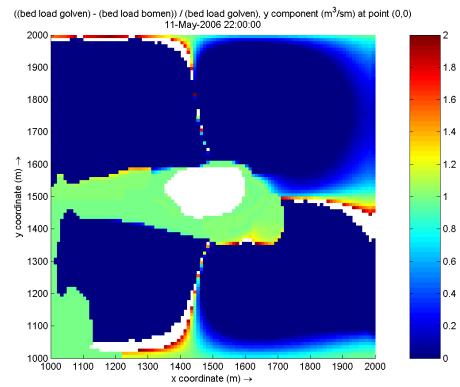
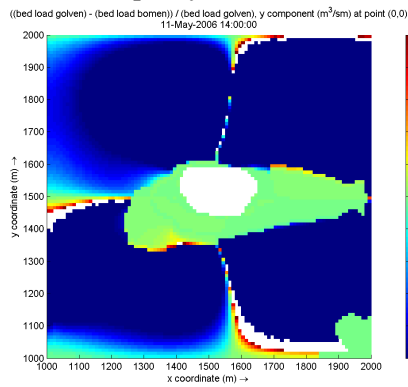
Suspended transport y-direction



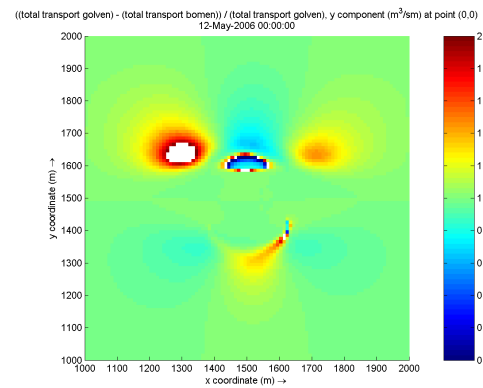
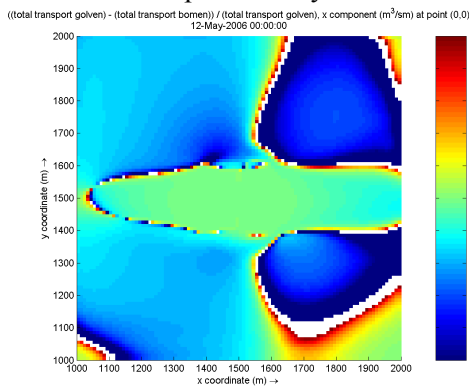
Bed load transport x-direction



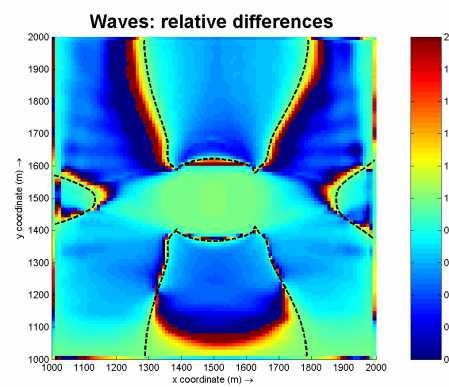
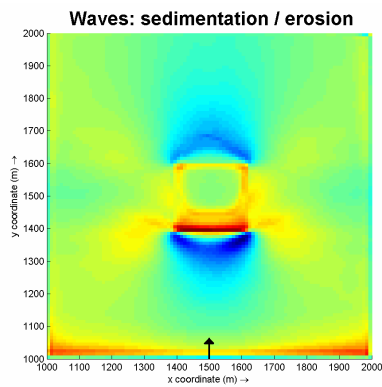
Bed load transport y-direction



Mean total transport x and y direction



F.1.3 Observations



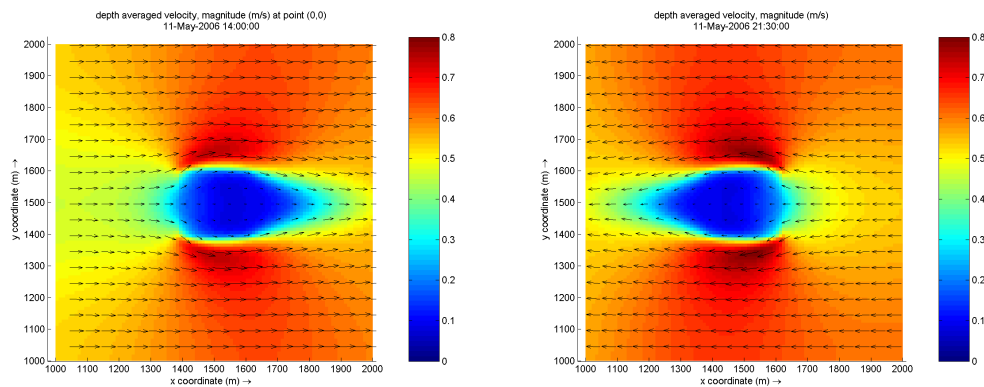
The following observations can be made:

- In the sedimentation/erosion plot it can be seen that waves are responsible for much more sedimentation at that side of the forest where the waves are ‘attacking’ at.
- Waves lead to much more sedimentation inside the forest (values in the difference plot at the location of the forest are 1)
- Waves also lead to more sedimentation behind the forest in the sedimentation area. Values in the difference plot are around 0.5. This means that the basic model (without waves) results in 50% less sedimentation
- In the erosion area at the side where the waves are ‘attacking’ there is more erosion close to the forest (value around 0.6), but the differences are getting smaller when coming closer to the model boundary (values are going to 1)
- In the erosion area behind the forest (from a wave point of view), there is also much more erosion (values around 0.8).
- The erosion area in the situation with waves is also a little bit larger than for the standard situation. This can be concluded from the red colour (value >1), outside the erosion area in the basic model.
- The erosion areas at the sides show also much more erosion and are larger than the original erosion areas.
- Some boundary effects can also be noticed in the difference plot and also from the sedimentation/erosion plot. It is therefore that the erosion area in front of the forest for the situation with waves is smaller than in the original situation. This also leads to much more sedimentation at the boundaries of the model

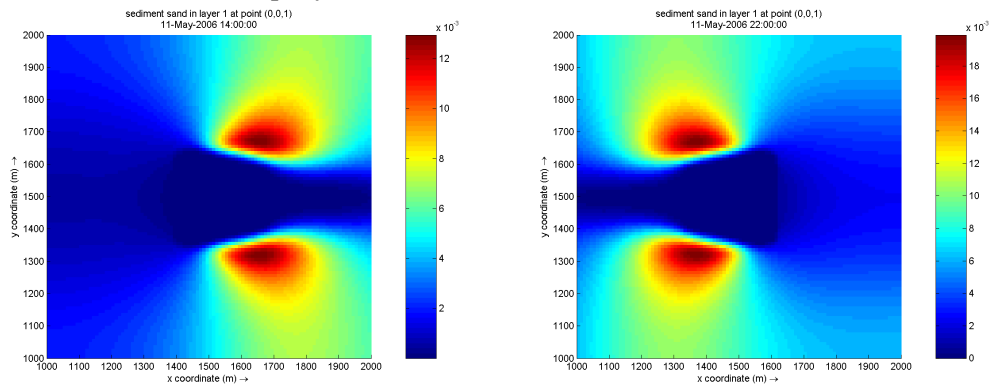
F.1.4 3D ~ magnitude

The resulting hydrodynamic, sediment dynamic and morphodynamic patterns for the 3D model calculations are shown below.

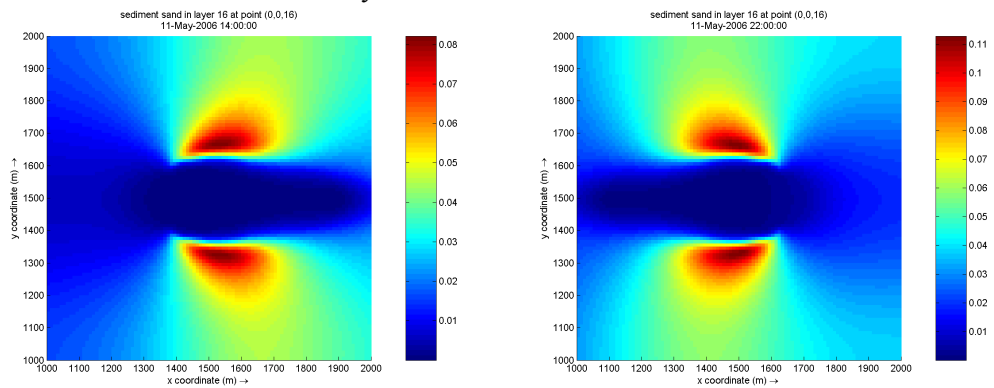
Velocities



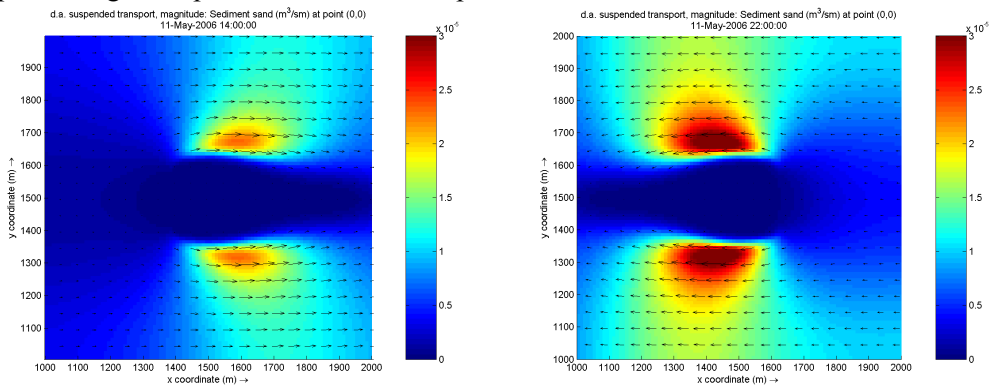
Sediment concentration top layer



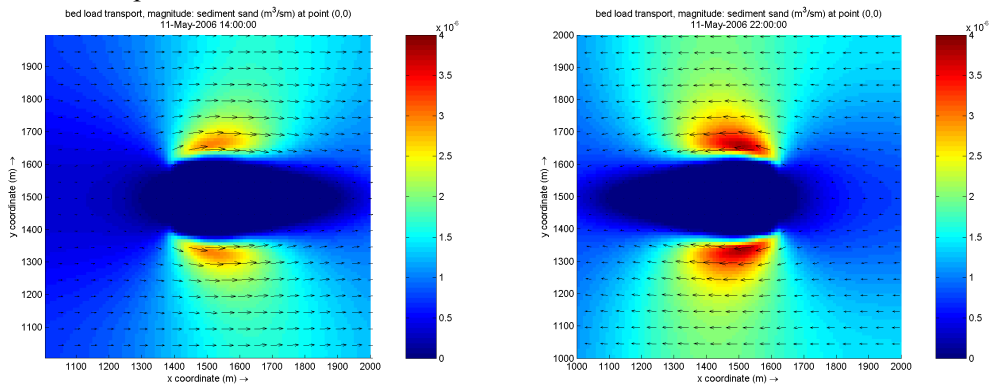
Sediment concentration bottom layer



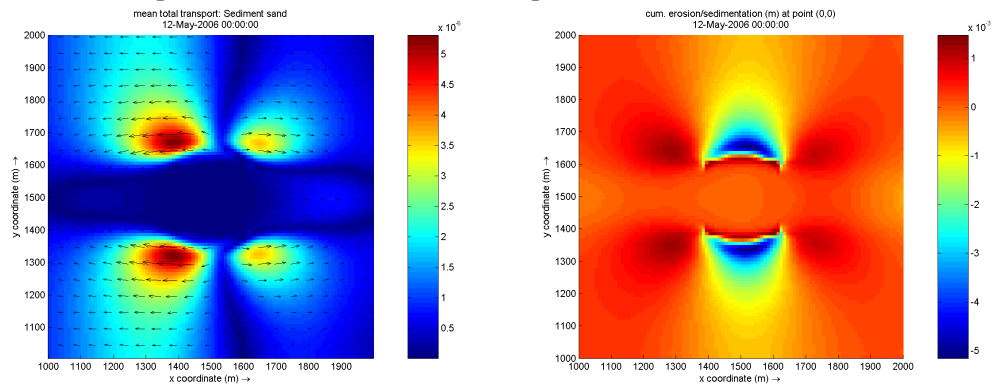
Depth averaged suspended sediment transport



Bed load transport



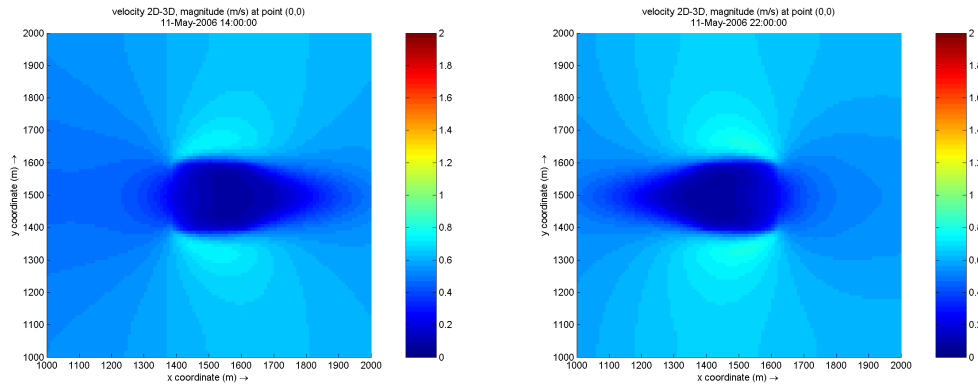
Mean total transport and Sedimentation/erosion pattern



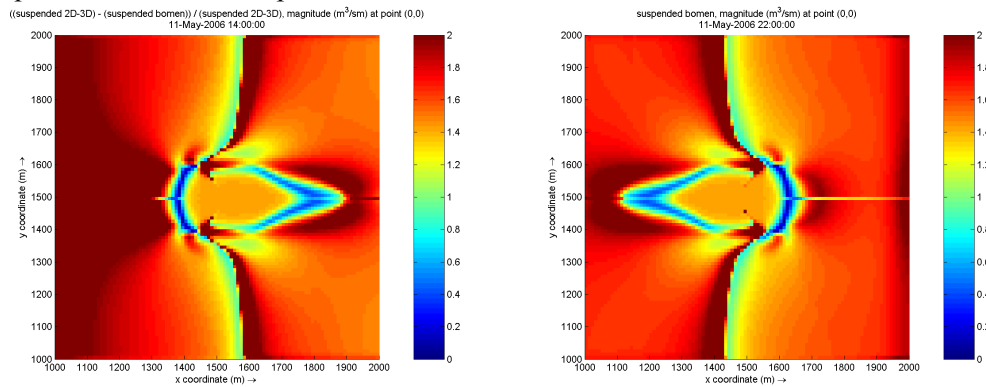
F.1.5 3D ~ Differences

The differences with the standard 2D, non-cohesive sediments modelling results are shown below.

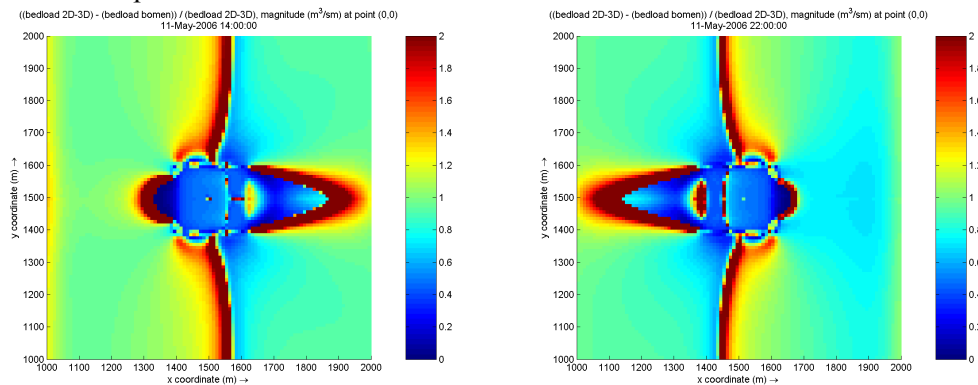
Velocities



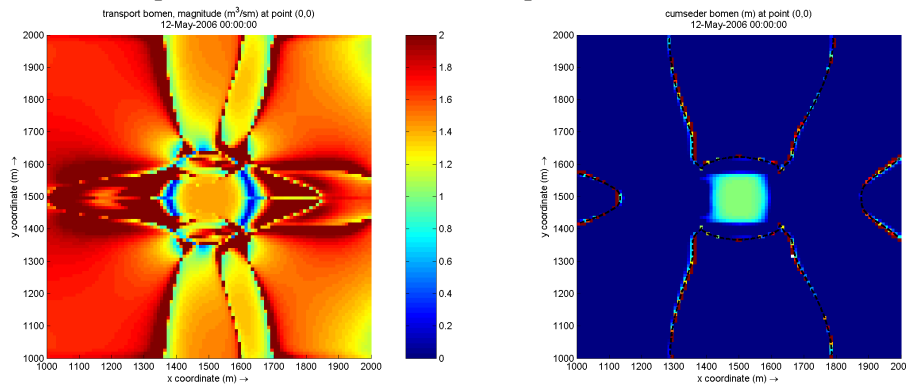
Suspended sediment transport



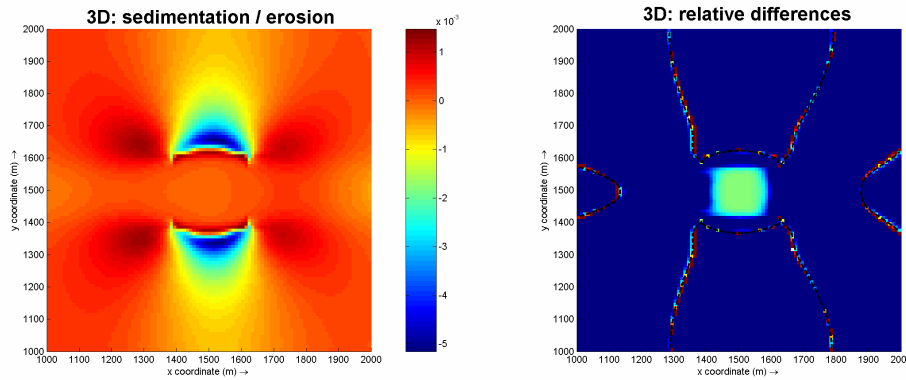
Bed load transport



Mean total transport and sedimentation/erosion pattern



F.1.6 Observations



The following things can be observed:

- The sedimentation erosion pattern does not change for the 3D model
- The effects of the basic 2D model and the 3D model are the same outside the forest. This can be seen to the value of 0 everywhere outside the forest
- Inside the forest the 3D model shows different results. The sedimentation inside the forest is much higher for the 3D simulation. This can be concluded from the value 1 inside the forest. However, the sedimentation inside the forest for the 3D simulation is still very low, in the order of 10⁻⁵ m per tide.

F.2 Parameter sensitivity

Figure F.1 contains a lot of information about the effect of five different parameters on the modelling results and the sensitivity of the model to these five parameters. The following can be observed from figure F.1:

- For cohesive sediment there is no net sediment transport into the forest through boundary 1 and 3. There might be some transport into the forest, just like in the other cases for non-cohesive sediment, but the transport out of the forest at the same time rules out the transport into the forest. That this is not the case for non-cohesive sediments can be attributed to the much lower settling velocity of cohesive sediments (factor 10). These sediments remain much longer in concentration than non-cohesive sediment. So, what is transported into the forest through boundary 2 and 4 is also transported out of the forest through boundary 1 and 3. There might be sediment transport into the forest through boundary 1 or 3, but the transport out of the forest at the same time is more, so the net sediment transport is directed out of the forest. This is not the case for non-cohesive sediments.

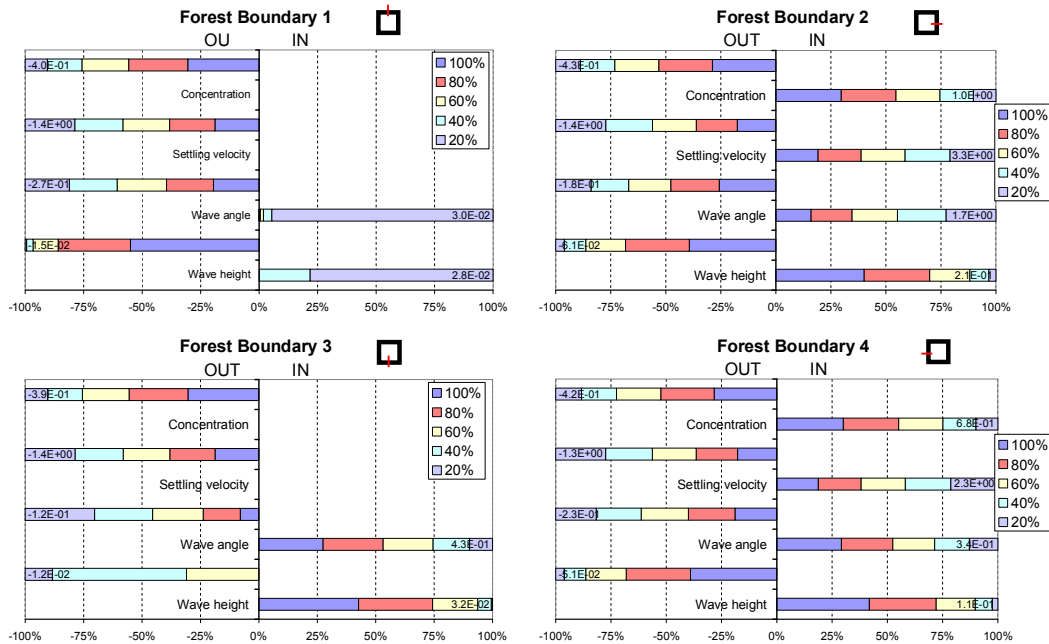


Figure F-1: sediment transport in and out of the forest (m³/s) during one tide. The red line in the square gives the boundary of the forest where the transport is going in or out. Each bar represents five different variations, shown by the five different colours. The different colours in the bar show their contribution to the total cumulative transport due to the five variations in 1 parameter. The values present sediment transport in or out of the forest for the 20% variation parameter value.

- Transport through forest boundary 1 and 3 are sensitive for almost all (researched) parameters, except for the settling velocity. This can be seen in the length of the different colours in each bar. For settling velocity the colours are all equally large, so the variations in settling velocity do not influence the transport through boundary 1 and 3. Transport through boundary 2 and 4 is also not sensitive for the settling velocity. It would be expected that the higher the settling velocity, the faster the sediment would settle and less transport would occur. This is not the case, showing that the settling velocity is already that low, that it does not influence the sediment transport through the forest boundaries.
- When waves are taken into account, only for low waves there is transport into the forest through boundary 1. This also counts for lower wave angles. Wave angles lower than 144 (if the original wave angle is 180) result in transport into the forest through boundary 1. The main reason for this is that boundary 1 lies at the lee side of the forest (see figure 5.11). The resulting currents of the waves transport the sediment out of the forest through boundary 1. Only for very low waves, or low wave angles there will be some sediment transport into the forest. Although, comparing to the transport out of the forest this is almost nothing.
- For the basic model the varied parameter was tree density. Both transport into the forest and out of the forest through boundary 1 and 3 are sensitive for this parameter. It can be seen that the lower the tree density the more transport out of the forest will take place. For transport into the forest this is just the other way around: a high tree density results in high transport into the forest. This can be attributed to the turbulence generated by the trees. The denser the forest, the more turbulence around the forest, resulting in more transport into the forest through boundary 1 and 3.
- Because of lower sediment concentration of cohesive sediments, less sediment will be available and less transport will occur through the forest boundaries. This is the case for transport into the forest and out of the forest for all forest boundaries. Therefore it is important to know what the sediment concentration is, when modelling a mangrove forest, in the case of cohesive sediments.
- Transport through forest boundary 2 and 4 is less sensitive for the wave height parameter, comparing to forest boundary 1 and 3, but still highly sensitive. The larger the wave height, the more sediment transport through boundary 2 and 4 will occur. When wave height decreases from 0.833 m (100%) to 0.167 m (20%) transport into and out of the forest through boundary 2 and 4 decreases with a factor 10.
- Transport through boundary 2 and 4 increases when the waves are acting more directly on the forest boundary. This influences the transport into forest boundary 4 and out of forest boundary 2. Transport decreases when the wave angle decreases. It would be expected that transport into forest boundary 2 and out of forest boundary 4 would be more sensitive to the wave angle. This is not the case, showing that a changing wave angle does not bring more sediment through the boundaries, but only stops the transport of sediment through the boundaries.

- The transport into forest boundary 2 and 4 is also sensitive for tree density. A decreasing density results in increasing sediment transport into the forest through boundary 2 and 4. When the density is decreasing the water can easily flow through the forest, resulting in more sediment transport. Sediment transport out of the forest through boundary 2 and 4 is less sensitive for tree density. The flow is reduced in the forest, resulting in less sediment transport out of the forest. The reduction of the flow depends on the density of the trees and the length of the forest. For a certain tree density a maximum flow velocity will be established inside the forest (see Baptist, 2005). This velocity can transport some sediments out of the forest, but this is much less than what comes into the forest. The relationship between tree density, transport into the forest and transport out of the forest is not linear. This is why the transport into the forest through boundary 2 and 4 is more sensitive to tree density than transport out of the forest through boundary 2 and 4.

Looking to the amount of transport it can be seen that in general cohesive sediments lead to much more transport into and out of the forest comparing to non-cohesive sediments. The difference is more than a factor 10 for forest boundary 2 and 4, and about a factor 100 for forest boundary 1 and 3, comparing to the basic model with non-cohesive sediments. Waves also lead to more sediment transport through all boundaries, comparing to the basic model without waves. Especially transport through forest boundary 3 results in much higher values.

G Management issues

G.1 General management issues

In the introduction (chapter 1) three important functions of mangrove forests are mentioned underlining the importance of these forests:

- They are the most biologically diverse forests (Burger, 2005)
- They are of economical importance (Mazda et al., 2002 and Quartel, 2000)
- They protect the coastline (Burger, 2005, Schiereck and Booij, 1995, Mazda et al., 1997, Mazda et al., 2002)

To make use of the functions of mangrove forests, good management plays a key role. Three important management issues for mangrove forests can be defined (Lewis, 2005):

(1) *restoration*, (2) *protection* and (3) *conservation*.

Lewis (2005) describes the loss of mangrove ecosystems that cover shorelines from 198000 km in 1980, 157630 km in 1990 and 146530 km in 2000. These losses represent about 2% per year between 1980 and 1990, and 1% per year between 1990 and 2000. Besides the magnitude of loss these figures emphasize, they also show the opportunities to *restore* mangrove ecosystems. Construction of shrimp aquaculture ponds is one of the most important threats for mangrove ecosystems, leading to the huge loss of forests, described above (Armitage, 2003). Important is to *protect* mangrove areas from being destroyed and develop aquaculture ponds in a sustainable way. Wood production is also an important threat for mangrove forests (Ruitenbeek, 1994), leading to destruction of the forests.

Hydrology is an important boundary condition for healthy mangrove ecosystems (Lewis, 2005). Changes in hydrology, due to dam building, canalisation, building of levees for example, can destroy mangrove forests. For conservation of mangrove ecosystems, it is important to link mangroves to a watershed. Measures and plans for that watershed should be analysed on the effect for the mangrove ecosystem. *Conservation* of mangrove areas starts by seeing the relationships between the watershed and the mangroves surrounded by the watershed.

A key term and tool in the restoration, protection and conservation of mangrove ecosystems is ecological engineering. Lewis (2005) defines this term by three goals:

- The restoration of ecosystems that have been substantially disturbed by human activities
- The development of new sustainable ecosystems that have both human and ecological value
- To accomplish items (1) and (2) in a cost effective way

Box G.1: Restoration of mangroves

A well known 'mistake' in mangrove restoration is immediately planting mangroves. Often these projects fail because mangroves cannot survive in these areas. Mangroves are not for nothing disappeared in these areas. Roy R. Lewis is a world wide known expert in restoration of mangrove areas. Together with a fellow researcher he suggested five critical steps for successful restoration. Figure 6.1 presents a typical 'before' and 'after' picture of a mangrove restoration project. The five steps are (after Lewis and Marshall, 1997):

1. Understand the autecology of mangrove species at the site, in particular the patterns of reproduction, propagule distribution and successful seedling establishment
2. Understand the normal hydrological patterns that control the distribution and successful establishment and growth of targeted mangrove species
3. Assess the modifications of the previous mangrove environment that occurred that currently prevents natural secondary succession
4. Design the restoration program to initially restore the appropriate hydrology and utilize natural volunteer mangrove propagules recruitment for plant establishment

Only utilize actual planting of propagules, collected seedlings or cultivated seedlings after determining through Steps 1-4 that natural recruitment will not provide the quantity of successfully established seedlings, rate of stabilisation or rate of growth of saplings established as goals for the restoration project



Figure G.1: mangrove restoration: before and after

In order to manage mangrove ecosystems (i.e. restoration, protection and conservation), knowledge of autecology (individual species ecology) of mangroves (Lewis and Marshall (1997)) and the hydrology (Lewis (2005)) is necessary (see box G.1 for information about restoration of mangrove areas). The autecology gives insight in the conditions that an individual trees need to grow and reproduce. Hydrology (in terms of currents, water levels and inundation times) shapes the conditions around mangrove forest. Inundation time and water level are important for the oxygen condition and salt concentrations. Tidal currents determine propagule transport (Huiskes et al, 1995) and sediment transport. Modelling is an important instrument to get insight in the hydrology of mangrove areas. In the next paragraph it is tried to generate some basic principles in the effect of mangroves on hydrology.

G.2 General hydrodynamic principles

Considering hydrodynamic principles the effect of mangroves on water levels and the effect on flow velocities are important. Both will be described and it is tried to use the Delft3D model in generating basic principles in analysing the effects. Two questions are leading in deriving general hydrodynamic principles:

1. Are the effects significant?
2. In what way are the effects related to other parameters?

These two questions will be specified and elaborated in the sub-paragraphs. Based on chapter 4 and appendix C the fringe mangrove forest will also be taken into account in this analysis, because there is no reason to conclude that the hydrodynamics are not modelled well in this case. It is the sediment transport dynamics, causing the modelling problems.

G.2.1 Water levels

In the modelling experiment the effect of mangroves on the water level could be clearly seen in the fringe and overwash cases (not shown in chapter 4 and 5). Due to the friction of mangroves a new balance between water levels and flow velocities will be established (see § 2.2.1).

Figure G.2 shows a sketch of the effects of mangroves on water level gradients, based on the literature presented in chapter 3 and the modelling experiment. The effect of mangroves on the water level gradient is often small. However, due to the low gradient of mangrove shorelines (in the order of 1/500), small water level gradients can have a large effect. The effect of the water level gradient can be that the water would not reach a certain point above MSL, while it would reach that point if there were no mangroves (see figure G.2 point b). This effect would be the largest at the end of the mangrove forest (in case of fringe mangrove) or in the middle of the forest (in case of overwash mangroves). It can also be that the water stays longer (a longer inundation time) on a certain point, than it normally would do (see figure G.2 point a). This will only be observed in the fringe mangrove forest, in the beginning of the forest. At this point the friction field for the rising tide is smaller (only 50 m forest), comparing to the falling tide (more than 500 m forest). In an overwash mangrove forest this effect is compensated by the symmetric bi-directional currents and cannot be observed. These effects should be kept in mind when (re)planting mangrove trees. For both fringe and overwash mangroves this is worked out.

Fringe mangroves

It is difficult to derive general principles for the influence of a mangrove forest on water level gradients. The gradients depend on the bathymetry, size and shape of the forest, and the individual resistance force of a tree. There are many possible settings, resulting in many different water level gradients. To start with the analysis of the effect of mangroves on water level gradients a 2D model is constructed with a cross-shore bed level gradient of 1/500, a 12 hr 2 m harmonical tide and a Chezy friction factor of 40 m^{1/2}/s. Other parameters are presented in figure G.2. The mangroves are specified according to § 4.1.2 and waves are not taken into account. In this case resulting currents without mangroves are around 0.2 m/s.

The results of this experiment are shown in figure G.3. No differences in maximum water levels could be observed. This means that there is enough time for the water level to reach this value, indicating that the influence on the flow velocity inside the forest is not large.

The increased inundation time in the beginning of the forest can be seen well in figure G.3. In this case it is however not very large and the question rises how significant the increase in inundation time is.

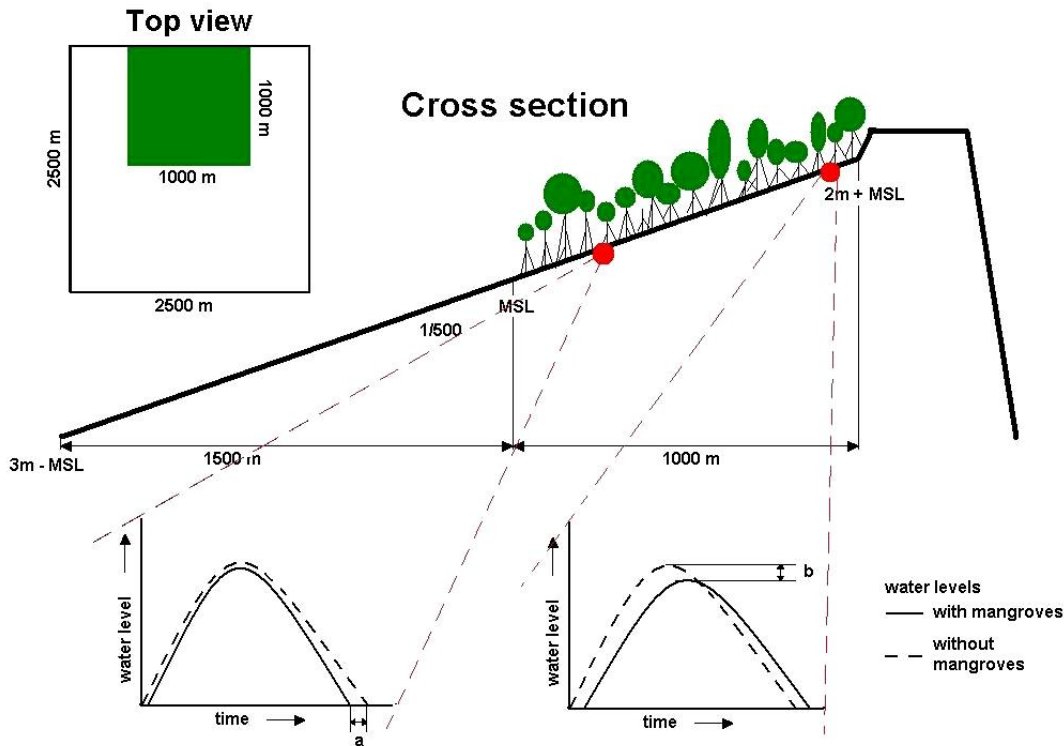


Figure G-2: Sketch of the model setup and the effects of mangroves on the water levels. Point a shows the increased inundation time and point b the decreased water levels

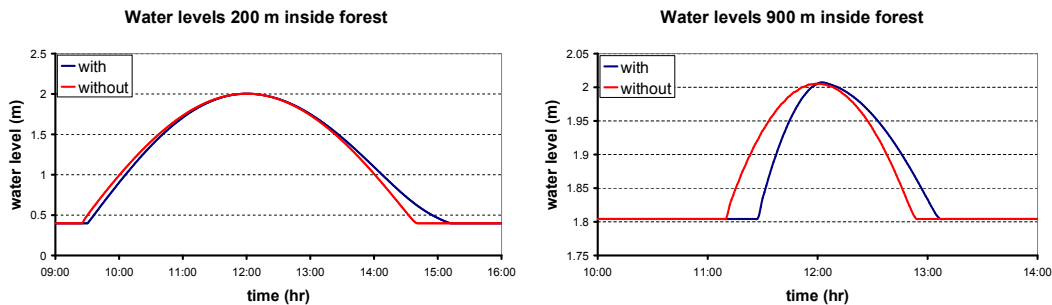


Figure G-3: water levels inside the mangrove forest

The differences in inundation time for the rising tide are 5 minutes and for the falling tide 21 minutes. So, in the case of mangroves the increased inundation time is 16 minutes. This is about 5 % of the total inundation time for mangroves (which is 5:41 hr) and only 2% of the tidal period. Lewis (2005) report inundation time values between 30% and 60% for different mangrove species on different locations. An increase of 5% lies in the reported range and is therefore not significant. The inundation time will probably increase when the forest length is increasing and/or the tidal currents are increasing. However in the modelled case both tidal currents (resulting from tidal water level differences) and the forest length are at the high side of the reported values (see chapter 3).

Overwash mangroves

Management implications considering water level gradients for the overwash case are analysed using the basic overwash model, described in § 5.1.2. It is said that for the overwash case the water levels in the middle of the forest are lower comparing to normal water levels. Some differences with the previous case are:

- larger tidal currents (maximum 0.7 m/s without mangroves)
- smaller forest (200x200 m)
- lower tidal amplitude (1m)

Figure G.4 shows the water levels in the middle and at the boundaries of the forest for this modelling experiment.

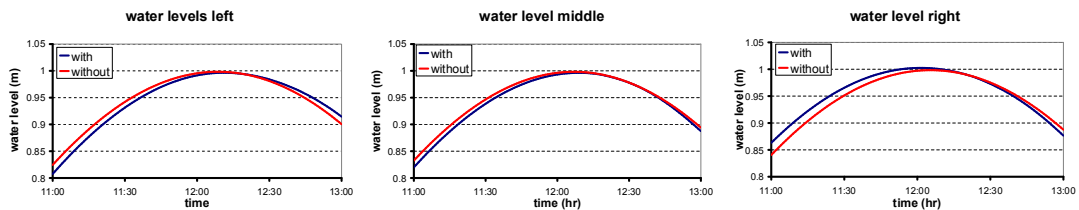


Figure G-4: water levels between 11:00 and 13:00 at the boundaries (left and right) of a mangrove forest and in the middle of a mangrove forest, compared to water levels on the same location without mangroves

It can be seen that there is no significant difference between maximum water levels with and without mangroves. An interesting observation which can be made is that the inundation time in the middle of the forest is smaller for the situation with mangroves. However, on one tide this difference is 3 minutes and not of huge influence. The small differences can be attributed to the relatively slow turn of the tide. In this time the water level can compensate the gradients and differences between water levels disappear.

The assumptions about the bathymetry made in the overwash case (uniform -2m MSL) influences the result. With decreasing water depth, velocity decreases as well and differences are getting smaller. The above standing results are probably an overestimation.

Conclusions

The main conclusion that can be drawn from the experiment is that there are no significant influences of mangrove trees on water levels. This implies that when (re)planting or removing a mangrove forest the effect on water levels does not have to be taken into account in the analysis of the effects. What should be kept in mind though is that the effect of waves is not taken into account in this model experiment. Waves are affected by mangrove trees and removing the trees has large effects on the wave heights (see chapter 2 and 3 for more information). Wave height affects the water levels by wave set-up and set down. It is also important to realise mangroves can influence the water levels during extreme natural events like (see also § 6.3.1).

G.2.2 Velocities

Mangroves have two effects on the magnitude of the velocity:

1. They increase the velocity outside the forest
2. They decrease the velocity inside the forest

Both effects will be analysed in this paragraph for the fringe and overwash case. For both the increase and decrease, it is tried to find a relationship between tree density and velocity. The velocity pattern will not be discussed here. It is already discussed in chapter 5 where the sensitivity to different forest types of the overwash mangroves is analysed.

Increase in velocity outside mangrove forest

Overwash mangroves

The velocity pattern of the overwash mangrove case is shown in figure 5.4. This pattern is consistent during the tide, so the highest velocities occur at one point during the tide. Figure G.5 shows the magnitude of the velocity, including the velocity vectors at $t = 22:00$ during a 12 hr harmonical tide. The maximum velocity is about 0.8 m/s at this time. The white dot in the graph is the point where the highest velocities occur. Figure G.6 gives a time plot of the velocities on that point for different tree densities. The tree densities are varied in the same way as presented in § 5.3.1. It can be seen that in the case of mangroves the maximum velocity is higher comparing to the ‘no-mangrove’ case. The maximum velocities for the different tree densities are almost equal to each other. The velocities are the highest if they are directed to the left. This is because the chosen point is located at the right side of the forest (see also figure G.5). The velocity pattern to the left shows the highest values at the right side of the forest. The right directed velocity pattern shows the highest values at the left side of the forest. It can be seen that the maximum velocity without mangroves is about 0.6 m/s. This means that the velocity in the case of mangroves shows an increase of 25%, which is significant.

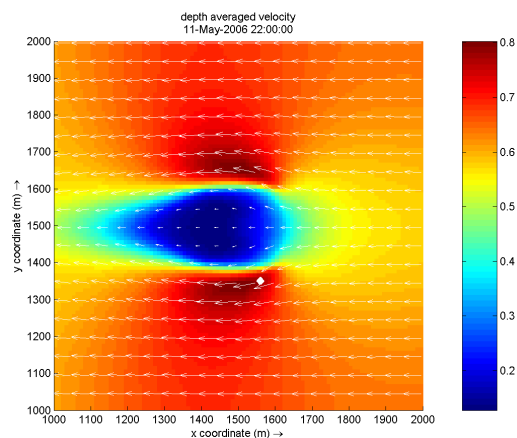


Figure G-5: velocity pattern for the overwash mangrove case at $t = 22:00$ hr. The white dot represents the location where the highest velocities occur.

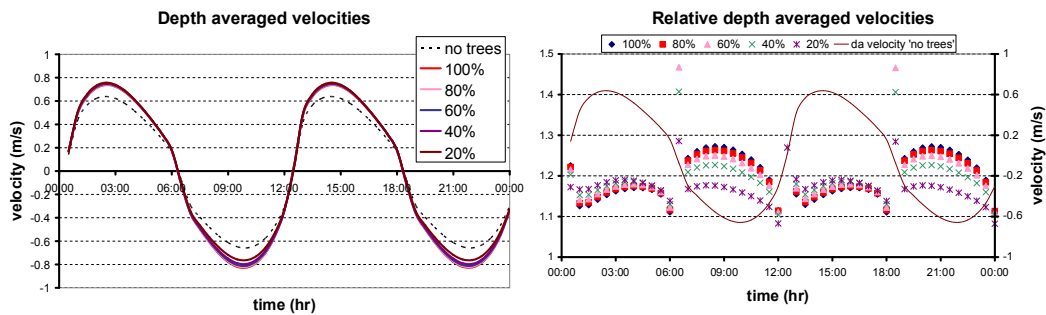


Figure G-5: depth averaged velocity during 2 tides for different tree densities (left) and relative depth averaged velocities for different tree densities (right) during one day. The brown line in the relative depth averaged velocity plot is the depth averaged for the ‘without trees’ case. A negative velocity is left directed

To analyse the effect of tree density on the velocity at this point the velocity is made relative to the case without trees, by dividing the ‘with tree’ case through the ‘without tree’ case. The result is shown in the right plot of figure G.6. Besides some strange points occurring at the time when the tide is turning, the relative velocities show interesting patterns. The following observations can be made:

- For left directed velocities the relative differences are larger
- For right directed velocities the lowest tree densities results in the highest increase in velocity. For left directed velocities this is the other way around
- Right directed velocities show a small range of increase in velocities. The maximum (relative) difference between the different tree densities is about 5%. Left directed velocities show a wider range of increase between the different tree densities (10% range). The range in velocity is constant in time
- The relative velocities are not constant during the time. This indicates that the increase in velocity depends on the velocity
- The maximum relative differences between velocities with and without mangrove trees do not occur at the maximum velocity for the ‘without trees’ case. Some lag effects can be observed, which can possibly be attributed to the forest shape and the resulting water level gradients. In the case with mangroves the maximum velocity increases faster, leading to higher relative differences. The relative differences however are small.

From figure G.6 it can be concluded that the maximum velocity outside the mangrove forest increases with about 25%, when the forest density is 100%. For lower densities this is between 15% and 20%. These values are valid for the left directed velocities at the right side of the forest (see figure 6.5), when the velocity is directed to the left. The increase is a little sensitive for incoming velocities.

Fringe mangroves

For fringe mangroves the maximum velocity occurs at the boundary of the forest when the water is flowing out of the forest. Figure G.7 shows this situation together with the modelled velocity during the tide on the location where the maximum velocity occurs. This location is at mean sea level. Therefore the depth averaged velocity is zero about half the time. It should be noticed that the velocity for the falling tide is higher comparing to the rising tide. This can be attributed to the water level gradients occurring inside the forest. Although the gradient is small and does not affect the water level significant, the effects on the velocity are large. The maximum velocity with mangroves is about 0.35 m/s and without mangroves 0.15 m/s, so the effect is significant.

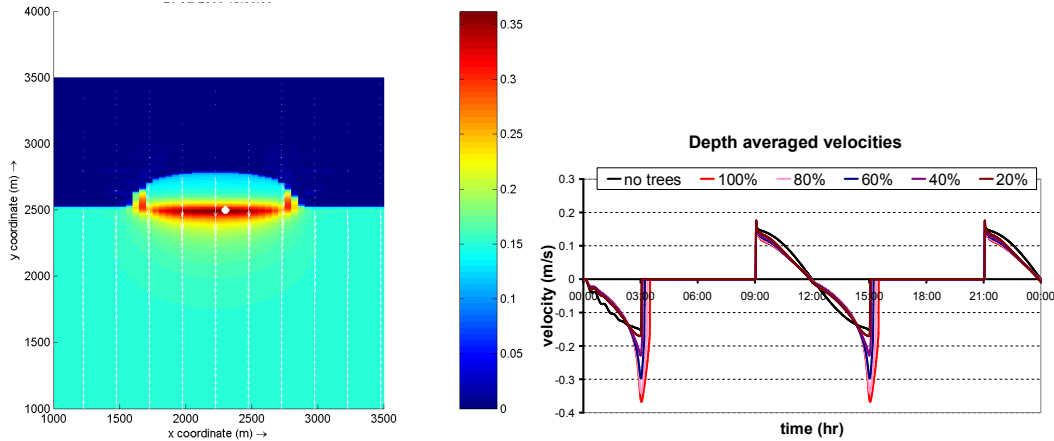


Figure G-6: depth averaged velocity pattern at time $t = 15:00$ (left) and velocity at the white spot, during the time for different tree densities

Contrasting to the overwash mangrove case the velocity shows a very sudden increase. The most interesting point is what the (relative) increase in maximum velocity will be. The maximum velocity is also interesting in the case of sediment transport. However by only looking to the maximum velocity in this case the relationship between tree density and other velocities cannot be analysed. The maximum velocity depends on tidal water level variation. Therefore this situation is also modelled with a 12 hr, 1 m amplitude tide. The results for the (relative) maximum velocity for both tides are shown in figure G.8. It can be seen that for the 2 m amplitude tide the maximum depth averaged flow velocity increases as the tree density increases. The increase seems flatten to a certain maximum value, depending on the tree density. For the 1 m tide there is no effect of the tree density on the maximum flow velocity. The flow velocity is so low that it can flow through the trees without acceleration.

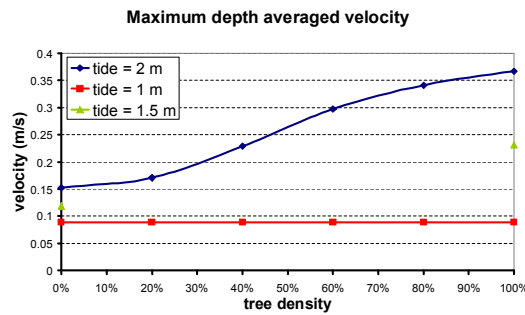


Figure G-8: maximum relative depth averaged velocity for different tree densities and different tides. For the 1.5 m tide (green triangle) only the cases with 100% and 0% tree densities are modelled

If there is or isn't an effect of vegetation on flow velocities can be based on the flow velocity without mangroves. When the (maximum) flow velocity is higher than about 10 cm/s the effect of mangroves will be seen, and will increase if density increases. To illustrate this an extra model calculation is carried out for a 100% forest and a 1.5 m amplitude tide. Without a forest the velocities during the tide are about 12 cm/s. It can be seen in figure G.8 that there is indeed an effect, supporting the statement of 10 cm/s.

An interesting observation which can be made is that the velocity for the 1.5 m tide without trees is in the middle of the velocities for the other tides without trees. For the 100% tree density case this velocity also lies in the middle between the other cases. It seems that the relation between the different tides remain the same for different tree densities.

Decrease in velocity inside mangrove forest

Overwash mangroves

When water flows into the mangrove forest the flow velocity will decrease. Questions that raises are:

- Is this decrease significant?
- Does the decrease depend on the incoming velocity?
- Is there a relationship between location in the forest and decrease of velocity?
- Can it also be related to tree density?

To answer these questions for the overwash mangrove case a transect of 9 observation points through the forest are analysed. The velocities for these points during the tide are shown in figure G.9. It can be seen that the decrease is significant.

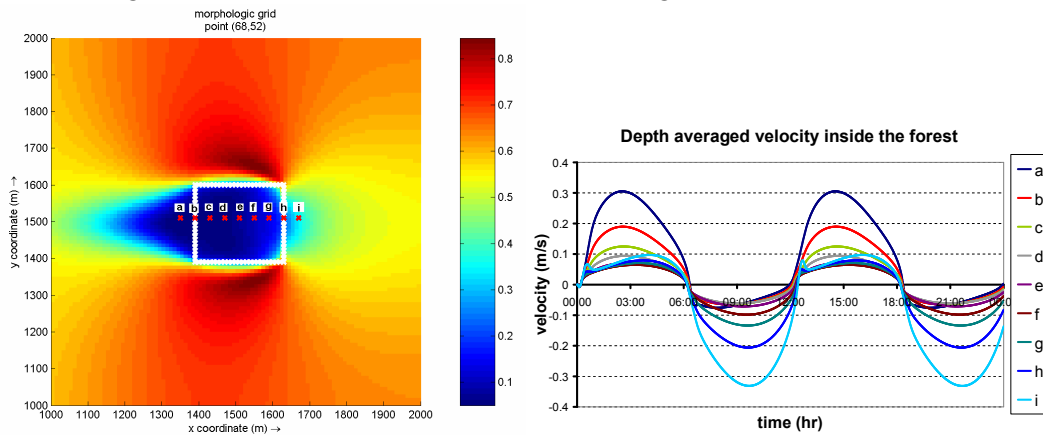


Figure G-9: location of velocity observation points and the tidal depth averaged flow velocity in these points during 2 tides

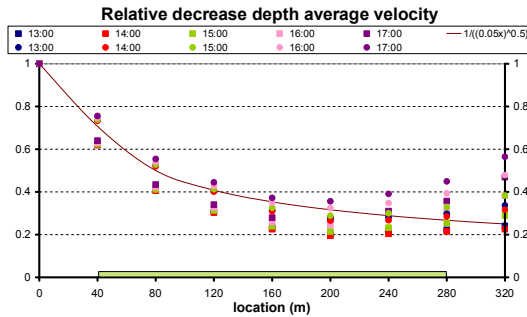


Figure G-10: relative depth averaged flow velocity for a 100% tree density (the square) and a 40% tree density (circle). The green bar represents the location of the mangrove forest, and the brown line is an approximation of the decrease in flow velocity

To analyse the decrease in velocity the tidal velocities between 13:00 and 17:00 are analysed. Figure G.10 shows the relative depth averaged tidal flow velocities for several times and two tree densities (100% and 40%). The locations of the values correspond to the a – i locations from figure G.8. The points are located 40 m from each other. Several times are taken to analyse the decrease of different incoming flow velocities. Two densities (100% and 40%) are taken to analyse the effect of tree density on the decrease in flow velocity. It can be seen that the decrease in flow velocity during the first 200 m, does not depend on the incoming flow velocity and on tree density as well. The 40% tree density results in a higher flow velocity through the forest, but the pattern of the decrease is the same as the 100% tree density. At the end and just outside the forest (from 240 m – 320 m) the relative depth averaged flow velocity increases for both forest densities. This increase is higher when the time increases. It is not clear what is behind this effect.

In figure G.10 the equation $\frac{1}{\sqrt{(0.05x)}}$ is plotted, where x is the distance inside the mangrove forest. It can be seen that with this simple equation the decrease in flow velocity can be approximated well for both tree densities.

Fringe mangroves

The decrease in flow velocity for fringe mangroves during the tide is shown in figure G 11 where the results of the 12hr, 2 m amplitud 1 corresponds with the point shown in figu 200m between each different point. For development of the flow velocity. This can little instability when the area is getting v tide, when the area gets dry again. Hardly the forest. The development of the velocity shown here). For the falling tide can be se goes to the beginning of the forest. The r velocity just at the border of the forest. Th will be made.

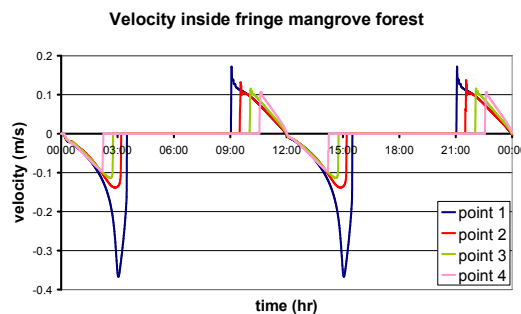


Figure G-11: depth averaged velocity development during the tide for different points inside the forest (point 1 = 0m, point 2 = 200m, point 3 = 400 m, point 4 = 600 m inside the forest)

G.2.3 Conclusion

The focus of this paragraph was trying to find general hydrodynamic principles which can be useful for mangrove management situations. Therefore the effects on water levels and the effects on velocities are analysed. Two questions were leading:

1. Are the effects significant?
2. In what way are the effects related to other parameters?

Considering the water levels the effect of mangroves on the water levels are not significant.

For velocities there are significant effects. The increase in maximum depth averaged flow velocity outside the forest for the overwash case is about 25% for a dense forest and 15%-20% for an open forest. The effect is a little sensitive for incoming velocities. For the fringe mangroves the velocity starts to increase when the normal tidal currents are larger than 10 cm/s. For currents of 15 cm/s without mangroves (a 2m amplitude tide) the resulting maximum depth averaged currents with mangroves are about 37 cm/s.

The decrease in flow velocity inside the forest is only interesting in the overwash case, because in the fringe case there is no significant decrease in velocity observed. For the overwash case the decrease for depth averaged flow velocities, for all forest densities, can

be approximated with $\frac{1}{\sqrt{(0.05x)}}$.